

**Development of Lanthanide-Binding Tags (LBTs) as Powerful and Versatile Peptides
For Use in Studies of Proteins and Protein Interactions**

by

Langdon James Martin

B.A. Chemistry
Kalamazoo College, 2003

Submitted to the Department of Chemistry
in Partial Fulfillment of the Requirements for the
Degree of Doctor of Philosophy

at the

Massachusetts Institute of Technology

May 2008

© 2008 Massachusetts Institute of Technology
All rights reserved

Signature of Author: _____
Department of Chemistry
May 14th, 2006

Certified by: _____
Barbara Imperiali
Class of 1922 Professor of Chemistry and Professor of Biology
Thesis Supervisor

Accepted by: _____
Robert W. Field
Haslam and Dewey Professor of Chemistry
Chairman, Departmental Committee on Graduate Students

This doctoral thesis has been examined by a committee of the Department of Chemistry as follows:

Timothy M. Swager
Chairman
John D. MacArthur Professor of Chemistry
Massachusetts Institute of Technology

Barbara Imperiali
Thesis Supervisor
Class of 1922 Professor of Chemistry and Professor of Biology
Massachusetts Institute of Technology

Stuart S. Licht
Assistant Professor of Chemistry
Massachusetts Institute of Technology

Karen N. Allen
Professor of Physiology and Biophysics
Boston University School of Medicine

**Development of Lanthanide-Binding Tags (LBTs) as
Powerful and Versatile Peptides
For Use in Studies of Proteins and Protein Interactions**

by

Langdon James Martin

Submitted to the Department of Chemistry
on May 14th, 2008 in partial fulfillment of the
requirements for the Degree of Doctor of Philosophy in
Organic Chemistry

ABSTRACT

To determine the function of proteins of interest, chemical biologists employ their full panoply of techniques, including X-ray crystallography and NMR spectroscopy for structural information, and luminescence spectroscopy to determine cellular localization and binding interactions. These techniques generally require a spectroscopic handle, and trivalent lanthanide ions (Ln^{3+}) are protean in this regard: an ordered Ln^{3+} can have many uses. Paramagnetic lanthanide ions can be exploited to align biomolecules in a magnetic field, and the anomalous signal of any lanthanide ion may be used to obtain phase information from X-ray diffraction data. Most lanthanide ions are luminescent upon sensitization by an organic fluorophore; for example, Tb^{3+} may be sensitized by the side chain of the amino acid tryptophan. Ln^{3+} emission profiles are distinct and long lived, and therefore ideal for imaging and resonance energy transfer experiments.

Lanthanide-binding tags (LBTs) are short peptide sequences developed to tightly and selectively chelate lanthanide ions. LBTs contain an appropriately placed tryptophan residue for sensitizing Tb^{3+} luminescence, and are composed entirely of encoded amino acids; incorporation at the genetic level into any protein of interest is thus facilitated. Subsequent expression of the tagged protein may be done using standard biochemical techniques, and the resultant protein contains a site for introducing an ordered lanthanide ion. Within this thesis is discussed the further optimization of LBTs for lanthanide affinity and structural stability. A combination of combinatorial peptide libraries and computational studies has resulted in the discovery of peptides that bind Tb^{3+} with dissociation constants of better than 20 nM. Furthermore, the concatenation of two LBT motifs has enabled the generation of so-called “double lanthanide-binding tags” (dLBTs). These slightly larger tags have additional advantages including the ability to bind two lanthanide ions, reduced mobility with respect to the tagged protein, and comparable or improved affinity for Ln^{3+} ions. Furthermore, since the lanthanide Gd^{3+} is a common handle for magnetic resonance imaging, progress has commenced to expand the utility of LBTs to include this type of experiment. Finally, LBT technology has been used to study the protein Calcineurin by uniquely modifying one calcium-binding loop to selectively bind and sensitize Tb^{3+} .

Thesis Supervisor: Barbara Imperiali

Title: Class of 1922 Professor of Chemistry and Professor of Biology

ACKNOWLEDGEMENTS

Intelligence is like four-wheel drive. It simply enables you to get stuck in more-remote locations.
-Garrison Keillor

I would be remiss if I did not first acknowledge my advisor, Barbara Imperiali. I cannot honestly say whether I myself would have had the audacity to accept a first-year graduate student who didn't know his twenty amino acids into my chemical biology lab, much less sell him on the LBT project, but Barbara did, and here I am. So, thank-you, Barbara, for promoting my development as a researcher—and giving advice when I did get stuck in more-remote locations, and for teaching me all sorts of chemistry and biology, for improving my ability to write like a scientist, for writing the grants that provided my funding, for providing a great environment for me to work in, and for putting up with my facetiousness through many a long minimeeting.

I also need to thank my fellow Imperiali lab rats (or “lablings,” as I am wont to call them). They helped make my days interesting, and I dare say I have learned something from all of them. Thank you all for your conversations, friendships, and for laughing at my jokes.

First and foremost, I thank my fellow LBT-ers for lots of helpful discussions, advice, and the occasional co-authorship. I am indebted to Mark Nitz, who really helped get my feet on the ground when I joined the lab, tolerated many inane babblings of a first-year grad student, provided loads of ideas of things to work on (many of which wound up in this thesis), and was the only person who also sported an “LBT-goatee”. Ryu Yoshida was unmatched in his motivation, and was an outstanding undergrad researcher. I thank Bianca Sculimbrene for her patience with me when she joined the lab, and for her panoply of insights, advice, and encouragement on chemistry, lab-work, and the world; also, she was the first to fully embrace the idea of LBT subgroup color-coordination at minimeetings. It has been a tremendous pleasure to work with Anne Reynolds, who is perpetually tenacious and unfailingly helpful, willing to lend an ear (or a car) when needed, and deserves credit for considerably improving my understanding of *d*-orbitals and expanding my enological palate. I have been glad to get to know Katja Barthelmes these past few months, and thank her for her explanations of protein NMR and her enthusiasm. Although I did not get to overlap with Kathy Franz, she initiated the LBT project, and therefore deserves accolades here as well.

As for the rest of you, I am going to run out of adjectives such as “friendly”, “kind”, “insightful”, “helpful”, “brilliant,” and “grad student/post-doc extraordinaire”; furthermore, the introduction “I am so glad I got to know and work with...” is hard to vary twenty-odd times, so suffice it to say that I could use these to describe any of you as both scientists and coworkers. Thank-you to Guofeng Zhang, Eranthie Weerapana, Beth Vogel Taylor, Eugenio Vazquez, Jay Troutman, Melissa Shults, Emi Sei, Matthieu “Chewie” Sainlos, Debbie Rothman, Debby Pheasant, Mary O'Reilly, Nelson Olivier, Elvedin Luković, Galen Loving, Angelyn Larkin, Wendy Iskenderian, Meredith Hartley, Christian Hackenberger, Susana Gordo, Juan Antonio “Nono” Gonzalez-Vera, Brenda Goguen, K. Jebrell Glover, Seungjib Choi, Mark Chen, Christina Carrigan, Dora Carrico-Moniz, Melanie Bonnekesel, Mayssam Ali, and Andreas Aemissegger. Good luck also to our rotator, Marcie Jaffee, and upcoming post-docs James Morrison and Cliff Stains.

I also owe some specific thank-yous. First, to Jebrell, Beth, and Guofeng, and also to Christina, Nelson, Mary, Eranthie, Bianca, both Marks, Angelyn, and Meredith for various insights into the workings of molecular biology and biochemistry. Thank-you to Mark Nitz and

Melissa for teaching me how to use the fluorometer. Thank-you to my editors, who are mentioned after each chapter; and to paraphrase Seungjib, I defer to them all responsibility for any typographical errors. A special thank-you, too, to my podmates (and pod-annex) Guofeng, Christina, Mark, Meredith, Wendy, and Brenda, who have made sitting at my computer fun and enjoyable. Thank you to those who have done their research in A-Lab hoods: Mark, Mayssam, Debbie, Seungjib, Eranthie, Galen, Bianca, Anne, Angelyn, Andreas, and Melanie, who have made doing experiments there more exciting. Thank-you to the Barbarians volleyball team members: Chieftans Mary and Meredith, and Eranthie, Jebrell, Melissa, Debbie, Christina, Christian, Guofeng, Matthieu, Emi, Mark, Andreas, Jay, and Galen, for glorious victories and enjoyable defeats. Thank-you to my outstanding grad-student classmates, Galen and Elvedin, for going through tribulations such as Orals and Proposal Writing with me, and for bonding experiences such as trips to the Muddy, dinner parties, and to Galen especially for organizing a sailing...adventure. Thank-you to Wendy and Meredith for an awesome baby shower. And thank-you to my fellow Red Sox fans Debbie, Beth, Melissa, Bianca, Seungjib, and Anne for going to games at Fenway, and for going nuts with me in 2004 and 2007.

I would also be remiss if I neglected to thank Elizabeth Fong, who does so much behind the scenes and keeps the lab running so very smoothly that we don't appreciate her enough.

Of course, my academic coworkers and mentors are in no way limited to my lab. I should first say thank-you to my thesis chair, Tim Swager, for helping to advise me the past five years. And I thank the rest of my committee, Stuart Licht and Karen Allen, as well.

The LBT project would have been nowhere near as exciting without our collaborators, who have been outstanding at filling in holes in my knowledge and skill set. Although I will say this in over half of my Thesis chapters, I am grateful for our collaboration with Karen Allen's lab at Boston University. Karen Allen herself has been a great mentor, and has put together an outstanding lab, including Nick Silvaggi, Manashi Sherawat, Kelly Daughtry, and Ezra Peisach, who are unceasing in their perseverance of LBT-crystallography and MRI. I thank Harald Schwalbe and his lab at Frankfurt University, especially Martin Hähnke and Jens Wöhnert. I have enjoyed collaborating with Bracken King in Bruce Tidor's lab at MIT, and learned a lot about *in silico* work from him. And it has been a fruitful collaboration with Patrick Hogan's lab at Harvard Medical School; he has given me a lot of helpful advice about the Calcineurin project, and Alina Iuga did a lot of the initial cloning and expression and control experiments, and Huiming Li will continue the project. I thank Becky Sommers in the lab of Dan Nocera at MIT for working with me to try and get their old fluorometer up and running. And I thank the lab of JoAnne Stubbe for occasionally letting me borrow chemicals and use their equipment.

As I one day hope to teach Organic Chemistry and/or Biochemistry, it has been a privilege to work as a Teaching Assistant under some great teachers here, including Sarah Tabacco, Tim Swager, Kimberly Berkowski, Dan Kemp, and Stuart Licht.

And I would not be writing a thesis today were it not for some outstanding mentors in chemistry and in other subjects as well. I especially thank my advisors at Kalamazoo College, Jeff Bartz and Greg Slough, along with the rest of the chemistry department there, for encouraging me to major in chemistry and to apply to grad school, and for plenty of helpful advice along the way. I thank Dean Webster and Vicky Johnston Gelling at North Dakota State University for allowing me to do a summer internship there, and to the Webster lab for making me feel welcome while I was there.

I have been in school now for something like 22 or 23 years, and have had many, many excellent teachers, who encouraged me to continue to learn and who also deserve thanks and mention. They include (in roughly chronological order, and with apologies for any misspellings), Mrs. Dairkee, Mrs. Dialwis, Becky Glass, Dawn Hill, Helene Carrasquillo, Donald Washington, Deb Neher, Millard Neiman, Eleanor Balbach, Art Froehle, Kyoko French, Mark Wanvig, Elaine Lindstrom, Carol Adelsman, Richard Anderson, Keith Liuzzi, Gina Lammers, Dick Schwartz, Michele Intermont, Steve Mackey, John Fink, Tom Evans, Rose Bundy, Tanaka-sensei, Tim Tikker, and Paula Romanaux. And a special thank-you to my piano teacher from 1st to 12th grade, Narissa Bach, who instilled in me the adage, “Knowledge for knowledge’s sake”.

I will round out the list with family, friends, and a handful of others who deserve thanks for expending time and energy and helping to shape and nurture me. Thank-you to my good friends Michael David, Pat Krefting, Sam Bunnett, Jim Li, Ben Berg, and Nick Chin. Thank-you to my godparents Sue Anderson and Tony Blodgett, and to Britta and Jamie Blodgett. I also thank Carol Wagner, Wayne and Peggy Krefting, John and Bonnie Rowell, Dick Masur, Nancy and Al Bunnett, Anne Walker and Torin Crissey, the Yokoyama family, Kit and Mitsuhiro and Léo Nagamura, Paul Johnson, Virginia Rickeman, Jim Gertmenian, and Philip Brunelle. (And I can’t forget about folks like Al Bumen, Dean A. Primer, Gene Vector, or Lou Minh Essons!)

I am privileged to have a family with so many wonderful aunts, uncles, and cousins, who have helped humor and inspire me. Thank-you Aunt Jean and Uncle Moffatt, Uncle Floyd and Aunt Becky, Uncle Aleck and Aunt Lynne, Uncle Martin and Aunt Bev, Uncle Gardiner and Aunt Jane, Uncle Kendall and Aunt Gwen, Great-Uncle Mart and Great-Aunt Marge, Great-Uncle Al and Great-Aunt Nell, and Great-Auntie Mabel. Thanks to my cousins Mary Rebecca, Katie Sue, Grier, Rachel, Megan, Martin, Walter, John, Julie, Amanda, Michael, and your families. Thank-you to my parents-in-law, Mark and Debbie Ward, to my sisters-in-law Erica and Meredith Ward, and to my brother-in-law-to-be, José Augustin “Jandin” Mejia-Comacho.

Thank-you, Granddaddy, for your warmth, your encouragement, your love, and your music, all of which have been an inspiration to me. Thank-you, Grandmother, for the kindness and the love that you gave me. Thank-you, Grandma, for the joy and the love that you gave me.

I dedicate this thesis to my mother, Elsie F. Myers Martin, to my father, Raymond J. Martin Jr., to my sister, Celia Grace Martin, and to my wife, Anna Ward Martin.

Mom and Dad, I feel like I am only now beginning to understand the love and energy that you put into raising me. I do know that you have been wonderful parents to me, and for that I thank you. I am deeply grateful to you both for your patience, your humor, your vivacity, your creativity, your wisdom, and your love.

Celia, thank-you for keeping me grounded, and for your tenacity and honesty and love. You are an awesome sister.

Anna, I am both lucky and happy to have you as my wonderful wife. I thank you for your encouragement, for your empathy, for your belief in me, for your trust and commitment, for your humor, and most of all for your love. I couldn’t have done this without you.

Finally, to my daughter, Eliza: you are not even a month old as I write this, and I look forward to being a father to you. May your life be long and happy, and may you be even smarter than your parents.

-Langdon James Martin. 26 April 2008

Table of Contents

Abstract.....	3
Acknowledgments.....	4
Table of Contents.....	7
List of Figures.....	10
List of Tables.....	12
List of Abbreviations.....	14

Chapter 1. Introduction

1-1. General Introduction to Biological Probes.....	19
1-2. General Introduction to Lanthanides.....	19
1-3. The Lanthanide Ions as Biological Probes.....	23
1-4. Introduction to Lanthanide-Binding Tags (LBTs).....	26
1-5. Preliminary, Disulfide Bond-Containing Lanthanide-Binding Tags.....	28
1-6. Development of a Powerful Combinatorial Screen.....	30
1-7. Lanthanide-Binding Tags Evolved Through the Combinatorial Screening Process...33	
1-8. Dissertation Objectives.....	36
Acknowledgements	37
References	37

Chapter 2. Sequence Refinement of Lanthanide-Binding Tags

Introduction	44
Results and Discussion	
2-1. Additional Combinatorial Libraries to Evolve the <u>SE2</u> Sequence.....	45
2-2. Tb ³⁺ -Bound Water Molecules and Relative Luminescence Intensity of LBTs.....	47
2-3. Results of Single Mutations at Specific Positions in the LBT.....	49
2-4. Studies on the Effects of Deleterious Mutations on the LBT Sequence.....	51
Conclusions	52
Experimental	53
Acknowledgements	60
References	61

Chapter 3. Attempts Towards and IR-Emitting Lanthanide-Binding Tag

Introduction	63
Results and Discussion	
3-1. Synthesis and Characterization of <u>LBT-IR1</u>	64
3-2. Synthesis and Characterization of <u>LBT-IR2</u>	66
Conclusions	67
Experimental	68
Acknowledgements	70
References	71

Chapter 4. Double-Lanthanide-Binding Tags

Introduction	72
Results and Discussion	
4-1. Design and Selection of the dLBT Sequences.....	73
4-2. Preparation of dLBT Peptides and a dLBT-Ubiquitin Construct.....	74
4-3. Photophysical Characterization of dLBT Peptides and Proteins.....	77
4-4. Characterization of GPGd <u>SE3</u> -ubiquitin by NMR.....	79
4-5. Characterization of GPGd <u>SE3</u> -ubiquitin by X-Ray Crystallography.....	81
Conclusions	83
Experimental	84
Acknowledgements	93
References	94

Chapter 5. LBT and dLBT Redesign based on dLBT Structural Data

Introduction	96
Results and Discussion	
5-1. Design of <u>SE3</u> Mutants to Address Conformational Questions.....	97
5-2. Synthesis and Photophysical Characterization of <u>SE3</u> Mutants.....	100
5-3. Crystallographic Studies of <u>SE3α</u> , <u>SE3β</u> , and <u>SE3ϵ</u>	102
5-4. Studies of dLBT-Ubiquitin Mutants Containing <u>SE3α</u> and <u>SE3β</u>	104
5-5. Optimization of the dLBT Expression System.....	106
5-6. Modification of the Gly-Pro-Gly Motif in the dLBT.....	107
5-7. Photophysical Characterization of Gly-Ala-Gly Motif-Containing dLBTs.....	110
5-8. dLBTs Based on <u>SE2</u> : Attempts to Generate the Brightest Possible dLBT.....	111
5-9. The Brightest Known dLBT Construct.....	113
Conclusions	113
Experimental	114
Acknowledgements	131
References	132

Chapter 6. Lanthanide-Binding Tags for Magnetic Resonance Imaging

Introduction	134
Results and Discussion	
6-1. Assessment of Existing LBT Sequences for Gd ³⁺ Binding.....	135
6-2. A Split-Pool Library to Optimize LBTs for MR-Imaging Studies.....	135
Conclusions	138
Experimental	139
Acknowledgements	143
References	143

Chapter 7. Using LBT Technology to Study the Protein Calcineurin

Introduction	145
Results and Discussion	
7-1. Preliminary Studies and Mutations to Eliminate Background Luminescence.....	148
7-2. Optimization of Site IV Luminescence Output in Calcineurin Mutants.....	149
7-3. Use of Competitive Ligands to Study the Interactions of Site IV with Sites I – III...	152
7-4. Initial LRET Experiments using the construct <u>CNm4^BA17C-TMR</u>	154
7-5. A <u>CNm4</u> Construct Labeled on the CaM-Binding Domain.....	158
7-6. Generation of a Simpler System, with Only CNB, for Use in LRET Studies.....	159
7-7. Generation of CNB-Binding Domain Peptides <u>CaNAα</u> and <u>P2465</u>	161
7-8. Photophysical Experiments with <u>CNBm7</u>	161
Conclusions	163
Experimental	164
Acknowledgements	179
References	180

Appendix

Select SPECFIT Data Files.....	183
<i>Curriculum Vitae</i>	184

List of Figures

Chapter 1. Introduction

Figure 1-1.	The Lanthanide metal series.....	20
Figure 1-2.	Emission spectrum of Tb ³⁺	21
Figure 1-3.	Excitation of Tb ³⁺ luminescence.....	22
Figure 1-4.	The security measures on euro banknotes.....	23
Figure 1-5.	Cartoon representation of X-ray crystallography.....	24
Figure 1-6.	Lanthanide ions promote orientation in a magnetic field.....	25
Figure 1-7.	Graphical representation of an LBT.....	27
Figure 1-8.	Comparison of the size of an LBT to GFP.....	28
Figure 1-9.	Expression of an LBT-protein construct is straightforward.....	28
Figure 1-10.	Generation of a split-and-pool combinatorial library.....	30
Figure 1-11.	The combinatorial libraries to generate tighter and brighter LBTs.....	32
Figure 1-12.	Results from Library 1.....	34
Figure 1-13.	Results from Library 2.....	34
Figure 1-14.	Results from Library 3.....	35
Figure 1-15.	Results from Library 4.....	36

Chapter 2. Sequence Refinement of Lanthanide-Binding Tags

Figure 2-1.	The Crystal Structure of <u>SE2</u> Bound to Tb ³⁺	44
Figure 2-2.	Results from Library 5.....	45
Figure 2-3.	Results from Library 6.....	46
Figure 2-4.	Results from Library 7.....	47
Figure 2-5.	Combination of Results from Libraries 5 and 6 to Optimize the LBT.....	47

Chapter 3. Attempts Towards and IR-Emitting Lanthanide-Binding Tag

Figure 3-1.	Lanthanide luminescence maxima range from the visible to the near-IR.....	63
Figure 3-2.	The IR-emitting phthalazine moiety.....	64
Figure 3-3.	Synthesis of <u>LBT-IR1</u>	65
Figure 3-4.	<u>LBT-IR1</u> sensitizes Tb ³⁺ and Eu ³⁺	66
Figure 3-5.	Normalized excitation scans of LBT-Tb ³⁺ complexes.....	67

Chapter 4. Double-Lanthanide-Binding Tags

Figure 4-1.	The design strategy to convert the single-LBT into the double-LBT.....	73
Figure 4-2.	Expression and purification strategy to obtain pure <u>GdSE3</u> peptide.....	75
Figure 4-3.	Expression and purification strategy to obtain pure <u>GPGdSE3</u> -ubiquitin.....	76
Figure 4-4.	Purification and gel-visualization of the dLBT constructs.....	77
Figure 4-5.	NMR data showing that the dLBT does not alter the structure of ubiquitin.....	80
Figure 4-6.	RDCs in single-LBT- or double-LBT-containing ubiquitin.....	80
Figure 4-7.	Crystallization of <u>GPGdSE3</u> -Ubiquitin.....	81
Figure 4-8.	The crystal structure of <u>GPGdSE3</u> -Ubiquitin.....	82
Figure 4-9.	Structure of the dLBT portion of the crystal.....	83

Chapter 5. LBT and dLBT Redesign based on dLBT Structural Data

Figure 5-1.	Structure of the dLBT portion of the crystal.....	96
Figure 5-2.	Comparison of Ramachandran space of four residues in the <u>SE2</u> and <u>GPGdSE3</u> crystals.....	97
Figure 5-3.	Comparison of the calculated folding energies of different residues at positions 4 and 6.....	98
Figure 5-4.	Differences in folding energies of all hypothetical double mutants.....	99
Figure 5-5.	Crystal Structure of <u>SE3β</u>	103
Figure 5-6.	System for generating <u>GPGdSE3</u> peptide for crystallization studies.....	106
Figure 5-7.	Cleavage of ubiquitin- <u>GPGdSE3</u> by mTEV protease was not facile.....	107
Figure 5-8.	Plasmids for generating <u>GAGdSE3</u> as a peptide and a ubiquitin tag.....	108
Figure 5-9.	Cleavage of H ₈ -ubiquitin- <u>ENLYFQGAGdSE3</u> by mTEV protease is extremely facile under a variety of conditions.....	109
Figure 5-10.	Purification of <u>GAGdSE3</u> -ubiquitin.....	110
Figure 5-11.	Purification of <u>GAGdSE2</u> -ubiquitin.....	112

Chapter 6. Lanthanide-Binding Tags for Magnetic Resonance Imaging

Figure 6-1.	Images of MRI contrast with the LBT <u>mSE3</u>	134
Figure 6-2.	Design of the linker region for the MRI-LBT library.....	136
Figure 6-3.	The synthesis and screening process for the “LanGdoN” combinatorial peptide libraries.....	137
Figure 6-4.	Library LanGdoN1.....	138

Chapter 7. Using LBT Technology to Study the Protein Calcineurin

Figure 7-1.	When a specific site in a calcium-binding protein is modified to be LBT-like, it may be selectively labeled with Ln ³⁺	145
Figure 7-2.	Crystal structure of calcineurin.....	146
Figure 7-3.	The effects of [Ca ²⁺] and CaM on the enzymatic activity of calcineurin.....	147
Figure 7-4.	Sequence of CNB used in this study.....	148
Figure 7-5.	Abilities of various LBTs and CN-mutants to sensitize Tb ³⁺	150
Figure 7-6.	Detail of calcineurin-B, metal-binding Site IV.....	152
Figure 7-7.	Addition of metal chelator to <u>CNm7</u> and Tb ³⁺	153
Figure 7-8.	Addition of metal chelator to <u>CNm7</u> and Tb ³⁺ with buffered [Ca ²⁺] _{free}	154
Figure 7-9.	Plans for three possible calcineurin LRET experiments.....	156
Figure 7-10.	Detail of the calcineurin structure, showing ^B Ala17 and ^A Cys153.....	156
Figure 7-11.	Gated luminescence scans of TMR-labeled calcineurin mutants.....	157
Figure 7-12.	Luminescence decay of <u>CNm4-^BA17C-TMR</u> is independent of [Ca ²⁺].....	158
Figure 7-13.	The plasmids for expressing <u>CNBm7</u> and <u>CNBm7-A17C</u>	159
Figure 7-14.	Generation and purification of <u>CNBm7-A17C-TMR</u>	160
Figure 7-15.	Gel of the purification of <u>CNBm7-A17C-TMR</u>	160
Figure 7-16.	Concentrations of [Tb ³⁺] and [Ca ²⁺] have no effect on the normalized emission spectrum of <u>CNBm7-A17C-TMR</u>	162
Figure 7-17.	The presence or absence of <u>CaNAdα</u> or <u>P2465</u> does not affect the Tb ³⁺ -to-TMR LRET of <u>CNBm7-A17C-TMR</u>	163

List of Tables

Chapter 1. Introduction

Table 1-1. Comparison of the Properties of Ca ²⁺ and Tb ³⁺	20
Table 1-2. Rationally-Designed LBT Sequences from Calcium-Binding Proteins.....	29

Chapter 2. Sequence Refinement of Lanthanide-Binding Tags

Table 2-1. Photophysical Data of Select Single-LBTs.....	49
Table 2-2. Mutational Analyses of <u>SE2</u> Amino Acid Residues.....	50
Table 2-3. Photophysical Data of LBT Mutants with Specific Deleterious Mutations.....	52
Table 2-4. Winning Peptides from the “TEN_DAYS” Library.....	58

Chapter 3. Attempts Towards and IR-Emitting Lanthanide-Binding Tag

Table 3-1. Sequence Design of Potential IR-Emitting-Ln ³⁺ -Sensitizing LBTs.....	64
---	----

Chapter 4. Double-Lanthanide-Binding Tags

Table 4-1. Tb ³⁺ -Binding Affinity and Luminescence Intensity of Select Single-LBTs.....	74
Table 4-2. Sequences of Double-LBTs and the Progenitor Single-LBT <u>SE3</u>	74
Table 4-3. Initial Double-LBT Peptide Photophysical Experiments.....	75
Table 4-4. Summary of Double-LBT Photophysical Data.....	78
Table 4-5. The GPG Motif and the Ubiquitin Protein Have No Inherent Effect on LBT Luminescence.....	79

Chapter 5. LBT and dLBT Redesign based on dLBT Structural Data

Table 5-1. Sequences of Computationally Designed <u>SE3</u> Mutants.....	100
Table 5-2. Photophysical Data from Computationally Designed <u>SE3</u> Mutants.....	101
Table 5-3. Competitive Titrations with <u>SE2</u> , <u>SE3β</u> and <u>SE3ε</u> , Between Tb ³⁺ and Various Lanthanide Ions.....	102
Table 5-4. Sequences of <u>SE3α</u> - and <u>SE3β</u> -Based dLBT-Ubiquitin Constructs.....	104
Table 5-5. Summary of Photophysical Data for <u>SE3α</u> - and <u>SE3β</u> -Containing dLBT-Ubiquitin Constructs.....	105
Table 5-6. Photophysical Characteristics of GAG Motif-Containing dLBT-Ubiquitin Constructs.....	110
Table 5-7. Sequences of the <u>SE2</u> -Based dLBTs.....	111
Table 5-8. Photophysical Characterization of Double-LBTs Based on <u>SE2</u>	112
Table 5-9. Photophysical Characterization of GPG <u>SE3</u> -NhPMM.....	113

Chapter 6. Lanthanide-Binding Tags for Magnetic Resonance Imaging

Table 6-1. Summary of LBT-Gd ³⁺ Affinity for Single-LBTs used in MRI Experiments.....	135
Table 6-2. Summary of GPG <u>SE3</u> -Ubiquitin <i>Log β</i> Values for Gd ³⁺ and Tb ³⁺	135

Chapter 7. Using LBT Technology to Study the Protein Calcineurin

Table 7-1. Alignment of the EF-Hand Motifs of Calcineurin-B with <u>SE3</u>	149
Table 7-2. CNB-Site IV Sequences of LBT-Like Calcineurin Mutants.....	150
Table 7-3. Luminescence Intensity and Bound Water Molecules for CN Mutants 4 – 7.....	151
Table 7-4. Metal-Chelation Buffers to Make a Variety of Free $[Ca^{2+}]$ Concentrations.....	154
Table 7-5. CNB-Binding Domain Peptides.....	161
Table 7-6. Gated Luminescence Scans and τ_{DA} Determination with 2 μM <u>CNm4-^BA17C-TMR</u>	171
Table 7-7. Gated Luminescence Scans and τ_{DA} Determination with 1 μM <u>CNBm7-A17C-TMR</u>	178
Table 7-8. Gated Luminescence Scans and τ_{DA} Determination with 1 μM <u>CNBm7-A17C-TMR</u> in the Presence of 5.82 μM <u>CaNAα</u> Peptide.....	179
Table 7-9. Gated Luminescence Scans and τ_{DA} Determination with 1 μM <u>CNBm7-A17C-TMR</u> in the Presence of 5.82 μM <u>P2465</u> Peptide.....	179

List of Abbreviations

Standard one- and three-letter codes are used for the amino acids.

One-letter code	Three-letter code	Amino Acid
A	Ala	Alanine
C	Cys	Cysteine
D	Asp	Aspartic acid (Aspartate)
E	Glu	Glutamic acid (Glutamate)
F	Phe	Phenylalanine
G	Gly	Glycine
H	His	Histidine
I	Ile	Isoleucine
K	Lys	Lysine
L	Leu	Leucine
M	Met	Methionine
N	Asn	Asparagine
P	Pro	Proline
Q	Gln	Glutamine
R	Arg	Arginine
S	Ser	Serine
T	Thr	Threonine
V	Val	Valine
W	Trp	Tryptophan
Y	Tyr	Tyrosine

Standard one-letter codes are used for the nucleotides.

One-letter code	Nucleotide
A	Adenosine
C	Cytidine
G	Guanosine
T	Thymidine

Other abbreviations are as follows.

<i>A'</i>	A lanthanide-specific constant used to determine <i>q</i>
Ac	Acetyl
Ac ₂ O	Acetic anhydride
AI	Auto-Inhibitory (domain)
ANP	3-amino-3-(2-nitrophenyl)propionic acid
<i>apo</i>	Unbound to metal-ion
β	Binding constant; $K_D = 10^{-\log \beta}$
β Ala	Beta-alanine (amino acid residue)
BME, β ME	Beta-mercaptoethanol; HOCH ₂ CH ₂ SH
BSA	Bovine serum albumin (protein)
C-terminus	The carboxy-terminal end of a peptide
calcd.	Calculated
CaM	The protein Calmodulin
CIP	Calf Intestinal alkaline Phosphatase
CN	The protein Calcineurin
CNA	Calcineurin subunit A (the larger, catalytic subunit)
CNB	Calcineurin subunit B (the smaller, Ca ²⁺ -binding, regulatory subunit)
CNm#	Calcineurin-B mutant (# = 1 - 7). This notation indicates that both subunits are present
CNBm7	Calcineurin-B mutant 7. This notation indicates that only the B-subunit is present
D ₂ O	Deuterated water; deuterium-oxide
DAPase	Diamino-peptidase (protease)
dATP	deoxyAdenosine TriPhosphate
DCM	Dichloromethane; CH ₂ Cl ₂
dCTP	deoxyCytidine TriPhosphate
<i>de novo</i>	Latin: "from the new"
dGTP	deoxyGuanosine TriPhosphate
DHB	Dihydroxybenzoic acid
DIC	<i>N,N'</i> -Diisopropylcarbodiimide
DIPEA	<i>N,N</i> -Diisopropylethyl amine; Hünig's base
dLBT	double-Lanthanide-Binding Tag
DMAP	4-(Dimethylamino)pyridine
DMF	<i>N,N</i> -Dimethylformamide; (CH ₃) ₂ NCHO
DMSO	Dimethylsulfoxide; (CH ₃) ₂ SO
DNA	Deoxyribonucleic acid
DTT	Dithiothreitol (Cleland's reagent); HSCH ₂ CH(OH)CH(OH)CH ₂ SH
dTTP, TTP	(deoxy)Thymidine TriPhosphate

<i>E</i>	The percentage of energy transferred
ϵ	Molar extinction coefficient (at a certain wavelength)
<i>E. coli</i>	<i>Escherichia coli</i> (bacteria)
EDT	1,2-Ethanedithiol; HSCH ₂ CH ₂ SH
EDTA	Ethylenediaminetetraacetic acid
EF-hand	A calcium-binding peptide consensus sequence found in native proteins
EGTA	Ethylene glycol-bis-(2-aminoethylether)- <i>N,N,N',N'</i> -tetraacetic acid
eLB	Enhanced LB bacterial growth media, based on Autoinduction buffers
eq.	Equation
equiv.	Equivalent
<i>et al.</i>	Latin: "and others"
ESI MS, ESI-TOF MS	ElectroSpray Ionization (Time-Of-Flight) Mass Spectroscopy
Fmoc	Fluoren-9-ylmethoxycarbonyl
FRET	Fluorescence Resonance Energy Transfer
GFP	Green Fluorescent Protein
GST	Glutathione- <i>S</i> -Transferase (protein)
η	Refractive index
HATU	O-(7-azabenzotriazole-1-yl)-1,1,3,3-tetramethyluronium hexafluorophosphate
HBTU	2-(1 <i>H</i> -benzotriazole-1-yl)-1,1,3,3-tetramethyluronium hexafluorophosphate
HEDTA	<i>N</i> -(hydroxyethyl)-ethylenediaminetriacetic acid
HEPES	<i>N</i> -(2-hydroxyethyl)piperazine- <i>N'</i> -ethanesulfonic acid
His ₆ , H ₆ , His ₆ -tag, His-tag	Protein purification tag comprised of six consecutive histidine residues
HMBA	4-hydroxymethylbenzoic acid
HOBt	<i>N</i> -hydroxybenzotriazole
HPLC	High-Performance (or -Pressure) Liquid Chromatography
<i>I(t)</i>	Luminescence intensity at time (<i>t</i>)
IMAC	Immobilized Metal-ion-Affinity Chromatography; purification using Ni-NTA resin and a His-tag
<i>In vitro</i>	Performed outside the context of the cell; Latin: "in glass"
<i>In vivo</i>	Performed in the context of living cells; Latin: "in life"
IPTG	Isopropyl- β -D-thiogalactopyranoside
IR	Infrared
<i>J</i>	Spectral overlap term
<i>J</i> -coupling	In NMR, indirect dipole-dipole coupling
κ^2	The orientation factor, taken as $2/3$
kDa	kiloDaltons

K_D	Dissociation constant
K_M	Michaelis constant for enzyme-substrate binding
λ	Wavelength
LB	Lysogeny Broth, a nutrient-rich bacterial growth medium
LBT	Lanthanide-Binding Tag
λ_{em}	Emission wavelength
λ_{ex}	Excitation wavelength
Ln	Any lanthanide metal
LRET	Luminescence Resonance Energy Transfer
MALDI, MALDI-TOF MS	Matrix-Assisted Laser-Desorption-Ionization (Time-Of-Flight) Mass Spectroscopy
MBP	Maltose-Binding Protein
MeCN	Acetonitrile; CH ₃ CN
MES	2-morpholinoethanesulfonic acid
MESNA	2-mercaptoethanesulfonic acid
min	Minutes
Mmt	Monomethoxytrityl
MOPS	3-(<i>N</i> -morpholino)propanesulfonic acid
MR	(Nuclear) Magnetic Resonance
MRI	(Nuclear) Magnetic Resonance Imaging
MS	Mass Spectroscopy
mTEV	mutant Tobacco Etch Virus protease
N-terminus	The amino-terminal end of a peptide
NaCl	Sodium chloride
NaOAc	Sodium acetate
Ni-NTA	Nickel-NTA agarose resin
NMP	<i>N</i> -MethylPyrrolidinone (1-methyl-2-pyrrolidinone)
NMR	Nuclear Magnetic Resonance
NOE	Nuclear Overhauser Effect
NTA	Nitrilo Triacetic acid
OAc	Acetate
OD	Optical Density
PAGE	PolyAcrylamide Gel Electrophoresis
PAL	Peptide Amide Linker
PBS	Phosphate Buffered Saline solution
PCR	Polymerase Chain Reaction
PEG	Polyethyleneglycol
Phe- <i>p</i> NO ₂	para-nitrophenylalanine residue
pip	Piperidine
PS	Polystyrene
PyBOP	Benzotriazole-1-yl-oxy-tris-pyrrolidino-phosphonium hexafluorophosphate

Q_D	Quantum yield of the donor
q	Number of lanthanide-ion-coordinated water molecules
R	Distance
R_0	The Förster distance
RCF	Relative Centrifugal Force
RDC	Residual Dipolar Coupling values
RET	Resonance Energy Transfer
RMSD	Root Mean Square Deviation
RNA	Ribonucleic acid
RP-HPLC	Reverse-Phase HPLC
RPM	Rotations per minute
SAD	Single-wavelength Anomalous Diffraction
SDS-PAGE	Sodium Dodecyl-Sulfate PolyAcrylamide Gel Electrophoresis
sLBT	single-Lanthanide-Binding Tag
SPPS	Solid Phase Peptide Synthesis
std. dev.	Standard deviation
τ	Lifetime
τ_D	Lifetime of the donor
τ_{DA}	Lifetime (of the donor) in the presence of the acceptor
$t_{1/2}$	Half-life
TBS	Tris-buffered saline
<i>t</i> Bu	<i>tert</i> -butyl
TCEP	<i>tris</i> -(2-carboxyethyl)phosphine P(CH ₂ CH ₂ CO ₂ H) ₃
TEV	Tobacco Etch Virus
TFA	Trifluoroacetic acid; CF ₃ CO ₂ H
TIS	Triisopropyl silane; (CH ₃) ₃ SiH
TMG	Tetramethylguanidine
TMR	Tetramethylrhodamine
TNBS	Trinitrobenzene sulfonic acid
Tris	Tris(hydroxymethyl)aminomethane
Trt	Trityl
Ubiqu	Ubiquitin (protein)
UV	Ultraviolet
UV-Vis	Ultraviolet-visible
<i>vide infra</i>	Latin: "see below"
<i>vide supra</i>	Latin: "see above"
V_{max}	Maximum (enzymatic) turnover velocity
Xaa	Used to denote any amino acid

Chapter 1

Introduction

Portions of this chapter have been published in *QSAR & Combinatorial Science*¹ and in *Journal of the American Chemical Society*² as noted in the text. Copyright © 2005, WILEY-VCH Verlag GmbH & Co and © 2007, American Chemical Society, respectively.

1-1. General Introduction to Biological Probes¹

With the sequencing of the human genome, it has become widely accepted that dynamic protein/protein interactions are an essential component of biological complexity. Chemical tools to detect and probe proteins and biomolecular interactions will provide a deeper understanding of the nature, regulation and function of protein interactions, which are central to cellular existence. Many of the currently available protein tags permit the incorporation only of a single functionality, such as the Green Fluorescent Proteins (GFPs) and GFP variants for fluorescence,^{3,4} selenomethionine to provide a heavy atom for X-ray crystallography,^{5,6} and paramagnetic metal ions for NMR spectroscopy.⁷ Of great use would be a versatile protein tag, which should display diverse physical and spectroscopic properties, enabling researchers to monitor proteins of interest with different and potentially complementary biophysical techniques.

Lanthanide ions are endowed with an extensive list of physical properties that are amenable to a variety of spectroscopic and crystallographic studies (*vide infra*). This, in tandem with the absence of lanthanides from living systems, makes these ions ideal handles for the study of proteins' structure and interactions. To be useful, the lanthanide ion (or ions) must be site-specifically attached to the target protein. This thesis will discuss the development of one such tool: the Lanthanide-Binding Tag.

1-2. General Introduction to Lanthanides

The lanthanide metals, elements 57 – 71, are shown in Figure 1-1. The lanthanide moniker “Rare Earths” comes not so much from the natural abundance of these elements (which ranges from 2 – 4 orders of magnitude more common than gold, for example)⁸, but from the initial difficulties encountered in purification.⁹ (It apparently required 15,000 fractional crystallizations to isolate lutetium!)¹⁰ Many are named after locations in Sweden, where these metals were originally isolated: the mining village of Ytterby is eponymous for three lanthanides

(ytterbium, terbium, and erbium) and yttrium—a distinction no other person or place can claim.¹⁰ Terbium is central to this thesis and to the Lanthanide-Binding Tag technology.

57 138.91	58 140.12	59 140.91	60 144.24	61 (145)	62 150.36	63 151.96	64 157.25	65 158.93	66 162.50	67 164.93	68 167.26	69 168.93	70 173.04	71 174.97
La	Ce	Pr	Nd	Pm	Sm	Eu	Gd	Tb	Dy	Ho	Er	Tm	Yb	Lu
LANTHANUM	CERIUM	PRASEODYMIUM	NEODYMIUM	PROMETHIUM	SAMARIUM	EUROPIUM	GADOLINIUM	TERBIUM	DYSPROSIUM	HOLMIUM	ERBIUM	THULIUM	YTTTERBIUM	LUTETIUM

Figure 1-1. The Lanthanide metal series.¹¹

Many of the interesting and useful photophysical properties of lanthanide ions are due to the electrons in the $4f$ orbitals. The $4f$ electrons are located within the outermost orbitals (the $5s^25p^6$), and are shielded from the surroundings, and making the luminescent $f-f$ transitions nearly ligand-independent.¹² In general, lanthanides are most stable as Ln^{3+} ions, in the $[\text{Xe}]4f^{N-57}$ configuration, where N is the atomic number of the lanthanide. As aqueous ions, all Ln^{3+} ions are remarkable similar to Ca^{2+} , with only a slight difference in atomic radius, as shown in Table 1-1, although the lanthanides are absent from normal living systems. Both are very “hard” ions and therefore oxophilic, with coordination spheres that are determined by sterics, and are capable of rapid ligand-exchange.^{12,13}

Table 1-1. Comparison of the Properties of Ca^{2+} and Tb^{3+} (the lanthanide most important to this thesis)

<i>Atom</i>	<i>Most stable oxidation state</i>	<i>Ionic radius^a</i>	<i>Preferred coordination</i>	<i>Ligand preference</i>
Calcium (Ca)	+2	1.18 Å	8-9 ligands, spherical	O > N > S
Terbium (Tb)	+3	1.10 Å ^b	8-9 ligands, spherical	O > N > S

^a Ionic radii shown are for the nine-coordinate complexes.¹⁴

^b Lanthanide(III) nine-coordinate ionic radii range from 1.03 Å (for Lu^{3+}) to 1.22 Å (for La^{3+}).^{13,14}

Many lanthanide ions, including Tb^{3+} , exhibit distinct luminescence emission spectra, due to $f-f$ electronic transitions. Figure 1-2 shows the (false-color) emission spectrum for Tb^{3+} , along with the $^{2S+1}L_J$ transitions that give rise to each peak. Because $f-f$ electric dipole transitions are forbidden by parity rules (‘Laporte-forbidden’), it is much more facile to excite Ln^{3+} ions via an organic fluorophore.^{12,15} This is accomplished as diagrammed in Figure 1-3 (based on Ref. 12). First, an organic fluorophore—the side-chain indole of tryptophan is used throughout this thesis—is excited (A) by irradiation from a source such as a fluorometer, making an excited singlet. This singlet may give up a photon and fluoresce (B), or it may undergo intersystem-crossing and become an excited triplet. If the triplet gives up a photon, the process

is known as phosphorescence (C), but it may instead undergo another (non-radiative) exchange of energy with a nearby Tb^{3+} ion. The energy of now-excited Tb^{3+} may be lost by a non-radiative process (*vide infra*), or the Tb^{3+} may luminesce (D), giving rise to the spectrum in Figure 1-2. It should be noted that this process is formally known as “luminescence”, and is referred to as such throughout this text, because the ground state of Tb^{3+} is not a singlet (having six unpaired *f* electrons) and therefore is neither fluorescence nor phosphorescence.

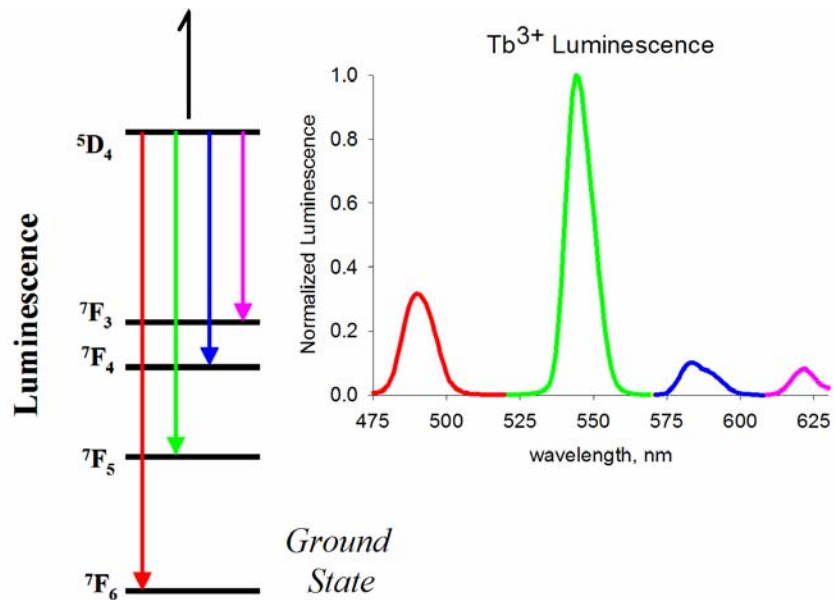


Figure 1-2. Emission spectrum of Tb^{3+} , shown in false-color to highlight the origins of the peaks.

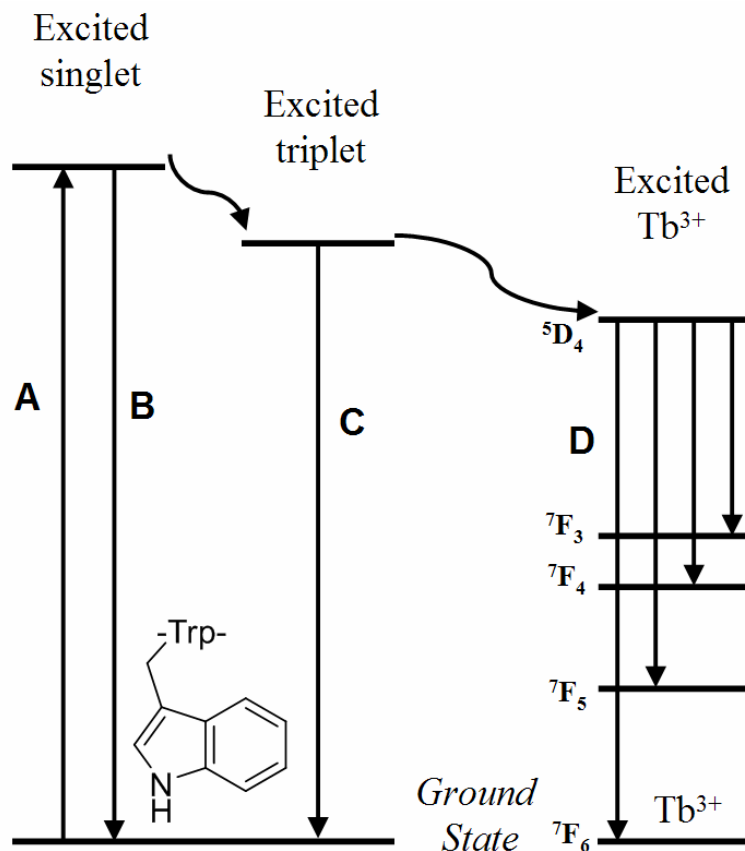


Figure 1-3. Excitation of Tb³⁺ luminescence. **A.** An organic fluorophore, such as the indole ring of tryptophan, is excited by UV light. **B.** The excited state singlet may fluoresce. **C.** If the excited singlet undergoes intersystem crossing, the excited triplet state may phosphoresce. **D.** Or, the energy may be transferred to the nearby Tb³⁺, which can luminesce. (Based on Ref. 12.)

Lanthanides and lanthanide luminescence have found a variety of uses in both biological and non-biological systems.¹⁶ Perhaps one of the most interesting (and appropriate) “real-world” applications is in the security measures of bank-notes. Luminescent europium chelates are believed to be responsible for the red color that shows up on the Euro paper currency under ultraviolet light (Figure 1-4);¹⁷ it need not be pointed out that the metal and the currency share a common eponym!

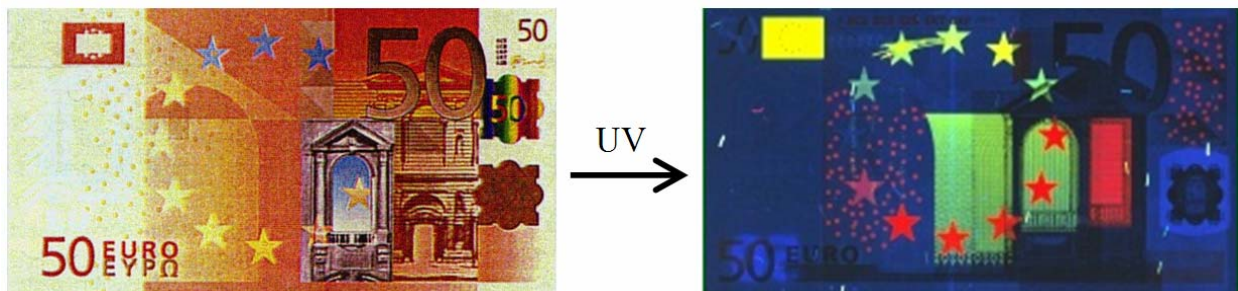


Figure 1-4. The security measures on euro banknotes are believed to contain europium chelates that emit red luminescence under ultraviolet light.

1-3. The Lanthanide Ions as Biological Probes^{1,2}

Complementing the unique emission profile, perhaps the most useful property of Tb^{3+} luminescence is that it is extremely long-lived, with a lifetime in the milliseconds; this, too, is a result of the parity-forbidden $f-f$ transitions. Eu^{3+} , while it cannot be sensitized by any canonical amino acid, also has a millisecond-length lifetime, making these lanthanides popular for use in time-resolved luminescence measurements.¹⁸⁻²⁰ Other lanthanides luminesce as well, although most of these have slightly shorter (microsecond) lifetimes.¹⁶ Some, such as Nd^{3+} and Yb^{3+} , emit in the near-IR, and are growing in interest for applications such as tissue-imaging.^{19,21,22}

The broad availability of spectroscopic equipment has made luminescence a popular choice for studying biological processes. The millisecond lifetimes of Tb^{3+} and Eu^{3+} luminescence, being significantly longer than the nanosecond lifetimes of most organic fluorophores, provide greatly increased sensitivity by elimination of background fluorescence. This, in turn, has generated considerable interest for the use of these ions in biological and biochemical assays,^{15,23-27} and in resonance energy transfer experiments.²⁸⁻³⁰ With regards to lanthanide luminescence it is important to note, as was alluded to previously, that excited lanthanide ions may also undergo nonradiative decay. When a molecule of water is present in the inner coordination sphere of Tb^{3+} or Eu^{3+} , excited-state energy is rapidly transferred into vibrational energy of the O-H bond.³¹ Lanthanide complexes used for bioluminescent assays are therefore almost invariably made of ligands of sufficient number or bulk such that water molecules are prevented from directly coordinating the metal ion.

Although this thesis is concerned exclusively with the study of proteins, it should be noted that non-protein analytes are also amenable to study via lanthanide-based sensors: recent studies were published utilizing terbium luminescence in the detection of sugars³² and

phosphopeptides.³³ In addition, there have been preliminary explorations into the use of lanthanides as probes of protein redox processes.³⁴

Lanthanide ions have also greatly assisted protein structure determination both in the solid and solution state. This versatility is a result of various physical properties. For example, the abundant non-valence electrons interact strongly with X-rays. In protein X-ray crystallography, a series of crystal diffraction patterns are collected, integrated, and scaled. These contain information about the amplitude of the X-rays, but the phase information is needed to solve the structure *via* Fourier Transformation (Figure 1-5). The strong scattering power and anomalous scattering of lanthanides can be used to phase X-ray diffraction data in macromolecular crystallography;³⁵⁻³⁷ the anomalous signal is calculated to be roughly four times as powerful as that from a selenomethionine.³⁸

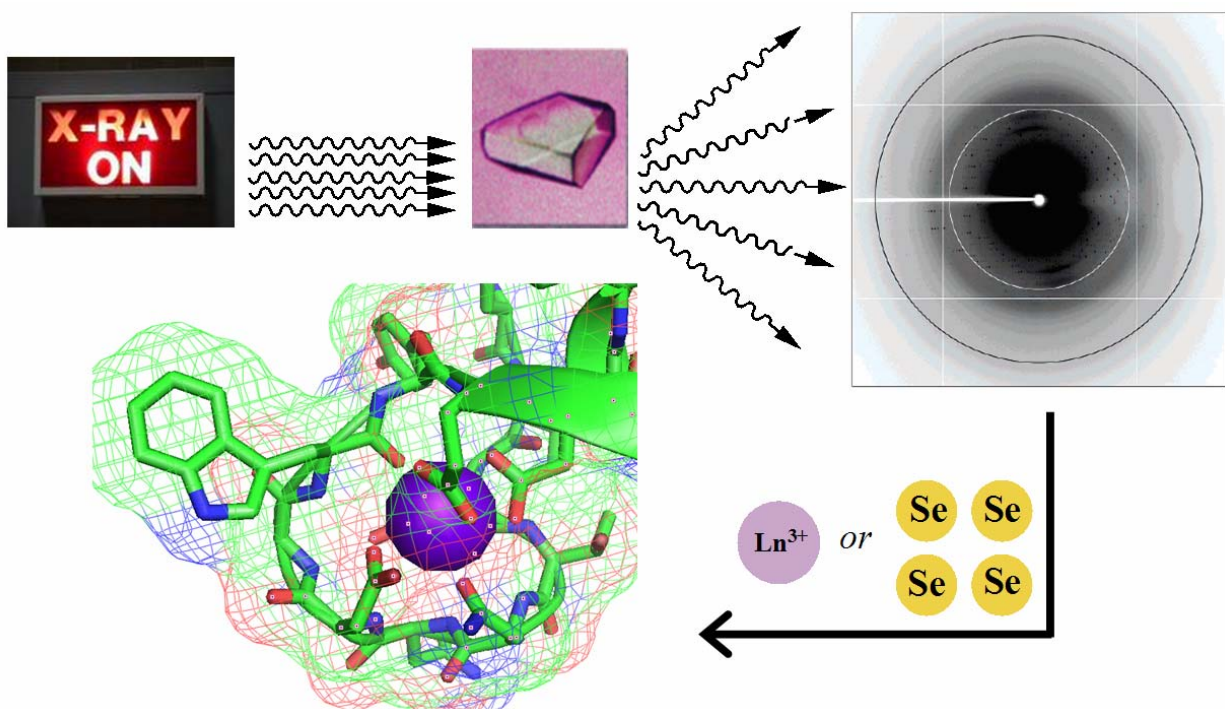


Figure 1-5. Cartoon representation of X-ray crystallography. A protein crystal is bombarded with X-rays, yielding diffraction patterns that are integrated and scaled. In order to solve the phase information, the presence of an ordered, anomalously scattering heavy atom such as a lanthanide ion or selenium can be used. One lanthanide ion has the phasing power of about four selenium atoms.

Furthermore, all lanthanide ions, with the exception of La^{3+} and Lu^{3+} , have one or more unpaired electrons in f orbitals. And because these paramagnetic ions have an anisotropic susceptibility tensor, ordered Ln^{3+} ions can be used in NMR spectroscopy to partially orient proteins in the magnetic field, represented in Figure 1-6.³⁹⁻⁴² This leads to magnetic dipolar

interactions between nearby spins that are otherwise averaged to zero in solution due to molecular tumbling. These so-called residual dipolar couplings (RDCs) can be observed and have proven to yield useful long-range restraints for structure determination, and in fact the measurement and use of RDCs has become an essential tool for structure determination of proteins.⁴³⁻⁴⁵ Unlike NOEs and scalar 3J -couplings that report on short-range distances ($< 5 \text{ \AA}$) and dihedral angles, RDCs deliver valuable long-range orientational information. In addition, paramagnetic pseudocontact shifts can be used for the determination of the binding geometry of small ligands to protein receptors.⁴⁶

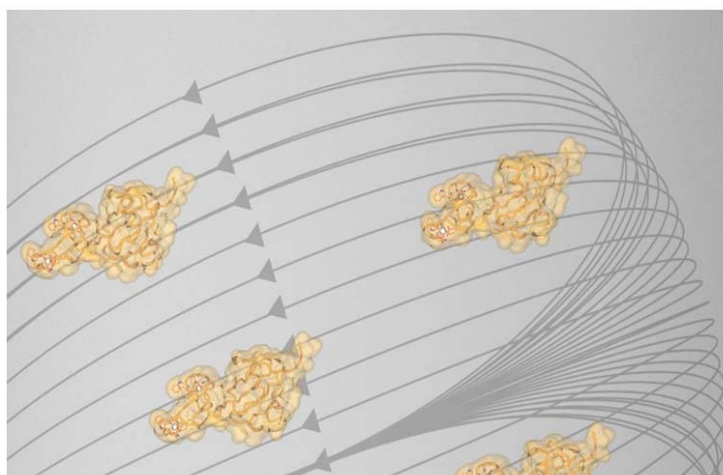


Figure 1-6. When biomolecules such as proteins contain one or more lanthanide ions, the ions' anisotropic magnetic susceptibility promote orientation in a magnetic field. This enables long-range coupling interactions to be observed. (This figure was designed and created by Nicholas Silvaggi.)

Finally, Gd^{3+} is unique among the trivalent lanthanide ions in that, with a $[\text{Xe}]4f^7$ configuration, it contains seven unpaired electrons. It therefore has a strong paramagnetic relaxation enhancement effect as well as a relaxation time that is significantly longer than other lanthanides.³⁹ This, coupled with the aforementioned rapid ligand exchange, makes it a useful metal for chelates used in Magnetic Resonance Imaging (MRI).^{39,47,48} It is noteworthy, though, that in the case of MRI it is necessary to have a molecule of water in the inner coordination sphere of the Gd^{3+} (where the relaxation enhancement takes place), and it is beneficial to have two or more. Therefore, protein tags that work well for MRI will likely be suboptimal for luminescence-based applications and *vice versa*. Recently, other lanthanides have begun to attract interest for MRI applications as well.⁴⁸

1-4. Introduction to Lanthanide-Binding Tags (LBTs)^{1,2}

The wide range of physical information that can be obtained from the localization of different lanthanide ions, coupled with the absence of the rare earths from natural biological systems, has fostered significant interest in engineering tools to incorporate lanthanides into biomolecules. Various methods for the incorporation of lanthanide ions into proteins have been explored. In specialized applications, the similarity of trivalent lanthanides (Ln^{3+}) to divalent calcium (Ca^{2+}) in ionic radius and oxophilicity enables direct incorporation into calcium-binding proteins.^{35,40,42,49} The majority of proteins, however, lack native calcium-binding sites, and therefore this technique is clearly limited in scope. Another approach has been to incorporate lanthanide-chelating prosthetic groups as either the side-chain of a non-natural amino acid,⁵⁰ or via the chemical modification of a uniquely reactive amino acid residue.^{36,51,52} These chelates can bind the lanthanide extremely tightly, and may incorporate a sensitizer, but this method requires considerable manipulation and significant case-by-case optimization.

A more viable tool for proteomics would be a tag that is amenable to incorporation into proteins at the DNA level via standard molecular biology techniques, thereby avoiding cumbersome, and often inefficient, post-translational chemical modifications. Indeed, despite the relatively large size (ca. 240 residues), the great success of the GFPs is in no small part due to the convenient methods for engineering GFP-fusion proteins.⁵³ Short peptide sequences that comprise encoded amino acids and selectively bind lanthanide ions would be advantageous probes for proteomic analysis. These sequences would enable the introduction of the physical properties of lanthanide ions while retaining the ease of protein tagging via genetic manipulation. An early example of this, by Szabo and coworkers, involved a calcium-binding protein in which one of the calcium-binding loops was modified to show greater preference for terbium.⁵⁴ Kaback and coworkers went further and expressed a similar loop on a membrane protein so as to be able to conduct terbium-based Resonance Energy Transfer experiments.⁵⁵

Utilizing information about calcium-binding loops,^{56,57} previous members of the Imperiali lab conducted design and engineering studies which resulted in the development of short polypeptides that bind tightly and selectively to lanthanide ions, specifically terbium.^{58,59} These peptides, dubbed “Lanthanide Binding Tags” (LBTs), show low-nM affinities and are selective for lanthanides over other common metal ions.^{1,58-60} An LBT is depicted in Figure 1-7.

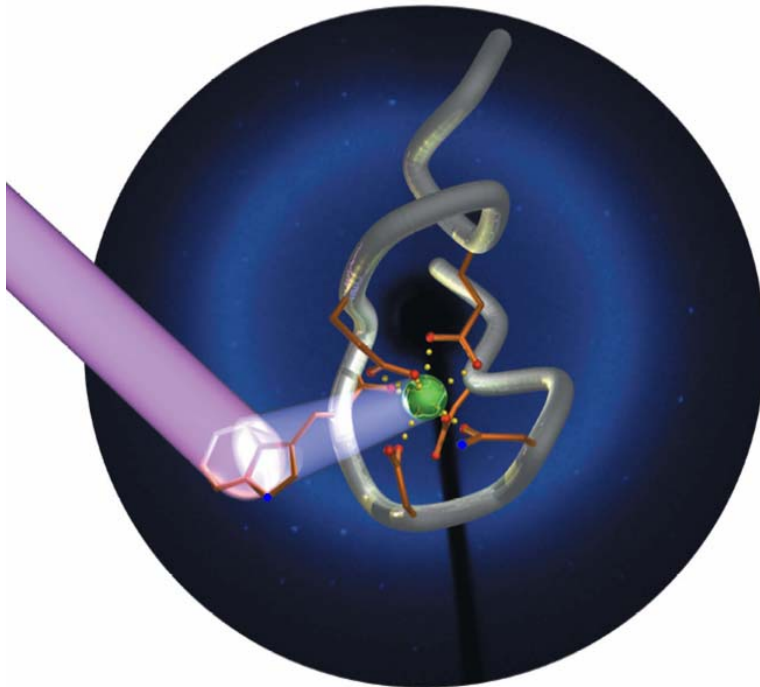


Figure 1-7. Graphical Representation of an LBT, based on the crystal structure of SE2.⁶⁰ (The sequence of SE2 is YIDTNNDGWYEGDELLA; see also section 1-6, *vide infra*). The peptide backbone is shown in grey, and the chelating side-chains and back-bone carbonyl are shown in orange, with oxygen red and nitrogen blue. The side-chain indole of Trp7 is excited by UV light, and may transfer energy to Tb³⁺, shown in green, leading to luminescence. The diffraction pattern of this crystal was used as the background. (This figure was designed and created by Ezra Peisach.)

Lanthanide-Binding Tags are composed of twenty or fewer amino acids, and are thus less than 10% the size of GFP (Figure 1-8). Use of only encoded amino acids facilitates the incorporation of LBTs at the genetic level, and thus expression of the tagged protein may be accomplished by the natural cellular machinery. Once expressed, addition of the cofactor Ln³⁺ arms the tag for exploitation of the unique and versatile properties conferred by the metal ion (Figure 1-9).

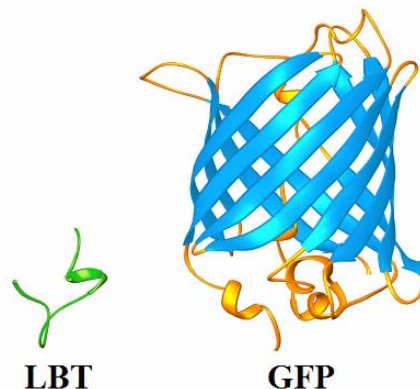


Figure 1-8. Comparison of the size of a Lanthanide-Binding Tag to that of Green Fluorescent Protein. (This figure was created by Ryu Yoshida.)

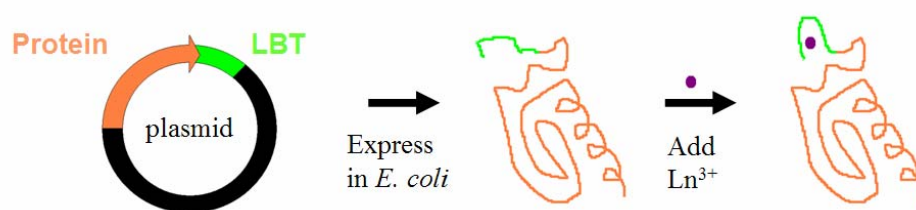


Figure 1-9. Expression of an LBT-protein construct is straightforward.

1-5. Preliminary, Disulfide Bond-Containing Lanthanide-Binding Tags¹

The similarity in atomic radii and oxophilic ligand preference of Ca^{2+} and Ln^{3+} ions (Table 1-1, *vide supra*) inspired researchers to base the design of lanthanide-binding sequences on ion-binding motifs selected from native calcium-binding proteins. Initially, studies by Richardson and Martin began with full length calcium-binding proteins to test for sensitization of Tb^{3+} luminescence.⁶¹ Two important factors were found to govern the luminescence. First, a sensitizing group such as the aromatic side chain of tryptophan or tyrosine must be in close proximity (5-10 Å) to the Tb^{3+} to excite it, due to the inherently low absorbance of lanthanides.⁶² Second, the coordination sites of the terbium need to be fully occupied to avoid luminescence quenching due to the O-H bonds in water.^{31,63,64} In order to identify a binding motif for terbium luminescence, Szabo and coworkers conducted a small screen of short peptide sequences to optimize the type and position of the sensitizing agent.⁵⁷ In this study, researchers found that a tryptophan residue at position 7 of the reference peptide (LBT-0, which has the sequence GDYNADGWIEFEEL; see also Table 1-2 below) was optimal for terbium luminescence. Unfortunately, once this short peptide sequence is removed from the native protein architecture,

the affinity for lanthanide ions decreases precipitously (by around two orders of magnitude) and dissociation constants on the order of 10 μM are observed.

In order for LBTs to be useful tags for proteins that do not already include native calcium-binding loops, an increase in lanthanide affinity is critical. The lanthanide-binding tag should be of sufficient affinity to preclude protein aggregation from non-specific interactions of lanthanide ion with the protein. Members of our lab therefore implemented methods to identify peptide motifs which demonstrated both increased affinity for lanthanide ions and improved luminescence. An initial attempt to rationally design short peptides with increased lanthanide affinity was spearheaded by Dr. Kathy Franz. It was hypothesized that tethering the ends of the loop might pre-organize the peptide backbone and facilitate lanthanide binding. For this reason, disulfide-bridge containing peptides based on LBT-0 were synthesized and the dissociation constants for Tb^{3+} determined (Table 1-2).⁵⁸ From this small library, binding affinity was improved by over an order of magnitude to yield LBT-8 with a K_D for Tb^{3+} of 220 nM (Table 1-2). While these initial results were encouraging, this method was not high-throughput, and therefore unsuitable for obtaining protein tags of even stronger lanthanide affinity without depending on disulfide bond formation. With this in mind, a more rapid and comprehensive screen was desired, both to increase the likelihood of success and to reduce the time-consuming, and often fallible, method of rational design, which allows only individual testing of a limited number of sequences.

Table 1-2. Rationally-Designed LBT Sequences Derived from Calcium-Binding Proteins.^{a,b} (This table was designed by Bianca Sculimbrene.)

Position Peptide	-4	-3	-2	-1	0	1	2	3	4	5	6	7	8	9	10	11	12	13	14	15	16	17	K_D, Tb^{3+} [μM]
<u>LBT-0</u>			Ac	G	D	Y	N	A	D	G	W	I	E	F	E	E	L						9 \pm 1
<u>LBT-1</u>	A	A	C	G	D	Y	N	A	D	G	W	I	E	F	E	E	L	A	C	A			9.3 \pm 0.4
<u>LBT-2</u>			Ac	G	G	D	Y	N	A	D	G	W	I	E	F	E	E	L	L				8 \pm 1
<u>LBT-3</u>	A	C	A	G	D	Y	N	A	D	G	W	I	E	F	E	E	L	A	C	A			6.4 \pm 0.8
<u>LBT-4</u>	A	C	A	G	D	Y	N	A	D	G	W	I	E	F	E	E	L	A	A	C	A		5.9 \pm 0.5
<u>LBT-5</u>	A	C	A	A	G	D	Y	N	A	D	G	W	I	E	F	E	E	L	A	C	A		5.3 \pm 0.9
<u>LBT-6</u>	A	A	C	G	D	Y	N	A	D	G	W	I	E	F	E	E	L	A	A	C	A		5.0 \pm 0.3
<u>LBT-7</u>				C	G	D	Y	N	A	D	G	W	I	E	F	E	E	L	C				0.6 \pm 0.1
<u>LBT-8</u>	A	C	A	G	D	Y	N	A	D	G	W	I	E	F	E	E	L	C	A	A			0.220 ^c

^a Peptides LBT1 and LBT3 to LBT8 were oxidized to afford disulfide-containing macrocycles. Amino acids in bold-face correspond to Tb^{3+} -ligating residues. The tryptophan residue at position 7 coordinates Tb^{3+} through the backbone carbonyl and sensitizes Tb^{3+} luminescence. Amino acids are given as one-letter codes. Ac corresponds to an acetyl-capped N-terminus; all others are free amines. All peptides were synthesized as C-terminal amides.

^b All LBTs are aligned to LBT-0. The residue numbering system is based on the literature.^{56,57}

^c Error of 0.003 μM .

1-6. Development of a Powerful Combinatorial Screen¹

The limiting step in the discovery of new peptides with a particular function is not the synthesis but the screening process. An enormous number of compounds would be generated from a library of completely randomized peptides, even if each position were limited to the encoded amino acids. Thousands of individual peptides can be made by solid-phase peptide synthesis (SPPS), and the ability to generate random peptide sequences in SPPS is easily achieved via split-and-pool combinatorial libraries (diagrammed in Figure 1-10).⁶⁵⁻⁶⁷ Therefore, development of a rapid screening method was undertaken to take advantage of all the diversity available from this method.

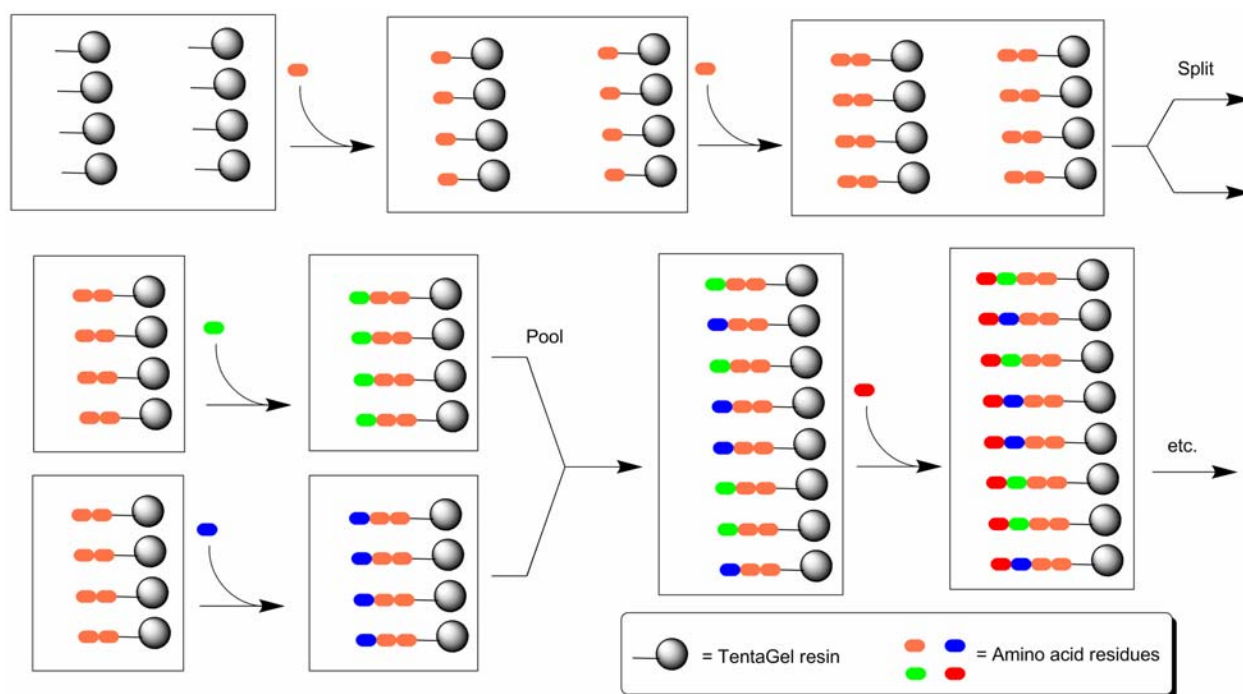


Figure 1-10. Generation of a split-and-pool combinatorial library. Resin is loaded with peptide residues until the location in the sequence to be varied. The resin is then split into equal portions corresponding to the number of variations (two in the diagram). One of the varied amino acids is added to each portion, and then all the resin is pooled. Amino acids are added until the next variation, where the split-react-pool cycle is repeated, or until the N-terminus is reached. This methodology enables every permutation in the library to be made, while maintaining a single sequence on each individual bead.

Fluorescence spectroscopy has emerged as a highly efficient method for screening combinatorial libraries.⁶⁸⁻⁷¹ The sensitivity of fluorescence allows small quantities of material to be analyzed using instrumentation including fluorescence microscopes and fluorescence plate readers. For this study, it was reasoned that screening combinatorial peptide libraries for Tb^{3+}

luminescence could chemically evolve tighter and brighter LBTs. Hundreds of individual peptides could be screened on-bead simultaneously, identifying the brightest ones for selection and sequencing.

A new screen was developed in our lab to select tight and bright LBT sequences, spearheaded by Dr. Mark Nitz. Peptide sequences with high lanthanide affinity are of particular importance, to enable LBTs to be fully occupied in the presence of few equivalents of Tb^{3+} ; high $[Tb^{3+}]$ often induces protein aggregation. The screen utilizes Tb^{3+} luminescence with experimental strategies to avoid signal interference from the solid support and to reduce the cost and time associated with peptide sequencing by Edman degradation. This strategy is diagrammed in Figure 1-11.⁵⁹ As solid support, TentaGel macrobeads (280-320 μm) were chosen based on compatibility with both organic solvents (during the peptide synthesis) and aqueous solution (during the Tb^{3+} luminescence screening). The high loading capacity of 2-3 nmol per bead ensures that sufficient peptide will be available for the orthogonal screen and sequence determination procedures. The resin is first derivatized with *para*-nitrophenylalanine to help quench background fluorescence. Resin is then co-functionalized with 20% of a photocleavable linker (3-amino-3-(2-nitrophenyl)propionic acid, ANP) and 80% of a base-labile linker (4-hydroxymethylbenzoic acid, HMBA). This co-functionalization allows a small amount of the peptide to be released from the bead with long wavelength UV light during screening, while the remaining portion of the peptide remains on the resin for sequencing after the selection process. A five-residue spacer is then added to facilitate ionization and to allow the shortest capped sequences to be above the background level of MALDI mass spectroscopy (MALDI-MS), which is used for sequence deconvolution.

The peptide is elongated using standard Fmoc-based SPPS protocols, including piperidine deprotection and amino-acid activation with HOBt/HBTU. Some of the varied residues are introduced simultaneously with an encoded capping reagent to generate a mass ladder for sequence determination. This method, developed by Griesinger and coworkers, utilizes an algorithm to calculate the minimum number of encoded capping steps necessary to generate a non-degenerate mass ladder.⁷² This approach necessitates fewer truncation sequences on each bead, compared with conventional mass spectroscopy ladder techniques that cap after every variation.

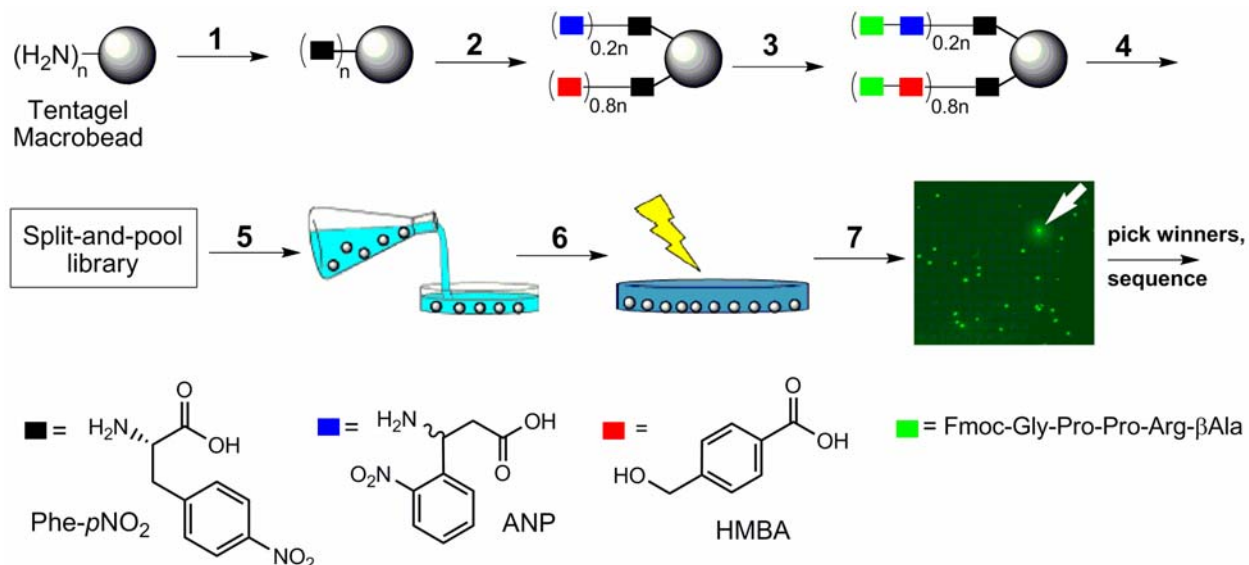


Figure 1-11. The synthesis and screening process for the combinatorial libraries to generate tighter and brighter LBTs. Reproduced and modified from the literature.⁶⁰ (1) Coupling of Fmoc-4-nitrophenylalanine. (2) Coupling of orthogonal linkers (ANP/HMBA, 1:4). (3) Introduction of the spacer peptide sequence. (4) Coupling of the split-and-pool peptide library and mass-spectral ladder capping groups. (5) Amino acid side-chain deprotection, and casting of 2% agarose gel containing 50 μM Tb^{3+} , 100 mM NaCl and 10 mM HEPES at pH 7.0 in a Petri dish. (6) Photolysis of the ANP linker using > 320 nm light. (7) Visualization of the beads at 280 nm. Beads are then selected that have bright luminescent halos, removal of agarose from selected beads followed by cleavage of the HMBA linker in 28% NH_4OH , followed by MALDI-MS sequence deconvolution and single-bead Tb^{3+} -affinity titrations. (This figure was originally designed and created by Mark Nitz, and has been previously published.¹⁻⁵⁹)

Once the split-and-pool encoded library is generated and side-chain protecting groups are cleaved by treatment with 94% trifluoroacetic acid, 2.5% water, 2.5% ethanedithiol and 1% triisopropylsilane, several hundred beads are dispersed in a buffered agarose gel containing Tb^{3+} ions. Nitrilotriacetic acid (NTA) or another competitive ligand may be included to ensure that only the tightest LBTs are bound to Tb^{3+} . Release of the peptide portion attached via the photolabile linker is accomplished by illuminating the gel for six minutes on a long-wavelength UV transilluminator. The gel is visualized on a transilluminator with excitation at 280 nm; beads that contain the best LBTs exhibit a green, luminescent “halo” as shown in Figure 1-11. Beads with these halos are selectively removed from the gel. Treatment with ammonium hydroxide enables the release of these beads’ remaining peptide, the sequence of which is then determined by MALDI-MS. This selection assay avoids signal interference from the solid support while still taking advantage of the large number and diversity of peptides accessible through solid phase chemistry.

1-7. Lanthanide-Binding Tags Evolved Through the Combinatorial Screening Process^l

Despite the power that comes with the ability to screen large numbers of peptides for a specific function on resin, a certain amount of rational design is still required when developing a library. For instance, complete randomization of a trideca-peptide to all twenty natural amino acids would require a library of $20^{13} = 8.2 \times 10^{16}$ individual sequences. Approximately five grams of resin are required to make 100,000 peptides, meaning that four billion kilograms of resin would be necessary to synthesize the aforementioned library! It is thus imperative to limit the number of variations or randomizations in order to avoid a prohibitively monumental screen or inadequate coverage of sequence space. Therefore, for the LBT libraries, no more than seven residues were ever varied in any screen, and selections were based on known or presumed function of the position whenever possible. Also, because MALDI-MS was used in sequence deconvolution, mass-degenerate amino acids were generally avoided at any one positional variation.

This prohibition on complete randomization led to the use of the original LBT-0 as the initial terbium-binding model. From this sequence, a series of four combinatorial libraries were designed, with each consensus peptide serving as the starting point for future library generations.⁵⁹ The first library (Figure 1-12) contained 3,600 peptides, and addressed primarily whether the ligating glutamate residues (E9 and E12) were indeed optimized for Tb³⁺-binding. The sequence at positions 10 and 11 was varied to include residues biased towards turn formation by introduction of glycine and proline residues. Lastly, in order to compensate for the lack of a pre-organizational disulfide bond, explorations towards a stronger interaction between the N- and C-termini of the LBT were commenced. This results of library conclusively showed that the glutamate residues at positions 9 and 12 in LBT-0 were already optimized. Nevertheless, the best LBT, dubbed SE1, had a dissociation constant for Tb³⁺ that was lowered from 9 μ M to 4 μ M. (LBTs discovered through these combinatorial libraries were nicknamed “Sticky-Ends”, abbreviated “SE” in appreciation of the fact that the goal was to stick the termini together via non-covalent interactions.)

Position	-1	0	1	2	3	4	5	6	7	8	9	10	11	12	13	K_D, Tb^{3+}		
Peptide																		
<u>LBT-Ref</u>		G	D	Y	N	K	D	G	W	Y	E	E	L	E	L	~9 μ M		
	L	A									D	G	G	D	L			
	T	G									E	P	P	E	T			
	V	W									N			N	V			
		Y									Q			Q				
											S			S				
<u>SE1</u>			V	Y	D	Y	N	K	D	G	W	Y	E	G	P	E	L	~4 μ M

Figure 1-12. Results from Library 1: “Bidentate Ligating Residues and Turn Sequence”. Residues at varied positions in the starting LBT-O are shown in red. Residues selected as optimal for each position are shown in blue. The resulting consensus sequence, the LBT “SE1,” is outlined in blue.

The second library (Figure 1-13) involved a much more thorough study—utilizing 14,700 peptides—of possible interactions between the two termini. By creating this sort of interaction, the entropic penalty upon metal-binding and organization could be minimized, lowering the dissociation constant. Calcium-binding motifs, for example, have a much stronger affinity while embedded within a protein, as a result of the more rigid structure around the loop holding the ends together. It was therefore logical to create stronger, hydrophobic interactions between the termini in an attempt to better mimic this environment. The resulting peptides from this second generation library, SE1a- α and SE1a- β , showed that increasing the length and modifying the terminal residues was indeed extremely beneficial. These sequences were significantly more selective terbium-binders than SE1, with dissociation constants now in the high nanomolar range.

Position	-1	0	1	2	3	4	5	6	7	8	9	10	11	12	13	14	15	K_D, Tb^{3+}		
Peptide																				
<u>SE1</u>	V	Y	D	Y	N	K	D	G	W	Y	E	G	P	E	L			~4 μ M		
	A	A		W											A	A	A			
	L	L		Y											L	L	L			
	V	V													P	P	T			
	W	P													T	T	V			
	Y	W													V	V	Y			
		Y													W	W				
															Y	Y				
<u>SE1a-α</u>			W	V	D	W	N	K	D	G	W	Y	E	G	P	E	L	L	A	~700 nM
<u>SE1a-β</u>			Y		Y															

Figure 1-13. Results from Library 2: “Interactions at the Termini”. Varied positions in the parent SE1 LBT are shown in red. Residues selected as optimal for each position are shown in blue. The resulting consensus sequences, the LBTs “SE1a- α ” and “SE1a- β ,” are outlined in blue.

The third library (Figure 1-14) was the largest of the libraries, involving 18,000 peptides. It continued the variation of the aromatic residues at the -1 position, introduced an additional variation at position 0 (isoleucine was not included in the previous library because it is indistinguishable from leucine by MALDI-MS), and randomized the internal, non-ligating residues at positions 4, 10 and 11. Finally, the aromatic residues at positions 7 and 8 were varied in an attempt to identify brighter LBTs. The large investment in peptide quantities paid off, for the resulting SE1b- α , SE1b- β , and SE1b- γ were an order-of-magnitude improved in K_D from the SE1a generation. This was the most significant improvement observed in any of the libraries.

Position	-1	0	1	2	3	4	5	6	7	8	9	10	11	12	13	14	15	K_D, Tb^{3+}
<u>SE1a</u>	X	V	D	X	N	K	D	G	W	Y	E	G	P	E	L	L	A	~700 nM
	F	I		F		G			W	W		D	D					
	W	V		G		K			Y	Y		E	G					
	Y			L		N						G	N					
				P		P						N	P					
				W		R						S	S					
				Y														
<u>SE1b-α</u>	Y	I	D	F	N	N	D	G	W	Y	E	G	D	E	L	L	A	~70 nM
<u>SE1b-β</u>				L														
<u>SE1b-γ</u>				W														

Figure 1-14. Results from Library 3: “Internal, Non-ligating Residues”. Varied positions in the parent SE1a LBT are shown in red. Residues selected as optimal for each position are shown in blue. The resulting consensus sequences, the LBTs “SE1b- α ,” “SE1b- β ,” and “SE1b- γ ,” are outlined in blue.

While this result was exciting, the apparent variability of preference at position 2 was curious, so a fourth library (Figure 1-15) was constructed to address this. Position 2 was randomized with all sulfur-free, mass-non-degenerate amino acids. The resulting peptide, which Dr. Nitz dubbed “SE2,” unambiguously showed that threonine was optimal at this position, with a 57 nM dissociation constant for Tb^{3+} . Also, competitive titrations of SE2 between Tb^{3+} and most other Ln^{3+} metal ions clearly showed terbium to be the tightest binder.⁶⁰ The trend indicated a high dependence on effective ionic radius: while Dy^{3+} and Eu^{3+} were only marginally weaker, using lanthanides with ionic radii much different than Tb^{3+} (especially the larger lanthanides, e.g. La^{3+}) led to significant drops in affinity.⁶⁰ Furthermore, competitive titrations of SE2 between Tb^{3+} and Ca^{2+} or Mg^{2+} show only weak binding of the latter two ions. These results underscore that these libraries have successfully identified a selective terbium-binding

peptide. Similar screens should provide equally selective in creating peptides that chelate other metals, provided that a method exists for detecting binding.

Position	-1	0	1	2	3	4	5	6	7	8	9	10	11	12	13	14	15	K_D, Tb^{3+}	
Peptide																			
<u>SE1b</u>		Y	I	D	X	N	N	D	G	W	Y	E	G	D	E	L	L	A	~70 nM
					A, D, E, F, G, H, K, L, N, P, R, S, T, V, W, Y														
<u>SE2</u>		Y	I	D	T	N	N	D	G	W	Y	E	G	D	E	L	L	A	57 nM

Figure 1-15. Results from Library 4: “Variation at Position 2”. The varied position in the parent, SE1b, is shown in red. The optimal residue is shown in blue. The resulting consensus sequence, the LBT “SE2,” is outlined in blue.

1-8. Dissertation Objectives

Early work on LBTs was extremely successful. The combinatorial screen enabled the selection of a sequence, SE2 (Figure 1-15), that was more than two orders of magnitude tighter than the original LBT-0. Since the inception of SE2, this sequence has been used, in collaboration with other labs, in preliminary experiments regarding applicability of LBTs to NMR studies,⁷³ and to determine the crystal structure of the terbium-bound peptide complex.⁶⁰ In addition, the protean nature of Lanthanide-Binding Tags as probes has since been demonstrated, by our lab and by others, through the use of LBTs for luminescent visualization on gels,⁵⁸ as magnetic-field paramagnetic alignment agents in protein-NMR experiments,⁷³⁻⁷⁵ in fluorescence microscopy,⁷⁶ and as partners in luminescence resonance energy transfer (LRET) studies.⁷⁷ Recent work includes the development of LBTs containing unnatural amino acids at position 7, with side chains that can be excited at lower-energy wavelengths and sensitize Eu^{3+} .⁷⁸

Nevertheless, a tool being used as a biological probe nearly always has room for improvement. Still-tighter sequences are desirable: although not yet available, picomolar or sub-picomolar K_D values would be needed for use *in vivo*, for example. This thesis will detail the continued development of the LBT peptide for use in a variety of applications. Additional libraries and residue-studies have been used to further optimize the SE2 sequence, especially with respect to insight gained from the peptide crystal structure,⁶⁰ thus obtaining the best known LBT, with a low-nM K_D for Tb^{3+} (Chapter 2). A brief attempt to make an LBT that emits in the near-IR region is discussed in Chapter 3. Despite the improvement in affinity shown in Chapter 2, the single-lanthanide-binding peptides have not yet been successful in conjunction with

protein crystallography, and therefore the LBT-repertoire has been expanded to include two-lanthanide-binding motifs (“double-LBTs”), which show even greater promise as protein probes (Chapter 4). Computational studies of the double-LBT sequence furthered insight into sub-optimal portions of the LBT sequence, culminating in the design of additional LBT and dLBT improvements (Chapter 5). In Chapter 6, a preliminary library to evolve an LBT that would be useful for magnetic resonance imaging experiments is discussed. Finally, knowledge about the LBT sequences has enabled it to be used in the study of a calcium-binding protein, Calcineurin (Chapter 7).

Acknowledgements

Much of this chapter has been previously published, and I am thus indebted to all of my co-authors, but especially to Dr. Bianca Sculimbrene for her help with writing and editing, and to Dr. Mark Nitz, who made the original design of Figure 1-11. I am also grateful for our collaboration with Prof. Karen Allen’s lab at Boston University, as many of that lab’s members have superior artistic talents: Dr. Nicholas Silvaggi created Figure 1-6, and Dr. Ezra Peisach created Figure 1-7. A UROP in the Imperiali lab, Ryu Yoshida, designed Figure 1-8. I am eternally grateful to Wendy Iskenderian for editing this chapter.

References

- (1) Martin, L. J.; Sculimbrene, B. R.; Nitz, M.; Imperiali, B. "Rapid Combinatorial Screening of Peptide Libraries for the Selection of Lanthanide-Binding Tags (LBTs)." *QSAR Comb. Sci.* **2005**, *24(10)*, 1149-1157.
- (2) Martin, L. J.; Hähnke, M. J.; Nitz, M.; Wöhnert, J.; Silvaggi, N. R.; Allen, K. N.; Schwalbe, H.; Imperiali, B. "Double-Lanthanide-Binding Tags: Design, Photophysical Properties, and NMR Applications." *J. Am. Chem. Soc.* **2007**, *129(22)*, 7106-7113.
- (3) Tsien, R. Y. "The green fluorescent protein." *Annu. Rev. Biochem.* **1998**, *67*, 509-544.
- (4) Schmid, J. A.; Neumeier, H. "Evolutions in science triggered by green fluorescent protein (GFP)." *ChemBioChem* **2005**, *6(7)*, 1149-1156.
- (5) Doublet, S. "Preparation of selenomethionyl proteins for phase determination." *Meth. Enzymol.* **1997**, *276*, 523-530.

- (6) Hendrickson, W. A.; Horton, J. R.; LeMaster, D. M. "Selenomethionyl proteins produced for analysis by multiwavelength anomalous diffraction (MAD): a vehicle for direct determination of three-dimensional structure." *EMBO J.* **1990**, *9*(5), 1665-1672.
- (7) Banci, L.; Bertini, I.; Huber, J. G.; Luchinat, C.; Rosato, A. "Partial Orientation of Oxidized and Reduced Cytochrome b5 at High Magnetic Fields: Magnetic Susceptibility Anisotropy Contributions and Consequences for Protein Solution Structure Determination." *J. Am. Chem. Soc.* **1998**, *120*(49), 12903-12909.
- (8) Wedepohl, K. H. "The composition of the continental crust." *Geochim. Cosmochim. Acta* **1995**, *59*(7), 1217-1232.
- (9) Evans, W. J. "The Importance of Questioning Scientific Assumptions: Some Lessons from f Element Chemistry." *Inorg. Chem.* **2007**, *46*(9), 3435-3449.
- (10) Venetsky, S. I., *On Rare and Scattered Metals: Tales about Metals*. Mir Publishers: Moscow, 1983;
- (11) Vardhan, A. Periodic Table of the Elements. <http://www.ktf-split.hr/periodni/en> (2004),
- (12) Cotton, S., *Lanthanides and Actinides*. Oxford University Press: New York, 1991;
- (13) Bünzli, J.-C. G. "Benefiting from the unique properties of lanthanide ions." *Acc. Chem. Res.* **2006**, *39*(1), 53-61.
- (14) Shannon, R. D. "Revised effective ionic radii and systematic studies of interatomic distances in halides and chalcogenides." *Acta Cryst.* **1976**, *A32*(5), 751-767.
- (15) Richardson, F. S. "Terbium(III) and europium(III) ions as luminescent probes and stains for biomolecular systems." *Chem. Rev.* **1982**, *82*(5), 541-552.
- (16) Bünzli, J.-C. G.; Piguet, C. "Taking advantage of luminescent lanthanide ions." *Chem. Soc. Rev.* **2005**, *34*, 1048 - 1077.
- (17) Cotton, S., *Lanthanide and Actinide Chemistry*. John Wiley & Sons Ltd.: West Sussex, England, 2006;
- (18) Gudgin Dickson, E. F.; Pollak, A.; Diamandis, E. P. "Time-resolved detection of lanthanide luminescence for ultrasensitive bioanalytical assays." *J. Photochem. Photobiol., B* **1995**, *27*(1), 3-19.
- (19) Faulkner, S.; Pope, S. J. A.; Burton-Pye, B. P. "Lanthanide complexes for luminescence imaging applications." *Appl. Spec. Rev.* **2005**, *40*, 1-31.
- (20) Yuan, J.; Wang, G. "Lanthanide Complex-Based Fluorescence Label for Time-Resolved Fluorescence Bioassay." *J. Fluorescence* **2005**, *15*(4), 559-568.

- (21) Piszczek, G.; Gryczynski, I.; Maliwal, B. P.; Lakowicz, J. R. "Multi-Photon Sensitized Excitation of Near Infrared Emitting Lanthanides." *J. Fluorescence* **2002**, *12*(1), 15-17.
- (22) Zhang, J.; Badger, P. D.; Geib, S. J.; Petoud, S. "Sensitization of Near-Infrared-Emitting Lanthanide Cations in Solution by Tropolonate Ligands." *Angew. Chem. Int. Ed.* **2005**, *44*, 2508-2512.
- (23) Brennan, J. D.; Capretta, A.; Yong, K.; Gerritsma, D.; Flora, K. K.; Jones, A. "Sensitization of lanthanides by nonnatural amino acids." *Photochem. Photobiol.* **2002**, *75*(2), 117-121.
- (24) Nadi, S.; Santos, M.; Haldar, M. K.; Roy, B. C.; Mallik, S.; Campiglia, A. D. "Solid-supported synthesis of polymerizable lanthanide-ion chelating lipids for protein detection." *Inorg. Chem.* **2005**, *44*, 2234-2244.
- (25) Elbanowski, M.; Makowska, B. "The lanthanides as luminescent probes in investigations of biochemical systems." *J. Photochem. Photobiol., A* **1996**, *99*(2-3), 85-92.
- (26) Handl, H. L.; Gillies, R. J. "Lanthanide-based luminescent assays for ligand-receptor interactions." *Life Sci.* **2005**, *77*(4), 361-371.
- (27) Hemmilä, I.; Laitala, V. "Progress in lanthanides as luminescent probes." *J. Fluorescence* **2005**, *15*(4), 529-542.
- (28) Selvin, P. R. "The renaissance of fluorescence resonance energy transfer." *Nature Struct. Biol.* **2000**, *7*, 730-734.
- (29) Selvin, P. R. "Principles and biophysical applications of lanthanide-based probes." *Annu. Rev. Biophys. Biomol. Struct.* **2002**, *31*, 275-302.
- (30) Selvin, P. R.; Hearst, J. E. "Luminescence energy transfer using a terbium chelate: Improvements on fluorescence energy transfer." *Proc. Natl. Acad. Sci. USA* **1994**, *91*, 10024-10028.
- (31) Horrocks, W. D., Jr.; Sudnick, D. R. "Lanthanide ion probes of structure in biology. Laser-induced luminescence decay constants provide a direct measure of the number of metal-coordinated water molecules." *J. Am. Chem. Soc.* **1979**, *101*(2), 334-340.
- (32) Koshi, Y.; Nakata, E.; Hamachi, I. "Luminescent saccharide biosensor by using lanthanide-bound lectin labeled with fluorescein." *ChemBioChem* **2005**, *6*(8), 1349-1352.
- (33) Liu, L. L.; Franz, K. J. "Phosphorylation of an α -Synuclein Peptide Fragment Enhances Metal Binding." *J. Am. Chem. Soc.* **2005**, *127*(27), 9662-9663.

- (34) Supkowski, R. M.; Bolender, J. P.; Smith, W. D.; Reynolds, L. E. L.; Horrocks, W. D., Jr. "Lanthanide ions as redox probes of long-range electron transfer in proteins." *Coord. Chem. Rev.* **1999**, *185-186*, 307-319.
- (35) Pidcock, E.; Moore, G. R. "Structural characteristics of protein binding sites for calcium and lanthanide ions." *J. Biol. Inorg. Chem.* **2001**, *6(5-6)*, 479-489.
- (36) Purdy, M. D.; Ge, P.; Chen, J.; Selvin, P. R.; Wiener, M. C. "Thiol-reactive lanthanide chelates for phasing protein X-ray diffraction data." *Acta Crystallogr. D* **2002**, *D58(7)*, 1111-1117.
- (37) Pompidor, G.; D'Aléo, A.; Vicat, J.; Toupet, L.; Giraud, N.; Kahn, R.; Maury, O. "Protein Crystallography through Supramolecular Interactions between a Lanthanide Complex and Arginine." *Angew. Chem. Int. Ed.* **2008**, *47(18)*, 3388-3391.
- (38) Silvaggi, N. R.; Martin, L. J.; Schwalbe, H.; Imperiali, B.; Allen, K. N. "Double-Lanthanide-Binding Tags for Macromolecular Crystallographic Structural Determination." *J. Am. Chem. Soc.* **2007**, *129(22)*, 7114-7120.
- (39) Pintacuda, G.; John, M.; Su, X.-C.; Otting, G. "NMR Structure Determination of Protein-Ligand Complexes by Lanthanide Labeling." *Acc. Chem. Res.* **2007**, *40(3)*, 206-212.
- (40) Barbieri, R.; Bertini, I.; Cavallaro, G.; Lee, Y.-M.; Luchinat, C.; Rosato, A. "Paramagnetically induced residual dipolar couplings for solution structure determination of lanthanide binding proteins." *J. Am. Chem. Soc.* **2002**, *124(19)*, 5581-5587.
- (41) Veglia, G.; Opella, S. J. "Lanthanide Ion Binding to Adventitious Sites Aligns Membrane Proteins in Micelles for Solution NMR Spectroscopy." *J. Am. Chem. Soc.* **2000**, *122(47)*, 11733-11734.
- (42) Lee, L.; Sykes, B. D. "Use of lanthanide-induced nuclear magnetic resonance shifts for determination of protein structure in solution: EF calcium binding site of carp parvalbumin." *Biochemistry* **1983**, *22(19)*, 4366-4373.
- (43) Tolman, J. R. "Dipolar couplings as a probe of molecular dynamics and structure in solution." *Curr. Opin. Struct. Biol.* **2001**, *11(5)*, 532-539.
- (44) Lipsitz, R. S.; Tjandra, N. "Residual dipolar couplings in NMR structure analysis." *Annu. Rev. Biophys. Biomol. Struct.* **2004**, *33*, 387-413.
- (45) Schwalbe, H.; Grimshaw, S. B.; Spencer, A.; Buck, M.; Boyd, J.; Dobson, C. M.; Redfield, C.; Smith, L. J. "A refined solution structure of hen lysozyme determined using residual dipolar coupling data." *Prot. Sci.* **2001**, *10(4)*, 677-688.

- (46) John, M.; Pintacuda, G.; Park, A. Y.; Dixon, N. E.; Otting, G. "Structure Determination of Protein-Ligand Complexes by Transferred Paramagnetic Shifts." *J. Am. Chem. Soc.* **2006**, *128*(39), 12910-12916.
- (47) Caravan, P.; Ellison, J. J.; McMurry, T. J.; Lauffer, R. B. "Gadolinium(III) Chelates as MRI Contrast Agents: Structure, Dynamics, and Applications." *Chem. Rev.* **1999**, *99*(9), 2293-2352.
- (48) Bottrill, M.; Kwok, L.; Long, N. J. "Lanthanides in magnetic resonance imaging." *Chem. Soc. Rev.* **2006**, *35*(6), 557-571.
- (49) Burroughs, S. E.; Horrocks, W. D., Jr.; Ren, H.; Klee, C. B. "Characterization of the Lanthanide Ion-Binding Properties of Calcineurin-B Using Laser-Induced Luminescence Spectroscopy." *Biochemistry* **1994**, *33*(34), 10428-10436.
- (50) Becker, C. F. W.; Clayton, D.; Shapovalov, G.; Lester, H. A.; Kochendoerfer, G. G. "On-Resin Assembly of a Linkerless Lanthanide(III)-Based Luminescence Label and Its Application to the Total Synthesis of Site-Specifically Labeled Mechanosensitive Channels." *Bioconjugate Chem.* **2004**, *15*(5), 1118-1124.
- (51) Rodriguez-Castaneda, F.; Haberz, P.; Leonov, A.; Griesinger, C. "Paramagnetic tagging of diamagnetic proteins for solution NMR." *Magn. Reson. Chem.* **2006**, *44*(Spec. Issue), S10-S16 and references therein.
- (52) Weibel, N.; Charbonnière, L. J.; Guardigli, M.; Roda, A.; Ziessel, R. "Engineering of highly luminescent lanthanide tags suitable for protein labeling and time-resolved luminescence imaging." *J. Am. Chem. Soc.* **2004**, *126*(15), 4888-4896.
- (53) Zhang, J.; Cambell, R. E.; Ting, A. Y.; Tsien, R. Y. "Creating New Fluorescent Probes for Cell Biology." *Nat. Rev. Mol. Cell Biol.* **2002**, *3*(12), 906-918.
- (54) MacKenzie, C. R.; Clark, I. D.; Evans, S. V.; Hill, I. E.; MacManus, J. P.; Dubuc, G.; Bundle, D. R.; Narang, S. A.; Young, N. M.; Szabo, A. G. "Bifunctional fusion proteins consisting of a single-chain antibody and an engineered lanthanide-binding protein." *Immunotechnology* **1995**, *1*(2), 139-150.
- (55) Vázquez-Ibar, J. L.; Weinglass, A. B.; Kaback, H. R. "Engineering a terbium-binding site into an integral membrane protein for luminescence energy transfer." *Proc. Natl. Acad. Sci. USA* **2002**, *99*(6), 3487-3492.
- (56) Marsden, B. J.; Hodges, R. S.; Sykes, B. D. "Proton NMR studies of synthetic peptide analogs of calcium-binding site III of rabbit skeletal troponin C: Effect on the lanthanum affinity of the interchange of aspartic acid and asparagine residues at the metal ion coordinating positions." *Biochemistry* **1988**, *27*(11), 4198-4206.

- (57) MacManus, J. P.; Hogue, C. W.; Marsden, B. J.; Sikorska, M.; Szabo, A. G. "Terbium luminescence in synthetic peptide loops from calcium-binding proteins with different energy donors." *J. Biol. Chem.* **1990**, *265*(18), 10358-10366.
- (58) Franz, K. J.; Nitz, M.; Imperiali, B. "Lanthanide-binding tags as versatile protein coexpression probes." *ChemBioChem* **2003**, *4*(4), 265-271.
- (59) Nitz, M.; Franz, K. J.; Maglathlin, R. L.; Imperiali, B. "A powerful combinatorial screen to identify high-affinity terbium(III)-binding peptides." *ChemBioChem* **2003**, *4*(4), 272-276.
- (60) Nitz, M.; Sherawat, M.; Franz, K. J.; Peisach, E.; Allen, K. N.; Imperiali, B. "Structural origin of the high affinity of a chemically evolved lanthanide-binding peptide." *Angew. Chem. Int. Ed.* **2004**, *43*(28), 3682-3685.
- (61) Brittain, H. G.; Richardson, F. S.; Martin, R. B. "Terbium(III) emission as a probe of calcium(II) binding sites in proteins." *J. Am. Chem. Soc.* **1976**, *98*(25), 8255-8260.
- (62) Kirk, W. R.; Wessels, W. S.; Prendergast, F. G. "Lanthanide-dependent perturbations of luminescence in indolythylenediaminetetraacetic acid-lanthanide chelate." *J. Phys. Chem.* **1993**, *97*(40), 10326-10340.
- (63) Horrocks, W. D., Jr.; Sudnick, D. R. "Lanthanide ion luminescence probes of the structure of biological macromolecules." *Acc. Chem. Res.* **1981**, *14*(12), 384-392.
- (64) Beeby, A.; Clarkson, I. M.; Dickins, R. S.; Faulkner, S.; Parker, D.; Royle, L.; de Sousa, A. S.; Williams, J. A. G.; Woods, M. "Non-radiative deactivation of the excited states of europium, terbium and ytterbium complexes by proximate energy-matched OH, NH and CH oscillators: an improved luminescence method for establishing solution hydration states." *J. Chem. Soc., Perkin Trans. 2* **1999**, (3), 493-504.
- (65) Lam, K. S.; Lebl, M.; Krchnak, V. "The "One-Bead-One-Compound" Combinatorial Library Method." *Chem. Rev.* **1997**, *97*(2), 411-448.
- (66) Lam, K. S.; Salmon, S. E.; Hersh, E. M.; Hruby, V. J.; Kazmierski, W. M.; Knapp, R. J. "A new type of synthetic peptide library for identifying ligand-binding activity." *Nature* **1991**, *354*, 82-84.
- (67) Furka, A.; Sebestyen, F.; Asgedom, M.; Dibo, G. "General method for rapid synthesis of multicomponent peptide mixtures." *Int. J. Pept. Prot. Res.* **1991**, *37*(6), 487-493.
- (68) Finney, N. S. "Fluorescence assays for screening combinatorial libraries of drug candidates." *Curr. Opin. Drug Dis. Develop.* **1998**, *1*(1), 98-105.
- (69) Burbaum, J. J.; Sigal, N. H. "New technologies for high-throughput screening." *Curr. Opin. Chem. Biol.* **1997**, *1*(1), 72-78.

- (70) Harris, R. F.; Nation, A. J.; Copeland, G. T.; Miller, S. J. "A Polymeric and Fluorescent Gel for Combinatorial Screening of Catalysts." *J. Am. Chem. Soc.* **2000**, *122*(45), 11270-11271.
- (71) Evans, C. A.; Miller, S. J. "Proton-activated fluorescence as a tool for simultaneous screening of combinatorial chemical reactions." *Curr. Opin. Chem. Biol.* **2002**, *6*(3), 333-338.
- (72) Hoffman, C.; Blechschmidt, D.; Krueger, R.; Karas, M.; Griesinger, C. "Mass spectrometric sequencing of individual peptides from combinatorial libraries via specific generation of chain-terminated sequences." *J. Comb. Chem.* **2002**, *4*(1), 79-86.
- (73) Wöhnert, J.; Franz, K. J.; Nitz, M.; Imperiali, B.; Schwalbe, H. "Protein alignment by a coexpressed lanthanide-binding tag for the measurement of residual dipolar couplings." *J. Am. Chem. Soc.* **2003**, *125*(44), 13338-13339.
- (74) Su, X.-C.; Huber, T.; Dixon, N. E.; Otting, G. "Site-specific labeling of proteins with a rigid lanthanide-binding tag." *ChemBioChem* **2006**, *7*(10), 1599-1604.
- (75) Su, X.-C.; McAndrew, K.; Huber, T.; Otting, G. "Lanthanide-Binding Peptides for NMR Measurements of Residual Dipolar Couplings and Paramagnetic Effects from Multiple Angles." *J. Am. Chem. Soc.* **2008**, *130*, 1681-1687.
- (76) Goda, N.; Tenno, T.; Inomata, K.; Iwaya, N.; Sasaki, Y.; Shirakawa, M.; Hiroaki, H. "LBT/PTD dual tagged vector for purification, cellular protein delivery and visualization in living cells." *Biochim. Biophys. Acta* **2007**, *1773*(2), 141-146.
- (77) Sculimbrene, B. R.; Imperiali, B. "Lanthanide-Binding Tags as Luminescent Probes for Studying Protein Interactions." *J. Am. Chem. Soc.* **2006**, *128*(22), 7346-7352.
- (78) Reynolds, A. M.; Sculimbrene, B. R.; Imperiali, B. "Lanthanide-Binding Tags with Unnatural Amino Acids: Sensitizing Tb³⁺ and Eu³⁺ Luminescence at Longer Wavelengths." *Bioconjugate Chem.* **2008**, *19*(3), 588-591.

Chapter 2

Sequence Refinement of Lanthanide-Binding Tags

Portions of this chapter have been published in *QSAR & Combinatorial Science*¹ as noted in the text. Copyright © 2005, WILEY-VCH Verlag GmbH & Co.

Introduction

The first disulfide-free LBT sequence that was published, known as SE2 (with a sequence of YIDTNNDGWYEGDELLA, Figure 1-15), has a dissociation constant of 57 nM for Tb³⁺.² The peptide was crystallized in the Tb³⁺-bound form to determine the nature of the structural evolution from a native calcium-binding EF-hand motif from the protein Troponin C.³ Figure 2-1 shows the crystal structure of SE2 from three different angles and highlights certain features that promoted design of subsequent combinatorial peptide libraries (as in Figure 1-11). The result of the analyses of these libraries led to the discovery of the LBT sequence FIDTNNDGWIEGDELLLEEG, known as SENG, which is the tightest single Lanthanide-Binding Tag to date, with a dissociation constant of 18 nM for Tb³⁺. In addition to K_D values, LBT sequences are characterized by relative brightness compared to a standard sequence, since brighter sequences may be more useful in certain applications involving luminescence spectroscopy. Mutational studies have also been conducted to compare the importance of various residues in photophysical measurements.

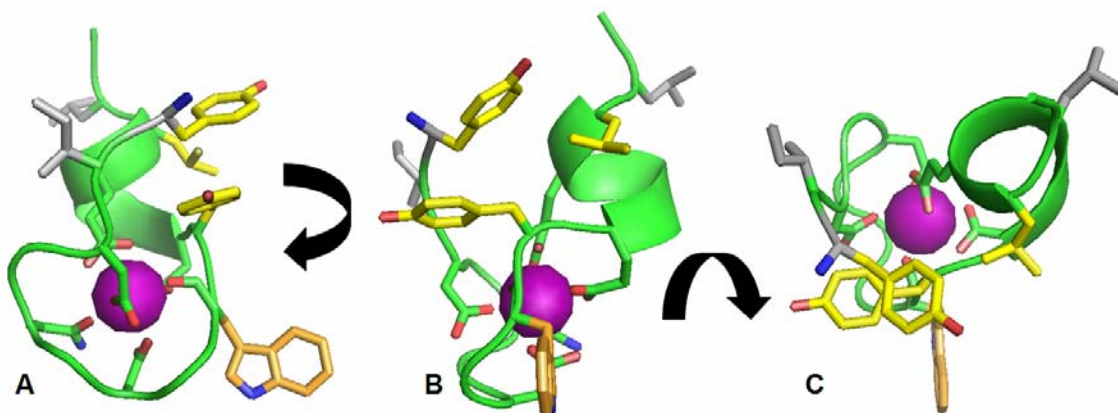


Figure 2-1. The crystal structure of SE2 bound to Tb³⁺, shown from three different perspectives. **B** is a rotation of **A** by about 90° around a vertical axis. **C** is a rotation of **B** by about 90° through a horizontal axis. Tb³⁺ is shown as a violet sphere, and the peptide backbone is shown in green in cartoon form. All side chains that are shown have oxygen atoms colored red and nitrogen atoms in blue. The side chain of Trp7 is shown in orange. The Tb³⁺-chelating side chains of Asp1, Asn3, Asp5, Glu9 and Glu12, as well as the main-chain carbonyl of Trp 7 are shown in green. The side chains of Tyr-1, Tyr8 and Leu13 that form a hydrophobic core are shown in yellow. The side chains of Ile0 and Leu14, as well as the N-terminus (of Tyr-1) are shown in grey. This figure was created using PyMOL based on the crystal structure 1TJB.³

Results and Discussion

2-1. Additional Combinatorial Libraries to Evolve the SE2 Sequence'

The impetus for preparing the fifth library (shown in Figure 2-2) was the observation that in the crystal structure of SE2 bound to Tb^{3+} ,³ the C-terminus of the peptide crystallized with α -helical-like character. (This helix is visible in Figure 2-1, especially 2-1A and 2-1B.) It was hypothesized that an extended α -helix might improve Tb^{3+} -binding. The C-terminus was therefore extended by three additional residues, some of which were selected due to a high propensity for helix-formation, for a total screen of 240 peptides. The results, however, indicated that making this region helical (such as with three additional alanine residues) does not necessarily improve binding. Instead, an additional leucine residue, and two additional glutamic acid residues were found to be optimal. These residues may assist in the pre-organization of the unbound-LBT, and the negatively charged residues are likely to further attract the Tb^{3+} ion. Additionally, this result indicates that while a certain amount of rational design may be useful, the ability to screen libraries of peptides is essential for determining the tightest binders.

Position	-1	0	1	2	3	4	5	6	7	8	9	10	11	12	13	14	15	16	17	18	K_D, Tb^{3+}
<u>Peptide</u>																					
<u>SE2</u>	Y	I	D	T	N	N	D	G	W	Y	E	G	D	E	L	L	A				57 nM
																	A	A	A	A	
																	K	E	E	G	
																	L	K	K	K	
																		L	L	L	
																				R	
<u>SE2a</u>	Y I D T N N D G W Y E G D E L L L E E G																36 nM				

Figure 2-2. Results from Library 5: “Extension of the C-Terminus”. Varied positions in the parent SE2 LBT are shown in red. Residues selected as optimal for each position are shown in blue. The resulting consensus sequence, the LBT “SE2a,” is outlined in blue.

The crystal structure further indicated that the side chains of residues Tyr-1, Tyr8, and Leu13 in SE2 were packed in a hydrophobic core in the Tb^{3+} -bound peptide,³ as can be seen by the yellow colored side-chains in Figure 2-1. Library 6, containing 175 peptides (Figure 2-3), was therefore designed to examine a variety of hydrophobic residues that might improve the packing of this core, and thus offset the entropic penalty of binding. Two sequences were recovered from this screen, named SE3 and SE4. These indicated that leucine was already optimized at position 13, an aromatic residue was desirable at position -1, and isoleucine was

optimal at position 8. For the tighter SE4 sequence, position -1 was also mutated to phenylalanine, thereby improving the dissociation constant to about 30 nM.

Position	-1	0	1	2	3	4	5	6	7	8	9	10	11	12	13	14	15	K_D, Tb^{3+}
<u>SE2</u>	Y	I	D	T	N	N	D	G	W	Y	E	G	D	E	L	L	A	57 nM
	F									F					F			
	I									I					L			
	M									M					M			
	W									T					W			
	Y									V					Y			
										W								
										Y								
<u>SE3</u>	Y	I	D	T	N	N	D	G	W	I	E	G	D	E	L	L	A	38 nM
<u>SE4</u>	F	I	D	T	N	N	D	G	W	I	E	G	D	E	L	L	A	30 nM

Figure 2-3. Results from Library 6: “The Hydrophobic Core”. Varied positions in the parent SE2 LBT are shown in red. Residues selected as optimal for each position are shown in blue. The resulting consensus sequences, the LBTs “SE3” and “SE4,” are outlined in blue.

The hydrophobic side chains at positions 0 (an isoleucine residue) and 14 (a leucine residue) in SE2 appear to be solvent-exposed in the crystal structure, as seen in Figure 2-1 (the orientations of the grey side chains of these residues are most visible in Figure 2-1C). Hence, Library 7 (Figure 2-4) was designed in part to address whether these residues were optimal through experimentation with a variety of hydrophilic residues at these two positions. This 320-peptide library enabled assessment of whether a single additional N-terminal (position -2) residue would be beneficial. (The N-terminus of SE2, also colored grey with nitrogen in blue, is visible in Figure 2-1 as well.) Analysis of results of this library clearly indicated that Ile0 and Leu14 are in fact already optimized, and that a single additional N-terminal residue was unnecessary. The parent LBT, SE2, was therefore re-isolated from this library.

Position	-2	-1	0	1	2	3	4	5	6	7	8	9	10	11	12	13	14	15	K_D, Tb^{3+}	
Peptide																				
<u>SE2</u>			Y	I	D	T	N	N	D	G	W	Y	E	G	D	E	L	L	A	57 nM
	A		A																	
	D		D																	
	E		E																	
	N		I																	
	S		N																	
	T		Q																	
	Y		T																	
			Y																	

SE2 **Y I D T N N D G W Y E G D E L L A** 57 nM

Figure 2-4. Results from Library 7: “Interactions with the Solvent” (or “TEN_DAYS,” from an anagram of the position -2 variations). Varied positions in the parent SE2 LBT are shown in red. Residues selected as optimal for each position are shown in blue. The resulting consensus sequence, the parent LBT “SE2,” is outlined in blue.

Following the completion of Libraries 5, 6, and 7, the hypothesis that results from multiple libraries on different parts of the LBT sequence could be combined was tested and validated. Integrating the data of the “Extension of the C-Terminus” library (Library 5) and “The Hydrophobic Core” library (Library 6) yields a new peptide, SENG (“Sticky Ends the Next Generation”), which has a tighter binding constant than any of the progenitor sequences (Figure 2-5). This is the tightest known, “disulfide-bond free” LBT to date, being nearly three orders of magnitude tighter than the original LBT-Ref. SENG has a dissociation constant for Tb^{3+} of 18 nM, which is comparable to that of many native, calcium-binding proteins.

Position	-1	0	1	2	3	4	5	6	7	8	9	10	11	12	13	14	15	16	17	18	K_D, Tb^{3+}	
Peptide																						
<u>SE2</u>		Y	I	D	T	N	N	D	G	W	Y	E	G	D	E	L	L	A			57 nM	
<u>SE2a</u>		Y	I	D	T	N	N	D	G	W	Y	E	G	D	E	L	L	L	E	E	G	36 nM
<u>SE4</u>		F	I	D	T	N	N	D	G	W	I	E	G	D	E	L	L	A			30 nM	
<u>SENG</u>		F	I	D	T	N	N	D	G	W	I	E	G	D	E	L	L	L	E	E	G	18 nM

Figure 2-5. Combination of Results from Libraries 5 and 6 to Optimize the LBT. Varied positions from Libraries 5 and 6 in the parent LBT, SE2, are shown in red. Residues changed as a result of these libraries for SE2a and SE4 are shown in blue. The cumulative consensus sequence, the LBT “SENG,” is outlined in blue.

2-2. Tb^{3+} -Bound Water Molecules and Relative Luminescence Intensity of LBTs

In order to optimize LBTs for applications utilizing luminescence, such as Luminescence Resonance Energy Transfer (LRET), the luminescence intensity and lifetime should both be

maximized. The main potential hindrance to optimal lifetime is the presence of water molecules in the inner coordination sphere of Tb^{3+} , because this enables excited-state energy to be rapidly transformed into vibrational energy of the O–H bond, in a process much faster than luminescence emission.⁴ The crystal structure of SE2 showed only peptide ligands coordinated to the central Tb^{3+} ion. However, as a more rapid way to determine the number of coordinated water molecules, the method of Beeby *et al.* was used.⁵ Briefly, solutions of 2 μM LBT were made in water with varying percentages of deuteration. (The O–D bond is much less efficient at quenching excited- Tb^{3+} than is the O–H bond.) The LBT was saturated with Tb^{3+} and the time-gated luminescence decay was measured and fit to equation (1), where I is the luminescence intensity at time t , and τ is the luminescence lifetime.

$$I(t) = I(0)e^{-t/\tau} \quad (1)$$

Values of τ were then compared at different ratios of $\text{H}_2\text{O}:\text{D}_2\text{O}$, and $\tau_{\text{H}_2\text{O}}$ and $\tau_{\text{D}_2\text{O}}$ were determined (where the subscript denotes the calculated value in 100% of that solvent). These values were then substituted into equation (2), where A' is a constant ($A' = 5$ for Tb^{3+}) and q is the number of coordinated water molecules.⁵

$$q = A' \left(\frac{1}{\tau_{\text{H}_2\text{O}}} - \frac{1}{\tau_{\text{D}_2\text{O}}} - 0.06 \right) \quad (2)$$

Starting with the LBT SE2, determination of the value of q was performed routinely as part of the photophysical characterization experiments, in addition to determination of the K_{D} for Tb^{3+} by luminescence titration. (When q is reported, values of 0.15 or less indicate an absence of bound water molecules.) In addition, the relative luminescence intensities of LBTs saturated with Tb^{3+} are compared, for ease of sequence-selection for applications that require brighter LBTs. In this thesis, the LBT SE3 will be nominally defined to have a luminescence intensity of 1.0, and all others will be compared to it.

Finally, it should be mentioned that, unless otherwise noted, luminescence titrations to determine K_{D} are conducted at $[\text{LBT}] = 50 \text{ nM}$. For some of the LBTs included herein, this concentration is higher than the K_{D} , and the accuracy of K_{D} values much tighter than this could be limited. Therefore, in addition to the titrations in buffer containing 0.1 M NaCl at pH 7.0 for maintenance of constant ionic strength, “Acetate-Buffer Titrations” (which instead use 0.1 M NaOAc at pH 7.0) are also conducted. Acetate weakly coordinates Ln^{3+} ions,⁶ artificially

weakening the binding. These numbers enable a qualitative (though not necessarily quantitative) comparison of tight-binding LBTs. A summary of photophysical data for the LBTs SE2, SE3, and SENG is included in Table 2-1. (The value of q was determined for SE3 in both normal and acetate buffer, and there was no significant difference, indicating that this buffer does not have a significant effect on the mode of binding.)

Table 2-1. Photophysical Data of Select Single-LBTs.^a

<u>LBT</u>	K_D, Tb^{3+}		<i>Relative Intensity</i>	q
	<i>Direct Tb^{3+} Titrations</i>	<i>Acetate-Buffer Titrations</i>		
<u>SE2</u>	57 nM	1900 nM	1.9	0.03
<u>SE3</u>	38 nM	980 nM	1.0	0.08
<u>SENG</u>	18 nM	540 nM	1.3	0.11

^a Portions of the data in this table have been previously published.^{1,2,7}

2-3. Results of Single Mutations at Specific Positions in the LBT¹

Uses have emerged for lanthanide-binding peptides beyond those of a simple protein tag.⁸ If further applications of LBTs require unavoidable mutations or modifications, it should be noted that certain residues show greater flexibility to variation than others. Table 2-2 includes a variety of single amino-acid mutations from SE2 (K_D of 57 nM for Tb^{3+}) and the approximate resulting dissociation constant for Tb^{3+} , as well as a hypothesized role for each amino acid.

Table 2-2. Mutational Analyses of SE2 Amino Acid Residues

Position	SE2	Hypothesized role	Mutational analysis
-1	Y	Part of the hydrophobic core with positions 8 and 13. ²	Y-1→W shows comparable Tb ³⁺ affinity, and Y-1→F is optimal for lanthanide-binding at this position. Deletion causes a precipitous drop in affinity. This position appears to have a small effect on luminescence output.
0	I	Side-chain exposed to solution, but Library 7 (Figure 2-4) established Ile as optimal. Possibly involved in the organization of the <i>apo</i> state.	I0→T gives a small but noticeable drop in affinity, yet is still a reasonable tag. I0→R is much weaker, with a K _D for Tb ³⁺ near 350 nM.
1	D	Monodentate lanthanide-ligating residue.	Sykes and coworkers established that even D1→N is inferior. ⁹
2	T	Appears to form a hydrogen-bond with E12 in the crystal structure. ³	T2→V and most <u>SE1b</u> variants (see Figure 1-14) bind Tb ³⁺ in the 100 nM range; some variation at this residue is tolerable.
3	N	Monodentate lanthanide-ligating residue.	Sykes and coworkers established that even N3→D is inferior. ⁹
4	N	A spacer between ligating positions; accepts variation.	Substitution of Asn with Ala, Asp, Glu, and Gly at this position show comparable or improved affinity. See also Chapter 5.
5	D	Monodentate lanthanide-ligating residue.	Sykes and coworkers established that even D5→N is inferior. ⁹
6	G	In a turn populating glycine Ramachandran space.	None; presumed necessary for position 7 backbone-carbonyl to orient properly, but see Chapter 5.
7	W	Contains the lanthanide-coordinating main-chain carbonyl.	Studies by Szabo and coworkers established W7 as the optimum sensitizer for Tb ³⁺ . ¹⁰ Non-natural antennae can also be used here. ¹¹
8	Y	Part of the hydrophobic core with positions -1 and 13. ³	Y8→I is optimal for Tb ³⁺ -binding. Y8R decimates affinity. This residue strongly influences relative luminescence intensity; Tyr is optimal in this regard.
9	E	Bidentate ligating residue.	Calcium-binding loops usually include D9 instead of E9. ¹² Falke and coworkers established E9 as optimal for lanthanides. ¹³
10	G	In a turn populating glycine Ramachandran space.	None; necessary for E12 to align appropriately.
11	D	Asp appears to be the best residue for this turn sequence.	D11→R gives μM affinity; other mutations may be acceptable. (See Figure 1-14.)
12	E	Bidentate ligating residue.	Firmly established by Library 1 (Figure 1-12).
13	L	Part of the hydrophobic core with positions -1 and 8. ³	Leucine is optimal, by Library 6 (Figure 2-3). L13→A gives a K _D in the μM range.
14	L	Side-chain is exposed to solution, but Library 7 (Figure 2-4) established Leu as optimal. Possibly involved in organization of the <i>apo</i> state.	L13→Q gives a small but noticeable reduction in affinity. Deletion and L13R yield progressively worse affinities.
15+	A	Unclear at present.	Library 5 (Figure 2-2) indicated that additional C-terminal, acidic residues were beneficial, as in the LBT <u>SENG</u> .

2-4. Studies on the Effects of Deleterious Mutations on the LBT Sequence

Early in the development of LBTs such as SE2, SE3, and SENG, studies were conducted to examine the coordination and sensitization of terbium ion (Tb^{3+}). Previous work by Sykes and coworkers had demonstrated that Asp, Asn, and Asp were optimal for Ln^{3+} -binding at positions 1, 3, and 5, respectively,⁹ and these residues were reselected by Dr. Mark Nitz in a library preceding Library 1.¹⁴ Library 1 (see Chapter 1) verified that Glu was optimal at positions 9 and 12, confirming the results of Falke and coworkers;¹³ these positions were not further tested.^{1,2} The crystal structure of the SE2- Tb^{3+} complex showed that the Glu at position 9 (usually an Asp in native calcium-binding motifs), along with the Gly at position 10 (which is necessary due to the Ramachandran space that residue occupies in SE2) precludes water-coordination.³ The optimal location for the Trp residue, at position 7, was discovered prior to the development of LBTs, in the Szabo lab.¹⁰

When using an LBT as an N- or C-terminal tag, it is clearly most advantageous to use one of the optimized sequences; however, it may also be of interest to mutate an inner portion of a protein target to be LBT-like. In this case, additional constraints may exist, such as side chains necessary for folding or catalysis, which would then be unmutatable residues. Furthermore, because position 9 in the EF-hand motif is Asp in the majority of known calcium-binding proteins,¹² it might be beneficial to know the effect of a Glu→Asp mutation at this position.

Therefore, using SE3 as the parent sequence, three new “suboptimal” LBT sequences were designed. The LBT qSE3 (“quiet-SE3”) moves the tryptophan sensitizer to position 2 (the second-best position found by Szabo and coworkers¹⁰). The LBTs wSE3 (“wet-SE3”) and mSE3 (“moist-SE3”) both contained a Glu9→Asp mutation; wSE3 also changed the glycine at position 10 back to the isoleucine found in native Troponin-C. Table 2-2 shows the full sequences and the pertinent photophysical data for these LBTs.

Table 2-3. Photophysical Data of LBT Mutants to Determine the Effects of Specific Deleterious Mutations

<i>LBT</i>	<i>Sequence</i> ^a	K_D , Tb^{3+} ^b	<i>Relative Intensity</i>	<i># of Tb^{3+}-bound water molecules</i> ^c
<u>SE3</u>	YIDTNNDGWIEGDELLA	38 nM	1.00	0
<u>qSE3</u>	YIDWNNNDGLIEGDELLA	~10 nM ^d	0.17	0
<u>wSE3</u>	YIDTNNDGWIDIDELLA	2000 nM	0.10	1
<u>mSE3</u>	YIDTNNDGWIDGDELLA	1200 nM	0.14	1

^a Mutations from the parent SE3 sequence are shown in bold-face.

^b Determined by direct titrations; titrations in acetate buffer were not performed. The titrations of qSE3 had to be performed at a concentration well above the K_D , so the value should be considered more of an estimate.

^c Values of q , rounded to the nearest integer.

^d The value of 10 nM should be considered approximate; the low luminescence of this complex required the use of 100 nM peptide in the luminescence titration, which is well above the K_D value.

Clearly, any of these mutations are quite deleterious to the luminescence output of the LBT, and the admission of a water molecule is the most detrimental to luminescence (although see also Chapter 6). More importantly, the Glu9→Asp mutation significantly reduces affinity, although mutation of the amino acids at positions 2 and 7 show no negative effects. Therefore, if an LBT is to be inserted into a protein using site-directed mutagenesis (rather than inserting it at a terminus or within a loop), it is vital that the residues with ligating side-chains (Asp1, Asn3, Asp5, Glu9 and Glu12) be unaltered. Some LBT applications, such as NMR and crystallography, do not require a sensitizer,^{15,16} obviating the necessity for a tryptophan residue. However, to take full advantage of the versatile properties of the Tb^{3+} ion, Trp7 should also be included.

Conclusions

Combinatorial libraries have resulted in the generation of the tightest single Lanthanide-Binding Tag to date, SENG, which binds Tb^{3+} with a 18 nM dissociation constant. Titration in a buffer containing sodium acetate (instead of the normal sodium chloride) artificially weakens the affinity of LBTs for Tb^{3+} , enabling a qualitative comparison of the best LBTs. For applications of LBTs that do not require a luminescent signal, mutation of Trp7 has no negative effects on LBT- Ln^{3+} affinity. However, in the context of the current structural framework, mutation of the ligating residues of even the best LBTs to date should be avoided, as this lowers affinity by more than an order of magnitude.

Experimental

2-OE. General Procedures

Peptide Synthesis and Purification.

Peptides were prepared by standard N-fluorenylmethoxycarbonyl (Fmoc)-based solid phase peptide synthesis (SPPS) procedures. Single-LBT peptides were synthesized on either Fmoc-PAL-PEG-PS (peptide amide linker-polyethyleneglycol-polystyrene) resin macrobeads (190 $\mu\text{mol/g}$) (Applied Biosystems, Foster City, CA), or on NovaPEG Rink Amide LL resin (EMD Biosciences, San Diego, CA). Peptides were synthesized on an automated ABI 431A Peptide Synthesizer (Applied Biosystems).

All Fmoc-protected amino acids and peptide coupling reagents including HOBt (N-hydroxybenzotriazole) and HBTU (2-(1H-benzotriazole-1-yl)-1,1,3,3-tetramethyluronium hexafluorophosphate) were purchased from Applied Biosystems, EMD Biosciences, or GenScript (Piscataway, NJ). All other reagents, including solvents, were purchased from Sigma-Aldrich (St. Louis, MO).

HPLC (high-performance liquid chromatography) was performed using a Waters 600E HPLC fitted with a Waters 600 automated control module and a Waters 2487 dual wavelength absorbance detector recording at 228 and 280 nm. The standard linear gradient for preparatory HPLC was 95:5 to 5:95 (water : acetonitrile, 0.1% TFA) over 30 minutes. Five minutes of 95:5 was run before the gradient, and five minutes of 5:95 was run after the gradient. The flow rate was 15 mL/min. Peptide identification and purity were confirmed by MALDI mass spectroscopy on a PerSeptive Biosystems Voyager MALDI-TOF instrument using a 2,5-dihydroxybenzoic acid (DHB) matrix.

Coupling procedures that were used were standard for Fmoc-based SPPS. Deprotection was achieved by at least two treatments for five or more minutes with 20% 4-methylpiperidine (in lieu of “regular” piperidine)¹⁷ in NMP (1-methyl-2-pyrrolidinone, Sigma-Aldrich). In general, automated synthesis (on the ABI 431A) was used. For all automated peptide syntheses, a double-coupling was used, as well as acetic anhydride capping after each step to minimize deletion peptides. Peptide coupling steps used 4 equiv. Fmoc-amino acid per equiv. resin, 4 equiv. (each) HOBt and HBTU activating agents, with 8 equiv. diisopropylethylamine (DIPEA) in NMP, for at least one hour at room temperature. (Chemistry files for the ABI are included in the appendix). For manual couplings, 4 equiv. of PyBOP (benzotriazole-1-yl-oxy-tris-pyrrolidino-phosphonium hexafluorophosphate) was used instead of HOBt/HBTU, and after

each coupling reaction, a few beads of resin were tested with TNBS (trinitrobenzene sulfonic acid) to verify complete coupling. The full-length peptide N-terminus was used as a free amine.

Side chain deprotection and cleavage from the resin (to yield a C-terminal amide) was carried out using a cocktail of 94% trifluoroacetic acid (TFA), 2.5% 1,2 ethanedithiol (EDT), 2.5% H₂O, and 1% triisopropyl silane (TIS), shaking for 2 hours at room temperature. Peptides were purified by HPLC and confirmed by MALDI-MS. Expected masses were calculated using a web-based calculator.¹⁸ Purified peptides were lyophilized, and dissolved in a buffer of 100 mM NaCl, 20 mM HEPES, pH 7.0. Concentrations of these stock solutions were determined by the UV absorption of tryptophan ($\epsilon_{280} = 5690 \text{ cm}^{-1}\text{M}^{-1}$), tyrosine ($\epsilon_{280} = 1280 \text{ cm}^{-1}\text{M}^{-1}$) and cysteine ($\epsilon_{280} = 120 \text{ cm}^{-1}\text{M}^{-1}$) amino acid content in 6 M guanidinium chloride.¹⁹

Luminescence Titrations.

Titrations were recorded on a Jobin Yvon Horiba Fluoromax-3 Spectrometer in a 1 cm path-length quartz cuvette. Tryptophan-sensitized Tb³⁺ luminescence was collected by excitation at 280 nm and by recording emission at 544 nm; a 315 nm long-pass filter was used to avoid interference from harmonic doubling. Slit widths of 5 nm were used, with 1 second integration times. Spectra were recorded at 25°C, and were corrected for intensity using the manufacturer-supplied correction factors. Peptide or protein solutions were prepared in 3 mL buffer (pH 7.0). For direct titrations, the buffer was 100 mM NaCl, 10 mM MOPS (3-(N-morpholino)propanesulfonic acid), pH 7.0. For “relative” (qualitative comparison) titrations, the buffer was 100 mM NaOAc, 10 mM HEPES, pH 7.0.

Tb³⁺ stock solutions were prepared from the TbCl₃-hydrate salts (Sigma-Aldrich) as ~50 mM solutions in 1 mM HCl, and were diluted as needed. Exact concentrations were determined by colorimetric titrations using a standardized EDTA solution (Aldrich) and a Xylenol Orange indicator as described in the literature.²⁰ Aliquots of Tb³⁺ were added to a 3 mL solution of peptide or protein (50 nM for direct titrations, 100 nM for titrations in acetate buffer). For direct titrations, after a background data point was obtained, seven 1 μL aliquots of 40 μM Tb³⁺ were added, followed by three aliquots of 1 $\mu\text{L} \times 100 \mu\text{M}$ Tb³⁺, three aliquots of 1 $\mu\text{L} \times 200 \mu\text{M}$ Tb³⁺, and one aliquot of 1 $\mu\text{L} \times 1 \text{ mM}$ Tb³⁺. After each addition, the solution was mixed by pipet-aspiration and a data point taken. Relative titrations were conducted in the same manner, except

with three aliquots of $1 \mu\text{L} \times 200 \mu\text{M Tb}^{3+}$, seven aliquots of $1 \mu\text{L} \times 1 \text{mM Tb}^{3+}$, and four aliquots of $1 \mu\text{L} \times 5 \text{mM Tb}^{3+}$.

Luminescence titration spectra obtained in this fashion were analyzed with the program SPECFIT/32,²¹ which determines $\log \beta$ values (β = binding constant) using the equilibrium data. Calculated $\log \beta$ values were then translated into the dissociation constants ($K_D = 10^{-\log \beta}$). Reported values are the average of three or four trials. Sample SPECFIT data files are shown in the Appendix.

Relative Luminescence Intensity.

Comparative luminescence intensities of LBTs were determined by comparing the molar luminescence outputs, as determined in SPECFIT²¹ using the direct titration data (*vide supra*); that of the LBT SE3 was arbitrarily normalized to an output of 1.00.

Determination of Tb^{3+} -bound water molecules.

Luminescence lifetimes were measured in a Jobin Yvon Horiba Fluoromax-3 Spectrometer, equipped with a Spex 1934D3 phosphorimeter. Samples were excited by a pulse of 280 nm light for 70 ms. Data were collected at 544 nm for 15 ms in 30 μs increments following a 50 μs delay. Slit widths were 5 nm for excitation and 10 nm for emission. Samples were 2 μM peptide, with 2.5 equiv. Tb^{3+} , in 100 mM NaCl, 10 mM MOPS (pH 7.0) in a 500 μL cuvette. Data sets were fit to a single exponential decay, and lifetimes in varying percentages of D_2O (Cambridge Isotope Laboratories) were plotted on a curve to determine the lifetimes in pure H_2O and pure D_2O . The number of Tb^{3+} -bound water molecules, q , could then be calculated using equation (2) as described in the literature. $A'_{\text{Tb}} = 5 \text{ ms}$, τ is the lifetime in the specified solvent, and -0.06 ms^{-1} is the correction factor for outer-sphere water molecules.⁵

$$q = A' \left(\frac{1}{\tau_{\text{H}_2\text{O}}} - \frac{1}{\tau_{\text{D}_2\text{O}}} - 0.06 \right) \quad (2)$$

2-1E. Additional Combinatorial Libraries to Evolve the SE2 Sequence

Library screens were conducted and winners determined as described in the literature.^{1,2}

Library 7: “TEN DAYS”.

Figure 1-10 includes a diagram of split-and-pool synthesis for library generation.

Figure 1-11 includes a diagram of the library-generation protocol.

TentaGel Macrobeads (Rapp Polymere, Tübingen, Germany) were weighed into a fritted funnel (1 g, 0.21 mmol/g). Resin was swelled for 1 min. with DMF; for all swelling and reaction steps, N₂ gas was bubbled through to ensure complete mixing, and liquid was drained by vacuum filtration. All reactions were performed under air atmosphere at room temperature.

A *para*-nitrophenylalanine residue was first coupled to the resin, to help quench the auto-fluorescence of the TentaGel resin. Fmoc-*p*NO₂Phe-OH (274 mg, 3 equiv.) and PyBOP (benzotriazole-1-yl-oxy-tris-pyrrolidino-phosphonium hexafluorophosphate, 327 mg, 3 equiv.) were dissolved in ~6 mL of DMF, and added to the resin. DIPEA (290 μL, 8 equiv.) was then added to the mixture, and was allowed to react for one hour. Resin was drained, and the step was repeated with new reagents for another hour. The resin was then washed five times with DMF.

The Fmoc group was then removed by treatment with two 5 mL aliquots of 20% piperidine in DMF for about five minutes each. This solution was collected and diluted to 100 mL in methanol for UV analysis to determine yield ($\epsilon_{300(\text{Fulvene})} = 7800 \text{ M}^{-1}\text{cm}^{-1}$); obtained 154 μmol, so 73% yield.

Next, the orthogonal linkers (ammonium hydroxide-labile HMBA, 80%, and photolabile ANP, 20%) were coupled. In 4 mL DMF was dissolved HMBA (4-hydroxymethylbenzoic acid, 145 mg, 4 equiv.), Fmoc-ANP (3-amino-3-(2-nitrophenyl)propionic acid, 48 mg, 1 equiv.), HOBt (166 mg, 5 equiv.), and DIC (165 μL, 5 equiv.), and the solution was added to the resin and allowed to react for one hour. The resin was then filtered and washed five times with DMF.

To couple the β-alanine residue, the symmetric anhydride was made. In a 50 mL round-bottom flask equipped with a stir bar was added 665 mg Fmoc-βAla-OH and 10 mL DCM (the former did not completely dissolve). Next, 165 μL DIC was added and the solution turned clear, briefly. The mixture was stirred under open atmosphere for 30 minutes at room temperature, and the solvent was then removed by rotary evaporation. The residue was dissolved in DMF and immediately added to the resin, along with 20 mg of DMAP (4-(Dimethylamino)pyridine); the mixture was allowed to react for three hours. Resin was then washed five times with DMF, and twice with DCM. The four-residue spacer (–Gly-Pro-Pro-Arg–) was appended using standard Fmoc-based SPPS on the ABI 431A, as described above (2-0E). For storage, the terminal Fmoc

protecting group is left attached, and the resin was washed with DCM; it is stored at 4°C until use.

The C-terminal residue of the LBT, an alanine, was coupled on the ABI 431A, using standard Fmoc-based SPPS chemistry as described above (2-*OE*), on 200 mg (~60 μmol) of the resin. The resin was then divided into five equal portions, and each portion had one of the position 9 variable amino acids (Fmoc-Glu(*t*Bu)-OH, 8.9 mg; Fmoc-Leu-OH, 8.5 mg; Fmoc-Asn(*Trt*)-OH, 9.1 mg; Fmoc-Gln(*Trt*)-OH, 9.1 mg; or Fmoc-Tyr(*t*Bu)-OH, 9.0 mg; 24 μmol of each) coupled by hand using PyBOP (12.5 mg, 24 μmol) as an activating agent in DMF, with 8.2 μl (48 μmol) DIPEA. The resin was then pooled and the sequence **-DTNNDGWYEGDEL-** was coupled on the ABI.

The resin was split again, this time into eight equal portions. Using PyBOP (39 mg, 75 μmol, 10 equiv.) as an activating agent, onto each portion one of the following variations at position 0 was coupled. Fmoc-Ile-OH (24 mg, 90% of 75 μmol) and Boc-Ala-OH (1.4 mg, 10% of 75 μmol); or Fmoc-Thr(*t*Bu)-OH (25 mg, 85% of 75 μmol) and Boc-Thr(*Bzl*)-OH (3.5 mg, 15% of 75 μmol); or Fmoc-Tyr(*t*Bu)-OH (26 mg, 85% of 75 μmol) and Boc-Tyr(*Bzl*)-OH (4.2 mg, 15% of 75 μmol); or Fmoc-Asp(*t*Bu)-OH (26 mg, 85% of 75 μmol) and Boc-Glu(*Bzl*)-OH (3.8 mg, 15% of 75 μmol); or Fmoc-Glu(*t*Bu)-OH (24 mg, 85% of 75 μmol) and Boc-Arg(*Tos*)-OH (4.8 mg, 15% of 75 μmol); or Fmoc-Asn(*Trt*)-OH (23 mg, 85% of 75 μmol) and Ac-Leu-OH (1.9 mg, 15% of 75 μmol); or Fmoc-Gln(*Trt*)-OH (24 mg, 85% of 75 μmol) and Bz-Leu-OH (2.6 mg, 15% of 75 μmol); or Fmoc-Ala-OH (20 mg, 85% of 75 μmol) and Bz-Ala-OH (2.2 mg, 15% of 75 μmol); were coupled in DMF.

The resin was pooled again to couple the N-terminal tyrosine on the ABI. Finally, the resin was again split into eight equal portions and each portion had one of the position -2 variable amino acids coupled by hand. Except for the last portion, this was done using PyBOP (7.8 mg, 15 μmol) as an activating agent in DMF, with 5.1 μl (30 μmol) DIPEA. Onto seven of the portions were coupled one of the following: Fmoc-Thr(*t*Bu)-OH, 6.0 mg; Fmoc-Glu(*t*Bu)-OH, 6.4 mg; Fmoc-Asn(*Trt*)-OH, 9.0 mg; Fmoc-Asp(*t*Bu)-OH, 6.2 mg; Fmoc-Ala-OH, 4.7 mg; Fmoc-Tyr(*t*Bu)-OH, 6.9 mg; or Fmoc-Ser(*t*Bu)-OH, 5.8 mg; 15 μmol of each. Nothing was coupled to the eighth portion, to account for the possibility that the absence of an amino acid might be optimal at this position. The resin was pooled for Fmoc deprotection and N-terminal acetyl capping.

Side-chain protecting groups were removed by treatment with the TFA cocktail (94% TFA, 2.5% EDT, 2.5% H₂O, and 1% TIS). The resin was then washed with TFA, then washed twice with DCM, twice with DMF, thrice with H₂O, and then with 40 mL of 100 mM HEPES pH 7.0 buffer. Luminescent-bead experiments were then performed in an agarose gel as described, with 100 μ M NTA added to increase selection.^{1,2}

Five beads were successfully picked, and were washed to remove the agarose. The beads were treated with fresh 28% NH₄OH at room temperature overnight, and then concentrated to dryness on the speedivac. The white residue was dissolved in 50/50 water/acetonitrile; MALDI analyses showed peaks corresponding to masses for the following peptides. These peptides were then titrated with Tb³⁺ to obtain rough K_D values (Table 2-4).

Table 2-4. Winning Peptides from the “TEN_DAYS” Library

Ac-	-2	Y	\emptyset	DTNNDGWIEGDEL	I4	A	Approx K_D , Tb ³⁺
Ac-	Y	Y	I	DTNNDGWIEGDEL	N	A	1000 nM
Ac-	T	Y	I	DTNNDGWIEGDEL	E	A	374 nM
Ac-	E	Y	I	DTNNDGWIEGDEL	N	A	265 nM
Ac-	E	Y	I	DTNNDGWIEGDEL	Q	A	319 nM
Ac-	--	Y	I	DTNNDGWIEGDEL	E	A	321 nM

The peptides H₂N-**EYIDTNN**DGWYEGDELNA-CONH₂, H₂N-**EYIDTNN**DGWYEGDELEA-CONH₂, and H₂N-**YIDTNN**DGWYEGDELQA-CONH₂ were synthesized on the ABI 431A and found to have K_D values inferior to that of SE2 (all were in the 80 – 100 nM range); therefore, the parent LBT SE2 was declared the winner of this library.

2-2E. Tb³⁺-Bound Water Molecules and Relative Luminescence Intensity of LBTs

SE2: H₂N-**YIDTNN**DGWYEGDELLA-CONH₂

SE2 peptide was a gift from Mark Nitz² and was used without further purification.

$\text{Log } \beta$ (Tb³⁺, 1:1_{NaCl/MOPS}) (also previously reported)² = 7.23 \pm 0.01

$\text{Log } \beta$ (Tb³⁺, 1:1_{NaOAc/HEPES}) = 5.72 \pm 0.02

Molar luminescence intensity (1:1) = 9.76 \times 10¹² M⁻¹cm⁻¹

Luminescence decay (previously reported)³: τ_{H_2O} = 2.6 ms; τ_{D_2O} = 3.4 ms

SE3: H₂N-YIDTNN~~GW~~IEGDELLA-CONH₂

SE3 was prepared using standard Fmoc-based SPPS as described on PAL-PEG-PS resin, cleaved by TFA cocktail and purified as described by RP-HPLC ($t_R = 19.4$ min). Exact mass calcd., 1935.8 [M+H⁺]; found 1934.9 [M+H⁺], 1957.3 [M+Na⁺] by MS(MALDI).

$$\text{Log } \beta (\text{Tb}^{3+}, 1:1_{\text{NaCl/MOPS}}) = 7.42 \pm 0.05$$

$$\text{Log } \beta (\text{Tb}^{3+}, 1:1_{\text{NaOAc/HEPES}}) = 6.01 \pm 0.02$$

$$\text{Molar luminescence intensity (1:1)} = 5.50 \times 10^{12} \text{ M}^{-1}\text{cm}^{-1}$$

$$\text{Luminescence decay: } \tau_{\text{H}_2\text{O}} = 2.62 \text{ ms; } \tau_{\text{D}_2\text{O}} = 3.28 \text{ ms}$$

$$\text{Luminescence decay (acetate buffer): } \tau_{\text{H}_2\text{O}} = 2.59 \text{ ms; } \tau_{\text{D}_2\text{O}} = 3.23 \text{ ms}$$

SENG: H₂N-FIDTNN~~GW~~IEGDELLLEEG-CONH₂

SENG was prepared using standard Fmoc-based SPPS as described on PAL-PEG-PS resin, cleaved by TFA cocktail and purified as described by RP-HPLC ($t_R = 19.7$ min). Exact mass calcd., 2279.4 [M+H⁺]; found 2277.5 [M+H⁺], 2298.6 [M+Na⁺] by MS(MALDI).

$$\text{Log } \beta (\text{Tb}^{3+}, 1:1_{\text{NaCl/MOPS}}) = 7.74 \pm 0.01$$

$$\text{Log } \beta (\text{Tb}^{3+}, 1:1_{\text{NaOAc/HEPES}}) = 6.27 \pm 0.03$$

$$\text{Molar luminescence intensity (1:1)} = 7.21 \times 10^{12} \text{ M}^{-1}\text{cm}^{-1}$$

$$\text{Luminescence decay: } \tau_{\text{H}_2\text{O}} = 2.55 \text{ ms; } \tau_{\text{D}_2\text{O}} = 3.22 \text{ ms}$$

2-3E. Results of Single Mutations at Specific Positions in the LBT

Based on the literature.¹

2-4E. Studies on the Effects of Deleterious Mutations on the LBT Sequence

Peptides were photophysically characterized as described above.

qSE3: H₂N-YIDWNN~~DGL~~IEGDELLA-CONH₂

qSE3 was prepared using standard Fmoc-based SPPS as described on PAL-PEG-PS resin, cleaved by TFA cocktail and purified as described by RP-HPLC ($t_R = 19.8$ min). Exact mass calcd., 1950.1 [M+H⁺]; found 1949.5 [M+H⁺], 1970.6 [M+Na⁺] by MS(MALDI).

$$\text{Log } \beta (\text{Tb}^{3+}, 1:1_{\text{NaCl/MOPS}}) = 8.00 \pm 0.07$$

$$\text{Molar luminescence intensity (1:1)} = 0.91 \times 10^{12} \text{ M}^{-1}\text{cm}^{-1}$$

$$\text{Luminescence decay: } \tau_{\text{H}_2\text{O}} = 2.56 \text{ ms; } \tau_{\text{D}_2\text{O}} = 3.32 \text{ ms}$$

wSE3: H₂N-YIDTNNDGWIDIDELLA-CONH₂

wSE3 was prepared using standard Fmoc-based SPPS as described on PAL-PEG-PS resin, cleaved by TFA cocktail and purified as described by RP-HPLC ($t_R = 21.6$ min). Exact mass calcd., 1980.1 [M+H⁺]; found 1977.4 [M+H⁺], 1999.5 [M+Na⁺] by MS(MALDI).

$$\text{Log } \beta (\text{Tb}^{3+}, 1:1_{\text{NaCl/MOPS}}) = 5.70 \pm 0.05$$

$$\text{Molar luminescence intensity (1:1)} = 0.54 \times 10^{12} \text{ M}^{-1} \text{ cm}^{-1}$$

$$\text{Luminescence decay: } \tau_{\text{H}_2\text{O}} = 0.56 \text{ ms; } \tau_{\text{D}_2\text{O}} = 1.56 \text{ ms}$$

mSE3: H₂N-YIDTNNDGWIDGDELLA-CONH₂

mSE3 was prepared using standard Fmoc-based SPPS as described on PAL-PEG-PS resin, cleaved by TFA cocktail and purified as described by RP-HPLC ($t_R = 19.8$ min). Exact mass calcd., 1922.9 [M+H⁺]; found 1922.3 [M+H⁺], 1943.0 [M+Na⁺] by MS(MALDI).

$$\text{Log } \beta (\text{Tb}^{3+}, 1:1_{\text{NaCl/MOPS}}) = 5.93 \pm 0.04$$

$$\text{Molar luminescence intensity (1:1)} = 0.91 \times 10^{12} \text{ M}^{-1} \text{ cm}^{-1}$$

$$\text{Luminescence decay: } \tau_{\text{H}_2\text{O}} = 0.71 \text{ ms; } \tau_{\text{D}_2\text{O}} = 2.07 \text{ ms}$$

Acknowledgements

Much of this chapter has been previously published, and I am thus indebted to my co-authors, especially Dr. Bianca Sculimbrene for her writing and editorial work. The design and bead-selection of Libraries 5 and 6 was done entirely by Dr. Mark Nitz, and he helped me design Library 7. Assistance from Dr. Nitz and from Dr. Melissa Shults on use of the fluorometer is also gratefully acknowledged. I am eternally grateful to Mark Chen for editing this chapter.

References

- (1) Martin, L. J.; Sculimbrene, B. R.; Nitz, M.; Imperiali, B. "Rapid Combinatorial Screening of Peptide Libraries for the Selection of Lanthanide-Binding Tags (LBTs)." *QSAR Comb. Sci.* **2005**, *24(10)*, 1149-1157.
- (2) Nitz, M.; Franz, K. J.; Maglathlin, R. L.; Imperiali, B. "A powerful combinatorial screen to identify high-affinity terbium(III)-binding peptides." *ChemBioChem* **2003**, *4(4)*, 272-276.
- (3) Nitz, M.; Sherawat, M.; Franz, K. J.; Peisach, E.; Allen, K. N.; Imperiali, B. "Structural origin of the high affinity of a chemically evolved lanthanide-binding peptide." *Angew. Chem. Int. Ed.* **2004**, *43(28)*, 3682-3685.
- (4) Horrocks, W. D., Jr.; Sudnick, D. R. "Lanthanide ion probes of structure in biology. Laser-induced luminescence decay constants provide a direct measure of the number of metal-coordinated water molecules." *J. Am. Chem. Soc.* **1979**, *101(2)*, 334-340.
- (5) Beeby, A.; Clarkson, I. M.; Dickins, R. S.; Faulkner, S.; Parker, D.; Royle, L.; de Sousa, A. S.; Williams, J. A. G.; Woods, M. "Non-radiative deactivation of the excited states of europium, terbium and ytterbium complexes by proximate energy-matched OH, NH and CH oscillators: an improved luminescence method for establishing solution hydration states." *J. Chem. Soc., Perkin Trans. 2* **1999**, (3), 493-504.
- (6) Martell, A. E.; Smith, R. M., *Critical Stability Constants, Vol. 1: Amino Acids*. Plenum Press: New York, 1974;
- (7) Martin, L. J.; Hähnke, M. J.; Nitz, M.; Wöhnert, J.; Silvaggi, N. R.; Allen, K. N.; Schwalbe, H.; Imperiali, B. "Double-Lanthanide-Binding Tags: Design, Photophysical Properties, and NMR Applications." *J. Am. Chem. Soc.* **2007**, *129(22)*, 7106-7113.
- (8) Lim, S.; Franklin, S. J. "Lanthanide-binding peptides and the enzymes that might have been." *Cell. Mol. Life Sci.* **2004**, *61*, 2184-2188.
- (9) Marsden, B. J.; Hodges, R. S.; Sykes, B. D. "Proton NMR studies of synthetic peptide analogs of calcium-binding site III of rabbit skeletal troponin C: Effect on the lanthanum affinity of the interchange of aspartic acid and asparagine residues at the metal ion coordinating positions." *Biochemistry* **1988**, *27(11)*, 4198-4206.
- (10) MacManus, J. P.; Hogue, C. W.; Marsden, B. J.; Sikorska, M.; Szabo, A. G. "Terbium luminescence in synthetic peptide loops from calcium-binding proteins with different energy donors." *J. Biol. Chem.* **1990**, *265(18)*, 10358-10366.
- (11) Reynolds, A. M.; Sculimbrene, B. R.; Imperiali, B. "Lanthanide-Binding Tags with Unnatural Amino Acids: Sensitizing Tb³⁺ and Eu³⁺ Luminescence at Longer Wavelengths." *Bioconjugate Chem.* **2008**, *19(3)*, 588-591.

- (12) Grabarek, Z. "Structural Basis for Diversity of the EF-hand Calcium-binding Proteins." *J. Mol. Biol.* **2006**, *359*, 509-525.
- (13) Drake, S. K.; Lee, K. L.; Falke, J. J. "Tuning the Equilibrium Ion Affinity and Selectivity of the EF-Hand Calcium Binding Motif: Substitutions at the Gateway Position." *Biochemistry* **1996**, *35*(21), 6697-6705.
- (14) Nitz, M.; Franz, K. J.; Imperiali, B., Unpublished results.
- (15) Su, X.-C.; Huber, T.; Dixon, N. E.; Otting, G. "Site-specific labeling of proteins with a rigid lanthanide-binding tag." *ChemBioChem* **2006**, *7*(10), 1599-1604.
- (16) Su, X.-C.; McAndrew, K.; Huber, T.; Otting, G. "Lanthanide-Binding Peptides for NMR Measurements of Residual Dipolar Couplings and Paramagnetic Effects from Multiple Angles." *J. Am. Chem. Soc.* **2008**, *130*, 1681-1687.
- (17) Hachmann, J.; Lebl, M. "Alternative to Piperidine in Fmoc Solid-Phase Synthesis." *J. Comb. Chem.* **2006**, *8*(2), 149.
- (18) Rozenski, J. Peptide Mass Calculator v3.2.
<http://rna.rega.kuleuven.ac.be/masspec/pepcalc.htm>
- (19) Chazan, A. Peptide Property Calculator.
<http://www.basic.northwestern.edu/biotools/proteincalc.html>
- (20) Pribil, R. "Present state of complexometry. IV. Determination of rare earths." *Talanta* **1967**, *14*(6), 619-627.
- (21) Binstead, R.; Jung, B.; Zuberbühler, A. *SPECFIT/32 for Windows; Original Release 2000*, Version 3.0.39; Spectrum Software Associates, Marlborough, MA.: SPECFIT/32 provides global analysis of equilibrium and kinetic systems using singular value decomposition and nonlinear regression modeling by the Levenberg-Marquardt method., 2007.

Chapter 3

Attempts Towards an IR-Emitting Lanthanide-Binding Tag

Introduction

While many lanthanide ions are capable of luminescence (Figure 3-1),¹ terbium (Tb^{3+}) is the only one that can be sensitized by the side chain of the encoded amino acid tryptophan. Although sensitizing Tb^{3+} via tryptophan at 280 nm is acceptable for most *in vitro* applications, such high-energy radiation would be damaging to living cells. Recent efforts from our lab have generated LBTs in which the tryptophan is replaced with unnatural amino acids that are excited at longer, lower-energy wavelengths, and has resulted in the generation LBTs that can sensitize Eu^{3+} luminescence.² It is further desirable to expand the scope of LBTs to include some of the other lanthanides shown in Figure 3-1.

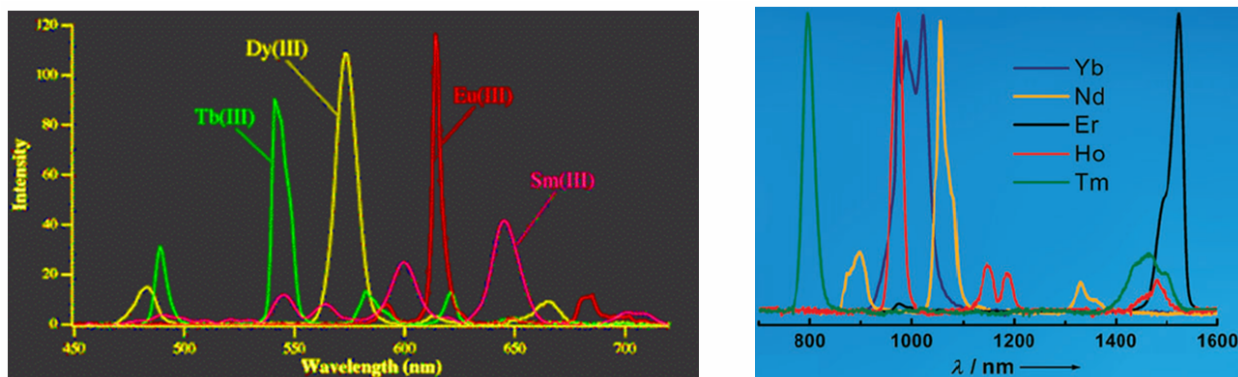


Figure 3-1. Many lanthanides luminesce, with maxima spanning a range of wavelengths from the visible to the near-IR. (The picture of the visible lanthanide emissions was appropriated from the internet,³ and the infrared lanthanide emissions from the publication of J. Zhang *et al.*⁴)

Lanthanides including Nd^{3+} , Ho^{3+} , Er^{3+} , Tm^{3+} and Yb^{3+} emit in the near-infrared (near-IR) region of the spectrum (Figure 3-1, right). Because tissue is essentially transparent to these wavelengths of light, the aforementioned lanthanides are currently growing in interest for imaging applications.⁴⁻⁶ Likewise, we attempted to expand the utility of LBTs to include the sensitization of some or all of these lanthanide ions. Recently, the synthesis of the compound 1,4,7,10-tetraazacyclododecane 1,4,7-trisacetic acid 10-methyltriazolo[3,4- α]phthalazine complexed with lanthanide ions, (**1**), was reported by the Faulkner lab.⁷ These researchers successfully reported using this compound to sensitize emission from complexes of Nd^{3+} , Eu^{3+} , Er^{3+} and Yb^{3+} . Therefore, we decided to incorporate the sensitizer triazolo[3,4- α]phthalazine

moiety, **(2)** (Figure 3-2), into an LBT, in an attempt to generate an LBT capable of sensitizing Ln^{3+} ions that emit in the infrared.

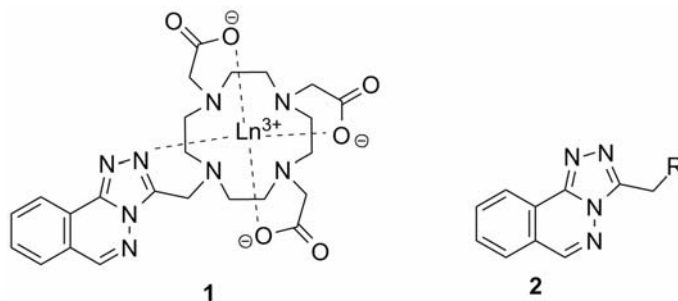


Figure 3-2. The IR-emitting lanthanide-sensitizing compound **(1)** synthesized by Faulkner and coworkers.⁷ The phthalazine moiety **(2)** could potentially be used as an amino acid side-chain in an IR-emitting LBT.

Results and Discussion

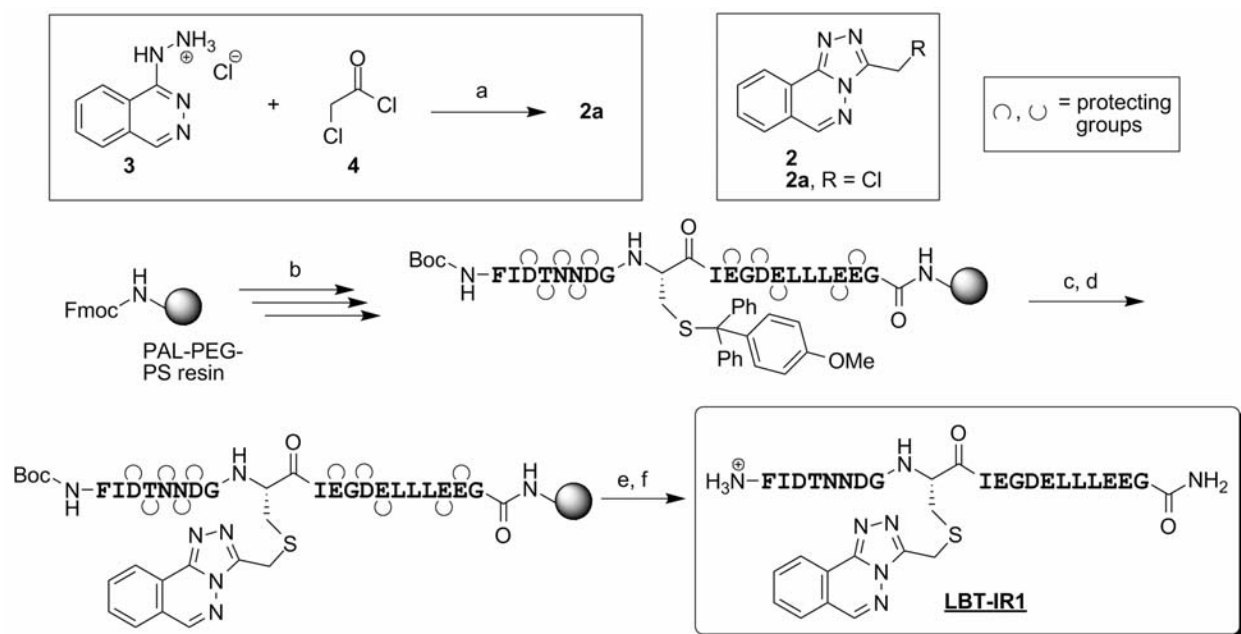
3-1. Synthesis and Characterization of LBT-IR1

Although compound **(1)** showed direct coordination to the lanthanide ion by the phthalazine sensitizer,⁷ it was decided to design the first potential IR-emitting LBT simply by replacing the indole side chain on Trp7 with a derivative **(2)**, using the sequence for SENG (see Table 3-1, below). To do so, **(2a)** was synthesized on gram scale from hydralazine-HCl **(3)** and chloroacetyl chloride **(4)** in aqueous sodium bicarbonate using a procedure based on the one previously reported⁷ (Figure 3-3). Using the methodology diagrammed in Figure 3-3, LBT-IR1 (Table 3-1) was successfully synthesized. Briefly, a peptide was synthesized on PAL-PEG-polystyrene resin using standard Fmoc-based SPPS, using a modified SENG sequence in which position 7 was a cysteine residue with a monomethoxytrityl (Mmt) protecting group on the side chain. The Mmt was removed by 1% trifluoroacetic acid (TFA) in dichloromethane, leaving the remaining protecting groups intact, and the free-cysteine-containing peptide was then treated with **(2a)**. After extensive washing, cleavage with a TFA cocktail and HPLC purification yielded free LBT-IR1.

Table 3-1. Sequence Design of Potential IR-Emitting- Ln^{3+} -Sensitizing LBTs^a

<i>LBT</i>	-1	0	1	2	3	4	5	6	7	8	9	10	11	12	13	14	15	16	17	18
<u>SENG</u>	F	I	D	T	N	N	D	G	W	I	E	G	D	E	L	L	L	E	E	G
<u>LBT-IR1</u>	F	I	D	T	N	N	D	G	C _{φθ}	I	E	G	D	E	L	L	L	E	E	G
<u>LBT-IR2</u>	F	I	D	T	N	N	D	G	W	I	E	G	D	C _{φθ}	A	A				

^a Amino acid residues are denoted by their one-letter codes. The entry “C_{φθ}” indicates a cysteine residue that has been modified by the phthalazine **(2)** moiety. Side-chain-ligating positional numbers on SENG are shown in bold.



Conditions: a) Aqueous NaHCO₃, reflux 12 hours. b) Standard Fmoc Solid Phase Peptide Synthesis on a peptide synthesizer. c) 1% TFA in CH₂Cl₂. d) Freshly distilled TMG, DMF, **2a**. e) 94% TFA cleavage cocktail. f) HPLC purification.

Figure 3-3. Synthesis of LBT-IR1.

The ability of LBT-IR1 to sensitize lanthanide ions was then examined. In a fluorometer cuvette, 2 μM lanthanide ion was added (Tb³⁺, Eu³⁺, Ho³⁺, Tm³⁺, or Yb³⁺), followed by 2 μM LBT-IR1. The solutions were excited and emission was monitored around a known emission maximum for each lanthanide. Strong, distinct peaks were observed of Tb³⁺ and Eu³⁺ emission (Figure 3-4), but none of the IR-emitting Ln³⁺ ion-bound LBT-IR1 complexes showed a signal above baseline (data not shown). Based on the Tb³⁺ and Eu³⁺ data, it is clear that LBT-IR1 is still capable of binding lanthanide ions. However, we conclude that a different process of energy transfer must be necessary for Ho³⁺, Tm³⁺ and Yb³⁺ than for Tb³⁺ and Eu³⁺, and the former group appears to require direct coordination by the aromatic sensitizer.⁸

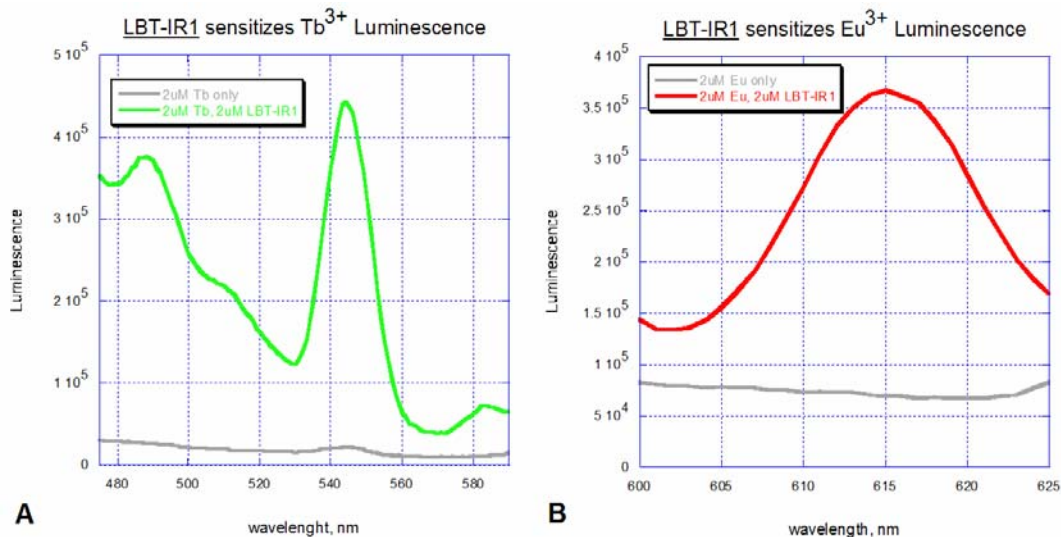


Figure 3-4. LBT-IR1 sensitizes Tb³⁺ (shown in **A**) and Eu³⁺ (shown in **B**). Baseline is shown in grey in both graphs; LBT-IR1-Tb³⁺ emission is shown in green and LBT-IR1-Eu³⁺ emission is shown in red.

3-2. Synthesis and Characterization of LBT-IR2

Due to the apparent necessity for direct sensitizer-coordination for the infrared-emitting lanthanides, an alternate approach was taken. A new LBT was designed to test the possibility of replacing one lanthanide-ion-ligating side chain with a phthalazine-(2)-modified cysteine residue. Based on the crystal structure of SE2⁹ (see also Figure 2-1), it appears that Glu12 (the most C-terminal of the ligating residues) swings around to bind Tb³⁺. This seemed to present an ideal target to replace. Therefore, the final LBT shown in Table 3-1 (*vide supra*) was designed. The sequence of LBT-IR2 has a direct replacement of the glutamate-12 with the phthalazine-labeled cysteine; it was hoped that the sensitizer would be able to swing around and coordinate the Ln³⁺ ion. Also, because the C-terminal structure would likely be significantly altered by the new ligating residue, these residues were omitted. Instead, the C-terminal alanine residues were designed primarily as a spacer from the resin; this would minimize steric hindrance when the Cys12 was labeled with (**2a**) in a manner analogous to that shown in Figure 3-3.

Despite this new design, LBT-IR2 was not observed to sensitize the IR-emitting Ln³⁺ ions tested (Ho³⁺, Tm³⁺ and Yb³⁺). The most likely reason is that the phthalazine moiety is not making the necessary contact with the metal ion. Evidence for this is shown by the excitation scans (Figure 3-5) of various LBT-Tb³⁺ complexes, which compares the emission output at 544 nm at different excitation wavelengths. The SE2-Tb³⁺ trace is a positive control for sensitization by tryptophan; the LBT-IR1-Tb³⁺ spectrum is indicative of sensitization by phthalazine (**2**). The

spectrum for LBT-IR2-Tb³⁺ is nearly identical to that of SE2-Tb³⁺; therefore, sensitization must come almost exclusively from the indole side-chain, and not from the expected efficient transfer of energy from the phthalazine moiety.

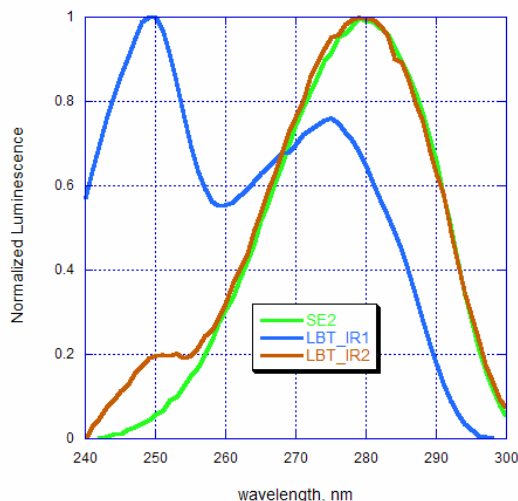


Figure 3-5. Normalized excitation scans of LBT-Tb³⁺ complexes, measured at 544 nm emission. The trace for SE2 is shown in green; for LBT-IR1 in blue; and for LBT-IR2 in brown.

Conclusions

Two new LBTs have been designed containing a phthalazine moiety, which is known to sensitize lanthanide ions that have an emission profile in the near-IR region. However, neither of these LBTs were successful at sensitizing this subgroup of lanthanides. We suspect that a different method of energy transfer is necessary in this case, in which the sensitizer-fluorophore is directly coordinated the Ln³⁺. Although LBT-IR2 was designed with this criterion in mind, it does not appear to adequately sensitize in the orientation provided by the current design. A larger library will be necessary to find a true “IR-LBT”. Nevertheless, LBT-IR1 is capable of sensitizing Eu³⁺ luminescence, and may be added to the arsenal² of LBTs with sensitizers that do so.

Experimental

3-0E. General Procedures

Additional chemical reagents were purchased from Sigma-Aldrich (St. Louis, MO).

Peptides were prepared by standard Fmoc-based SPPS procedures, purified by HPLC and verified by MALDI-TOF MS as described in Chapter 2 (2-0E). Concentrations of stock solutions were determined by the UV absorption using the extinction coefficients of the tryptophan ($\epsilon_{280} = 5690 \text{ cm}^{-1}\text{M}^{-1}$)¹⁰ and phthalazine (**2**) ($\epsilon_{274} = 12500 \text{ cm}^{-1}\text{M}^{-1}$ and $\epsilon_{306} = 2400 \text{ cm}^{-1}\text{M}^{-1}$)⁷ content in 6 M guanidinium chloride.

3-1E. Synthesis and Characterization of LBT-IR1.

3-chloromethyl triazolo[3,4-*a*]phthalazine, (2a)

Compound (**2a**) was synthesized using a procedure slightly modified from the literature.⁷ Briefly, hydralazine hydrochloride (1 g, 5.1 mmol) and sodium bicarbonate (700 mg, 8.4 mmol) were dissolved in 10 mL of deionized water, forming a yellow solution. Chloroacetyl chloride (670 μL , 8.4 mmol) was added drop-wise to this solution. The reaction was heated to reflux for 90 minutes, and was then allowed to cool to room temperature over 90 minutes. The product formed as a white precipitate, which was collected by filtration and recrystallized from ethanol, forming 166 mg of white needles (15% yield; 36% reported⁷). ESI MS [$\text{M}+\text{H}^+$] 219 for $\text{C}_{10}\text{H}_7\text{N}_4\text{Cl}$; found 219.4. The ¹H NMR spectrum (300 MHz, CDCl_3) matched that from the literature.⁷

LBT-IR1: $\text{H}_2\text{N-FIDTNNDGC}_\phi\text{-IEGDELLLEEG-CONH}_2$

The fully-protected peptide Fmoc-**FIDTNNDGC**(Mmt)**IEGDELLLEEG-PAL-PEG-PS** was a gift from Dr. Bianca Sculimbrene. The Mmt protecting group was removed by dilute acid: 100 mg of resin was added to a fritted funnel, and swelled with five \times 5 mL DCM. It was then treated with 10 mL of DCM containing 1% TFA and 5% TIS, and was mixed by bubbling N_2 through for about 20 – 30 minutes. The resin was drained, and the 1% TFA-treatment process was repeated about ten times. The resin was then washed five times with DCM followed by five times with DMF. To couple the phthalazine, 33 mg of (**2a**) was added to the resin, followed by 3 mL of Sure/Seal™ DMF, and 40 μL of freshly distilled TMG (tetramethylguanidine). The reaction was allowed to run overnight, with N_2 bubbling through.

The next morning, the resin was washed five times with DMF, and the N-terminal Fmoc group was removed with 20% 4-methylpiperidine, as for standard Fmoc-SPPS. The resin was washed five times with DMF, then five times with DCM. The peptide was cleaved and fully deprotected using the standard 94% TFA cocktail (see Chapter 2, 2.0E), and purified as described by RP-HPLC ($t_R = 19.2$ min). Exact mass calcd., 2337.6 [M+H⁺]; found 2337.4 [M+H⁺] by MS(MALDI).

Emission Spectra.

Luminescence spectroscopy was performed on the aforementioned Jobin Yvon Horiba Fluoromax-3 Spectrometer in a 1 cm path-length quartz cuvette. Peptide solutions were prepared in 0.5 mL buffer, which consisted of 100 mM NaCl, 10 mM HEPES (*N*-(2-hydroxyethyl)piperazine-*N'*-ethanesulfonic acid), pH 7.0. Emission scans were recorded at 2 μ M peptide, 2 μ M Ln³⁺. Phthalazine-sensitized (LBT-IR1) Ln³⁺ luminescence was collected by excitation at 304 nm for Tb³⁺ and Eu³⁺, and at 337 nm for all other lanthanides tested (Ho³⁺, Tm³⁺, and Yb³⁺). (These excitation wavelengths were chosen based on the literature.⁷) Slit widths of 4 nm (excitation) and 10 nm (emission) were used. Spectra were recorded at 25°C, and were corrected for intensity using the manufacturer-supplied correction factors. Data points were collected at 1 nm increments with 0.5 second integration times. Emission spectra were collected 20 – 50 nm on either side of an emission maximum of each lanthanide.

3-2E. Synthesis and Characterization of LBT-IR2.

LBT-IR2: H₂N-**FIDTNNDGWIEGDC** _{ϕ} -**AA**-CONH₂

The peptide Boc-**FIDTNNDGC**(Mmt)**IEGDELLLEEG**-PAL-PEG-PS was prepared using standard Fmoc-SPPS as described (see 2-0E) on PAL-PEG-PS resin. The amino acid Boc-Phe-OH was used in the final step, so that the N-terminus would be capped for the alkylation step, while obviating the need for an additional Fmoc-deprotection. The Mmt protecting group was removed by dilute acid, using an identical procedure as with IR-LBT1 (see above), and (**2a**) was coupled in an analogous fashion. The peptide was cleaved and fully deprotected using the standard 94% TFA cocktail and purified as described by RP-HPLC ($t_R = 18.5$ min). Exact mass calcd., 1922.3 [M+H⁺]; found 1921.0 [M+H⁺], 1942.3 [M+Na⁺] by MS(MALDI).

Excitation Spectra.

Excitation spectra were also performed on the Jobin Yvon Horiba Fluoromax-3 Spectrometer in a 1 cm path-length quartz cuvette. Peptide solutions were prepared in 0.5 mL buffer (100 mM NaCl, 10 mM HEPES, pH 7.0). Excitation scans were recorded at 2 μ M peptide, 2 μ M Tb^{3+} . Phthalazine- and tryptophan-sensitized Tb^{3+} luminescence was collected at the emission maximum of 544 nm. Slit widths of 5 nm (excitation) and 10 nm (emission) were used. Spectra were recorded at 25°C, and were corrected for intensity using the manufacturer-supplied correction factors. Excitation scans were collected from 240 nm – 300 nm, using 1 nm increments with 0.5 second integration times.

Acknowledgements

I thank Bianca Sculimbrene for the precursor-peptide that was used to make LBT-IR1. I am eternally grateful to Mark Chen for editing this chapter.

References

- (1) Cotton, S., *Lanthanides and Actinides*. Oxford University Press: New York, 1991;
- (2) Reynolds, A. M.; Sculimbrene, B. R.; Imperiali, B. "Lanthanide-Binding Tags with Unnatural Amino Acids: Sensitizing Tb³⁺ and Eu³⁺ Luminescence at Longer Wavelengths." *Bioconjugate Chem.* **2008**, *19*(3), 588-591.
- (3) Werts, M. H. V. Luminescent Lanthanides. <http://perso.univ-rennes1.fr/martinus.werts/lanthanides/>
- (4) Zhang, J.; Badger, P. D.; Geib, S. J.; Petoud, S. "Sensitization of Near-Infrared-Emitting Lanthanide Cations in Solution by Tropolonate Ligands." *Angew. Chem. Int. Ed.* **2005**, *44*, 2508-2512.
- (5) Piszczek, G.; Gryczynski, I.; Maliwal, B. P.; Lakowicz, J. R. "Multi-Photon Sensitized Excitation of Near Infrared Emitting Lanthanides." *J. Fluorescence* **2002**, *12*(1), 15-17.
- (6) Faulkner, S.; Pope, S. J. A.; Burton-Pye, B. P. "Lanthanide complexes for luminescence imaging applications." *Appl. Spec. Rev.* **2005**, *40*, 1-31.
- (7) Burton-Pye, B. P.; Heath, S. L.; Faulkner, S. "Synthesis and luminescence properties of lanthanide complexes incorporating a hydralazine-derived chromophore." *Dalton Trans.* **2005**, (1), 146-149.
- (8) The limit of the emission monochromator on the fluorometer used in these experiments is 1000 nm. The emission maxima of Ho³⁺ and Yb³⁺ are above 900 nm and therefore approach the limits of the instrument, but Tm³⁺ emission is only about 800 nm. The ability of our instrument to detect emission from these lanthanide ions was verified by repeating experiments reported in Reference (4) (J. Zhang *et al.*), using tropolonate ligands as sensitizers.
- (9) Nitz, M.; Sherawat, M.; Franz, K. J.; Peisach, E.; Allen, K. N.; Imperiali, B. "Structural origin of the high affinity of a chemically evolved lanthanide-binding peptide." *Angew. Chem. Int. Ed.* **2004**, *43*(28), 3682-3685.
- (10) Chazan, A. Peptide Property Calculator. <http://www.basic.northwestern.edu/biotools/proteincalc.html>

Chapter 4

Double-Lanthanide-Binding Tags

Portions of this chapter have been published in the *Journal of the American Chemical Society*¹ as noted in the text. Copyright © 2007, American Chemical Society.

Introduction¹

The 17 – 20 residue Lanthanide-Binding Tags described in Chapter 2 show low-nM affinities for Tb³⁺, and are selective for lanthanides over other common metal ions.²⁻⁵ The versatility of these tags as probes has been demonstrated, including use for luminescent visualization on gels,² as magnetic-field paramagnetic alignment agents in protein NMR experiments,⁶⁻⁸ in fluorescence microscopy,⁹ and as partners in luminescence resonance energy transfer (LRET) studies.¹⁰ However, X-ray crystallography is notably absent from this list. Although multiple proteins had been examined as both N- and C-terminal fusions, in collaboration with Professor Karen Allen's lab (Boston University School of Medicine), the few proteins that crystallized did not show an anomalous lanthanide signal that could be used to obtain phase information. It was hypothesized that the current LBT prototype might be poorly constructed for making adequate contacts with the fusion protein, and thus be too short to be effective as a crystallographic tag. Therefore, an attempt was made to lengthen the LBT sequence for applications including X-ray crystallography.

While most applications of lanthanide ions in protein studies require only one metal ion per protein, a construct that selectively incorporates two ions could potentially confer advantages in luminescence output, X-ray scattering power, and anisotropic magnetic susceptibility. To this end, we built upon our initial structure/function analyses with LBTs (such as SE2) to design double-LBTs (dLBTs) that simultaneously bind and sensitize two lanthanide ions (Figure 4-1). Herein is described the generation and characterization of dLBT peptides, which are superior tags in many applications. Furthermore, based on results of collaborative studies involving NMR spectroscopy and X-ray crystallography, the goal of creating a less mobile tag has been achieved.

Results and Discussion

4-1. Design and Selection of the dLBT Sequences¹

The dLBT prototype was designed with the intent of balancing high terbium-ion affinity with strong luminescence. Figure 4-1 conceptualizes the dLBT design process. The hydrophobic core at positions -1, 8 and 13 (revealed in the crystal structure of SE2)⁴ led to the design of a combinatorial peptide library to optimize these residues,⁵ as discussed in Chapter 2. Initial results yielded SE3, in which the tyrosine residue at position 8 was mutated to isoleucine (Table 4-1; see also Figure 2-3 and Table 2-1). Although the luminescence output of this LBT was reduced, the improved K_D prevailed in the selection of the SE3 sequence as the prototype for the first generation of dLBTs; furthermore, concatenation of two lanthanide-binding motifs was expected to compensate for the reduced luminescence. Ultimately, refinement of the seventh combinatorial library (see Chapter 2, Figure 2-3) further optimized the hydrophobic core (Tyr-1 was mutated to Phe), yielding SE4. This single-LBT showed improved terbium-binding affinity and luminescence; future studies on dLBTs may therefore take advantage of this mutation. It should be noted that not all applications of LBTs require a sensitizer (e.g. NMR and crystallography), enabling non-luminescent LBTs to be used successfully.^{7,8} However, for maximum utility, it is advantageous to include a sensitizer such as tryptophan for exploitation of the luminescence properties of the LBT.

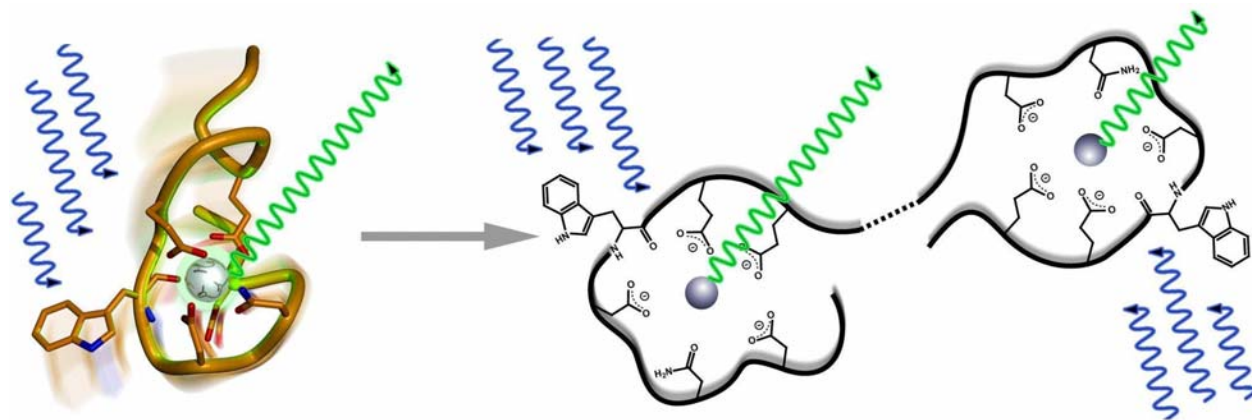


Figure 4-1. Representation of the design strategy for converting the single-LBT into the double-LBT. The image depicts the peptide backbone based on the crystal structure of SE2.⁴ The side chains that chelate Tb^{3+} are shown, along with the tryptophan sensitizer with the Tb^{3+} -coordinating peptide backbone carbonyl. The indole ring is excited at 280 nm, thereby sensitizing the Tb^{3+} which emits at 544 nm. The design goal for the dLBT is to incorporate two Tb^{3+} -binding sites within a contiguous sequence—potentially conferring advantages in luminescence output, X-ray scattering power, and anisotropic magnetic susceptibility—together with reduced mobility relative to the tagged protein. (Dr. Nicholas Silvaggi created this figure.)

Table 4-1. Comparison of Tb³⁺-Binding Affinity and Luminescence Intensity of Select Single-LBTs

<i>single-LBT</i>	<i>position</i> ^a															<i>K_D, Tb³⁺</i>	<i>relative intensity</i>		
	-1	0	1	2	3	4	5	6	7	8	9	10	11	12	13	14	15	(nM)	
<u>SE2</u>	Y	I	D	T	N	N	D	G	W	Y	E	G	D	E	L	L	A	57	1.9
<u>SE3</u>	Y	I	D	T	N	N	D	G	W	I	E	G	D	E	L	L	A	38	1.0
<u>SE4</u>	F	I	D	T	N	N	D	G	W	I	E	G	D	E	L	L	A	18	1.3

^a The LBT residue numbering system is based on the literature.^{11,12} Ln³⁺-coordinating side chains' position number is shown in bold-faced font.

The linker region connecting the N- and C-terminal lanthanide-binding motifs was designed to preserve the interactions in the hydrophobic core. Position 13 of the N-terminal motif was set adjacent to position -1 of the C-terminal motif with the goal of promoting intramolecular hydrophobic interactions, thereby creating the sequence for “dSE3” (“double-SE3”), the first double-LBT: **YIDTNNNDGWIEGDELYIDTNNNDGWIEGDELLA** (Table 4-2).

Table 4-2. Sequences of Double-LBTs and the Progenitor Single-LBT SE3

LBT	residues from protease cleavage ^a	N-terminal Ln ³⁺ -binding motif	C-terminal Ln ³⁺ -binding motif
<u>SE3</u>			YIDTNNNDGWIEGDELLA
<u>dSE3</u>		YIDTNNNDGWIEGDEL	YIDTNNNDGWIEGDELLA
G <u>dSE3</u>		G YIDTNNNDGWIEGDEL	YIDTNNNDGWIEGDELLA
GPG <u>dSE3</u>		GPG YIDTNNNDGWIEGDEL	YIDTNNNDGWIEGDELLA

^a The N-terminal glycine on GdSE3 is residual from the mTEV protease cleavage site, and the corresponding glycine-proline-glycine sequence on GPGdSE3 is residual from the DAPase stop site.

4-2. Preparation of dLBT Peptides and a dLBT-Ubiquitin Construct¹

Initially, the prototype double-LBT (dSE3, Table 4-2) was synthesized by solid phase peptide synthesis. However, the efficiency of amino acid coupling became significantly reduced after the first twenty residues, leading to a number of truncation products (so-called “sesqui-LBTs”) that could not be purified from full-length dSE3. (A superior resin for peptide synthesis was eventually found and used successfully; see Chapter 5.) Instead, an alternate production strategy involving expression of the dLBT sequence as a fusion protein was pursued. Pure, full-length dLBT peptide could be obtained via overexpression in *E. coli* using a glutathione *S*-transferase (GST)-fusion strategy. DNA encoding the dLBT was inserted into the pGEX-4T-2 plasmid (Amersham Biosciences) to generate the gene for a GST-fusion protein with a C-terminal dLBT and an intervening mTEV-protease recognition sequence (the Tobacco Etch

Virus cleaves the sequence ENLYFQX between Q and X, where X is any residue except proline¹³). (This strategy has since been modified to include His-tagged ubiquitin instead of GST as the N-terminal tag; see Chapter 5.)

The fusion protein was overexpressed, purified on glutathione-sepharose resin, and cleaved with mTEV protease (Figure 4-2; see also Figure 4-4). The protease cleavage site resulted in the additional N-terminal glycine residue, yielding GdSE3 (Table 4-2), which was purified by HPLC. Initial photophysical experiments on GdSE3 were promising (Table 4-3): binding of Tb^{3+} to the first site was even stronger than the parent sequence, SE3 (which was not unexpected, given the numerous proximal unligated Asp and Glu residues),⁵ and the second Tb^{3+} bound with nearly identical affinity to the parent LBT. Finally, the (normalized) molar luminescence intensity was roughly double that of the progenitor, also as expected.

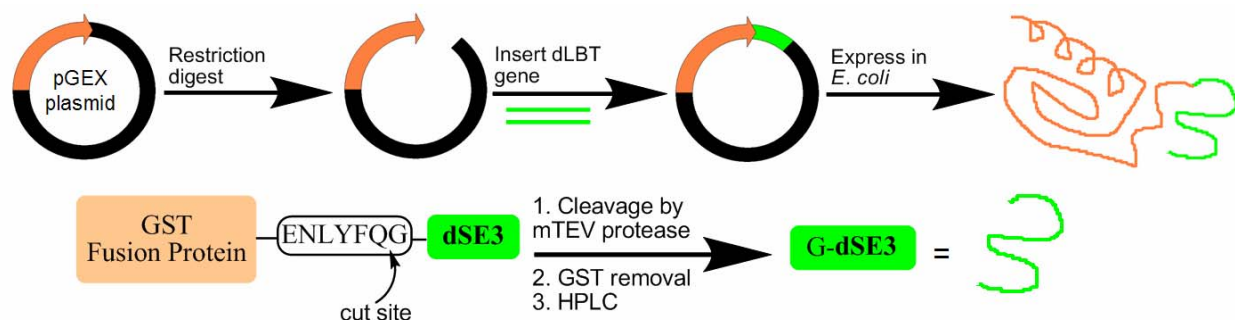


Figure 4-2. Expression and purification strategy for obtaining pure GdSE3 peptide via a GST-fusion protein

Table 4-3. Initial Double-LBT Peptide Photophysical Experiments

<u>LBT</u>	K_D, Tb^{3+} (nM) ^a		Relative intensity ^b	q ^c
	<i>First</i> Tb^{3+}	<i>Second</i> Tb^{3+}		
<u>SE3</u>	38	--	1.0	0.08
<u>GdSE3</u>	9.8	35	2.1	0.08

^a Determined by luminescence titration in 100 mM NaCl, 10 mM MOPS buffer (pH 7.0). All values are the average of at least three titrations.

^b Luminescence comparison of equal concentrations of peptide or protein construct saturated with Tb^{3+} , normalized to that of SE3.

^c The number of bound water molecules, q , was determined by luminescence decay experiments as described in the literature.^{4,14}

Next, it was important to examine the efficacy of the dLBT as part of a fusion protein. The protein ubiquitin was chosen as a prototype, since it is highly soluble and has a known crystal structure.¹⁵ The expression and purification of the LBT-ubiquitin construct was carried

out using standard molecular biology techniques and protein purification approaches. The pET-18a plasmid (Invitrogen) was modified to contain the gene for dSE3-ubiquitin with an N-terminal hexa-histidine tag and an intervening DAPase stop site (Figure 4-3; see also the Experimental section). (DAPase is an exopeptidase that cleaves dipeptides from the N-termini of proteins.) This strategy has since been modified to use a TEV protease cleavage site in lieu of DAPase; see Chapter 5.

The H₆-GPGdSE3-ubiquitin fusion protein was overexpressed, purified on Ni-NTA-agarose resin (Qiagen), and the His-tag was excised with DAPase (Qiagen). The protease stop site resulted in the additional N-terminal glycine-proline-glycine motif, yielding GPGdSE3-ubiquitin, which was purified by reverse-IMAC (see the Experimental section). Protein yields were excellent—at least 30 mg/L in LB (Lysogeny Broth, which contains 10 g/L tryptone, 5 g/L yeast extract, and 5 g/L NaCl)—with the size of the construct verified by SDS-PAGE.

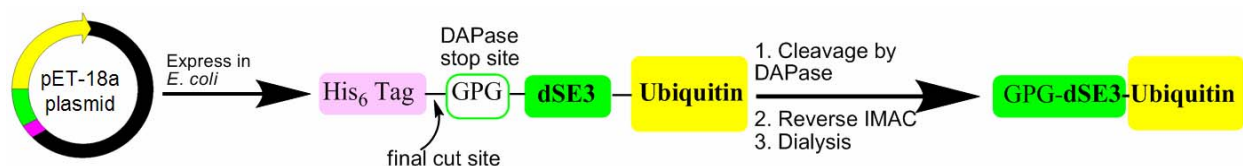


Figure 4-3. Expression and purification strategy for obtaining pure GPGdSE3-ubiquitin construct.

The purification of the GST-GdSE3 and GPGdSE3-ubiquitin constructs also highlights the utility of the LBT as a co-expression tag for in-gel visualization (Figure 4-4). Specifically, for confirmation of the presence of an LBT, the gel was briefly incubated with Tb³⁺, and bands containing a LBT were visualized on a UV transilluminator (Figure 4-4A). The gel was then stained in order to visualize total protein (Figure 4-4B). For corroborating identification, Western blot analysis, utilizing a monoclonal antibody generated to recognize the sequence **IEGDELL** (residues 8 – 14 of SE3), was carried out (Figure 4-4C). (The antibody was generated in rabbits by Quality Controlled Biosystems, Hopkinton, MA.)

We anticipate that the success of dLBTs as N- and C-terminal tags in these model systems will be transferable to other proteins. Despite the increased length (35 residues for GPGdSE3), we have not encountered any additional complications with expression or purification.

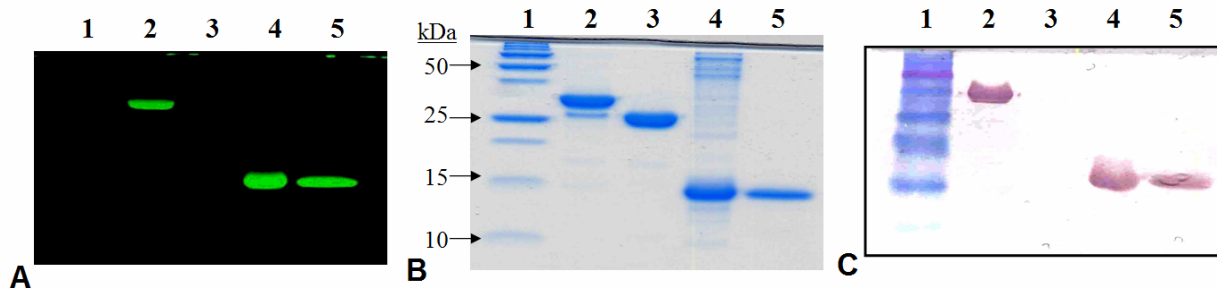


Figure 4-4. Purification and visualization of the dLBT constructs. For all panels, lane 1: protein mass ladder; lane 2: *GST-ENLYFQ-GdSE3*; lane 3: *GST-ENLYFQ*; lane 4: *MKH₆-GPGdSE3-Ubiquitin*; lane 5: *GPGdSE3-Ubiquitin*. **A.** 15% SDS-PAGE gel treated with 4 μM Tb^{3+} and visualized on UV transilluminator, with enhancement for color and contrast. **B.** The same gel, subsequently stained with GelCode[®] Blue Stain Reagent. **C.** Western blot analysis of an identical gel run in parallel, using a primary anti-LBT antibody.

4-3. Photophysical Characterization of dLBT Peptides and Proteins^l

To compare the photophysical properties of the newly designed and generated dLBTs with those of the corresponding single-LBTs, luminescence titration (to ascertain maximum intensity and affinity) and terbium-bound water molecule determination was carried out as described previously³⁻⁵ (Table 4-4). Water molecules directly coordinating the chelated terbium ion are highly detrimental to luminescence, causing excited Tb^{3+} to undergo rapid, nonradiative energy transfer to the vibrational states of the water O–H bonds.¹⁶ The original screen for brightly luminescent LBTs selected for peptides that excluded water from the inner coordination sphere upon chelation. Using methods described in the literature,^{4,14,17} it was verified that the water-excluded state was also a property of the dLBTs, shown by near-zero q values in Table 4-4.

Terbium affinities were assessed via luminescence titration studies, which reveal that the dLBTs bind Tb^{3+} with similar affinity as do the single LBTs. Two different systems were used for titration experiments at pH 7.0: NaCl/MOPS (used for direct K_D determination³⁻⁵) and NaOAc/HEPES (used for analysis under competitive conditions). In the latter case, acetate is known to weakly coordinate lanthanides (the 1:1 complex with Tb^{3+} has a K_D of 12 mM);¹⁸ thus, titrations performed in the presence of an acetate buffer show a weakened apparent dissociation constant due to competition with excess acetate. This enables improved qualitative comparison of the *relative* K_D values of two tight-binding LBTs or dLBTs. As shown in Table 4-4, in the direct titrations the binding affinity of dLBTs for the first equivalent of terbium is stronger than that of SE3, however, the second equivalent of Tb^{3+} binds with comparable affinity to that single-LBT analogue. Whether the first binding event represents binding solely to one of the two

LBT motifs is unclear. We have previously noted that additional non-ligating acidic residues increase affinity, presumably because of bulk electrostatic interactions with the metal ion.⁵ Therefore, it is likely that the first terbium binding event may be promoted by the presence of the highly negatively charged, unliganded side chains in the remainder of the sequence, and that the second binding event is unaffected and more comparable to the single-LBT.

For titrations in acetate buffer, the two dissociation constants are similar, suggesting that the electrostatic effects seen in the direct titrations may be less important. Using acetate buffer (or in the presence of any competing ligand) the LBT binding affinities can be fine-tuned, by shifting the equilibrium of high-affinity ligands, which can be an advantage for NMR experiments. We also note that the N-terminal residues (G or GPG) that result from incorporation of the protease cleavage sites (Table 4-2; Figures 4-2 and 4-3), are not detrimental to binding. Finally, it is noteworthy that we observe that in the case of the protein construct GPGdSE3-ubiquitin, binding of the two metals appears to be cooperative: the second K_D is lower than the first. It is unclear whether this is related to the luminescence enhancement, and why this is not observed in NaCl/MOPS buffer. Since this phenomenon is not observed in either of the peptides, it could be that the ubiquitin is playing a role, perhaps by altering the accessibility or structure of the C-terminal binding site.

Table 4-4. Summary of Double-LBT Photophysical Data

<i>LBT</i>	K_D , Direct titrations ^a		K_D , Acetate buffer titrations ^b		Relative intensity ^c	q ^d
	<i>First Tb³⁺</i>	<i>Second Tb³⁺</i>	<i>First Tb³⁺</i>	<i>Second Tb³⁺</i>		
<u>SE3</u>	38 nM	--	980 nM	--	1.0	0.08
GdSE3	9.8 nM	35 nM	590 nM	1100 nM	2.1	0.08
GPGdSE3	3.6 nM	62 nM	570 nM	1000 nM	2.5	0.08
GPGdSE3-Ubiq	2.4 nM	23 nM	710 nM	500 nM	3.0	0.05

^a Determined by luminescence titration in 100 mM NaCl, 10 mM MOPS buffer (pH 7.0). All values are the average of at least three titrations.

^b Determined by luminescence titration in 100 mM NaOAc, 10 mM HEPES buffer (pH 7.0). All values are the average of at least three titrations.

^c Luminescence comparison of equal concentrations of peptide or protein construct saturated with Tb^{3+} , normalized to that of SE3.

^d The number of bound water molecules, q , was determined by luminescence decay experiments as described in the literature.^{4,14}

The luminescence intensities of the peptide GdSE3 and the GPGdSE3-ubiquitin construct saturated with Tb^{3+} were compared to that of the progenitor SE3 (Table 4-4). The free peptide GPGdSE3, generated in parallel to GdSE3, was also included to assess the effect of the

additional N-terminal residues. Remarkably, although GdSE3 is approximately twice as bright as SE3, the peptide GPGdSE3 is 2.5 times as bright as the prototype, and the construct GPGdSE3-ubiquitin shows a full three-fold increase over the original brightness. The reason for this luminescence enhancement is not entirely clear; however, it is advantageous (also, see section 4-5). It is notable that neither the N-terminal GPG motif nor the presence of the ubiquitin protein result in enhanced LBT luminescence: the single-LBT-containing construct GPGSE2-ubiquitin has a luminescence intensity that is identical to the SE2 peptide (Table 4-5).

Table 4-5. The GPG Motif and the Ubiquitin Protein Have No Inherent Effect on LBT Luminescence

<i>LBT</i>	K_D, Tb^{3+}		Relative Intensity ^c	q^d
	<i>Direct Titrations</i> ^a	<i>Acetate Buffer Titrations</i> ^b		
SE2	57 nM	1900 nM	1.9	0.03
GPG-SE2-Ubiq	130 nM	4400 nM	1.9	0.13

Determined by luminescence titration in 100 mM NaCl, 10 mM MOPS buffer (pH 7.0). All values are the average of at least three titrations.

^b Determined by luminescence titration in 100 mM NaOAc, 10 mM HEPES buffer (pH 7.0). All values are the average of at least three titrations.

^c Luminescence comparison of equal concentrations of peptide or protein construct saturated with Tb^{3+} , normalized to that of SE3.

^d The number of bound water molecules, q , was determined by luminescence decay experiments as described in the literature.^{4,14}

4-4. Characterization of GPGdSE3-ubiquitin by NMR^l

Experiments to study the construct GPGdSE3-ubiquitin by Nuclear Magnetic Resonance spectroscopy were conducted by Dr. Martin Hähnke and Dr. Jens Wöhnert in the laboratory of Prof. Harald Schwalbe at Frankfurt University. These results are germane to this thesis, and are therefore reviewed here.

Previously, the introduction of an N-terminal single-LBT to ubiquitin (as the construct GPGSE2-ubiquitin; see Table 4-5) allowed the analysis of induced Residual Dipolar Couplings (RDCs) of about 8 Hz at 600 MHz, suggesting some degree of mobility of the LBT tag relative to the protein.⁶ NMR analysis was conducted in order to assess the impact of the dLBT on the structure of the conjugated protein. The Schwalbe lab comparison of ¹H and ¹⁵N chemical shift perturbations using GPGdSE3-ubiquitin loaded with diamagnetic Lu³⁺ demonstrated that the dLBT does not alter the core structure of ubiquitin (Figure 4-5).

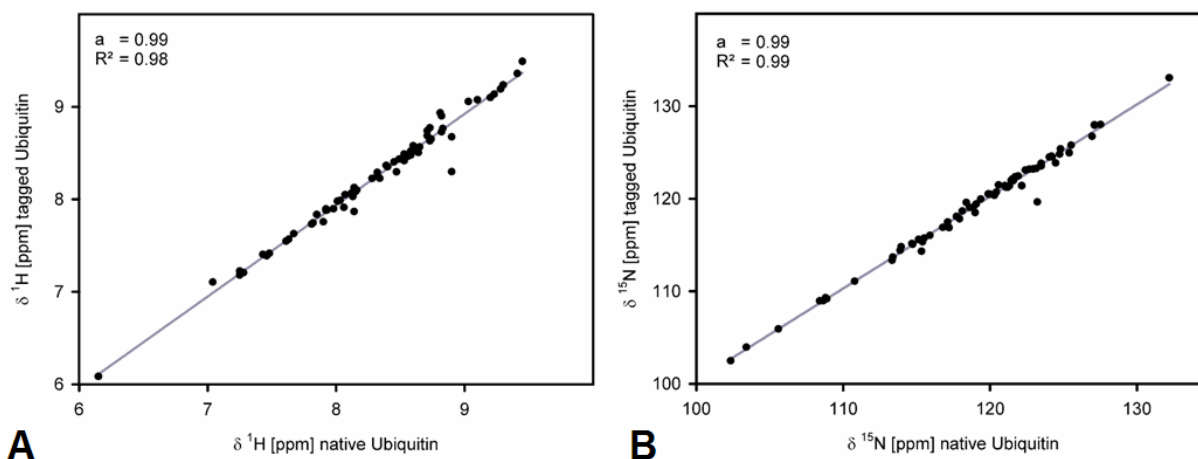


Figure 4-5. Chemical shifts of GPGdSE3-ubiquitin loaded with Lu³⁺, plotted against the chemical shifts of native ubiquitin show that the dLBT does not alter the solution structure of ubiquitin. **A.** ¹H. **B.** ¹⁵N. (Dr. Martin Hähnke created these graphs.)

The RDCs measured at 18.8 T (800 MHz) with thulium (Tm³⁺) as paramagnetic ion in GPGdSE3-ubiquitin exceed the values measured in GPGSE2-ubiquitin (a single-LBT ubiquitin construct described previously⁶) by a factor of 3 as shown in Figure 4-6. However, the maximal increase in alignment expected for addition of a second lanthanide binding site is only a factor of two. Thus, the more-than-linear increase in the residual dipolar coupling obtained must originate from a different source, which is most likely the reduced mobility of the dLBT relative to the protein.

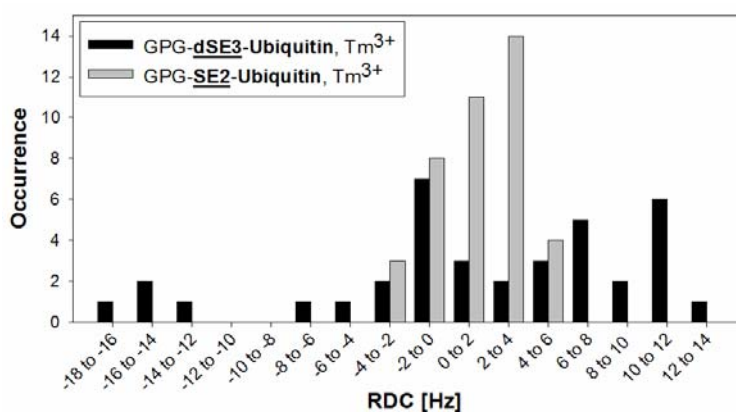


Figure 4-6. Histogram of Residual Dipolar Couplings measured with Tm³⁺ in either single-LBT- or double-LBT-containing ubiquitin (GPGSE2-Ubiquitin or GPGdSE3-Ubiquitin), demonstrating a more-than-linear increase in RDC size for the latter. (Martin Hähnke created this histogram.)

The induced alignment in this construct also exceeds that reported from approaches using EDTA-based chelators.¹⁹ Therefore, despite the lower binding affinity of the dLBTs relative to

the synthetic multidentate chelators, the relatively rigid association of the dLBT with the attached protein provides a fundamental advantage in the application of the dLBTs in these types of experiments. The two LBT modules apparently rigidify one another through secondary interactions that are formed during lanthanide binding. Clearer evidence for this is shown by the crystal structure of GPGdSE3-ubiquitin (*vide infra*).

4-5. Characterization of GPGdSE3-ubiquitin by X-Ray Crystallography

Experiments to study the construct GPGdSE3-ubiquitin by X-ray crystallographic analysis were conducted by Dr. Nicholas Silvaggi in the laboratory of Prof. Karen Allen at Boston University. These results are germane to this thesis, and are therefore included here.

Many previous attempts at solving the structure of a terbium-loaded LBT-protein fusion had met with failure. In some cases, the construct had failed to crystallize, and in some instances, there simply was no density in the LBT region (if the phases were solved by molecular replacement using the known protein structure), thus there was no anomalous Tb^{3+} signal to use when obtaining *de novo* phase information.²⁰ Initial crystallography screens on the GPGdSE3-ubiquitin construct were promising, and protein crystals began forming almost immediately upon concentration and screening (Figure 4-7A). More importantly, when illuminated with a handheld UV lamp, the crystals emitted green luminescence, indicating the presence of Tb^{3+} -bound (and -sensitizing) LBT (Figure 4-7B). One technique that may have been advantageous was loading the protein with Tb^{3+} at low concentration with multiple aliquots of lanthanide ion, followed by concentration.²¹ Ultimately, the optimized crystals gave a reasonable diffraction pattern (Figure 4-7C).

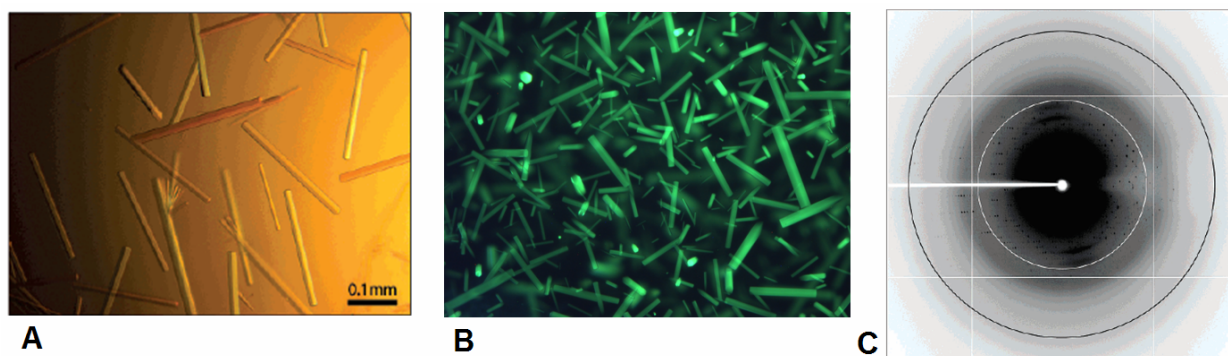


Figure 4-7. Crystallization of GPGdSE3-Ubiquitin. (These images have been previously published.²¹) **A.** Photograph of the optimized narrow, hexagonal rod crystals that GPGdSE3-ubiquitin forms. **B.** The crystals of this construct emit green luminescence under UV light. **C.** A representative diffraction image from one of the crystals. (These photographs were taken by Dr. Nicholas Silvaggi.)

Using the distinct anomalous signals from the Tb^{3+} atoms, the crystal structure of GPGdSE3-Ubiquitin was solved using the SAD (single-wavelength anomalous diffraction) method.²¹ (Ironically, this made us happy.) The full structure is shown in Figure 4-8A, and was deposited in the PDB with ID# 2OJR. A comparison was made of the ubiquitin portion of the GPGdSE3-ubiquitin construct with the structure of native ubiquitin, to determine the effect of the presence of the dLBT. As shown in Figure 4-8B, these structures overlay extremely well, with an RMSD of only about 0.8 Å. This evidence corroborates with the NMR data (Figure 4-5) to show that the presence of the dLBT minimally perturbs the structure of the protein to which it is tagged, an essential quality for either of these methods of structural determination. This was the first time a protein structure had been solved using a genetically encoded, coexpressed tag for incorporating heavy atoms; generalization of this method would be an outstanding addition to the protein crystallography tool kit.

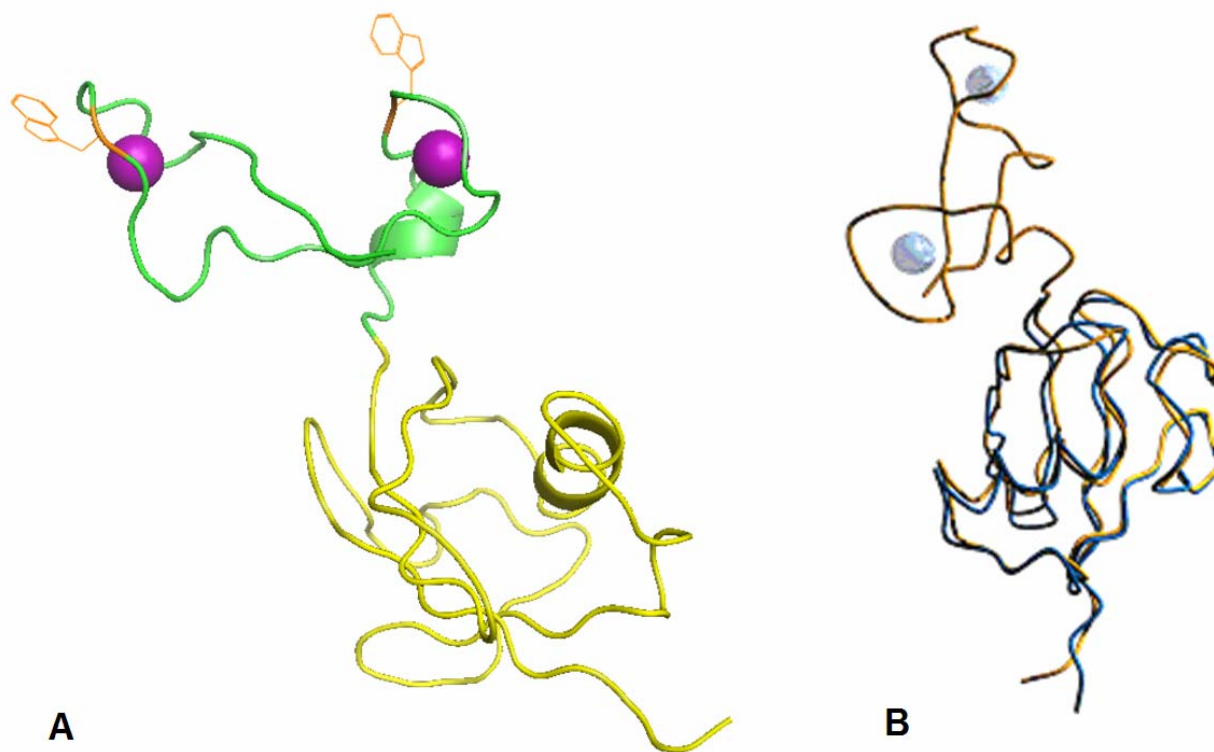


Figure 4-8. The crystal structure of GPGdSE3-Ubiquitin. **A.** The full structure in cartoon form, with the Tb^{3+} ions shown as magenta spheres, the dLBT shown in green, the tryptophan sensitizers shown in orange, and the ubiquitin shown in yellow. It is notable that this structure looks like an alien: the Tb^{3+} ions are the alien's eyes, the dLBT the alien's head, the tryptophan residues the alien's antennae, and the ubiquitin the alien's body—and the alien's weapon. **B.** Overlay of GPGdSE3-Ubiquitin (PDB ID# 2OJR), shown in orange with Tb^{3+} ions as silver spheres, with native Ubiquitin (PDB ID# 1UBQ, colored blue) showing the minimal change in the structure of the ubiquitin protein. (The image in **A** was created using the program PyMOL. The image in **B** was designed and created by Dr. Nicholas Silvaggi, and has been previously published.²¹)

The dLBT portion of the crystal is diagrammed in Figure 4-9. Figure 4-9B highlights the most interesting feature of this structure: the N-terminal Gly-Pro-Gly motif, which is merely present as a residual site from proteolysis site, forms a β -sheet-like structure with the intervening sequence (Leu-Tyr-Ile) between the two LBT motifs. This structure was completely unexpected, but it appears to enhance certain properties of the dLBT. For example, this may help to explain some of the strong RDCs observed in the protein NMR experiments (*vide supra*). Also, it is notable in Table 4-4 that, while the luminescence of GdSE3 is double that of SE3, GPGdSE3 is 2.5 times as bright as SE3. This Gly-Pro-Gly motif does not inherently enhance single-LBT luminescence (Table 4-5), and neither glycine nor proline residues include any sort of fluorophore. Therefore, it seems reasonable to hypothesize that the added structure is somehow beneficial to luminescence. It also seems likely to improve the ability of the substructure to crystallize.

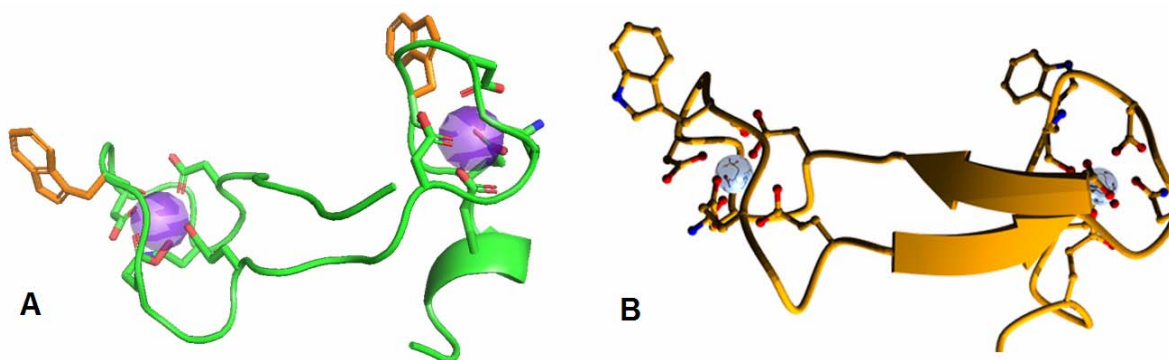


Figure 4-9. Structure of the dLBT portion of the crystal. **A.** The backbone is shown in green as a cartoon, with the indole side chains of Trp shown in orange, the Tb³⁺ ions shown as purple spheres, and the metal-chelating side chains and backbone carbonyls shown as sticks with carbon colored green, oxygen red and nitrogen blue. (This image was generated using PyMOL.). **B.** Shown at a slightly different angle, with coloration as in Figure 4-8B, and metal-chelating side chains shown. The β -sheet region, formed with the GPG motif, is clearly presented in cartoon form. (This image in **B** was created by Dr. Nicholas Silvaggi, and has been previously published.²¹)

Conclusions¹

We have successfully generated double-LBTs of fewer than 40 amino acids capable of simultaneously binding two lanthanide ions. The peptides GdSE3 and GPGdSE3 have been expressed as C-terminal fusions to GST, and then cleaved to yield free peptides, which were photophysically characterized to reveal that the concatenation of two LBTs resulted in superior binding and luminescence properties. When GPGdSE3 was expressed on the N-terminus of

ubiquitin, the lanthanide binding and luminescence characteristics of the construct were improved. NMR studies on GPGdSE3-ubiquitin reveal that in addition to the improved photophysical properties, the efficiency of the tag in mediating alignment between the lanthanide ions and the protein is increased dramatically by the lower mobility of the dLBT. This finding was corroborated by the use of the dLBT to solve the phases during the crystallographic structure determination of the same ubiquitin construct. Both NMR and crystallographic data revealed minimal structural perturbation by the dLBT on the ubiquitin protein. The crystallographic data showed that the N-terminal GPG formed a β -sheet structure as part of the dLBT, and this seems to be one factor that helps improve the luminescence output. The luminescence can be used for in-gel visualization, and furthermore the LBT can be used as the antigen in a Western blot analysis, because an antibody has been generated against a portion of the LBT sequence. The outstanding luminescence of the dLBT, together with the extension of applications for X-ray crystallography and NMR spectroscopy, is the focus on continuing efforts. The dLBT adds a unique, versatile tool that enables new approaches for the study of the structure, function, dynamics and interactions of proteins.

Experimental

4-OE. General Procedures

Peptide Synthesis and Purification.

Preparation of single-LBT peptides, and initial attempts at dLBT-peptide preparation, were by standard Fmoc-based SPPS procedures as described in Chapter 2 (2-OE). Peptides generated in this manner, and through the GST-fusion construct, were purified by HPLC and verified by MALDI-TOF MS as described in Chapter 2 (2-OE). Concentrations of stock solutions of peptides and the GPGdSE3-ubiquitin fusion protein were determined by the UV absorption using the extinction coefficients of the tryptophan ($\epsilon_{280} = 5690 \text{ cm}^{-1}\text{M}^{-1}$) and tyrosine ($\epsilon_{280} = 1280 \text{ cm}^{-1}\text{M}^{-1}$) content in 6 M guanidinium chloride.²²

Luminescence Titrations.

Titrations were recorded on a Jobin Yvon Horiba Fluoromax-3 Spectrometer in a 1 cm path-length quartz cuvette, as described in Chapter 2 (2-OE). As before, for direct titrations, the buffer was 100 mM NaCl, 10 mM MOPS; it was 100 mM NaOAc, 10 mM HEPES, pH 7.0 for qualitative comparisons. Aliquots of Tb^{3+} were added as described in section 2-OE.

Luminescence titration spectra were again analyzed with the program SPECFIT/32,²³ and calculated $\log \beta$ values were translated into the dissociation constants ($K_D = 10^{-\log \beta}$). Reported values are the average of three or four trials. For all titrations of double-LBTs (peptides or proteins), the luminescence intensity of the 1:1 (Tb³⁺:dLBT) complex was set, as part of the SPECFIT, to be exactly half of that of the 2:1 complex.

Relative Luminescence Intensity.

Comparative luminescence intensities of LBTs were determined using SPECFIT²³ as described in Chapter 2 (2-0E), normalized to that of SE3. For all dLBT constructs, the luminescence of the 1:1 (Tb³⁺:dLBT) complex was set in SPECFIT to exactly half of the luminescence of the 2:1 complex.

Determination of Tb³⁺-bound water molecules.

Luminescence lifetimes were measured as described in Chapter 2 (2-0E), to determine τ_{H2O} and τ_{D2O} . The number of Tb³⁺-bound water molecules, q , could then be calculated as described in the literature.¹⁴

4-1. Design and Selection of the dLBT Sequences.

Peptides were photophysically characterized as described above.

SE2: H₂N-YIDTNNDGWYEGDELLA-CONH₂

SE2 was a gift from Mark Nitz³ and was used without further purification, and was characterized as described in Chapter 2 (2-2E).

SE3: H₂N-YIDTNNDGWIEGDELLA-CONH₂

SE3 was prepared and characterized as described in Chapter 2 (2-2E).

SE4: H₂N-FIDTNNDGWIEGDELLLEEG-CONH₂

SE4 was a gift from Mark Nitz⁵ and was used without further purification, and was characterized as described in Chapter 2 (2-2E).

dSE3: H₂N-YIDTNNDGWIEGDELYIDTNNDGWIEGDELLA-CONH₂

Attempts at preparing dSE3 were by standard Fmoc-based SPPS as described on PAL-PEG-PS resin, with cleavage by TFA cocktail and purification by RP-HPLC. The major HPLC peak ($t_R \approx 20.5 - 21.5$ min) was never clean, even after three consecutive purifications. By MALDI, numerous truncation products were observed, especially in the N-terminal IEGDE region.

4-2E. Preparation of dLBT peptides and a dLBT-Ubiquitin construct.

Peptides were photophysically characterized as described above.

Generation of “megaprimer” inserts by PCR.

Primers were obtained from Operon Biotechnologies, Inc. (Huntsville, AL). Desalting purification was used. (Sequences of primers are included with the procedures for the specific construct.) Primers were dissolved in biological (sterile, deionized) water to a concentration of 0.5 mg/mL. Polymerase and polymerase buffer were obtained from Invitrogen (Carlsbad, CA); all other reagents were obtained from New England Biolabs (Ipswich, MA) and used as received.

In a sterile, 500 μ L Eppendorf tube was added 380 μ L of biological water, 50 μ L of 10 \times HIFI polymerase buffer, 32.5 μ L of dNTP mix (which contained 10 mM each of dATP, dCTP, dGTP, and dTTP), 19.5 μ L of 50 mM Mg^{2+} (either $MgCl_2$ or $MgSO_4$), and 6.5 μ L each of the forward and reverse primers. These were gently mixed by pipetting, and then 5 μ L of *Taq* DNA polymerase was added, and gently mixed. The solution was aliquoted into 10 \times 50 μ L, and placed in the PCR machine (BIO-RAD, Hercules, CA).

The PCR was cycled as follows (all temperatures in Celsius; 50 μ L reaction volume; 100 $^\circ$ C cover temperature):

- 1.) 92 $^\circ$, 3 min
- 2.) 92 $^\circ$, 45 sec
- 3.) 55 $^\circ$, 30 sec
- 4.) 72 $^\circ$, 1 minute
- 5.) Repeat steps 2 – 4 two more times (three times total)
- 6.) 72 $^\circ$, 1 min
- 7.) 04 $^\circ$, for storage

The PCR product was then concentrated. The 10 \times 50 μ L aliquots were combined into two \times 250 μ L in 1.5 mL Eppendorf tubes. To each was added 25 μ L of 3 M NaOAc, pH 5.5,

mixed by gentle vortex, and then 550 μL of absolute ethanol. Both were vortexed briefly, and then put on dry ice for at least 10 minutes. The tubes were then centrifuged for 30 minutes at maximum speed (14.1 RCF) at 4°C. The supernatant was aspirated, and the DNA pellet was dissolved in Buffer EB (10 mM Tris-Cl, pH 8.5, Qiagen), and purified on an agarose gel. Desired bands were excised and purified using the QIAquick gel extraction kit (Qiagen).

Digestion of plasmids and inserts by restriction enzymes.

Buffers and reagents were obtained from New England Biolabs and used without purification.

In a sterile, 500 μL Eppendorf tube was added 42.5 μL of DNA solution. (Plasmids were obtained from purification from DH5 α cells, *vide infra*, and inserts were generally from purification of the megaprimer, e.g. *vide supra*.) To each was added 5 μL of 10 \times restriction enzyme buffer (based on the double digestion recommendation from New England Biolabs), 0.5 μL of 100 \times BSA stock, and 1.0 μL each of the two restriction enzymes (e.g. *Bam*HI and *Xho*I). The reaction was mixed by pipetting, and allowed to react at 25°C overnight.

The next morning, 1.5 μL of *CIP* alkaline phosphatase was (usually) added to the plasmid digestion solution, and placed at 37°C for 90 minutes. Both reactions were then quenched with 12.5 μL of 5 \times nucleic acid loading buffer (Bio-Rad) and purified by agarose gel.

Ligation of new plasmids.

Purified, linear plasmid and insert DNA (from the restriction digests, above) were run on a quantitative agarose gel, to determine the stock concentrations. In a small, sterile tube were combined plasmid (~40 ng), insert (~60 ng or 5 equiv.), 1 μL 10 \times ligation buffer and 1 μL T4-ligase enzyme (Promega, Madison, WI), and biological water to 10 μL . Ligation reactions were carried out at 16°C overnight. The next morning, ultra competent XL10-gold cells (Stratagene, La Jolla, CA) were transformed with 5 μL of the ligation reaction, and plated on an LB-agar plate containing the appropriate antibiotic(s).

Transformation of competent cells.

A Falcon tube (BD Biosciences, San Jose, CA) was chilled on ice. Competent cells (XL10-gold, DH5 α , or BL21(DE3)gold, e.g.) were thawed on ice, and 30 – 40 μL of cells was transferred to the Falcon tube using a sterile pipet. If XL10-gold cells were used, 2 μL of molecular-biology grade β ME was also added to the Falcon tube, and let sit for 10 minutes.

Next, 1 – 10 μ L of ice-cold plasmid DNA was added to the cells and swirled to mix. Cells were incubated on ice for 30 minutes, heat-shocked at 42°C for 20 – 25 seconds, and incubated on ice for 2 minutes more.

To the tube was then added 270 μ L of sterile SOC medium (Invitrogen), and it was shaken at 37°C for one hour. Finally, 50 – 200 μ L of the growth was plated on an LB-agarose plate containing the appropriate antibiotic (e.g. carbenicillin or kanamycin) and incubated overnight at 37°C. The next morning, single colonies could be picked using a sterile tip.

Cloning of the *GST-ENLYFQGdSE3* construct.

The pGEX-4T-2 plasmid (Amersham Biosciences) was a gift from Dr. Elizabeth Vogel. DH5 α cells (Stratagene) were transformed with this plasmid, plated on LB-carbenicillin-agar plates, and incubated overnight. A colony was picked and grown overnight; usable quantities of plasmid were extracted using a Miniprep (Qiagen) kit.

The gene for ENLYFQG-dSE3 was inserted into the pGEX-4T-2 plasmid, using a megaprimer strategy. The TEV (Tobacco Etch Virus) protease cleavage site was included to facilitate removal of the N-terminal GST (glutathione-S-transferase) fusion protein; the recognition sequence, ENLYFQ/G, is cleaved such that the dLBT fragment is left with an N-terminal glycine. Two smaller primers (obtained from Operon; see the nucleotide sequences below) were elongated by PCR with Platinum Taq polymerase (Invitrogen), using the procedure described above, to generate the double-stranded dLBT insert.

“TEV-GdSE3 for *Bam*HI”

(CGGGATCCGAAAACCTGTA~~CTT~~CCAGGGTTACATCGACACCAACAACGATGGTTG
GATTGAAGGCGACGAACTGTATAT)

“dLBT_rev_ *Xho*I”

(CCGCTCGAGTCACGCCAGCAGTTCATCGCCTTCGATCCAACCGTCGTTGTTGGTA
TCGATATACAGTTCGTCGCCTTC)

The PCR products and the pGEX-4T-2 vector were digested using *Bam*HI and *Xho*I restriction enzymes, purified, and annealed as described; miniprep quantities of the desired plasmid were obtained from transformed XL10 gold cells. For expression, BL21 cells (Stratagene) were transformed with the plasmid.

Gene of the LVPRGSENL^YFQ**GdSE3** Portion:

CTGGTTCGCGTGGATCCGAAAACCTGTACTTCCAGGGTTACATCGACACCAACAA
CGATGGTTGGATTGAAGGCGACGAAGTGTATATCGATAACCAACAACGACGGTTGG
ATCGAAGGCGATGAACTGCTGGCGTGA

Protein Sequence of GST-ENLYFQ**GdSE3**:

MSPILGYWKIKGLVQPTRLLLEYLEEKYEEHLYERDEGDKWRNKKFELGLEFPNLPYYIDGDVK
LTQSMAIIRYIADKHNMLGGCPKERAEISMLEGAVLDIRYGVSR IAYS KDFETLKVDFLSKLPE
MLKMFEDRLCHKTYLNGDHVTHPDFMLYDALDVVLYMDPMCLDAFPKLVCFKKRIEAI PQIDKY
LKSSKYIAWPLQGWQATFGGGDHPKSDLVPRGSENL^YFQ**GYIDTNNDGWIEGDELYIDTNNDG
WIEGDELLA**

Expression and purification of the GST-GdSE3 construct.

Starting from an overnight culture, BL21-(DE3)-Gold cells (Stratagene) expressing the desired GST-fusion were grown in 10 L of LB media containing carbenicillin antibiotic in a fermenter (BIOFLO 110, New Brunswick Scientific), at 37 °C. When the OD₆₀₀ reached 0.45, the temperature was reduced to 30 °C, and protein production was induced with 0.2 mM isopropyl-β-D-1-thiogalactopyranoside (IPTG) at OD₆₀₀ of about 0.65. After 5 hours, the cells were harvested by centrifugation and frozen at -80 °C until needed.

All purification was performed at 4 °C unless otherwise noted. The cell pellet was thawed and resuspended in a lysis buffer (400 mL PBS pH 7.4, 1 mg/mL lysozyme, 400 μL Protease Inhibitor Cocktail Set III (Calbiochem), 1 mM DTT), and incubated at 4 °C for about 20 minutes. 50 mL of a 5% NP40 detergent solution (in PBS) was then added, followed by 10 minutes of rocking. Cells were lysed by sonication, and cellular debris was pelleted by centrifugation. Supernatant was incubated for 45 minutes with Glutathione-sepharose resin (Amersham Biosciences) at room temperature, washed extensively with PBS, and the GST-construct was then eluted using a 10 mM glutathione solution in 50 mM Tris (pH 8.0) buffer containing the same protease inhibitor cocktail. Elution fractions were analyzed by 15% SDS-PAGE and quantified using the Biorad BCA/BSA protein assay. Purified protein was stored at 4°C until cleavage by mTEV protease.

Cleavage by mTEV protease and purification of the dLBT peptide.

Mutant Tobacco Etch Virus protease (mTEV protease) was expressed on site from expression vector pRK793,¹³ which was obtained from Addgene (Cambridge, MA). The cleavage reaction was conducted in 50 mM Tris, 5 mM EDTA, 5 mM βME, pH 8.0, at room temperature overnight, and analyzed by 15% SDS-PAGE (*vide infra*) for completeness.

The solution was then prepared for HPLC. DMF (dimethylformamide, Sigma-Aldrich) was added to a concentration of up to 20%, and the mixture was acidified to pH < 5.0 using 2 M acetic acid. Precipitated (undesired) protein was pelleted by centrifugation, and the supernatant was filtered and then purified by reverse phase HPLC as described in Chapter 2 (2-0E).

GdSE3: H₂N-GYIDTNN~~GWIEGDELYIDTNN~~GWIEGDELLA-CO₂H

GdSE3 was prepared using the expression method described above. It was purified as described (section 4-0E) by RP-HPLC ($t_R = 21.7$ min). Exact mass calcd., 3729.6 [M+H⁺]; found 3727.7 [M+H⁺] by MS(MALDI).

$$\begin{aligned} \text{Log } \beta (\text{Tb}^{3+}, 1:1_{\text{NaCl/MOPS}}) &= 8.01 \pm 0.22 \\ \text{Log } \beta (\text{Tb}^{3+}, 2:1_{\text{NaCl/MOPS}}) &= 15.46 \pm 0.18 \\ \text{Log } \beta (\text{Tb}^{3+}, 1:1_{\text{NaOAc/HEPES}}) &= 6.23 \pm 0.02 \\ \text{Log } \beta (\text{Tb}^{3+}, 2:1_{\text{NaOAc/HEPES}}) &= 12.18 \pm 0.09 \\ \text{Molar luminescence intensity (1:1)} &= 11.6 \times 10^{12} \text{ M}^{-1}\text{cm}^{-1} \\ \text{Luminescence decay: } \tau_{\text{H}_2\text{O}} &= 2.63 \text{ ms; } \tau_{\text{D}_2\text{O}} = 3.29 \text{ ms} \end{aligned}$$

Gene Sequence of His₆-GPGdSE3-Ubiquitin:

ATGAAACATCACCATCACCATCACGGCCCAGGTTATATTGACACTAATAACGACGG
ATGGATTGAGGGTGATGAACTGTATATTGACACCAACAATGATGGGTGGATTGAAG
GAGATGAGTTACTGGCGATGCAAATTTTCGTCAAACGCTGACAGGCCAAAACGATC
ACCCTGGAAGTTGAGCCGAGCGATACAATCGAAAACGTGAAAGCAAAAATCCAGG
ACAAAGAAGGCATCCCGCCTGATCAGCAACGGCTGATTTTTGCCGGTAAACAGCT
GGAAGATGGCCGTACCCTGTCTGATTACAATATTCAGAAAGAAAGTACTCTGCATC
TGGTATTACGTCTGCGCGGTGGGTAAGGATCC

Cloning, expression and purification of GPGdSE3-Ubiquitin.

The construct for the expression of GPGdSE3-Ubiquitin was generated as described in the literature, by inserting the appropriate MKHHHHHHGPGdSE3-encoding gene into the pET11a plasmid (Novagen).¹ In general, experiments on this construct were done on protein that was prepared by Dr. Nicholas Silvaggi.²¹

GPGdSE3-Ubiquitin:

GPGYIDTNN~~GWIEGDELYIDTNN~~GWIEGDELLA**MQIFVKTLTGKTITLEVEPSDTIENVKAKIQDKEGIPPDQQRLLIFAGKQLEDGRTLSDYNIQKESTLHLVLRRLRGG**

GPGdSE3-ubiquitin was prepared and photophysically characterized as described above.

$$\begin{aligned} \text{Log } \beta (\text{Tb}^{3+}, 1:1_{\text{NaCl/MOPS}}) &= 8.63 \pm 0.07 \\ \text{Log } \beta (\text{Tb}^{3+}, 2:1_{\text{NaCl/MOPS}}) &= 16.27 \pm 0.19 \\ \text{Log } \beta (\text{Tb}^{3+}, 1:1_{\text{NaOAc/HEPES}}) &= 6.15 \pm 0.06 \\ \text{Log } \beta (\text{Tb}^{3+}, 2:1_{\text{NaOAc/HEPES}}) &= 12.45 \pm 0.05 \end{aligned}$$

Molar luminescence intensity (1:1) = $8.25 \times 10^{12} \text{ M}^{-1}\text{cm}^{-1}$ (determined by comparing luminescence of Tb^{3+} -saturated GPGdSE3-ubiquitin with that of Tb^{3+} -saturated SE3)
Luminescence decay: $\tau_{H_2O} = 2.70 \text{ ms}$; $\tau_{D_2O} = 3.33 \text{ ms}$

Ubiquitin:

*MQIFVKTLTGKTITLEVEPSDTIENVKAKIQDKEGIPPDQQRLLIFAGKQLEDGRTLSDYNIQKES
TLHLVLRGG*

Native ubiquitin was expressed and characterized in Prof. Schwalbe's lab as described.¹

SDS-PAGE and Western Blot Analysis.

Proteins were loaded onto 15% SDS-polyacrylamide gels in denaturing buffer, and subjected to electrophoresis at 120 V for about two hours. The gel was then washed twice for 15 minutes (each wash) with 100 mM NaCl, 10 mM HEPES pH 7.0 buffer, followed by incubation for 20 minutes in the same buffer containing 4 μM Tb^{3+} . Luminescent bands were visualized and processed as described previously.² The same gel was then stained with Gel Code Blue (Pierce) to visualize total protein.

Alternatively, an "anti-LBT" Western blot analysis could be conducted. Protein was transferred from the 15% PAGE to nitrocellulose at 105V for 90 minutes in Western blotting transfer buffer (made by dissolving 57.6 g glycine, 12.1 g Tris base, and 800 mL methanol in water to a volume of 4 liters). The nitrocellulose is then blocked with milk. The primary (monoclonal) antibody was generated in rabbits by Quality Controlled Biochemicals (Hopkinton, MA). (Two rabbits were utilized for this purpose. The injected antigen was the peptide sequence AcNH-**IEGDELLLEEG**-CONH₂. Antibody from one rabbit recognizes the sequence Ile-Glu-Gly-Asp-Glu-Leu-Leu; antibody from the other rabbit recognizes the sequence Glu-Gly-Asp-Glu-Leu-Leu.) A goat-anti-rabbit secondary antibody and an alkaline phosphatase stain were used for visualization.

4-3E. Photophysical Characterization of dLBT peptides and proteins.

Cloning of the *GST-ENLYFQGPGdSE3* construct.

This construct was cloned into the pGEX-4T-2 plasmid using a process identical to that for *GST-ENLYFQGdSE3*. The two primers used in the PCR generation of the megaprimer insert are shown below.

“TEV-GPGdSE3 for BamHI”
(CGGGATCCGAAAACCTGTACTTCCAGGGTCCGGGCTACATCGACACCAACAACG
ATGGTTGGATTGAAGGCGACGAACTGTATAT)

“dLBT_rev_XhoI”
(CCGCTCGAGTCACGCCAGCAGTTCATCGCCTTCGATCCAACCGTCGTTGTTGGTA
TCGATATACAGTTCGTCGCCTTC)

The PCR product and the pGEX-4T-2 vector were digested using *BamHI* and *XhoI* restriction enzymes, purified, and annealed as before; miniprep quantities of the desired plasmid were obtained from transformed XL10 gold cells.

Gene of the LVPRGSENL_YFQ**GPGdSE3** Portion:

CTGGTTCCGCGTGGATCCGAAAACCTGTACTTCCAGGGTCCGGGCTACATCGACA
CCAACAACGATGGTTGGATTGAAGGCGACGAACTGTATATCGATACCAACAACGAC
GGTTGGATCGAAGGCGATGAACTGCTGGCGTGA

Protein Sequence of GST-ENLYFQ**GPGdSE3**:

MSPILGYWKIKGLVQPTRLLEYLEEKYEEHLYERDEGDKWRNKKFELGLEFPNLPYYIDGDVKL
TQSMAIIRYIADKHNMLGGCPKERAEISMLEGAVLDIRYGVSRIAYSKDFETLKVDFLSKLP
KMFEDRLCHKTYLNGDHVTHPDFMLYDALDVVLYMDPMCLDAFPKLVCFKKRIEAI
PQIDKYLKSKYIAWPLQGWQATFGGGDHPPKSDLVPRGSENL_YFQ**GPGYIDT**
TNNDGWIEGDELYIDT
**TNNDGWI
EGDELLA**

Expression and purification of the GST-GPGdSE3 construct.

This construct was expressed and purified using a procedure identical to the *GST-GdSE3* construct (see section 4-2E). Cleavage by mTEV protease was significantly less efficient for this construct, but sufficient quantities of *GPGdSE3* peptide were obtained to run the described photophysical experiments.

GPGdSE3: H₂N-**GPGYIDT****TNNDGWIEGDELYIDT****TNNDGWIEGDELLA**-CO₂H

GPGdSE3 was prepared using the expression method described above. It was purified as described (section 4-2E) by RP-HPLC ($t_R = 20.8$ min). Exact mass calcd., 3883.7 [M+H⁺]; found 3883.8 [M+H⁺], 3903.6 [M+Na⁺] by MS(MALDI).

$$\text{Log } \beta (\text{Tb}^{3+}, 1:1_{\text{NaCl/MOPS}}) = 8.44 \pm 0.18$$

$$\text{Log } \beta (\text{Tb}^{3+}, 2:1_{\text{NaCl/MOPS}}) = 15.65 \pm 0.08$$

$$\text{Log } \beta (\text{Tb}^{3+}, 1:1_{\text{NaOAc/HEPES}}) = 6.24 \pm 0.02$$

$$\text{Log } \beta (\text{Tb}^{3+}, 2:1_{\text{NaOAc/HEPES}}) = 12.25 \pm 0.04$$

$$\text{Molar luminescence intensity (1:1)} = 6.65 \times 10^{12} \text{ M}^{-1} \text{ cm}^{-1}$$

$$\text{Luminescence decay: } \tau_{\text{H}_2\text{O}} = 2.71 \text{ ms; } \tau_{\text{D}_2\text{O}} = 3.41 \text{ ms}$$

Protein Sequence of His₆-GPGSE2-Ubiquitin:

MKHHHHHHGPGYIDTNNDGWYEGDELLAMQIFVKTLTGKTITLEVEPSDTIENVKAKIQDKEGIP
PDQQRLLIFAGKQLEDGRTLSDYNIQKESTLHLVLRLLRGG

Cloning, expression and purification of GPGSE2-Ubiquitin.

The construct for the expression of GPGSE2-Ubiquitin was generated as described in the literature.⁶ The GPGSE2-Ubiquitin used in the experiments described was a gift from Dr. Manashi Sherawat and Dr. Nicholas Silvaggi.

4-4E. Characterization of GPGdSE3-ubiquitin by NMR.

NMR experiments were conducted by Martin Hähnke and Dr. Jens Wöhnert in Prof. Harald Schwalbe's lab at Johann Wolfgang Goethe Universität Frankfurt am Main, and have been previously described.¹

4-5E. Characterization of GPGdSE3-ubiquitin by X-Ray Crystallography.

X-ray crystallography experiments and structural determination were conducted by Dr. Nicholas Silvaggi in Prof. Karen Allen's lab at Boston University School of Medicine, and have been previously described.²¹

Acknowledgements

Much of this chapter has been previously published, and I am thus indebted to all of my coauthors. Dr. Mark Nitz deserves credit for the original conceptualization of the dLBT. I am grateful for our collaboration with Prof. Harald Schwalbe's lab at Johann Wolfgang Goethe University in Frankfurt, Germany; Dr. Martin Hähnke did most of the NMR work, and made Figures 4-5 and 4-6. I am also grateful for our collaboration with Prof. Karen Allen's lab at Boston University School of Medicine; Dr. Nicholas Silvaggi did most of the crystallography work, and made Figures 4-1, 4-7, 4-8B and 4-9B. Nick and Dr. Manashi Sherawat purified the GPGdSE3-ubiquitin and GPGSE2-ubiquitin constructs; Dr. Jens Wöhnert (Schwalbe lab) did the original cloning for the former construct, and Dr. Kathy Franz (Imperiali lab) did the cloning for the latter. I thank Dr. K. Jebrell Glover and Dr. Elizabeth Vogel Taylor (Imperiali lab) for teaching me molecular biology and PCR techniques. I am eternally grateful to Meredith Hartley for editing this chapter.

References

- (1) Martin, L. J.; Hähnke, M. J.; Nitz, M.; Wöhnert, J.; Silvaggi, N. R.; Allen, K. N.; Schwalbe, H.; Imperiali, B. "Double-Lanthanide-Binding Tags: Design, Photophysical Properties, and NMR Applications." *J. Am. Chem. Soc.* **2007**, *129*(22), 7106-7113.
- (2) Franz, K. J.; Nitz, M.; Imperiali, B. "Lanthanide-binding tags as versatile protein coexpression probes." *ChemBioChem* **2003**, *4*(4), 265-271.
- (3) Nitz, M.; Franz, K. J.; Maglathlin, R. L.; Imperiali, B. "A powerful combinatorial screen to identify high-affinity terbium(III)-binding peptides." *ChemBioChem* **2003**, *4*(4), 272-276.
- (4) Nitz, M.; Sherawat, M.; Franz, K. J.; Peisach, E.; Allen, K. N.; Imperiali, B. "Structural origin of the high affinity of a chemically evolved lanthanide-binding peptide." *Angew. Chem. Int. Ed.* **2004**, *43*(28), 3682-3685.
- (5) Martin, L. J.; Sculimbrene, B. R.; Nitz, M.; Imperiali, B. "Rapid Combinatorial Screening of Peptide Libraries for the Selection of Lanthanide-Binding Tags (LBTs)." *QSAR Comb. Sci.* **2005**, *24*(10), 1149-1157.
- (6) Wöhnert, J.; Franz, K. J.; Nitz, M.; Imperiali, B.; Schwalbe, H. "Protein alignment by a coexpressed lanthanide-binding tag for the measurement of residual dipolar couplings." *J. Am. Chem. Soc.* **2003**, *125*(44), 13338-13339.
- (7) Su, X.-C.; Huber, T.; Dixon, N. E.; Otting, G. "Site-specific labeling of proteins with a rigid lanthanide-binding tag." *ChemBioChem* **2006**, *7*(10), 1599-1604.
- (8) Su, X.-C.; McAndrew, K.; Huber, T.; Otting, G. "Lanthanide-Binding Peptides for NMR Measurements of Residual Dipolar Couplings and Paramagnetic Effects from Multiple Angles." *J. Am. Chem. Soc.* **2008**, *130*, 1681-1687.
- (9) Goda, N.; Tenno, T.; Inomata, K.; Iwaya, N.; Sasaki, Y.; Shirakawa, M.; Hiroaki, H. "LBT/PTD dual tagged vector for purification, cellular protein delivery and visualization in living cells." *Biochim. Biophys. Acta* **2007**, *1773*(2), 141-146.
- (10) Sculimbrene, B. R.; Imperiali, B. "Lanthanide-Binding Tags as Luminescent Probes for Studying Protein Interactions." *J. Am. Chem. Soc.* **2006**, *128*(22), 7346-7352.
- (11) Marsden, B. J.; Hodges, R. S.; Sykes, B. D. "Proton NMR studies of synthetic peptide analogs of calcium-binding site III of rabbit skeletal troponin C: Effect on the lanthanum affinity of the interchange of aspartic acid and asparagine residues at the metal ion coordinating positions." *Biochemistry* **1988**, *27*(11), 4198-4206.

- (12) MacManus, J. P.; Hogue, C. W.; Marsden, B. J.; Sikorska, M.; Szabo, A. G. "Terbium luminescence in synthetic peptide loops from calcium-binding proteins with different energy donors." *J. Biol. Chem.* **1990**, *265*(18), 10358-10366.
- (13) Kapust, R. B.; Toezser, J.; Fox, J. D.; Anderson, D. E.; Cherry, S.; Copeland, T. D.; Waugh, D. S. "Tobacco etch virus protease: mechanism of autolysis and rational design of stable mutants with wild-type catalytic proficiency." *Protein Eng.* **2001**, *14*(12), 993-1000.
- (14) Beeby, A.; Clarkson, I. M.; Dickins, R. S.; Faulkner, S.; Parker, D.; Royle, L.; de Sousa, A. S.; Williams, J. A. G.; Woods, M. "Non-radiative deactivation of the excited states of europium, terbium and ytterbium complexes by proximate energy-matched OH, NH and CH oscillators: an improved luminescence method for establishing solution hydration states." *J. Chem. Soc., Perkin Trans. 2* **1999**, (3), 493-504.
- (15) Vijay-Kumar, S.; Bugg, C. E.; Cook, W. J. "Structure of ubiquitin refined at 1.8 Å resolution." *J. Mol. Biol.* **1987**, *194*(3), 531-544.
- (16) Horrocks, W. D., Jr.; Sudnick, D. R. "Lanthanide ion probes of structure in biology. Laser-induced luminescence decay constants provide a direct measure of the number of metal-coordinated water molecules." *J. Am. Chem. Soc.* **1979**, *101*(2), 334-340.
- (17) Horrocks, W. D., Jr.; Sudnick, D. R. "Lanthanide ion luminescence probes of the structure of biological macromolecules." *Acc. Chem. Res.* **1981**, *14*(12), 384-392.
- (18) Martell, A. E.; Smith, R. M., *Critical Stability Constants, Vol. 1: Amino Acids*. Plenum Press: New York, 1974;
- (19) Rodriguez-Castaneda, F.; Haberz, P.; Leonov, A.; Griesinger, C. "Paramagnetic tagging of diamagnetic proteins for solution NMR." *Magn. Reson. Chem.* **2006**, *44*(Spec. Issue), S10-S16 and references therein.
- (20) Silvaggi, N. R.; Sherawat, M.; Peisach, E.; Nitz, M.; Imperiali, B.; Allen, K. N., Unpublished results.
- (21) Silvaggi, N. R.; Martin, L. J.; Schwalbe, H.; Imperiali, B.; Allen, K. N. "Double-Lanthanide-Binding Tags for Macromolecular Crystallographic Structural Determination." *J. Am. Chem. Soc.* **2007**, *129*(22), 7114-7120.
- (22) Chazan, A. Peptide Property Calculator.
<http://www.basic.northwestern.edu/biotools/proteincalc.html>
- (23) Binstead, R.; Jung, B.; Zuberbühler, A. *SPECFIT/32 for Windows; Original Release 2000*, Version 3.0.39; Spectrum Software Associates, Marlborough, MA.: SPECFIT/32 provides global analysis of equilibrium systems using singular value decomposition and nonlinear regression modeling by the Levenberg-Marquardt method. 2007.

Chapter 5

LBT and dLBT Redesign based on dLBT Structural Data

Introduction

With one protein crystal structure solved using the dLBT,¹ and promising results using NMR spectroscopy,² we were excited about the potential generalization of the dLBT “GPGdSE3” (Figure 5-1). Nevertheless, this was the first dLBT that we had used to study a fusion protein, and it seemed unlikely that this sequence was optimal. However, the length of this peptide (35 residues) made it prohibitive to study *via* a synthetic combinatorial peptide library^{3,4} (as in Chapters 1 and 2); an alternative method was needed. Therefore, we engaged in collaboration with Bracken King in the laboratory of Professor Bruce Tidor at M.I.T. The aim of the collaboration was to improve single- and double-LBTs using computational design based on the known crystal structures. This approach has enabled the discovery of a single-LBT with improved properties, along with some promising leads for superior dLBT sequences. We have made modifications to the GPG region of the dLBT sequence to improve compatibility with purification systems utilizing the mTEV protease without affecting photophysical properties of the dLBT. Finally, we have begun studies to optimize the luminescence output of the dLBT

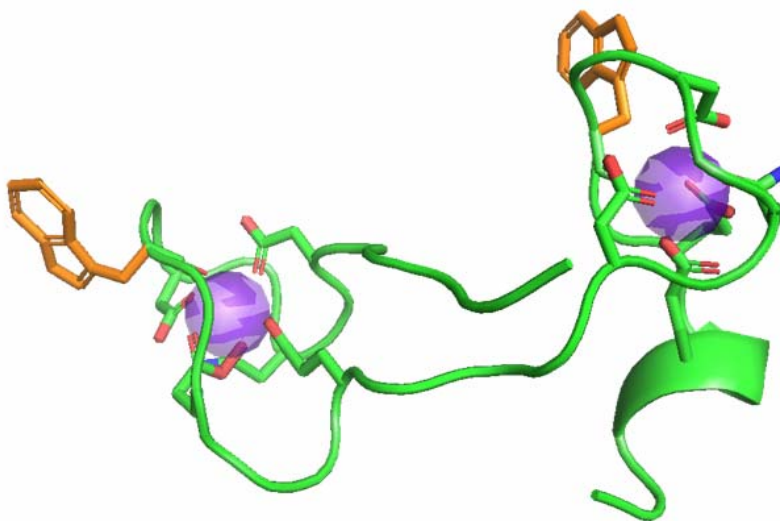


Figure 5-1. Structure of the dLBT portion of the crystal of GPGdSE3-ubiquitin (from PDB# 2OJR)¹. The backbone is shown in green as a cartoon, with the indole side chains of Trp shown in orange, the Tb³⁺ ions shown as purple spheres, and the metal-chelating side chains and backbone carbonyls shown as sticks with carbon colored green, oxygen red and nitrogen blue. The N-terminal lanthanide-binding motif is on the left; ubiquitin connects to the chain that terminates in the bottom right. (This image was generated using PyMOL.).

Results and Discussion

5-1. Design of SE3 Mutants to Address Conformational Questions

Bracken King, a graduate student in Professor Bruce Tidor's lab (M.I.T.), compared the orientation and flexibility of the terbium-binding peptides in the crystal structures of the single-LBT SE2⁵ (see Figure 2-1 and Table 4-1), and of the GPGdSE3 motif (Figure 5-1) in the ubiquitin construct¹. When superimposed, all three binding motifs appear nearly identical. However, the ϕ/ψ angles (and therefore Ramachandran space) of a few residues (Asn3, Asn4, Asp5, Gly6) in the N-terminal loop and the SE2 crystal differ significantly from those in the C-terminal loop of GPGdSE3, as shown in Figure 5-2. The related terbium-bound conformations will be called conformation 1 (which includes the SE2 peptide crystal) and conformation 2.

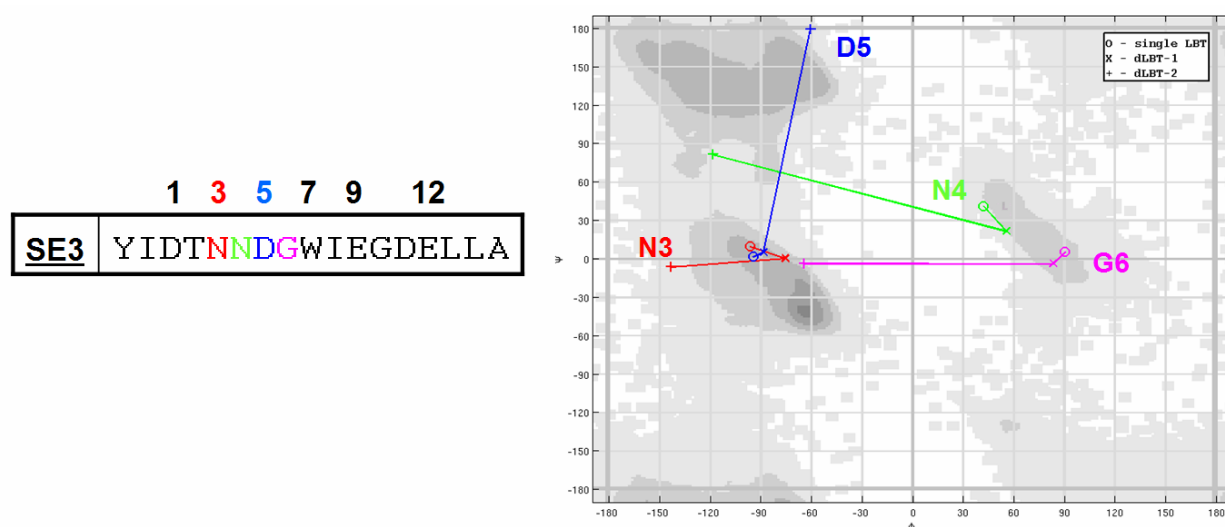


Figure 5-2. Comparison of Ramachandran space of four residues in the SE2 and GPGdSE3 crystals. The sequence of SE3 is shown at left for reference (SE2 has I8→Y). Asn3 is shown in red, Asn4 in green, Asp5 in blue and Gly6 in magenta. On the diagram, the position in ϕ/ψ space is indicated by a circle for SE2, by an X for the N-terminal motif of GPGdSE3, and by a cross for the C-terminal motif of GPGdSE3. (The Ramachandran diagram was created by Bracken King.)

The existence of these different conformations, coupled with repeated failures to generate crystals of a protein fusion with a single-LBT, leads to the hypothesis that this may have been caused by the failure of the terbium-bound LBT to adopt a single, unique conformation. Although Asn3 and Asp5 both chelate Tb^{3+} and are therefore effectively unmutatable, both Asn4 and Gly6 are not theoretically optimized (especially the former; see also Table 2-3). No significant libraries of peptides have ever been designed to study the importance Asn4, for

example.⁴ Also, Gly6 was believed to be necessary to allow the proper orientation of the coordinated carbonyl on Trp7 and so has never been varied. However, results from the computational study of the dLBT indicated that further refinement of these residues may be beneficial.

Using a program that Bracken designed, positions 4 and 6 were varied between all of the natural amino acids except proline (which the program was unable to use). The relative energies of folding ($\Delta\Delta G_{\text{fold}}$) into conformation 1 and conformation 2 were compared to that of the “wild-type” Asn4 and Gly6. These energy differences were graphed, and are shown in Figure 5-3.

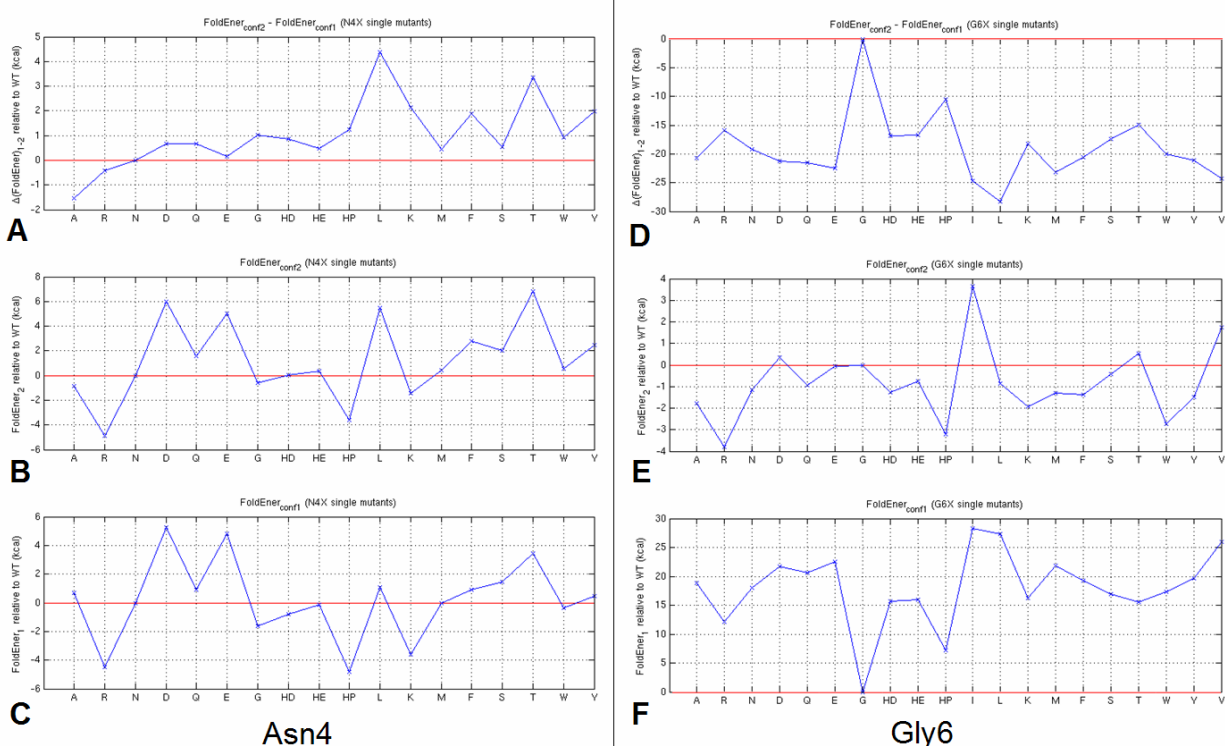


Figure 5-3. Comparison of the calculated folding energies of different residues at positions 4 and 6 of the Tb³⁺-bound LBT, in either conformation 1 or conformation 2. Plots **A** and **D** show the relative residue preferences for conformations 1 and 2. Plots **A**, **B**, and **C** are for mutations at position 4 (Asn in **SE3**); plots **D**, **E**, and **F** are for mutations at position 6 (Gly in **SE3**). In all graphs, the amino acid point mutations are plotted along the abscissa, and energy is plotted along the ordinate. The red line is at $\Delta E = 0$. Plots **B** and **E** compare the folding energies of the different residues in conformation 2 compared to Asn4 or Gly6, respectively. Plots **C** and **F** compare the folding energies of the different residues in conformation 1 compared to Asn4 or Gly6, respectively. Plot **A** represents the energy of plot **B** minus plot **C**; plot **D** represents the energy of the plot in **E** minus the plot in **F**, thus the relative preference of the residue for conformation 2 vs. conformation 1. (Bracken King made these plots.)

The lower plots (Figures 5-3C and 5-3F) show the difference in folding energy of mutant to “wild type” in conformation 1, and the center plots show the difference for conformation 2. The uppermost plots show the difference between the center and the lower plots in the same

column (that is, plot 5-3A = 5-3B – 5-3C, and 5-3D = 5-3E – 5-3F). Therefore, a more negative value in Figures 5-3A and 5-3D indicates a stronger preference for conformation 2 than “wild type”, whereas a more positive value indicates that conformation 1 should be favored; values at or near 0 for a specific residue indicate that the difference in energy between the two conformations is similar to that for Asn4 or for Gly6. Figure 5-4 is a compilation these hypothetical variations, simultaneously taking into account the values in Figures 5-3A and 5-3D. A dark red color indicates that the peptide should favor conformation 1 more strongly than “wild type” SE3, and the dark blue color indicates that conformation 2 should be more strongly favored. Note that the changes in each position are essentially additive; there is virtually no “cross-talk” between the two sites.

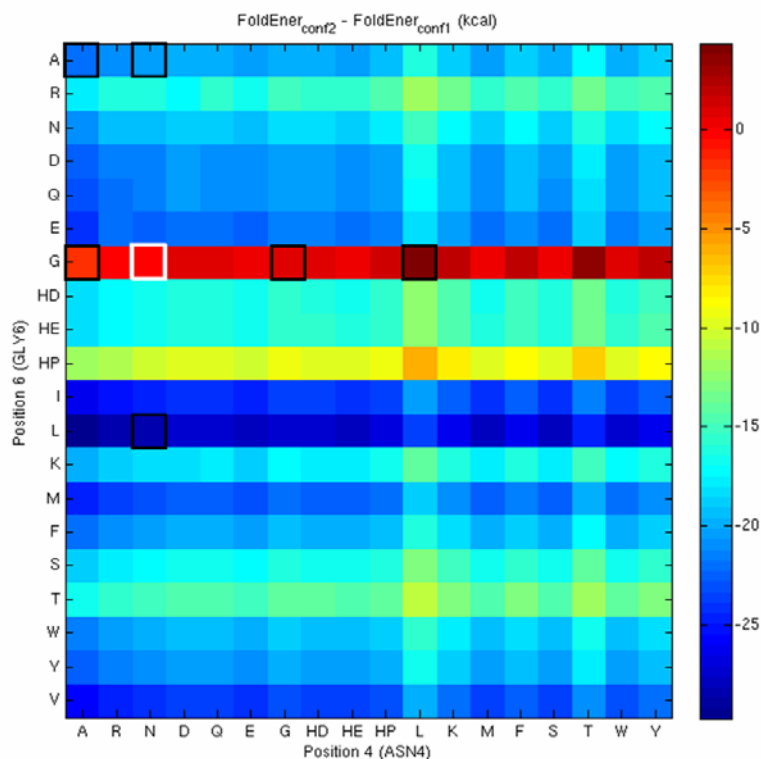


Figure 5-4. Differences in folding energies of all hypothetical Asn4, Gly6 SE3 double mutants. Mutations at Asn4 are shown on the horizontal axis, and mutations at Gly6 along the vertical axis. “Wild type” SE3 is indicated by the white box; black boxes indicate the non-proline-containing mutants that were made. A dark red color indicates that the peptide should favor conformation 1 more strongly than SE3, and the darker blue indicates that conformation 2 should be more strongly favored. (Bracken King created this figure.)

Based on these calculations, eight promising mutants were selected for synthesis and photophysical characterization, to screen for LBTs that might give enhanced crystallization

properties. Four are from mutation at position 4, three at position 6, with one double-mutant. These mutants are summarized in Table 5-1; see also the black squares in Figure 5-4. The mutation N4→L clearly appears (based on Figures 5-3 and 5-4) to most significantly favor conformation 1, and while N4→G is only slightly more conformation 1-promoting than in “wild type” SE3, glycine is generally well-modeled and was therefore chosen. Alanine is also easily modeled, and was therefore selected as a single mutation at both positions, and at both for the double mutant. Asn4→Ala was especially promising as a conformation 2-promoting mutant, given that it appears both to favor conformation 2 (Figure 5-3B) and disfavor conformation 1 (Figure 5-3C). Finally, while proline could not be modeled, neither of the Pro-containing mutants could possibly bind Tb³⁺ in conformation 1.

Table 5-1. Sequences of Computationally Designed SE3 Mutants

Mutation	LBT	Sequence ^a	Modeled preference ^b
--	<u>SE3</u>	YIDT N R D G WIEGDELLA	--
N4→A	<u>SE3α</u>	YIDT N A DGWIEGDELLA	Conformation 2
N4→G	<u>SE3β</u>	YIDT N G DGWIEGDELLA	Conformation 1
N4→L	<u>SE3γ</u>	YIDT N L DGWIEGDELLA	Conformation 1
N4→P	<u>SE3δ</u>	YIDT N P DGWIEGDELLA	Conformation 2
G6→A	<u>SE3ϵ</u>	YIDT N N D A WIEGDELLA	Conformation 2
G6→L	<u>SE3ζ</u>	YIDT N N D L WIEGDELLA	Conformation 2
G6→P	<u>SE3η</u>	YIDT N N D P WIEGDELLA	Conformation 2
N4→A, G6→A	<u>SE3θ</u>	YIDT N A D A WIEGDELLA	Conformation 2

^a SE3 residues N3, N4, D5 and G6 are colored as in Figure 5-2.

^b Based on Figures 5-3 and 5-4. Conformation 1 is SE2-crystal-conformation-like.

5-2. Synthesis and Photophysical Characterization of SE3 Mutants

All eight mutants were successfully synthesized using standard solid-phase peptide synthesis procedures and purified by HPLC. Peptides were subjected to the standard photophysical characterizations including the determination of the number of Tb³⁺-bound water molecules, measurement of dissociation constants (in normal buffer and also acetate buffer for the tight binders), and relative brightness. This data is summarized in Table 5-2.

Encouragingly, six of the eight mutants bound Tb³⁺. The two proline-containing mutants were the only peptides that failed to bind Tb³⁺; it is therefore concluded that proline puts too strong of a conformational restriction on LBTs, thereby abrogating binding. Perhaps the most surprising result was that the other Gly6 mutants—including the double mutant—all bound Tb³⁺, although we had believed that this position in the LBT sequence required the flexibility

conferred by glycine Ramachandran space in order to make the proper turn. In fact, the Gly6 mutants all somehow allow a molecule of water into the terbium-bound core; thus, the structure of these mutants is perturbed beyond either of the predicted conformations.

Table 5-2. Summary of Photophysical Data from Computationally Designed SE3 Mutants

Mutation	<u>LBT</u> ^{a,b}	K_D , Tb ³⁺		Relative intensity ^c	# of Tb ³⁺ -bound water molecules ^d
		Standard buffer	Acetate buffer		
--	<u>SE3</u>	38 nM	980 nM	1.0	0
N4→A	<u>SE3α</u> ^b	76 nM	2100 nM	0.8	0
N4→G	<u>SE3β</u> ^a	19 nM	760 nM	1.0	0
N4→L	<u>SE3γ</u> ^a	69 nM	1800 nM	1.0	0
N4→P	<u>SE3δ</u> ^b	***Does not bind Tb ³⁺ ***		--	--
G6→A	<u>SE3ε</u> ^b	1600 nM	n/d ^e	0.9	1
G6→L	<u>SE3ζ</u> ^b	1900 nM	n/d ^e	0.7	1
G6→P	<u>SE3η</u> ^b	***Does not bind Tb ³⁺ ***		--	--
N4→A, G6→A	<u>SE3θ</u> ^b	3800 nM	n/d ^e	0.5	1

^a Calculated to prefer conformation 1, which is SE2-crystal-conformation-like.

^b Calculated to prefer conformation 2.

^c Luminescence comparison of equal concentrations of peptide or protein construct saturated with Tb³⁺, normalized to that of SE3.

^d Values of q , rounded to the nearest integer.

^e These values were not determined, given the already weak K_D values seen in standard buffer.

Some exciting results were observed from the Asn4 mutants. SE3β, with the N4→G mutation, binds terbium with a K_D of 19 nM—virtually identical to SENG (19 nM, Table 2-1). SENG still appears slightly tighter based on the dissociation constants observed in acetate, but the peptide with the sequence FIDTNGDGWIEGDELLLEEG (SENG with N4→G) may yet be a tighter LBT. Interestingly, the two mutants that were designed to promote conformation 1 (SE3β and SE3γ) have luminescence intensity identical to that of SE3, whereas the conformation 2-promoting mutants such as SE3α were noticeably less bright. While this evidence is no better than circumstantial (there is nothing in the GPGdSE3 crystal structures to indicate why one conformation should be brighter than another), it is nevertheless worth noting.

To further examine the binding pocket, competitive titrations using three other lanthanides (Eu³⁺, Nd³⁺ and La³⁺) were performed on SE3β and SE3ε, in order to compare these relative affinities to those determined previously⁵ for SE2. It was hypothesized that SE3ε, with space in the binding pocket for an extra water molecule, might favor the larger lanthanides (La³⁺ > Nd³⁺ > Eu³⁺ ≈ Tb³⁺) more than would SE3β or SE2 (the atomic radii for these lanthanides are 1.22 Å, 1.16 Å, 1.12 Å, and 1.10 Å, respectively⁶). The data from these titrations is summarized

in Table 5-3. Although SE3ε is still optimized for the smaller lanthanide ions, it does appear less selective: the difference between the dissociation constants for this set of lanthanides is less than an order of magnitude for SE3ε, compared to nearly two orders of magnitude for SE2 and SE3β.

Table 5-3. Competitive Titrations with SE2,^a SE3β and SE3ε, Between Tb³⁺ and Various Lanthanide Ions

LBT	Sequence	Bound H ₂ O	K _D , Tb ³⁺	K _D , Eu ³⁺	K _D , Nd ³⁺	K _D , La ³⁺
<u>SE2</u>	YIDTNNDGWYEGDELLA	0	57 nM	62 nM	270 nM	3500 nM
<u>SE3β</u>	YIDTNGDGWIEGDELLA	0	19 nM	18 nM	78 nM	1000 nM
<u>SE3ε</u>	YIDTNNDAWIEGDELLA	1	1600 nM	1100 nM	2200 nM	6300 nM

^a Competitive titration values for SE2 are taken from the literature.⁵

5-3. Crystallographic Studies of SE3α, SE3β, and SE3ε

Based on the titration results, it was decided to attempt to crystallize the LBT mutants SE3α and SE3β. Based on the data in Table 5-2, these sequences seem the most likely to have structures corresponding to conformations 2 and 1, respectively. In addition, SE3ε seemed like a reasonable target for study of the unknown, water-containing conformation. All three peptides were therefore synthesized by SPPS and extensively purified to remove residual TFA before crystallization. All LBTs were prepared as crystallization stocks as for SE2:⁵ 1.20 mM peptide in 10 mM HEPES, pH 7.0, with 1.20 mM Tb³⁺. These stocks were filtered and stored at 4°C.

Crystallization screens were carried out by Dr. Manashi Sherawat in the laboratory of Prof. Karen Allen. Her initial screens of SE3β were promising. Screens of SE3α seemed to indicate that a higher stock concentration would be necessary, while screens of SE3ε indicated that this peptide did not behave as a normal LBT-Tb³⁺ complex, perhaps not surprisingly given the high K_D and the unusual conformation. The latter was therefore omitted from further studies. Refined screens were set up of SE3β, and a new SE3α stock was made: 2.5 mM SE3α, 2.5 mM Tb³⁺, 10 mM HEPES, 10 mM NaOAc, pH 7.0.

Ultimately, useful crystals of SE3β-Tb³⁺ were grown and the structure was solved (Figure 5-5A).⁷ As with SE2,⁵ there were two LBT-Tb³⁺ complexes in the asymmetric unit that were essentially identical, one of which is shown in Figure 5-5. Figure 5-5B shows the backbone traces of SE3β and SE2, which overlay very well. In addition, based on the calculations from the Tidor lab, the residues Asn3, Gly4, Asp5, and Gly6 of SE3β reside in Ramachandran space corresponding to the predicted crystal structure conformation 1. There was one unexpected feature observed in the structure, however: the hydrophobic core seen in SE2 (residues Tyr-1, Tyr8 and Leu13) does not appear to pack as such in SE3β. As shown in Figure 5-5C, the side

chains of these residues (Tyr-1, Ile8 and Leu13 in SE3 β) are not packed together, even though the Tb^{3+} - K_D of this LBT is lower (see Table 5-3). This is surprising, given that there are only two mutations between the two peptides (Asn4 \rightarrow Gly and Tyr8 \rightarrow Ile), and goes against the conclusion that this core is necessary for the tight binding. A brief analysis of the SE3 β crystal packing indicates that there may be inter-subunit crystal contacts (not shown) that contribute to the stability of the conformation. It is also possible that the solution structure is different than the crystal structure. Nevertheless, there may yet be other, undiscovered features of SE3 β (and possibly SE2 as well) that enable these sequences to chelate Tb^{3+} so effectively.

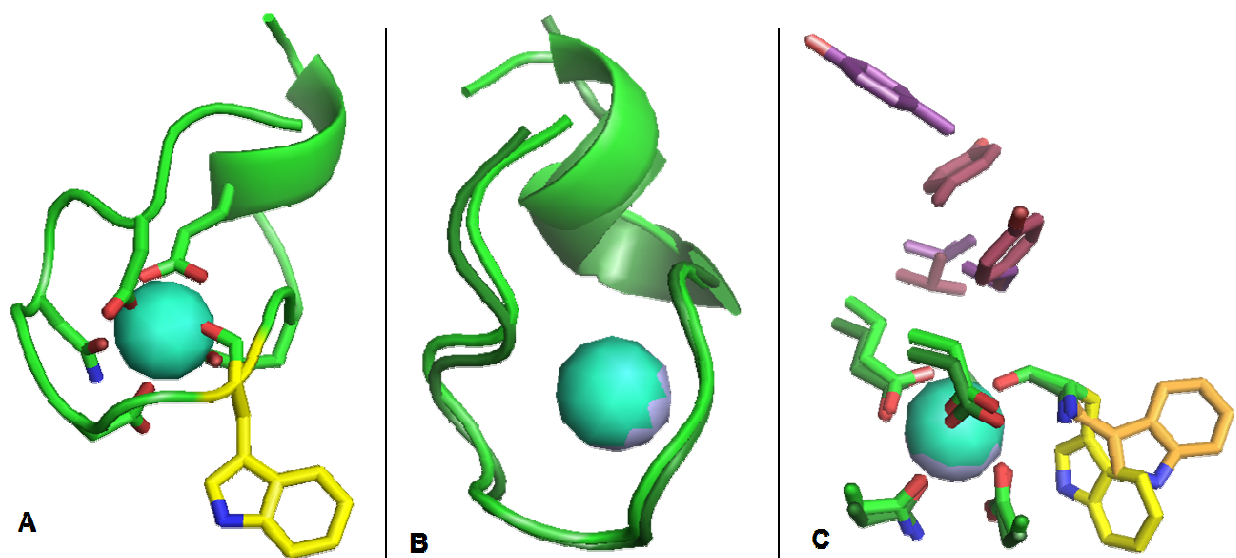


Figure 5-5. **A.** Crystal Structure of SE3 β . The backbone is shown in green cartoon form. The indole side chain of Trp 7 is in yellow; for all other side chain atoms, carbon is green, nitrogen is blue and oxygen is red. The Tb^{3+} is the central teal sphere. **B.** Overlay of the backbones of SE3 β (colored as in **A**) and SE2 (dark green). The Tb^{3+} is grey for SE2. **C.** Overlay of important side chains of SE3 β and SE2. On all side chains, nitrogen atoms are blue and oxygen atoms are red. Tb^{3+} is colored as in **B**. The carbon atoms of the Tb^{3+} -ligating side chains are shown in green for SE3 β and in dark green for SE2. The carbon atoms of the indole ring on Trp7 are yellow for SE3 β and orange for SE2. The “hydrophobic core” carbon atoms (Tyr-1, Ile/Tyr8, Leu13) are purple for SE3 β and maroon for SE2.

Without a crystal structure of SE3 ϵ , it was impossible to discern the location of the unbound water molecule, and therefore we are unable to rationally design mutant(s) that might exclude it. Nevertheless, a single attempt was made: because the SE3 \rightarrow SE3 ϵ mutation was Gly6 \rightarrow Ala, it seemed reasonable to suppose that the neighboring Asp5 was the most perturbed residue. Therefore the LBT SE3 ι , with an additional Asp5 \rightarrow Glu mutation (and thus a sequence of **YIDTNNEAWIEGDELLA**) was designed, synthesized, and purified. Unfortunately, SE3 ι did not bind Tb^{3+} , refuting this hypothesis. No additional mutations on SE3 ϵ were examined.

Even with the concentrated solution, SE3 α also failed to crystallize; it behaved significantly differently to SE2 and SE3 β under the crystal screening conditions.⁸ Although sweeping conclusions cannot be made from negative results such as these, the combination of facts including the weaker K_D , the weaker luminescence intensity than SE3 and SE3 β (Table 5-2), and the unusual behavior under crystallization conditions, is at least suggestive that the calculations about the preference of SE3 α for conformation 2 are on the right track.

5-4. Studies of dLBT-Ubiquitin Mutants Containing SE3 α and SE3 β

Since repeated attempts at crystallizing SE3 α have failed, a new approach is underway. Since the dLBT-Ubiquitin construct (GPGdSE3-ubiquitin) seems to be a good model for crystallizations, a series of dLBT mutants has been made, by Kelly Daughtry in Prof. Allen's lab, such that the GPGdSE3-Ubiquitin construct will contain all possibilities (α - α , α - β , β - α , and β - β) in the double LBT. The hope is that the crystallization of these dLBT mutants will give us improved information about the SE3 α and SE3 β sequences, and will indicate whether it will be worth pursuing a single-LBT strategy as a crystallographic tag.

Kelly was successful at generating the His-tagged versions of the four double-LBT mutants. The DAPase removal of the N-terminal hexahistidine tag for these dLBT-ubiquitin constructs was not as straightforward as for GPGdSE3-ubiquitin, as there was difficulty getting the reaction to go to completion. Eventually, it was found that the addition of Ca^{2+} to the cleavage buffer, potentially giving the LBT motifs some defined structure, was suitable to drive the reaction.⁹ The mutants were purified (the sequences are shown in Table 5-4), and the standard gamut of photophysical characterizations were run (Table 5-5).

Table 5-4. Sequences of SE3 α - and SE3 β -Based dLBT-Ubiquitin Constructs, Along with that of GPGdSE3-Ubiquitin

<i>Construct</i>	DAPase stop site	N-terminal Ln^{3+} - binding motif	C-terminal Ln^{3+} - binding motif
GPG <u>dSE3</u> -ubiquitin		GPG YIDT<u>N</u>NDGWIEGDEL	YIDT<u>N</u>NDGWIEGDELLA - ubiquitin
GPG <u>dSE3$\alpha\alpha$</u> -ubiquitin		GPG YIDT<u>N</u>ADGWIEGDEL	YIDT<u>N</u>ADGWIEGDELLA - ubiquitin
GPG <u>dSE3$\alpha\beta$</u> -ubiquitin		GPG YIDT<u>N</u>ADGWIEGDEL	YIDT<u>N</u>GDGWIEGDELLA - ubiquitin
GPG <u>dSE3$\beta\alpha$</u> -ubiquitin		GPG YIDT<u>N</u>GDGWIEGDEL	YIDT<u>N</u>ADGWIEGDELLA - ubiquitin
GPG <u>dSE3$\beta\beta$</u> -ubiquitin		GPG YIDT<u>N</u>GDGWIEGDEL	YIDT<u>N</u>GDGWIEGDELLA - ubiquitin

Table 5-5. Summary of Photophysical Data for SE3 α - and SE3 β -Containing dLBT-Ubiquitin Constructs

<i>LBT</i>	K_D , Direct Titrations ^a		K_D , Acetate buffer Titrations ^b		Relative intensity ^c	q ^d
	First Tb^{3+}	Second Tb^{3+}	First Tb^{3+}	Second Tb^{3+}		
<u>SE3</u>	38 nM	--	980 nM	--	1.0	0.08
<u>SE3α</u>	76 nM	--	2100 nM	--	0.8	0.11
<u>SE3β</u>	19 nM	--	760 nM	--	1.0	0.05
GPGd <u>SE3</u> -Ubiq	2.4 nM	23 nM	710 nM	500 nM	3.0	0.05
GPGd <u>SE3$\alpha\alpha$</u> -Ubiq	28 nM	42 nM	1200 nM	980 nM	1.8	0.02
GPGd <u>SE3$\alpha\beta$</u> -Ubiq	36 nM	88 nM	1100 nM	2100 nM	1.8	0.05
GPGd <u>SE3$\beta\alpha$</u> -Ubiq	20 nM	140 nM	930 nM	2800 nM	1.3	0.03
GPGd <u>SE3$\beta\beta$</u> -Ubiq	15 nM	37 nM	730 nM	1200 nM	1.3	0.10

^a Determined by luminescence titration in 100 mM NaCl, 10 mM MOPS buffer (pH 7.0). All values are the average of at least three titrations.

^b Determined by luminescence titration in 100 mM NaOAc, 10 mM HEPES buffer (pH 7.0). All values are the average of at least three titrations.

^c Luminescence comparison of equal concentrations of peptide or protein construct saturated with Tb^{3+} , normalized to that of SE3.

^d The number of bound water molecules, q , was determined by luminescence decay experiments as described in the literature.^{5,10}

Many of the results of these photophysical studies were unexpected. The only one of the double-mutants that shows the photophysical enhancements that the parent GPGdSE3-ubiquitin construct experienced is GPGdSE3 $\alpha\alpha$ -ubiquitin. In NaCl/MOPS buffer, the K_D values for both the 1:1 and 2:1 complex are superior to the parent sequence, SE3 α . Also, in acetate buffer, both of these constructs show the apparent cooperativity of binding, with the K_D for the binding of second Tb^{3+} lower than that of the first. Finally, the GPGdSE3 $\alpha\alpha$ -ubiquitin construct shows a more-than twofold enhancement of luminescence over the SE3 α parent, although it is about 2.25-fold, rather than threefold.

None of the other three double-mutants have these qualities. For example, none show cooperativity in acetate buffer. The luminescence of GPGdSE3 $\alpha\beta$ -ubiquitin is exactly the sum of the SE3 α and SE3 β parents, while the other two constructs ($\beta\alpha$ and $\beta\beta$) have luminescence that is less than would be expected from combining the single-LBT parents. This is especially surprising for GPGdSE3 $\beta\alpha$ -ubiquitin: based on the calculations (see sections 5-1 and 5-2), this arrangement should favor the configuration observed in the crystal structure¹ of GPGdSE3-ubiquitin. Finally, even the K_D values observed in standard titration buffer are not as low as would have been expected; although SE3 β binds Tb^{3+} more strongly than SE3, none of the three SE3 β -containing dLBT constructs have lower K_D values than the dSE3 construct. The unusually high value for the 2:1 binding of GPGdSE3 $\beta\alpha$ -ubiquitin further contradicts expectations.

5-5. Optimization of the dLBT Expression System

Although the GST construct expression system described in Chapter 4 was sufficient for making quantities of dLBTs for photophysical characterization, the yield (7 mg of GST construct per 1 L of growth) and the low mass percentage of the dLBT (14%, or about 1 mg per liter of bacteria) gave insufficient quantities for peptide crystallization studies. Therefore, a different expression system was needed. We were provided with one by labmate Dr. K. Jebrell Glover's former advisor, Professor Elizabeth A. Komives (UC San Diego). This system uses a ubiquitin fusion protein, which can be purified by an N-terminal octa-His-tag; the desired peptide is as a C-terminal fusion. Using the “megaprimer” strategy described in Chapter 4, the gene encoding GPGdSE3 was inserted, along with a TEV protease recognition motif, generating the plasmid shown in Figure 5-6.

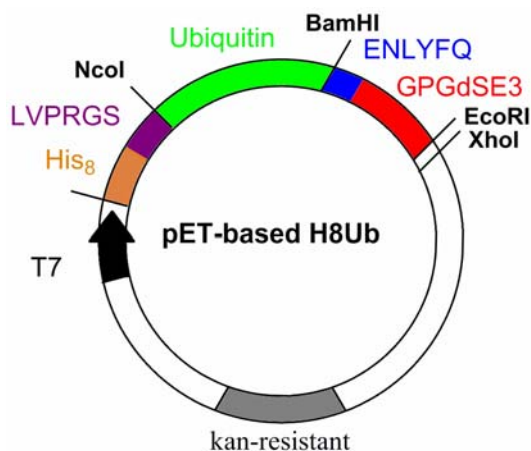


Figure 5-6. System for generating quantities of GPGdSE3 peptide for crystallization studies

In conjunction with the generation of the ubiquitin expression system, a new protein expression protocol was assessed. Developed by F. W. Studier, this protocol involves “autoinduction”, whereby the metabolism of lactose included in the growth medium turns on T7-promoted protein expression *via* a metabolite, without the need for IPTG.¹¹ Additional glucose and glycerol serve to significantly increase the cellular density—to the point that O₂ becomes the limiting “nutrient”—and further increasing the per-liter yield.

Expression of the His₈-ubiquitin-ENLYFQGPGdSE3 (the plasmid shown in Figure 5-6) gave protein yields in the 60 mg/L range, although there were occasional truncations in the dLBT portion of the product. The reason for these truncations is unclear, but has been seen for certain dLBTs by other members of the Imperiali lab as well. An alternative expression media was

therefore developed based on the Studier buffer system, although this system required IPTG induction (see the Experimental section). Nevertheless, yields obtained using this method were in the 40 mg/L range, potentially translating to nearly 10 mg of dLBT per liter of bacteria, an order-of-magnitude improvement over the GST construct.

Although a 10 mg/L yield of dLBT would make crystallographic studies accessible, the penultimate purification step, that of mTEV cleavage, proved problematic. A variety of different conditions were attempted (Figure 5-7); only extremely high concentrations of mTEV at room temperature for a week gave complete cleavage, making this route impractical.

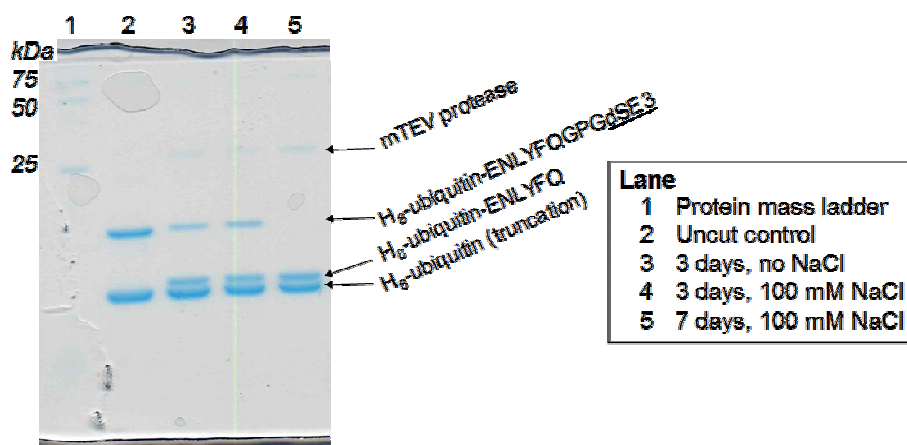


Figure 5-7. Cleavage of the ubiquitin-GPGdSE3 construct by mTEV protease is not facile.

5-6. Modification of the Gly-Pro-Gly Motif in the dLBT

The mTEV protease has been shown to be poor at cutting the ubiquitin-GPGdSE3 construct (Figure 5-7), and cut the GST-GPGdSE3 only enough for satisfactory amounts of GPGdSE3 for photophysical characterization. Other members of the Imperiali lab have had difficulty with constructs containing the sequence –ENLYFQGPG– failing to cut. Furthermore, a completely different construct, GST-ENLYFQ-IL1 β (studied by Dr. Anne Reynolds) proved essentially impervious to mTEV;¹² this construct contains an alanine in the P1' position and, similar to these constructs, a proline in the P2' position. Waugh and coworkers have studied the specificity of mTEV protease and found that, although smaller amino acids in the P1' position (glycine, alanine, serine, cysteine) are preferable, it can tolerate anything except proline.¹³ Therefore, it seems reasonable to hypothesize that the P2' position contains a similar selectivity, and a modification of this proline will be necessary for generating large quantities by this route.

Some very basic molecular modeling studies by Bracken King¹⁴ have indicated that a Pro→Ala mutation should not harm the β -sheet-like structure in the GPGdSE3-ubiquitin crystal. Therefore, two plasmid constructs (Figure 5-8) were generated to examine the effects of this mutation: His₈-ubiquitin-ENLYFQGAGdSE3 (Figure 5-8A) to obtain the peptide GAGdSE3, and His₆-ENLYFQGAGdSE3-ubiquitin (Figure 5-8B), with the goal of making GAGdSE3-ubiquitin. These both enabled the efficacy of this mutation for the TEV site to be checked, and to test the compatibility of this sequence with the dLBT. Because GAG is no longer a stop site for the DAPase enzyme, the TEV recognition sequence was added to facilitate removal of the His-tag. The construct in Figure 5-8A was generated by QuikChange[®] (Stratagene) mutagenesis, and the construct in Figure 5-8B by PCR (see the experimental section).

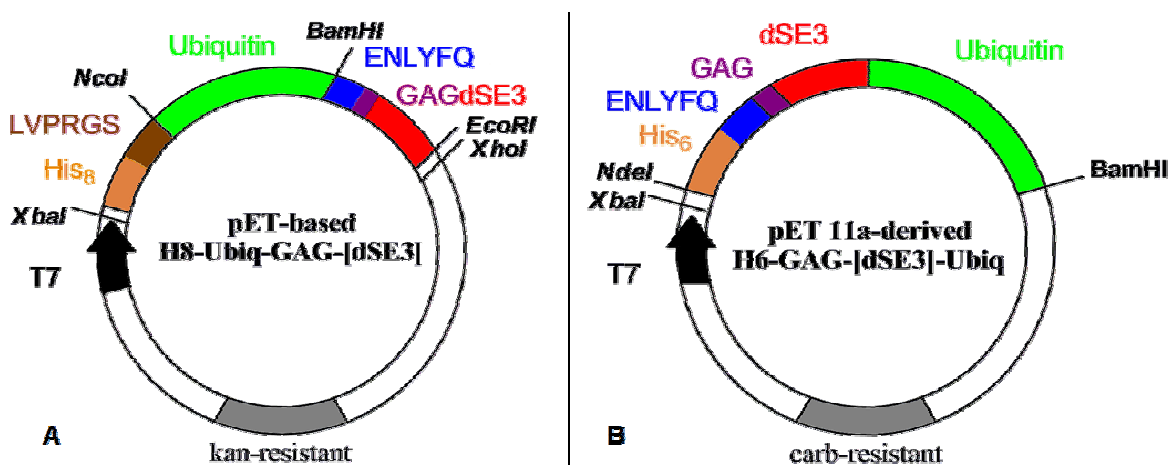


Figure 5-8. Plasmids for generating GAGdSE3 as a peptide and an N-terminal ubiquitin tag

The fusion protein His₈-ubiquitin-ENLYFQGAGdSE3 was expressed (from the gene in Figure 5-8A) and purified identically to the proline-containing protein, yielding about 40 mg of full-length construct per liter of culture (corresponding to about 10 mg of dLBT). Cleavage of this construct, releasing the peptide GAGdSE3, was extremely facile, requiring minimal mTEV protease, and achieving completion overnight at room temperature.

Because mTEV is a cysteine protease, it is extremely sensitive to oxidation in the presence of metals. Therefore, the normal mTEV protease cleavage buffer is 50 mM Tris, 0.5 mM EDTA, pH 8.0.¹⁵ However, reverse Ni-NTA IMAC (Immobilized Metal-ion Affinity Chromatography), which is necessary to remove the His-tagged ubiquitin byproduct and mTEV protease before HPLC purification, is impossible in the presence of EDTA. In order to obviate the need for dialysis (to remove EDTA), a variety of different buffer conditions were tried

(Figure 5-9). At pH 8.0, Tris and phosphate buffers both work well, with or without EDTA or extra MESNA (2-mercaptoethanesulfonic acid) reducing agent. All buffers also contained 100 mM NaCl. Because phosphate buffer is more compatible with IMAC, the large scale reaction was done in 100 mM NaCl, 50 mM phosphate, 2 mM β ME, pH 8.0. After reverse IMAC, the GAGdSE3 peptide was purified by HPLC (see the Experimental section).

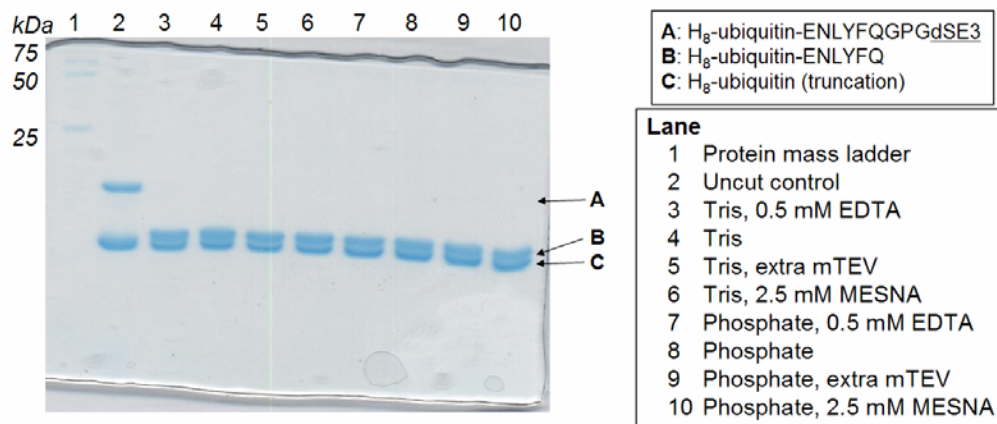


Figure 5-9. Cleavage of H₈-ubiquitin-ENLYFQGAGdSE₃ by mTEV protease is extremely facile under a variety of conditions. All buffers are at pH 8.0, 50 mM Tris or Phosphate, 100 mM NaCl, 5 mM β ME, and contain 5 μ L of His-tagged mTEV (“extra mTEV” reactions contain 10 μ L). All reactions were run overnight on the benchtop. Conditions in lane 8 are now used routinely for large scale purifications.

Expression of the protein H₆-ENLYFQGAGdSE₃-ubiquitin (from the gene in Figure 5-8B) was in the 150 mg/L range, with no apparent truncation product. Purification, cleavage by mTEV protease (under identical conditions: 100 mM NaCl, 50 mM PO₄³⁻, 5 mM β ME, pH 8.0), reverse IMAC and dialysis were without difficulty (Figure 5-10). Protein has been dialyzed into the published¹ buffer, and sent to the Allen Lab. Initial crystallization attempts are under way and have been promising.¹⁶

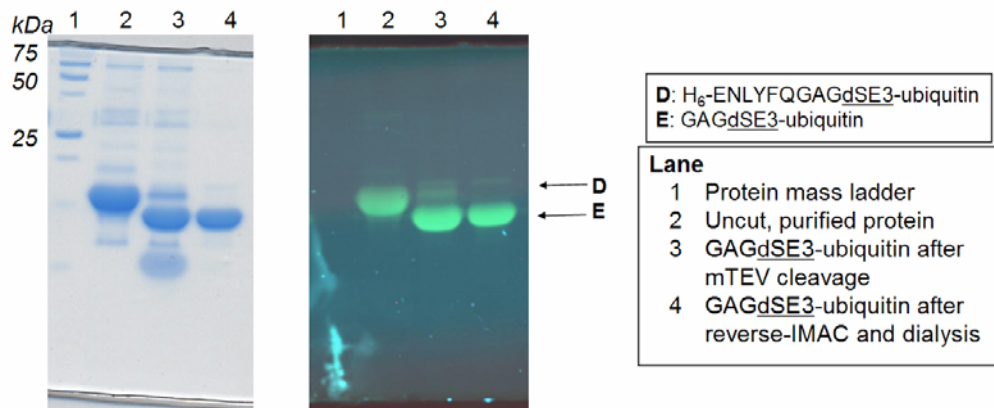


Figure 5-10. Purification of GAGdSE₃-ubiquitin from H₆ENLYFQGAGdSE₃-ubiquitin. The gel at left is stained with GelCode® Blue, the gel at right is stained with Tb³⁺ and shown without enhancement for contrast.

5-7. Photophysical Characterization of Gly-Ala-Gly Motif-Containing dLBTs

The peptide GAGdSE₃ and the fusion protein GAGdSE₃-ubiquitin were subjected to the standard photophysical characterizations: relative luminescence intensity, luminescence titrations in normal (NaCl/MOPS) and acetate (NaOAc/HEPES) buffers, and decay experiments to determine the number of terbium-bound water molecules. These results are summarized in Table 5-6. In fact, all of the photophysical constants are identical or nearly identical to the parent (GPG-containing) dLBT sequences, as expected, indicating that this modification causes minimal perturbation of the structure.

Table 5-6. Comparison of Photophysical Characteristics of GAG Motif-Containing dLBT-Ubiquitin Constructs to the Related GPG Motif-Containing Counterparts

<i>LBT</i>	K_D , Direct Titrations ^a		K_D , Acetate buffer Titrations ^b		Relative intensity ^c	q ^d
	<i>First Tb</i> ³⁺	<i>Second Tb</i> ³⁺	<i>First Tb</i> ³⁺	<i>Second Tb</i> ³⁺		
SE ₃	38 nM	--	980 nM	--	1.0	0.08
GPGdSE ₃	3.6 nM	62 nM	570 nM	1000 nM	2.5	0.08
GAGdSE ₃	6.9 nM	61 nM	630 nM	1200 nM	2.4	0.03
GPGdSE ₃ -Ubiq	2.4 nM	23 nM	710 nM	500 nM	3.0	0.05
GAGdSE ₃ -Ubiq	5.0 nM	24 nM	940 nM	400 nM	3.0	0.01

^a Determined by luminescence titration in 100 mM NaCl, 10 mM MOPS buffer (pH 7.0). All values are the average of at least three titrations.

^b Determined by luminescence titration in 100 mM NaOAc, 10 mM HEPES buffer (pH 7.0). All values are the average of at least three titrations.

^c Luminescence comparison of equal concentrations of peptide or protein construct saturated with Tb³⁺, normalized to that of SE₃.

^d The number of bound water molecules, q , was determined by luminescence decay experiments as described in the literature.^{5,10}

5-8. dLBTs Based on SE2: Attempts to Generate the Brightest Possible dLBT

When SE3 (**YIDTNN~~D~~GWIEGDELLA**) is the progenitor single-LBT, the double-LBT peptides are 2.1- to 2.5-fold brighter, and have been observed to be 3.0-fold brighter as an N-terminal tag on ubiquitin.² However, SE3 is not the brightest known single-LBT; SE2, with a Tyr at position 8 instead of Ile (**YIDTNN~~D~~GWYEGDELLA**) is nearly as bright as GdSE3 (see Tables 4-1 and 4-4). To determine if the brightness of dLBTs could be further optimized for luminescence-based applications, dLBTs based on the SE2 sequence have been generated.

Recently, EMD Biosciences has introduced a new resin: a PEG-based, low loading Rink Amide resin (NovaPeg Rink Amide LL). This resin has high swelling and low loading properties, and was designed for improving the yields of long and aggregation-prone peptides synthesized on the solid phase. We tested it using the GPGdSE3 sequence, and found that this resin enabled the synthesis of the full-length, 35 amino-acid peptide with essentially no truncation products, making HPLC purification feasible. (Although synthesis of this sequence was possible on the standard Fmoc-PAL-PEG-PS resin, a large number of “Sesqui-LBT” truncation products precluded purification of dLBT, as described in Chapter 4). The peptides dSE2 and GAGdSE2 (Table 5-7) have now been synthesized by standard Fmoc-based SPPS on this resin. HPLC showed truncation impurities to be largely absent, and MALDI of the major product showed only the desired mass.

Table 5-7. Sequences of the SE2-Based dLBTs Generated by Solid-Phase Peptide Synthesis

<u>Construct</u>	<i>N-terminus</i>	<i>N-terminal Ln³⁺- binding motif</i>	<i>C-terminal Ln³⁺- binding motif</i>
<u>SE2</u>			YIDTNNDGWIEGDELLA
<u>dSE2</u>		YIDTNNDGWYEGDEL	YIDTNNDGWIEGDELLA
GAGd <u>SE2</u>		GPG YIDTNNDGWYEGDEL	YIDTNNDGWIEGDELLA

Also, the construct H₆-ENLYFQGAGdSE2-Ubiquitin was generated by standard molecular biological cloning techniques. A series of two consecutive mutations were made based on the Quikchange mutagenesis kit. (The parent construct, H₆-ENLYFQGAGdSE3-Ubiquitin had been designed such that the DNA sequences encoding the N-terminal and C-terminal LBT motifs were sufficiently different that each could be mutated individually.) The gene encoding H₆-ENLYFQGAGdSE2-Ubiquitin (Figure 5-11A) was expressed and purified identically to the H₆-ENLYFQGAGdSE3-Ubiquitin construct (*vide supra*). Removal of the

hexa-histidine tag by mTEV protease was straightforward, and the GAGdSE2-ubiquitin protein was purified to homogeneity by reverse IMAC (Ni-NTA) chromatography (Figure 5-11B).

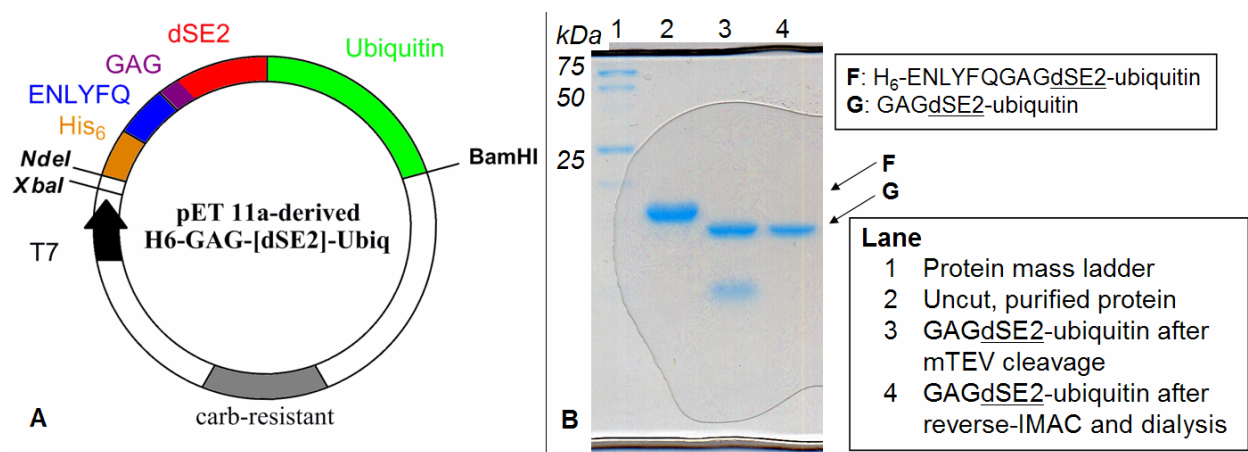


Figure 5-11. **A.** Plasmid for generating GAGdSE2-ubiquitin. **B.** Purification of GAGdSE2-ubiquitin from H₆ENLYFQGAGdSE2-ubiquitin.

The peptides dSE2 and GAGdSE2 have undergone a full photophysical characterization, as has the GAGdSE2-ubiquitin fusion protein, shown in Table 5-8. Interestingly, the SE2 sequence does not realize the advantages when it is concatenated as did the SE3 sequence. Although, like the dSE3-based peptides, dSE2 and GAGdSE2 have a K_D for the first metal that is lower than the parent sequence, SE2, the K_D for the second metal is noticeably higher. Also, dSE2 is only about 60 – 70% brighter than SE2; it does not have the doubling in relative brightness seen between SE3 and dSE3. The N-terminal GAG motif does not give the luminescence more than a marginal additional boost, either, and in this case, appending the C-terminal ubiquitin protein is actually detrimental to dSE2 luminescence. Neither is the apparent cooperativity seen of the protein construct in acetate buffer. Clearly, this Tyr8→Ile mutation causes some sort of fundamental alteration of the dLBT structure/function relationship.

Table 5-8. Photophysical Characterization of Double-LBTs Based on the SE2 Sequence.

<u>LBT</u>	K_D , Direct Titrations ^a		K_D , Acetate buffer Titrations ^b		Relative intensity ^c	q ^d
	First Tb^{3+}	Second Tb^{3+}	First Tb^{3+}	Second Tb^{3+}		
<u>SE3</u>	38 nM	--	980 nM	--	1.0	0.08
<u>SE2</u>	57 nM	--	1920 nM	--	1.9	0.03
<u>dSE2</u>	23 nM	280 nM	960 nM	4000 nM	3.1	0.11
GAG <u>dSE2</u>	38 nM	280 nM	1200 nM	4200 nM	3.2	0.11
GAG <u>dSE2</u> -Ubiq	70 nM	220 nM	2100 nM	4200 nM	2.3	0.12

^a Determined by luminescence titration in 100 mM NaCl, 10 mM MOPS buffer (pH 7.0). All values are the average of at least three titrations.

^b Determined by luminescence titration in 100 mM NaOAc, 10 mM HEPES buffer (pH 7.0). All values are the average of at least three titrations.

^c Luminescence comparison of equal concentrations of peptide or protein construct saturated with Tb³⁺, normalized to that of SE3.

^d The number of bound water molecules, *q*, was determined by luminescence decay experiments as described in the literature.^{5,10}

5-9. The Brightest Known dLBT Construct

Dr. Nicholas Sivaggi created a new dLBT construct that he is currently attempting to crystallize, GPGdSE3-NhPMM (“Nick’s homologue to PhosphoMannose Mutase”).¹⁷ He provided a sample stock solution for characterization, the data for which is shown in Table 5-9. This construct now holds the distinction of being the brightest dLBT construct known, at 3.7 times the intensity of SE3. It also appears to be the tightest dLBT construct: SPECFIT¹⁸ is unable adequately determine a *log β* value for the direct titrations. This may be explained by the fact that the numbers in the acetate buffer titrations are nearly an order of magnitude tighter than all other constructs; we posit that the direct titrations have passed the threshold of a being too tight to fit.

Table 5-9. Photophysical Characterization of GPGdSE3-NhPMM, and Comparison to Known Data

<i>LBT</i>	<i>K_D</i> , Direct Titrations ^a		<i>K_D</i> , Acetate buffer Titrations ^b		Relative intensity ^c	<i>q</i> ^d
	<i>First Tb³⁺</i>	<i>Second Tb³⁺</i>	<i>First Tb³⁺</i>	<i>Second Tb³⁺</i>		
<u>SE3</u>	38 nM	--	980 nM	--	1.0	0.08
GPG <u>dSE3</u>	3.6 nM	62 nM	570 nM	1000 nM	2.5	0.08
GPG <u>dSE3</u> -Ubiq	2.4 nM	23 nM	710 nM	500 nM	3.0	0.05
GPG <u>dSE3</u> -NhPMM	Unable to fit ^e		68 nM	370 nM	3.7	0.03

^a Determined by luminescence titration in 100 mM NaCl, 10 mM MOPS buffer (pH 7.0). All values are the average of at least three titrations.

^b Determined by luminescence titration in 100 mM NaOAc, 10 mM HEPES buffer (pH 7.0). All values are the average of at least three titrations.

^c Luminescence comparison of equal concentrations of peptide or protein construct saturated with Tb³⁺, normalized to that of SE3.

^d The number of bound water molecules, *q*, was determined by luminescence decay experiments as described in the literature.^{5,10}

^e SPECFIT¹⁸ was unable to converge this data. Based on a visual observation, and noting that the *K_D* values obtained in acetate buffer are roughly an order of magnitude lower than any other, it is believed that this is the first picomolar LBT.

Conclusions

Careful study of the crystallographic structure of GPGdSE3-ubiquitin revealed that certain residues in the two LBT motifs occupied slightly different Ramachandran space. Computational analysis then enabled us to predict mutations to favor one of the two

conformations. Based on photophysical and crystallographic analysis, at least one of these single-LBTs (SE3 β , and possibly SE3 α as well) follows the predictions. However, the four double-mutants of the GPGdSE3-ubiquitin construct that incorporate these two new LBTs do not show some of the improved photophysical properties seen in the original. Crystallographic analysis of these four constructs by our collaborators is underway.

A desire to obtain greater quantities of dLBT peptide led us to switch to using an N-terminal ubiquitin as a fusion protein rather than *GST*; the former can be expressed in yields of about 40 mg/L, from which 10 mg of dLBT peptide can be obtained. However, in the course of this study it was found that a proline residue in the P2' position significantly precludes cleavage by mTEV protease, making –ENLYFQGPGdLBT– an incompatible substrate. Additional modeling showed that a Pro→Ala mutation should be compatible with crystallography of the dLBT, and mTEV protease is highly active on substrates such as –ENLYFQGAGdLBT–. The GAG motif has no significant effect on the photophysical properties of dLBTs.

Double-LBT constructs incorporating the SE2 sequence have been generated and characterized. The peptides dSE2 and GAGdSE2 were synthesized using a superior resin for solid-phase peptide synthesis, and GAGdSE2-ubiquitin was expressed in *E. coli*. Although the two peptides are brighter than related dSE3 sequences, both are less than double that of the progenitor. Furthermore, the ubiquitin construct is significantly less bright than the dLBT peptides. Finally, the brightest known dLBT fusion protein is GPGdSE3-NhPMM. To date, all proteins studied have enhanced dLBT luminescence, but a more extensive screen would be necessary to see if this effect is general.

Experimental

5-0E. General Procedures

Peptide Synthesis and Purification.

Preparation of single and double-LBT peptides were by standard Fmoc-based SPPS procedures as described in Chapter 2 (2-0E), on an automated ABI 431A Peptide Synthesizer (Applied Biosystems). Preparation of double-LBT peptides was on NovaPEG Rink Amide LL resin (170 $\mu\text{mol/g}$) (EMD Biosciences, San Diego, CA). Peptides generated in this manner, and as *GST*- or ubiquitin-fusion constructs, were purified by HPLC and verified by MALDI-TOF MS as described in Chapter 2 (2-0E). Concentrations of stock solutions of peptides and of ubiquitin

fusion proteins were determined by the UV absorption using the extinction coefficients of the tryptophan ($\epsilon_{280} = 5690 \text{ cm}^{-1}\text{M}^{-1}$) and tyrosine ($\epsilon_{280} = 1280 \text{ cm}^{-1}\text{M}^{-1}$) content in 6 M guanidinium chloride.¹⁹

Luminescence Titrations.

Titration were recorded on a Jobin Yvon Horiba Fluoromax-3 Spectrometer in a 1 cm path-length quartz cuvette, as described in Chapter 2 (2-0E). As before, for direct titrations, the buffer was 100 mM NaCl, 10 mM MOPS; it was 100 mM NaOAc, 10 mM HEPES, pH 7.0 for qualitative comparisons. Aliquots of Tb^{3+} were added as described in section 2-0E. Luminescence titration spectra were again analyzed with the program SPECFIT/32,¹⁸ and calculated $\log \beta$ values were translated into the dissociation constants ($K_D = 10^{-\log \beta}$). Reported values are the average of three or four trials. For all titrations of double-LBTs (peptides or proteins), the luminescence intensity of the 1:1 (Tb^{3+} :dLBT) complex was set, as part of the SPECFIT, to be exactly half of that of the 2:1 complex.

Relative Luminescence Intensity.

Comparative luminescence intensities of LBTs were determined using SPECFIT¹⁸ as described in Chapter 2 (2-0E), normalized to that of SE3. For all dLBT constructs, the luminescence of the 1:1 (Tb^{3+} :dLBT) complex was set in SPECFIT to exactly half of the luminescence of the 2:1 complex.

Determination of Tb^{3+} -bound water molecules.

Luminescence lifetimes were measured as described in Chapter 2 (2-0E), to determine τ_{H2O} and τ_{D2O} . The number of Tb^{3+} -bound water molecules, q , could then be calculated as described in the literature.¹⁰

5-1E. Design of SE3 Mutants to Address Conformational Questions

Computational experiments were designed and performed by Bracken M. King in the laboratories of Professor Bruce Tidor (M.I.T., Department of Biological Engineering).

5-2E. Photophysical Characterization of SE3 Mutants

Peptides were photophysically characterized as described above.

SE3: H₂N-YIDTNNDGWIEGDELLA-CONH₂

SE3 was prepared and characterized as described in Chapter 2 (2-2E).

SE3 α : H₂N-YIDTNADGWIEGDELLA-CONH₂

SE3 α was prepared using standard Fmoc-based SPPS as described on PAL-PEG-PS resin, cleaved by TFA cocktail and purified as described by RP-HPLC ($t_R = 19.5$ min). Exact mass calcd., 1892.8 [M+H⁺]; found 1892.2 [M+H⁺], 1913.7 [M+Na⁺] by MS(MALDI).

$$\text{Log } \beta (\text{Tb}^{3+}, 1:1_{\text{NaCl/MOPS}}) = 7.18 \pm 0.04$$

$$\text{Log } \beta (\text{Tb}^{3+}, 1:1_{\text{NaOAc/HEPES}}) = 5.68 \pm 0.01$$

$$\text{Molar luminescence intensity (1:1)} = 4.34 \times 10^{12} \text{ M}^{-1} \text{ cm}^{-1}$$

$$\text{Luminescence decay: } \tau_{\text{H}_2\text{O}} = 2.60 \text{ ms; } \tau_{\text{D}_2\text{O}} = 3.31 \text{ ms}$$

SE3 β : H₂N-YIDTNGDGWIEGDELLA-CONH₂

SE3 β was prepared using standard Fmoc-based SPPS as described on PAL-PEG-PS resin, cleaved by TFA cocktail and purified as described by RP-HPLC ($t_R = 19.4$ min). Exact mass calcd., 1878.8 [M+H⁺]; found 1878.5 [M+H⁺], 1899.7 [M+Na⁺] by MS(MALDI).

$$\text{Log } \beta (\text{Tb}^{3+}, 1:1_{\text{NaCl/MOPS}}) = 7.78 \pm 0.08$$

$$\text{Log } \beta (\text{Tb}^{3+}, 1:1_{\text{NaOAc/HEPES}}) = 6.12 \pm 0.01$$

$$\text{Molar luminescence intensity (1:1)} = 5.59 \times 10^{12} \text{ M}^{-1} \text{ cm}^{-1}$$

$$\text{Luminescence decay: } \tau_{\text{H}_2\text{O}} = 2.73 \text{ ms; } \tau_{\text{D}_2\text{O}} = 3.39 \text{ ms}$$

SE3 γ : H₂N-YIDTNLDGWIEGDELLA-CONH₂

SE3 γ was prepared using standard Fmoc-based SPPS as described on PAL-PEG-PS resin, cleaved by TFA cocktail and purified as described by RP-HPLC ($t_R = 20.5$ min). Exact mass calcd., 1934.9 [M+H⁺]; found 1934.9 [M+H⁺], 1956.1 [M+Na⁺] by MS(MALDI).

$$\text{Log } \beta (\text{Tb}^{3+}, 1:1_{\text{NaCl/MOPS}}) = 7.19 \pm 0.04$$

$$\text{Log } \beta (\text{Tb}^{3+}, 1:1_{\text{NaOAc/HEPES}}) = 5.74 \pm 0.01$$

$$\text{Molar luminescence intensity (1:1)} = 5.50 \times 10^{12} \text{ M}^{-1} \text{ cm}^{-1}$$

$$\text{Luminescence decay: } \tau_{\text{H}_2\text{O}} = 2.76 \text{ ms; } \tau_{\text{D}_2\text{O}} = 3.41 \text{ ms}$$

SE3 δ : H₂N-YIDTNPDGWIEGDELLA-CONH₂

SE3 δ was prepared using standard Fmoc-based SPPS as described on PAL-PEG-PS resin, cleaved by TFA cocktail and purified as described by RP-HPLC ($t_R = 19.7$ min). Exact mass

calcd., 1918.9 [M+H⁺]; found 1918.7 [M+H⁺], 1939.3 [M+Na⁺] by MS(MALDI). SE3δ was photophysically characterized as described above, but did not measurably bind Tb³⁺.

SE3ε: H₂N-YIDTNNDAWIEGDELLA-CONH₂

SE3ε was prepared using standard Fmoc-based SPPS as described on PAL-PEG-PS resin, cleaved by TFA cocktail and purified as described by RP-HPLC (*t_R* = 19.5 min). Exact mass calcd., 1949.9 [M+H⁺]; found 1949.4 [M+H⁺], 1970.7 [M+Na⁺] by MS(MALDI).

Log β (Tb³⁺, 1:1_{NaCl/MOPS}) = 5.79 ± 0.02
Molar luminescence intensity (1:1) = 4.80 × 10¹² M⁻¹cm⁻¹
Luminescence decay: τ_{H₂O} = 1.38 ms; τ_{D₂O} = 2.30 ms

SE3ζ: H₂N-YIDTNNDLWIEGDELLA-CONH₂

SE3ζ was prepared using standard Fmoc-based SPPS as described on PAL-PEG-PS resin, cleaved by TFA cocktail and purified as described by RP-HPLC (*t_R* = 20.6 min). Exact mass calcd., 1991.9 [M+H⁺]; found 1992.2 [M+H⁺], 2013.1 [M+Na⁺] by MS(MALDI).

Log β (Tb³⁺, 1:1_{NaCl/MOPS}) = 5.72 ± 0.01
Molar luminescence intensity (1:1) = 4.06 × 10¹² M⁻¹cm⁻¹
Luminescence decay: τ_{H₂O} = 1.5 ms; τ_{D₂O} = 2.33 ms

SE3η: H₂N-YIDTNNDPWIEGDELLA-CONH₂

SE3η was prepared using standard Fmoc-based SPPS as described on PAL-PEG-PS resin, cleaved by TFA cocktail and purified as described by RP-HPLC (*t_R* = 19.7 min). Exact mass calcd., 1975.9 [M+H⁺]; found 1975.9 [M+H⁺], 1997.2 [M+Na⁺] by MS(MALDI). SE3η was photophysically characterized as described above, but did not measurably bind Tb³⁺.

SE3θ: H₂N-YIDTNADAWIEGDELLA-CONH₂

SE3θ was prepared using standard Fmoc-based SPPS as described on PAL-PEG-PS resin, cleaved by TFA cocktail and purified as described by RP-HPLC (*t_R* = 20.0 min). Exact mass calcd., 1906.9 [M+H⁺]; found 1906.1 [M+H⁺], 1927.9 [M+Na⁺] by MS(MALDI).

Log β (Tb³⁺, 1:1_{NaCl/MOPS}) = 5.43 ± 0.02
Molar luminescence intensity (1:1) = 2.83 × 10¹² M⁻¹cm⁻¹
Luminescence decay: τ_{H₂O} = 1.46 ms; τ_{D₂O} = 2.17 ms

Competitive Lanthanide Luminescence Titrations.

Competitive titrations were recorded on the same Jobin Yvon Horiba Fluoromax-3 Spectrometer in the 1 cm path-length quartz cuvette. Tryptophan-sensitized Tb³⁺ luminescence was collected by excitation at 280 nm and by recording emission at 544 nm; a 315 nm long-pass filter was used to avoid interference from harmonic doubling. Slit widths of 5 nm were used, with 1 second integration times. Spectra were recorded at 25°C, and were corrected for intensity using the manufacturer-supplied correction factors. Peptide or protein solutions were prepared in 3 mL buffer: 100 mM NaCl, 10 mM MOPS, pH 7.0.

La³⁺, Nd³⁺, Eu³⁺ and Tb³⁺ stock solutions were prepared from the LnCl₃-hydrate salts (Sigma-Aldrich) as ~50 mM solutions in 1 mM HCl, and were diluted as needed. Exact concentrations were determined by colorimetric titrations using a standardized EDTA solution (Aldrich) and a Xylenol Orange indicator as described in the literature.²⁰

LBT Peptide was added to a concentration of 200 nM in a 3 mL solution of the NaCl/MOPS buffer described above, and a background data point was obtained. Next, Tb³⁺ was added to a concentration of 400 nM (for SE3β) or 2 μM (for SE3ε, since it has a weaker affinity). Then, the competing Ln³⁺ (La³⁺, Nd³⁺, or Eu³⁺) was added. For competitive titrations of SE3β, five 2.0 μL aliquots of 100 μM Ln³⁺ were added, followed by five aliquots of 2.0 μL × 200 μM Ln³⁺, and six aliquots of 2.0 μL × 1 mM Ln³⁺. For competitive titrations of SE3ε, four 2.0 μL aliquots of 100 μM Ln³⁺ were added, followed by four aliquots of 2.0 μL × 200 μM Ln³⁺, and six aliquots of 2.0 μL × 1 mM Ln³⁺. After each addition, the solution was mixed by pipet-aspiration and a data point taken.

Competitive luminescence titration spectra obtained in this fashion were analyzed with the program SPECFIT/32,¹⁸ which determines $\log \beta$ values (β = binding constant) using the equilibrium data. The known SE3β-Tb³⁺ or SE3ε-Tb³⁺ $\log \beta$ was used as a constant in the algorithm. Calculated $\log \beta$ values were then translated into the dissociation constants ($K_D = 10^{-\log \beta}$). Reported values are based on one trial. A sample SPECFIT data file for a competitive titration is included in the Appendix.

SE3β: H₂N-YIDTNGDGWIEGDELLA-CONH₂

Log β (Tb³⁺, 1:1_{NaCl/MOPS}) \equiv 7.78 (*vide supra*)

Log β (Eu³⁺, 1:1_{NaCl/MOPS}) = 7.74 ± 0.01

Log β (Nd³⁺, 1:1_{NaCl/MOPS}) = 7.11 ± 0.02

Log β (La³⁺, 1:1_{NaCl/MOPS}) = 5.98 ± 0.05

SE3ε: H₂N-YIDTNNDAWIEGDELLA-CONH₂

Log β (Tb³⁺, 1:1_{NaCl/MOPS}) ≅ 5.79 (*vide supra*)

Log β (Eu³⁺, 1:1_{NaCl/MOPS}) = 5.95 ± 0.03

Log β (Nd³⁺, 1:1_{NaCl/MOPS}) = 5.65 ± 0.04

Log β (La³⁺, 1:1_{NaCl/MOPS}) = 5.20 ± 0.07

5-3E. Crystallographic Studies of SE3α, SE3β, and SE3ε

Preparation of stocks for crystallization.

Peptides were purified by HPLC as described above. The major peak was lyophilized, then dissolved again in 50% acetonitrile, 50% water and lyophilized once more, to remove residual TFA. Peptides were then dissolved in a minimum amount of buffer (10 mM HEPES, pH 7.0; or 10 mM HEPES, 10 mM sodium acetate, pH 7.0). Because the peptides are acidic, and because the Tb³⁺ stock contains 1 mM HCl, a small amount of concentrated NaOH was used to maintain a neutral pH, which was frequently checked by pH paper. The concentration was checked by UV A₂₈₀ (see 5-0E), and 1 equivalent of stock (56.7 mM) Tb³⁺ was added in 4 aliquots, with mixing after each addition. The peptide concentration was rechecked by UV A₂₈₀ and adjusted to the desired concentration as necessary with crystallization buffer.

The stocks were then filtered and stored at 4°C. Crystallization trays were set up and refined at Boston University by Manashi Sherawat. The structure of SE3β was solved by Manashi Sherawat and Prof. Karen Allen.⁷

SE3ι: H₂N-YIDTNNEAWIEGDELLA-CONH₂

SE3ι was prepared using standard Fmoc-based SPPS as described on PAL-PEG-PS resin, cleaved by TFA cocktail and purified as described by RP-HPLC (*t_R* = 20.1 min). Exact mass calcd., 1963.9 [M+H⁺]; found 1963.8 [M+H⁺], 1984.6 [M+Na⁺] by MS(MALDI). SE3ι was photophysically characterized as described above, but did not measurably bind Tb³⁺.

5-4E. Studies of dLBT-Ubiquitin Mutants Containing SE3α and SE3β

Cloning, expression and purification of GPGdSE3-Ubiquitin mutants αα, αβ, βα, and ββ.

Plasmids containing the genes for GPGdSE3αα-ubiquitin, GPGdSE3αβ-ubiquitin, GPGdSE3βα-ubiquitin, and GPGdSE3ββ-ubiquitin were generated by Kelly Daughtry in Prof.

Karen Allen's laboratory. These plasmids were made by QuikChange mutagenesis (*vide infra*) from the plasmid encoding GPGdSE3-ubiquitin (see Chapter 4, 4-2E). All constructs were based on the pET11a plasmid (Novagen), and contained an N-terminal His-tag (MKHHHHHH) that was used for the initial purification. Expression and removal of the His-tag was also accomplished by Kelly Daughtry, using the published procedure for GPGdSE3-ubiquitin,¹ although she found it was necessary to add a small amount of Ca²⁺ during the DAPase cleavage to push the reaction to completion.⁹

GPGdSE3-Ubiquitin:

GPGYIDTNNDGWIEGDELYIDTNNDGWIEGDELLAMQIFVKTLTGKTITLEVEPSDTIENVKAKIQDKEGIPPDQQRLIFAGKQLEDGRTLSDYNIQKESTLHLVLRRLGG

GPGdSE3-ubiquitin was prepared and photophysically characterized as described in Chapter 4 (4-2E).

GPGdSE3 $\alpha\alpha$ -Ubiquitin:

GPGYIDTNADGWIEGDELYIDTNADGWIEGDELLAMQIFVKTLTGKTITLEVEPSDTIENVKAKIQDKEGIPPDQQRLIFAGKQLEDGRTLSDYNIQKESTLHLVLRRLGG

GPGdSE3 $\alpha\alpha$ -ubiquitin was photophysically characterized as described above.

Log β (Tb³⁺, 1:1_{NaCl/MOPS}) = 7.56 ± 0.05
 Log β (Tb³⁺, 2:1_{NaCl/MOPS}) = 14.93 ± 0.05
 Log β (Tb³⁺, 1:1_{NaOAc/HEPES}) = 5.92 ± 0.01
 Log β (Tb³⁺, 2:1_{NaOAc/HEPES}) = 11.92 ± 0.04
 Molar luminescence intensity (1:1) = 5.06 × 10¹² M⁻¹cm⁻¹
 Luminescence decay: τ_{H_2O} = 2.68 ms; τ_{D_2O} = 3.24 ms

GPGdSE3 $\alpha\beta$ -Ubiquitin:

GPGYIDTNADGWIEGDELYIDTNGDGWIEGDELLAMQIFVKTLTGKTITLEVEPSDTIENVKAKIQDKEGIPPDQQRLIFAGKQLEDGRTLSDYNIQKESTLHLVLRRLGG

GPGdSE3 $\alpha\beta$ -ubiquitin was photophysically characterized as described above.

Log β (Tb³⁺, 1:1_{NaCl/MOPS}) = 7.44 ± 0.09
 Log β (Tb³⁺, 2:1_{NaCl/MOPS}) = 14.50 ± 0.10
 Log β (Tb³⁺, 1:1_{NaOAc/HEPES}) = 5.94 ± 0.01
 Log β (Tb³⁺, 2:1_{NaOAc/HEPES}) = 11.62 ± 0.03
 Molar luminescence intensity (1:1) = 4.94 × 10¹² M⁻¹cm⁻¹
 Luminescence decay: τ_{H_2O} = 2.68 ms; τ_{D_2O} = 3.30 ms

GPGdSE3 $\beta\alpha$ -Ubiquitin:

GPGYIDTNGDGWIEGDELYIDTNADGWIEGDELLAMQIFVKTLTGKTITLEVEPSDTIENVKAKIQDKEGIPPDQQRLIFAGKQLEDGRTLSDYNIQKESTLHLVLRRLGG

GPGdSE3 $\beta\alpha$ -ubiquitin was photophysically characterized as described above.

$\text{Log } \beta (\text{Tb}^{3+}, 1:1_{\text{NaCl/MOPS}}) = 7.65 \pm 0.05$
 $\text{Log } \beta (\text{Tb}^{3+}, 2:1_{\text{NaCl/MOPS}}) = 14.55 \pm 0.09$
 $\text{Log } \beta (\text{Tb}^{3+}, 1:1_{\text{NaOAc/HEPES}}) = 6.03 \pm 0.01$
 $\text{Log } \beta (\text{Tb}^{3+}, 2:1_{\text{NaOAc/HEPES}}) = 11.59 \pm 0.04$
Molar luminescence intensity (1:1) = $3.68 \times 10^{12} \text{ M}^{-1} \text{ cm}^{-1}$
Luminescence decay: $\tau_{\text{H}_2\text{O}} = 2.64 \text{ ms}$; $\tau_{\text{D}_2\text{O}} = 3.19 \text{ ms}$

GPGdSE3 β β -Ubiquitin:

**GPGYIDTNGDGWIEGDELYIDTNGDGWIEGDELLAMQIFVKTLTGKTITLEVEPSDTIENVKAKI
QDKEGIPPDQQRLLIFAGKQLEDGRTLSDYNIQKESTLHLVLRRLRGG**

GPGdSE3 β β -ubiquitin was photophysically characterized as described above.

$\text{Log } \beta (\text{Tb}^{3+}, 1:1_{\text{NaCl/MOPS}}) = 7.83 \pm 0.08$
 $\text{Log } \beta (\text{Tb}^{3+}, 2:1_{\text{NaCl/MOPS}}) = 15.26 \pm 0.10$
 $\text{Log } \beta (\text{Tb}^{3+}, 1:1_{\text{NaOAc/HEPES}}) = 6.14 \pm 0.03$
 $\text{Log } \beta (\text{Tb}^{3+}, 2:1_{\text{NaOAc/HEPES}}) = 12.07 \pm 0.04$
Molar luminescence intensity (1:1) = $3.51 \times 10^{12} \text{ M}^{-1} \text{ cm}^{-1}$
Luminescence decay: $\tau_{\text{H}_2\text{O}} = 2.54 \text{ ms}$; $\tau_{\text{D}_2\text{O}} = 3.01 \text{ ms}$

5-5E. Optimization of the dLBT Expression System

Generation of “megaprimer” inserts by PCR.

The generation of megaprimers is described in detail in Chapter 4 (4-2E).

Digestion of plasmids and inserts by restriction enzymes.

Digestion by restriction enzymes is described in detail in Chapter 4 (4-2E).

Ligation of new plasmids.

The ligation reaction strategy is described in detail in Chapter 4 (4-2E).

Autoinduction-based expression systems

The rationale for and mechanics behind autoinduction are discussed in detail in F. W. Studier’s publication; an extensive list of procedures and buffer recipes is included in the supplementary material therein.¹¹ Although autoinduction generally gave too many truncation products of dLBT constructs to be useful, it inspired the creation of “eLB” (Enhanced-LB) broth, which generally improved *E. coli* expression yields.

1L of eLB:

10 g tryptone
5 g yeast extract
2 mL of 1 M MgSO₄

20 mL of 50× “M” buffer (1.25 M Na₂HPO₄, 1.25 M KH₂PO₄, 2.50 M NH₄Cl, 0.25 M Na₂SO₄)

Deionized H₂O to 1 L, and autoclave

200 μL trace metals, added after autoclaving (to ultimately provide 50 μM Fe³⁺, 20 μM Ca²⁺, 10 μM Mn²⁺, 10 μM Zn²⁺, 2 μM Co²⁺, 2 μM Cu²⁺, 2 μM Ni²⁺, 2 μM Mo⁶⁺, 2 μM Se⁴⁺, 2 μM BO₃³⁻)

Cloning of the H₈-Ubiquitin-ENLYFQGPGdSE3 construct

The pET-based H₈-Ubiquitin plasmid was a gift from the labs of Prof. Elizabeth Komives. It is kanamycin-resistant. DH5α cells (Stratagene) were transformed with this plasmid, plated on LB-kanamycin-agar plates, and incubated overnight. A colony was picked and grown overnight; usable quantities of plasmid were extracted using a Miniprep (Qiagen) kit.

The gene for ENLYFQGPGdSE3 was inserted into the pET-H8Ubiquitin plasmid, using a megaprimer strategy. The TEV (Tobacco Etch Virus) protease cleavage site was included to facilitate removal of the N-terminal ubiquitin fusion protein. Two smaller primers (obtained from Operon; see the nucleotide sequences below) were elongated by PCR with Platinum Taq polymerase (Invitrogen), using the procedure described previously, to generate a double-stranded dLBT insert.

“TEV-GPGdSE3 for *Bam*HI”

(CGGGATCCGAAAACCTGTACTTCCAGGGTCCGGGCTACATCGACACCAACAACG
ATGGTTGGATTGAAGGCGACGAACTGTATAT)

“dLBT_rev *Xho*I”

(CCGCTCGAGTCACGCCAGCAGTTCATCGCCTTCGATCCAACCGTCGTTGTTGGTA
TCGATATACAGTTCGTCGCCTTC)

The PCR products and the pET vector were digested using *Bam*HI and *Xho*I restriction enzymes, purified, and annealed as described; miniprep quantities of the desired plasmid were obtained from transformed XL10 gold cells. For expression, BL21 cells (Stratagene) were transformed with the plasmid.

DNA sequence of the H₈-Ubiquitin-ENLYFQGPGdSE3 Plasmid:

ATGAAACACCACCACCACCACCACCACGGTGGTCTGGTTCCGCGTGGTTCCC
ATGGCATGCAAATTTTTGTCAAGACACTGACAGGTAAGACTATAACCCTAGAGGTT
GAATCTTCTGACACTATCGACAACGTTAAGTCGAAAATTCAAGACAAGGAAGGTAT
TCCTCCAGATCAACAAAGATTGATTTTTGCTGGTAAGCAACTGGAAGACGGTAGAA
CGCTGTCTGATTATAACATTCAGAAAGAGTCTACGTTGCATTTGGTGGTTGCGTTTGC
GTGGTGGATCCGAAAACCTGTACTTCCAGGGTCCGGGCTACATCGACACCAACAA

CGATGGTTGGATTGAAGGCGACGAACTGTATATCGATACCAACAACGACGGTTGG
ATCGAAGGCGATGAACTGCTGGCGTGA

Expression and purification of the H₈-Ubiquitin-ENLYFQGPGdSE3 construct.

Starting from an overnight culture, BL21-(DE3)-Gold cells (Stratagene) expressing the desired fusion protein were grown in 1.0 L of eLB media containing carbenicillin antibiotic in a shaker at 37 °C. When the OD₆₀₀ reached 0.6, the temperature was reduced to 25 °C, and protein production was induced with 0.25 mM IPTG. After 5 hours, the cells were harvested by centrifugation and frozen at -80 °C until needed.

All purification was performed at 4 °C unless otherwise noted. Half of the cell pellet (0.5 L of eLB worth) was thawed and resuspended in a lysis buffer (40 mL of 300 mM NaCl, 50 mM PO₄³⁻, 10 mM imidazole, 2 mM βME, pH 8.0), to which was added 1 mg/mL lysozyme (chicken egg white, Aldrich), and 1:1000 Protease Inhibitor Cocktail Set III (Calbiochem), and incubated at 4 °C for about 20 minutes. 10 mL of a 5% NP40 detergent solution (in lysis buffer) was then added, followed by 10 minutes of rocking. Cells were lysed by sonication (5 minutes at 3 intervals of 100 seconds with 100 second rests between intervals; 30% duty, 50% power), and cellular debris was pelleted by centrifugation (13K RPM for 55 min), and the soluble portion was filtered through a 2 micron filter. Supernatant was incubated for one hour with about 6 mL of NiNTA-agarose resin (Qiagen) at 4°, and poured into a 20 mL gravity-flow column, rerunning the flow-through to ensure complete binding. Resin was washed twice at room temperature with 30 mL wash buffer (identical to lysis buffer except for the concentration of imidazole, which was 20 mM). The ubiquitin construct was then eluted using ~40 mL of elution buffer (identical to the lysis buffer except for the concentration of imidazole, which was 250 mM), and moved immediately to the cold (4°C) room. The elution was analyzed by 15% SDS-PAGE and quantified using the Biorad BCA/BSA protein assay (obtained ~60 mg per L of eLB). Purified protein was immediately dialyzed to remove imidazole, and into a buffer suitable for TEV cleavage, and stored at 4°C until cleavage by mTEV protease.

Cleavage by mTEV protease and purification of the dLBT peptide.

Mutant Tobacco Etch Virus protease (mTEV protease) cleavage attempts were conducted as described in Chapter 4 (4-2E).

5-6E. Modification of the Gly-Pro-Gly Motif in the dLBT

“QuikChange[®]” Mutagenesis (Stratagene).

Primers were obtained from Operon Biotechnologies, Inc. (Huntsville, AL) by HPLC or PAGE purification. Primers were dissolved in biological (sterile, deionized) water to a concentration of 200 ng/μL. Polymerase and polymerase buffer were obtained from Invitrogen (Carlsbad, CA); all other reagents were obtained from New England Biolabs (Ipswich, MA) and used as received.

In a sterile PCR tube tube was added 35 μL of biological water, 5 μL of 10× Pfu buffer, 1.5 μL of the plasmid DNA template, 1.1 μL each of the forward and reverse primers, 2.5 μL of dNTP mix (which contained 10 mM each of dATP, dCTP, dGTP, and dTTP), and 2.8 μL of QuikSolution reagent (DMSO). These were gently mixed by pipetting, and then 1 μL of *Pfu Turbo* HIFI polymerase was added, and gently mixed using sterile tips.

The PCR was cycled as follows (all temperatures in Celsius; 50 μL reaction volume; 100°C cover temperature):

- 1.) 95°, 1 min
- 2.) 95°, 50 sec
- 3.) 60°, 50 sec
- 4.) 68°, 8 min
- 5.) Repeat steps 2 – 4 seventeen more times (eighteen times total)
- 6.) 68°, 8 min
- 7.) 04°, for storage

Next, 1 μL of *DpnI* restriction enzyme was added, and the parental (methylated) DNA was digested for two hours at 37°C. A test, 1.5% agarose gel was run on 4 μL of the reaction to verify the presence of plasmid DNA. Finally, XL10 gold cells were transformed (see procedure in 4-2E) using 5 μL of the reaction mixture, and useful quantities of plasmid were obtained from subsequent colonies.

PCR to remove genes from plasmids, enabling the potential alteration of 5' and 3' ends.

Primers were obtained from Operon Biotechnologies, Inc. (Huntsville, AL) by desalted purification. Primers were dissolved in biological (sterile, deionized) water to a concentration of 0.5 mg/mL. Polymerase and polymerase buffer were obtained from Invitrogen (Carlsbad, CA); all other reagents were obtained from New England Biolabs (Ipswich, MA) and used as received.

In a sterile, 500 μL Eppendorf tube was added 316 μL of biological water, 50 μL of 10× HIFI polymerase buffer, 32.5 μL of dNTP mix (which contained 10 mM each of dATP, dCTP,

dGTP, and dTTP), 20.0 μL of 50 mM Mg^{2+} (either MgCl_2 or MgSO_4), 35 μL each of the forward and reverse primers (such that equimolar quantities are included), and 10 μL of plasmid template. These were gently mixed by pipetting, and then 3 μL of *Taq* DNA polymerase was added, and gently mixed. The solution was aliquoted into 10 \times 50 μL , and placed in the PCR machine (BIO-RAD, Hercules, CA).

The PCR was cycled as follows (all temperatures in Celsius; 50 μL reaction volume; 100°C cover temperature):

- 1.) 94°, 2 min
- 2.) 94°, 30 sec
- 3.) 55°, 30 sec
- 4.) 68°, 1 min (based on gene length; longer for larger genes)
- 5.) Repeat steps 2 – 4 twenty-nine more times (thirty times total)
- 6.) 68°, 10 min
- 7.) 04°, for storage

The gene DNA was then purified on an agarose gel. Desired bands were excised and purified using the QIAquick gel extraction kit (Qiagen).

Cloning of the H₈-Ubiquitin-ENLYFQGAGdSE3 construct.

The pET-based plasmid encoding H₈-ubiquitin-ENLYFQGPdSE3 was used as a template. Usable quantities of plasmid were extracted from transformed DH5 α cells using a Miniprep (Qiagen) kit. Mutagenesis was conducted following the Quikchange (Stratagene) kit procedure (*vide supra*). The following primers were used (the altered nucleobases are shown in boldface.)

“**For_Ub(dLBT)SDM**”: (GTA**CT**TC**CA**GGGT**GC**GGGCTACATCGAC)

“**For_Ub(dLBT)SDM-r**”: (GTCGATGTAGCCCG**C**ACCCTGGAAGTAC)

For expression, BL21 cells (Stratagene) were transformed with the desired plasmid.

DNA sequence of the H₈-Ubiquitin-ENLYFQGAGdSE3 Plasmid:

```
ATGAAACACCACCACCACCACCACCACCGGTGGTCTGGTTCGCGTGGTTCCTCC
ATGGCATGCAAATTTTGTCAAGACACTGACAGGTAAGACTATAACCCTAGAGGTT
GAATCTTCTGACACTATCGACAACGTTAAGTCGAAAATTCAAGACAAGGAAGGTAT
TCCTCCAGATCAACAAAGATTGATTTTTGCTGGTAAGCAACTGGAAGACGGTAGAA
CGCTGTCTGATTATAACATTTCAGAAAGAGTCTACGTTGCATTTGGTGGTTCGTTTGC
GTGGTGGATCCGAAAACCTGTACTTCCAGGGTGCGGGCTACATCGACACCAACAA
CGATGGTTGGATTGAAGGCGACGAACTGTATATCGATACAACAACGACGGTTGG
ATCGAAGGCGATGAACTGCTGGCGTGA
```

Expression and purification of the H₈-Ubiquitin-ENLYFOGAGdSE3 construct.

The protocol was exactly analogous to that for H₈-ubiquitin-ENLYFQGPGdSE3. The elution was analyzed by 15% SDS-PAGE and quantified using the Biorad BCA/BSA protein assay (obtained ~40 mg per L of eLB). Purified protein was immediately dialyzed to remove imidazole, and into a buffer suitable for TEV cleavage, and stored at 4°C until cleavage by mTEV protease.

EDTA-free mTEV protease cleavage assay

The construct H₈-ubiquitin-ENLYFQGPGdSE3 was dialyzed into buffer containing either 100 mM NaCl, 50 mM Tris, pH 8.0, or 100 mM NaCl, 50 mM PO₄³⁻, pH 8.0. Eight conditions were set up. Conditions 1 – 4 contained 470 μL of the construct in Tris buffer; conditions 5 – 8 contained 470 μL of the construct in phosphate buffer. To all eight aliquots was added 25 μL of 20× βME stock (for a 5 mM final concentration), and 5 μL of His-tagged mTEV stock. To aliquots 1 and 5 was added 1 μL of 500 mM EDTA, pH 8.0. To aliquots 3 and 7 was added an extra 5 μL of mTEV protease. To aliquots 4 and 8 was added 5 μL of 500 mM MESNA. All aliquots were allowed to react at room temperature overnight on the bench-top. Reaction completeness was assayed by 15% SDS-PAGE analysis (procedure included in 4-2E).

Cleavage of constructs by mTEV protease.

The following procedure for cleavage by mTEV protease is used for the remainder of this Thesis. Mutant Tobacco Etch Virus protease (mTEV protease) was expressed on site from expression vector pRK793,¹⁵ which was obtained from Addgene (Cambridge, MA). The protein construct was dialyzed into a buffer consisting of 100 mM NaCl and 50 mM PO₄³⁻, pH 8.0. Immediately prior to cleavage, 5 mM βME was added (from a 20× stock), and the solution was filtered with a 2 micron filter. The mTEV protease was then added (usually at around 1:500 dilution), and the reaction was allowed to proceed at room temperature overnight; it was analyzed by 15% SDS-PAGE (see 4-2E for a procedure of SDS-PAGE) for completeness.

Cloning of the H₆-ENLYFOGAGdSE3-Ubiquitin construct.

The pET11a-based plasmid containing the gene encoding H₆-GPGdSE3-ubiquitin was used as a template for the PCR step and for the subsequent cloning. The plasmid was a gift from

the laboratory of Prof. Karen Allen. It is carbenicillin-resistant. DH5 α cells (Stratagene) were transformed with this plasmid, plated on LB-carbenicillin-agar plates, and incubated overnight. A colony was picked and grown overnight; usable quantities of plasmid were extracted using a Miniprep (Qiagen) kit. The gene for H₆-ENLYFQGAGdSE3-ubiquitin was generated by PCR, using the procedure to remove 5'- and 3'-modified DNA described above. The TEV (Tobacco Etch Virus) protease cleavage site was included to facilitate removal of the N-terminal His-tag. The following primers were used:

“**dSE3_Cryst_TEV-GAG_for**”:
(GGAATTCCATATGCACCACCATCATCACCACGAGAACCTGTACTTCCAGGGCGCG
GGTTATATTGACACTAATAACGAC)

“**For_Ub(dLBT)SDM-r**”: (GCGGGATCC TTACCCACCGCGCAGACGTAA)

For expression, BL21 cells (Stratagene) were transformed with the desired plasmid.

DNA sequence of the H₆-ENLYFQGAGdSE3-Ubiquitin Plasmid:

ATGCACCACCATCATCACCACGAGAACCTGTACTTCCAGGGCGCGGGTTATATTGA
CACTAATAACGACGGATGGATTGAGGGTGATGAACTGTATATTGACACCAACAATG
ATGGGTGGATTGAAGGAGATGAGTTACTGGCGATGCAAATTTTCGTCAAACGCTG
ACAGGCAAACGATCACCTGGAAGTTGAGCCGAGCGATACAATCGAAAACGTGA
AAGCAAAAATCCAGGACAAAGAAGGCATCCCGCCTGATCAGCAACGGCTGATTTTT
GCCGGTAAACAGCTGGAAGATGGCCGTACCCTGTCTGATTACAATATTCAGAAAGA
AAGTACTCTGCATCTGGTATTACGTCTGCGCGGTGGGTAA

Expression and purification of the H₆-ENLYFQGAGdSE3-Ubiquitin construct.

The protocol was exactly analogous to that for H₈-Ubiquitin-ENLYFQGAGdSE3. The elution was analyzed by 15% SDS-PAGE and quantified using the Biorad BCA/BSA protein assay (obtained ~60 mg per L of eLB). Purified protein was immediately dialyzed to remove imidazole, and into a buffer suitable for TEV cleavage (100 mM NaCl, 50 mM PO₄³⁻, pH 8.0), and stored at 4°C until cleavage by mTEV protease.

5-7E. Photophysical Characterization of Gly-Ala-Gly Motif-Containing dLBTs

GPGdSE3: H₂N-GPGYIDTNNDGWIEGDELYIDTNNDGWIEGDELLA-CO₂H

GPGdSE3 was prepared and photophysically characterized as described in Chapter 4 (section 4-3E).

GAGdSE3: H₂N-GAGYIDTNNDGWIEGDELYIDTNNDGWIEGDELLA-CO₂H

The construct H₈-ubiquitin-ENLYFQGAGdSE3 was prepared as described above (section 5-6E). Cleavage by TEV protease was carried out as described above (also section 5-6E), and purification of GAGdSE3 was as described for GdSE3 (see section 4-2E) by RP-HPLC ($t_R = 20.7$ min). Exact mass calcd., 3860.0 [M+H⁺]; found 3859.3 [M+H⁺] by MS(MALDI). Photophysical characterization was as described above.

$$\begin{aligned} \text{Log } \beta (\text{Tb}^{3+}, 1:1_{\text{NaCl/MOPS}}) &= 8.16 \pm 0.12 \\ \text{Log } \beta (\text{Tb}^{3+}, 2:1_{\text{NaCl/MOPS}}) &= 15.38 \pm 0.18 \\ \text{Log } \beta (\text{Tb}^{3+}, 1:1_{\text{NaOAc/HEPES}}) &= 6.20 \pm 0.02 \\ \text{Log } \beta (\text{Tb}^{3+}, 2:1_{\text{NaOAc/HEPES}}) &= 12.13 \pm 0.02 \\ \text{Molar luminescence intensity (1:1)} &= 6.24 \times 10^{12} \text{ M}^{-1}\text{cm}^{-1} \\ \text{Luminescence decay: } \tau_{\text{H}_2\text{O}} &= 2.67 \text{ ms; } \tau_{\text{D}_2\text{O}} = 3.26 \text{ ms} \end{aligned}$$

GAGdSE3-Ubiquitin:

GAGYIDTNNDGWIEGDELYIDTNNDGWIEGDELLAMQIFVKTLTGKTITLEVEPSDTIENVKAKIQDKEGIPDPQQLRIFAGKQLEDGRTLSDYNIQKESTLHLVLRRLGG

The construct H₆-ENLYFQGAGdSE3-ubiquitin was prepared as described above (section 5-6E). Cleavage by TEV protease was carried out as described above (also section 5-6E). After mTEV cleavage, NaCl was added to the buffer to a concentration of 300 mM, and imidazole to a concentration of 20 mM. His-tag peptide, uncleaved protein, and mTEV protease were removed by reverse IMAC (running the solution by gravity through NiNTA resin). The solution containing GAGdSE3-ubiquitin was then dialyzed into 100 mM NaCl, 20 mM HEPES pH 7.5. Purity was assessed by SDS-PAGE (15% gel; section 4-2E), and concentration determined by UV A₂₈₀ (section 2-0E). Photophysical characterization was as described above.

$$\begin{aligned} \text{Log } \beta (\text{Tb}^{3+}, 1:1_{\text{NaCl/MOPS}}) &= 8.30 \pm 0.14 \\ \text{Log } \beta (\text{Tb}^{3+}, 2:1_{\text{NaCl/MOPS}}) &= 15.92 \pm 0.19 \\ \text{Log } \beta (\text{Tb}^{3+}, 1:1_{\text{NaOAc/HEPES}}) &= 6.03 \pm 0.01 \\ \text{Log } \beta (\text{Tb}^{3+}, 2:1_{\text{NaOAc/HEPES}}) &= 12.43 \pm 0.02 \\ \text{Molar luminescence intensity (1:1)} &= 8.15 \times 10^{12} \text{ M}^{-1}\text{cm}^{-1} \\ \text{Luminescence decay: } \tau_{\text{H}_2\text{O}} &= 2.76 \text{ ms; } \tau_{\text{D}_2\text{O}} = 3.34 \text{ ms} \end{aligned}$$

5-8E. dLBTs Based on SE2: Attempts to Generate the Brightest Possible dLBT

SE2: H₂N-YIDTNNDGWYEGDELLA-CONH₂

SE2 was a gift from Mark Nitz,³ and was photophysically characterized as described in Chapter 2 (2-2E).

dSE2: H₂N-YIDTNNDGWYEGDELYIDTNNDGWYEGDELLA-CONH₂

dSE2 was prepared using standard Fmoc-based SPPS as described in section 2-0E on NovaPEG Rink Amide LL resin, cleaved by TFA cocktail and purified as described by RP-HPLC ($t_R = 20.6$ min). Exact mass calcd., 3774.9 [M+H⁺]; found 3776.6 [M+H⁺], 3796.2 [M+Na⁺] by MS(MALDI).

$$\text{Log } \beta (\text{Tb}^{3+}, 1:1_{\text{NaCl/MOPS}}) = 7.64 \pm 0.04$$

$$\text{Log } \beta (\text{Tb}^{3+}, 2:1_{\text{NaCl/MOPS}}) = 14.19 \pm 0.20$$

$$\text{Log } \beta (\text{Tb}^{3+}, 1:1_{\text{NaOAc/HEPES}}) = 6.04 \pm 0.02$$

$$\text{Log } \beta (\text{Tb}^{3+}, 2:1_{\text{NaOAc/HEPES}}) = 11.44 \pm 0.08$$

$$\text{Molar luminescence intensity (1:1)} = 8.55 \times 10^{12} \text{ M}^{-1}\text{cm}^{-1}$$

$$\text{Luminescence decay: } \tau_{\text{H}_2\text{O}} = 2.60 \text{ ms; } \tau_{\text{D}_2\text{O}} = 3.31 \text{ ms}$$

GAGdSE2: H₂N-GAGYIDTNNDGWYEGDELYIDTNNDGWYEGDELLA-CONH₂

GAGdSE2 was prepared using standard Fmoc-based SPPS as described in section 2-0E on NovaPEG Rink Amide LL resin, cleaved by TFA cocktail and purified as described by RP-HPLC ($t_R = 20.4$ min). Exact mass calcd., 3960.0 [M+H⁺]; found 3781.4 [M+Na⁺] by MS(MALDI).

$$\text{Log } \beta (\text{Tb}^{3+}, 1:1_{\text{NaCl/MOPS}}) = 7.64 \pm 0.04$$

$$\text{Log } \beta (\text{Tb}^{3+}, 2:1_{\text{NaCl/MOPS}}) = 14.19 \pm 0.20$$

$$\text{Log } \beta (\text{Tb}^{3+}, 1:1_{\text{NaOAc/HEPES}}) = 6.04 \pm 0.02$$

$$\text{Log } \beta (\text{Tb}^{3+}, 2:1_{\text{NaOAc/HEPES}}) = 11.44 \pm 0.08$$

$$\text{Molar luminescence intensity (1:1)} = 8.55 \times 10^{12} \text{ M}^{-1}\text{cm}^{-1}$$

$$\text{Luminescence decay: } \tau_{\text{H}_2\text{O}} = 2.60 \text{ ms; } \tau_{\text{D}_2\text{O}} = 3.31 \text{ ms}$$

Cloning of the H₆-ENLYFQGAGdSE2-Ubiquitin construct.

The pET11a-based plasmid containing the gene encoding H₆-ENLYFQGAGdSE3-ubiquitin (*vide supra*) was used as the initial template. Usable quantities of plasmid were extracted from transformed DH5 α cells using a Miniprep (Qiagen) kit. Two rounds of mutagenesis were conducted following the Quikchange (Stratagene) kit procedure (*vide supra*), the first to mutate the N-terminal LBT motif, and the second to mutate the C-terminal motif.

(The DNA sequences of the two motifs are sufficiently different to be distinguished by QuikChange primers.) The full procedure for Quikchange is included above in section 5-6E.

The following primers were used to mutate the N-terminal motif, generating the construct “H₆-ENLYFQGAGd**SE23**-ubiquitin” (the altered nucleobases are shown in boldface):

“QC_dLBT-Ub_N-I8Y_for”
(GACACTAATAACGACGGATGGT**TAT**GAGGGTGATGAACTGTATATTG)

“QC_dLBT-Ub_N-I8Y_rev”
(CAATATACAGTTCA**T**CACCCTCAT**ACC**ATCCGTCGTTATTAGTGTC)

The C-terminal motif was then mutated. The “H₆-ENLYFQGAGd**SE23**-ubiquitin” plasmid was used as the template. Usable quantities of plasmid were extracted from transformed XL10-gold cells using a Miniprep (Qiagen) kit. The following primers were used to mutate the C-terminal motif (the altered nucleobases are shown in boldface):

“QC_dLBT-Ub_C-I8Y_for”
(CACCAACAATGATGGGTGGT**AC**GGAAGGAGATGAGTTACTGGCG)

“QC_dLBT-Ub_C-I8Y_rev”
(CGCCAGTAACTCATCTCCTT**CGT**ACCACCCATCATTGTTGGTG)

For expression, BL21 cells (Stratagene) were transformed with the desired plasmid.

DNA sequence of the H₆-ENLYFQGAGd**SE2**-Ubiquitin Plasmid:

ATGCACCACCATCATCACCACGAGAACCTGTACTTCCAGGGCGCGGGTTATATTGACACTAATAACGACGGATGGTATGAGGGTGATGAACTGTATATTGACACCAACAATGATGGGTGGTACGAAGGAGATGAGTTACTGGCGATGCAAATTTTCGTCAAACGCTGACAGGCAAACGATCACCCTGGAAGTTGAGCCGAGCGATAACAATCGAAAACGTGAAAGCAAAAATCCAGGACAAAGAAGGCATCCCGCCTGATCAGCAACGGCTGATTTT TGCCGGTAAACAGCTGGAAGATGGCCGTACCCTGTCTGATTACAATATTCAGAAAGAAAGTACTCTGCATCTGGTATTACGTCTGCGCGGTGGGTAA

Expression and purification of the H₆-ENLYFQGAGd**SE2**-Ubiquitin construct.

The protocol was exactly analogous to that for H₆-ENLYFQGAGd**SE3**-Ubiquitin. The elution was analyzed by 15% SDS-PAGE and quantified using the Biorad BCA/BSA protein assay. Purified protein was immediately dialyzed to remove imidazole, and into the buffer suitable for TEV cleavage (100 mM NaCl, 50 mM PO₄³⁻, pH 8.0), and stored at 4°C until cleavage by mTEV protease.

GAGdSE2-Ubiquitin:

GAGYIDTNNNDGWYEGDELYIDTNNNDGWYEGDELLAMQIFVKTLTGKTITLEVEPSDTIENVKAKIQDKEGIPPDQORLIFAGKQLEDGRITLSDYNIQKESTLHLVLRRLRGG

The construct H₆-ENLYFQGAGdSE2-ubiquitin was prepared as described above. Cleavage by mTEV protease was carried out as described above (section 5-6E). After mTEV cleavage, NaCl was added to the buffer to a concentration of 300 mM, and imidazole to a concentration of 20 mM. His-tag peptide, uncleaved protein, and mTEV protease were removed by reverse IMAC (running the solution by gravity through NiNTA resin). The solution containing GAGdSE2-ubiquitin was then dialyzed into 100 mM NaCl, 20 mM HEPES pH 7.5. Purity was assessed by SDS-PAGE (15% gel; section 4-2E), and concentration determined by UV A₂₈₀ (section 2-0E). Photophysical characterization was as described above.

$$\begin{aligned}\text{Log } \beta (\text{Tb}^{3+}, 1:1_{\text{NaCl/MOPS}}) &= 7.16 \pm 0.03 \\ \text{Log } \beta (\text{Tb}^{3+}, 2:1_{\text{NaCl/MOPS}}) &= 13.82 \pm 0.03 \\ \text{Log } \beta (\text{Tb}^{3+}, 1:1_{\text{NaOAc/HEPES}}) &= 5.67 \pm 0.01 \\ \text{Log } \beta (\text{Tb}^{3+}, 2:1_{\text{NaOAc/HEPES}}) &= 11.04 \pm 0.03 \\ \text{Molar luminescence intensity (1:1)} &= 6.34 \times 10^{12} \text{ M}^{-1} \text{ cm}^{-1} \\ \text{Luminescence decay: } \tau_{\text{H}_2\text{O}} &= 2.56 \text{ ms; } \tau_{\text{D}_2\text{O}} = 3.26 \text{ ms}\end{aligned}$$

5-9. The Brightest Known dLBT Construct

GPGdSE3-NhPMM:

GPGdSE3-NhPMM was a gift from Dr. Nicholas Silvaggi and Prof. Karen Allen, and was used as received. It was photophysically characterized as described above.

$$\begin{aligned}\text{Log } \beta (\text{Tb}^{3+}, 1:1_{\text{NaCl/MOPS}}) &= \text{unable to converge} \\ \text{Log } \beta (\text{Tb}^{3+}, 2:1_{\text{NaCl/MOPS}}) &= \text{unable to converge} \\ \text{Log } \beta (\text{Tb}^{3+}, 1:1_{\text{NaOAc/HEPES}}) &= 7.17 \pm 0.08 \\ \text{Log } \beta (\text{Tb}^{3+}, 2:1_{\text{NaOAc/HEPES}}) &= 13.60 \pm 0.07 \\ \text{Molar luminescence intensity (1:1)} &= 10.3 \times 10^{12} \text{ M}^{-1} \text{ cm}^{-1} \\ \text{Luminescence decay: } \tau_{\text{H}_2\text{O}} &= 2.76 \text{ ms; } \tau_{\text{D}_2\text{O}} = 3.38 \text{ ms}\end{aligned}$$

Acknowledgements

I am grateful for our collaboration with Professor Bruce Tidor and Bracken M. King in the M.I.T. Department of Biological Engineering. Bracken did all of the computational analysis included in this chapter, and had to do some novel programming to do so. He made Figures 5-2, 5-3, and 5-4. He helped choose which SE3 mutants (a through q) to synthesize, and confirmed the promise of the GPG→GAG mutation. I am also grateful for our collaboration with Prof. Karen Allen's lab at Boston University School of Medicine. Dr. Nicholas Silvaggi provided the GPGdSE3-ubiquitin plasmid for me, and the GPGdSE3-NhPMM protein. He is currently working on crystallizing the GAGdSE3-ubiquitin protein. Dr. Manashi Sherawat did the crystallization

screens for SE3 α , SE3 β , and SE3 ϵ ; she and Prof. Allen solved the structure of SE3 β . Kelly Daughtry generated, expressed, and purified all of the dLBT mutants containing the SE3 α and SE3 β sequences. I thank Dr. K. Jebrell Glover for putting me in touch with the lab of Prof. Elizabeth Komives at UC San Diego, which provided the initial H₈-ubiquitin plasmid. I thank Dr. Anne M. Reynolds for helpful discussions about the proline issue with mTEV protease. I am eternally grateful to Angelyn Larkin for editing this chapter.

References

- (1) Silvaggi, N. R.; Martin, L. J.; Schwalbe, H.; Imperiali, B.; Allen, K. N. "Double-Lanthanide-Binding Tags for Macromolecular Crystallographic Structural Determination." *J. Am. Chem. Soc.* **2007**, *129*(22), 7114-7120.
- (2) Martin, L. J.; Hähnke, M. J.; Nitz, M.; Wöhnert, J.; Silvaggi, N. R.; Allen, K. N.; Schwalbe, H.; Imperiali, B. "Double-Lanthanide-Binding Tags: Design, Photophysical Properties, and NMR Applications." *J. Am. Chem. Soc.* **2007**, *129*(22), 7106-7113.
- (3) Nitz, M.; Franz, K. J.; Maglathlin, R. L.; Imperiali, B. "A powerful combinatorial screen to identify high-affinity terbium(III)-binding peptides." *ChemBioChem* **2003**, *4*(4), 272-276.
- (4) Martin, L. J.; Sculimbrenne, B. R.; Nitz, M.; Imperiali, B. "Rapid Combinatorial Screening of Peptide Libraries for the Selection of Lanthanide-Binding Tags (LBTs)." *QSAR Comb. Sci.* **2005**, *24*(10), 1149-1157.
- (5) Nitz, M.; Sherawat, M.; Franz, K. J.; Peisach, E.; Allen, K. N.; Imperiali, B. "Structural origin of the high affinity of a chemically evolved lanthanide-binding peptide." *Angew. Chem. Int. Ed.* **2004**, *43*(28), 3682-3685.
- (6) Shannon, R. D. "Revised effective ionic radii and systematic studies of interatomic distances in halides and chalcogenides." *Acta Cryst.* **1976**, *A32*(5), 751-767.
- (7) Sherawat, M.; Martin, L. J.; King, B. M.; Tidor, B.; Imperiali, B.; Allen, K. N., Unpublished results.
- (8) Sherawat, M.; Allen, K. N., Personal communication.
- (9) Daughtry, K.; Allen, K. N., Personal communication.
- (10) Beeby, A.; Clarkson, I. M.; Dickins, R. S.; Faulkner, S.; Parker, D.; Royle, L.; de Sousa, A. S.; Williams, J. A. G.; Woods, M. "Non-radiative deactivation of the excited states of europium, terbium and ytterbium complexes by proximate energy-matched OH, NH and CH oscillators: an improved luminescence method for establishing solution hydration states." *J. Chem. Soc., Perkin Trans. 2* **1999**, (3), 493-504.

- (11) Studier, F. W. "Protein Production by Auto-induction in high-density shaking cultures." *Protein Expr. Purif.* **2005**, *41*, 207-234 and supplementary information therein.
- (12) Reynolds, A. M., Personal communication.
- (13) Kapust, R. B.; Tözsér, J.; Copeland, T. D.; Waugh, D. S. "The P1' specificity of tobacco etch virus protease." *Biochem. Biophys. Res. Commun.* **2002**, *294*, 949-955.
- (14) King, B. M.; Tidor, B., Personal communication.
- (15) Kapust, R. B.; Toezser, J.; Fox, J. D.; Anderson, D. E.; Cherry, S.; Copeland, T. D.; Waugh, D. S. "Tobacco etch virus protease: mechanism of autolysis and rational design of stable mutants with wild-type catalytic proficiency." *Protein Eng.* **2001**, *14(12)*, 993-1000.
- (16) Silvaggi, N. R., Personal communication.
- (17) Silvaggi, N. R.; Allen, K. N., Unpublished results.
- (18) Binstead, R.; Jung, B.; Zuberbühler, A. *SPECFIT/32 for Windows; Original Release 2000*, Version 3.0.39; Spectrum Software Associates, Marlborough, MA.: SPECFIT/32 provides global analysis of equilibrium and kinetic systems using singular value decomposition and nonlinear regression modeling by the Levenberg-Marquardt method., 2007.
- (19) Chazan, A. Peptide Property Calculator.
<http://www.basic.northwestern.edu/biotools/proteincalc.html>
- (20) Pribil, R. "Present state of complexometry. IV. Determination of rare earths." *Talanta* **1967**, *14(6)*, 619-627.

Chapter 6

Lanthanide-Binding Tags for Magnetic Resonance Imaging

Introduction

Of the trivalent lanthanide ions, Gd^{3+} is uniquely endowed with a $[Xe]4f^7$ configuration and seven unpaired electrons, causing it to have a strong paramagnetic relaxation enhancement effect and by far the longest relaxation time of the lanthanides.¹ As with all Ln^{3+} ions, it undergoes rapid ligand exchange, and Gd^{3+} chelates are therefore frequently used in Nuclear Magnetic Resonance Imaging (MRI) experiments.¹⁻³ We are therefore interested in extending the scope of the *in vitro* LBT usage to include applications in this area, and have begun initial studies to this end, in collaboration with Kelly Daughtry and Professor Karen Allen at Boston University Medical Center. Figure 6-1 shows a representative contrast image.

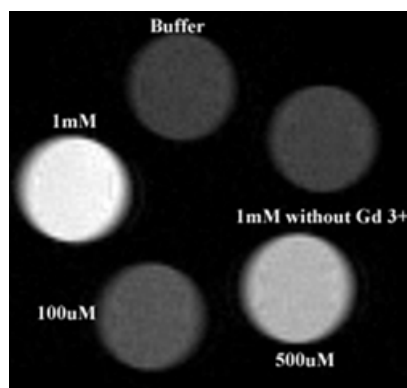


Figure 6-1. Images of MRI contrast with the LBT mSE3. Clockwise from top: buffer only, mSE3 only, mSE3 + 0.5 equiv. Gd^{3+} , mSE3 + 0.1 equiv. Gd^{3+} , mSE3 + 1.0 equiv. Gd^{3+} . (This image is courtesy of Kelly Daughtry.)

Whereas the chemically-selected LBTs (and dLBTs) mentioned thus far in this thesis exclude water from the inner coordination sphere of Tb^{3+} , a gadolinium-chelating water molecule is crucial for MRI; it is the relaxation of these protons that is enhanced. In fact, it is beneficial to have two or more molecules of water bound to the metal center if possible. Therefore, LBTs that work well for MRI will be suboptimal for luminescence-based applications and *vice versa*. Initial studies used existing LBTs, comparing water-excluding sequences such as SE3 with water-incorporating sequences such as mSE3. To further improve LBTs for this purpose, a new library has been designed, based on the original LBT-selecting library,^{4,5} but using MR contrast to select LBT sequences rather than Tb^{3+} luminescence.

Results and Discussion

6-1. Assessment of Existing LBT Sequences for Gd^{3+} Binding

Initial experiments focused on known LBT sequences. The binding affinity of a number of LBTs for Gd^{3+} has been assessed using competitive titrations, where the LBT is first coordinated to Tb^{3+} , and then Gd^{3+} is added. Since MRI is improved when there is at least one molecule of water coordinated to the Gd^{3+} , the LBTs mSE3 and SE3ε were studied in addition to SE3. (The design of the sequence of mSE3 was described in Chapter 2; the design of SE3ε was described in Chapter 5). A compilation of these binding constants is included in Table 6-1. Also, since an additional relaxation-enhancement site would be beneficial to this application, and to ascertain MRI in the context of a protein, the Gd^{3+} -affinity of the GPGSE3-ubiquitin construct was determined and is presented in Table 6-2. In all cases, the dissociation constant for Gd^{3+} is similar to that for Tb^{3+} . The contrast enhancement of these LBT peptides and dLBT-protein were assessed by Kelly Daughtry in Prof. Karen Allen's lab at Boston University. While all showed some promise, the mSE3 sequence gave the best contrast (shown above in Figure 6-1).⁶

Table 6-1. Summary of LBT- Gd^{3+} Affinity for Single-LBTs used in MRI Experiments

<u>LBT</u>	<i>Sequence</i>	q^a	$K_D, Tb^{3+ b}$	$K_D, Gd^{3+ c}$
<u>SE3</u>	YIDTNNDGWIEGDELLA	0	38 nM	38 nM
<u>mSE3</u>	YIDTNNDGWIDGDELLA	1	1200 nM	840 nM
<u>SE3ε</u>	YIDTNNDAWIEGDELLA	1	1700 nM	1600 nM

^a Values of q , the number of Ln^{3+} -coordinated water molecules, were determined by luminescence decay experiments as described in the literature^{7,8} and rounded to the nearest integer.

^b Determined by luminescence titration in 100 mM NaCl, 10 mM MOPS buffer (pH 7.0).

^c Determined by competitive luminescence titration between Tb^{3+} and Gd^{3+} in 100 mM NaCl, 10 mM MOPS buffer (pH 7.0). All values are the average of three titrations.

Table 6-2. Summary of GPGSE3-Ubiquitin $\log \beta$ Values for Gd^{3+} and $Tb^{3+ a}$

	1 Tb^{3+} , 0 Gd^{3+}	2 Tb^{3+} , 0 Gd^{3+}	1 Tb^{3+} , 1 Gd^{3+}	0 Tb^{3+} , 2 Gd^{3+}	0 Tb^{3+} , 1 Gd^{3+}
GPG <u>SE3</u> -Ubiq.	8.63	16.27	16.65	16.32	9.02

^a Determined by luminescence titration (for Tb^{3+} -only values), or by competitive luminescence titration between Tb^{3+} and Gd^{3+} in 100 mM NaCl, 10 mM MOPS (pH 7.0). All values are the average of three titrations.

6-2. A Split-Pool Peptide Library to Optimize LBTs for MRI Studies

As only the three LBTs detailed in Table 6-1 have been tested in the context of MRI studies, it is unlikely that the best of these (mSE3) is optimal. We therefore decided to design another series of libraries to optimize these “MRI-LBTs.” Based on the Split-Pool peptide

libraries designed by Mark Nitz^{4,5} and discussed in Chapters 1 and 2, a slightly modified methodology has been implemented. The same high-swelling TentaGel Macrobeads were used as solid support. For this series of libraries, the luminescence-quenching *para*-nitrophenylalanine is unnecessary; alanine was therefore used instead. Furthermore, the MRI-contrast screen will be performed entirely on-resin (*viz.* with the LBTs still attached), obviating the need for a photolabile linker; therefore only the ammonium hydroxide-labile HMBA linker was used. As before, a β -alanine residue was included as a spacer to the HMBA and, the sequence Gly-Pro-Pro-Arg was used to separate the LBT from the resin, with the arginine serving to facilitate ionization for MALDI (Figure 6-2).

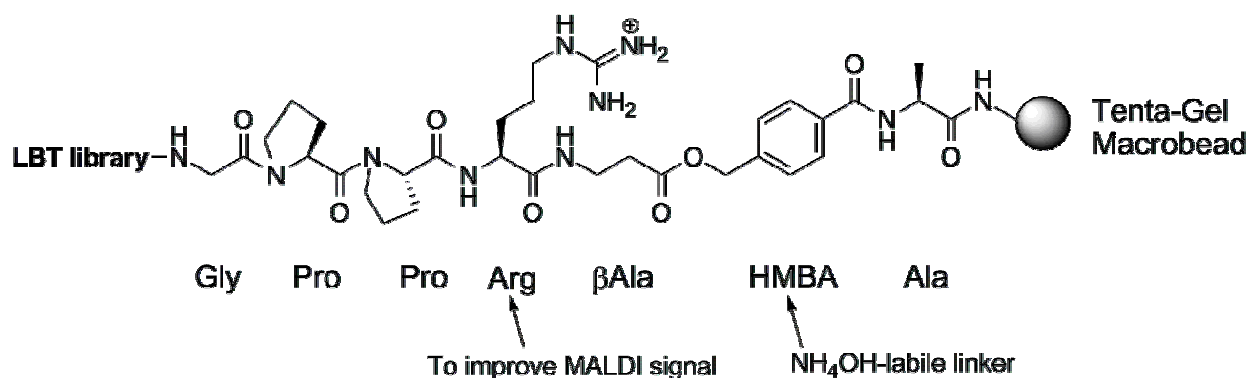


Figure 6-2. Design of the linker region for attachment of the MRI-LBT library to the resin.

Other features of the library (shown in Figure 6-3) closely follow the design for selecting bright, Tb^{3+} -binding LBTs (refer to Figure 1-11). Residue variations were introduced *via* split-and-pool library synthesis (see Figure 1-10), with capping as necessary to create a non-degenerate set of peptide masses. Beads were suspended in an agarose gel containing Gd^{3+} (and a metal-chelator such as NTA if necessary), and imaged on an MRI instrument. Ultimately, beads showing the highest contrast will be picked for sequence analysis and further screening.

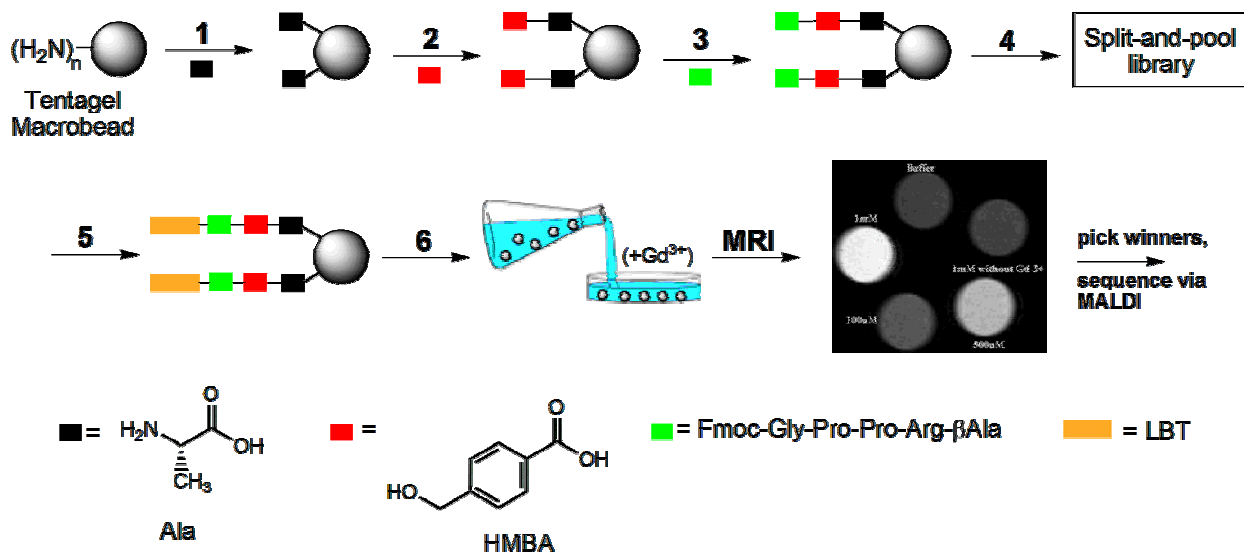


Figure 6-3. The synthesis and screening process for the “LanGdoN” combinatorial libraries to generate LBTs for use in *in vitro* MRI experiments. (1) Coupling of Fmoc-alanine. (2) Coupling of HMBA linker. (3) Introduction of the spacer peptide sequence. (4) Coupling of the split-and-pool peptide library and mass-spectral ladder capping groups. (5) Amino acid side-chain deprotection by TFA cocktail. (6) Casting of 2% agarose gel containing ~50 μM Gd³⁺, 100 mM NaCl and 10 mM HEPES at pH 7.0 in a Petri dish. LBTs are then tested on-resin for MRI contrast, and a photograph will be taken. Beads with the best MRI contrast are then selected and removed by hand from the agarose. The HMBA linker will then be cleaved in 28% NH₄OH, followed by MALDI-MS sequence deconvolution.

These libraries have been dubbed “LanGdoN” (Libraries assessing nuances of Gd³⁺-binding optimization for Nuclear Magnetic Resonance Imaging). The first, LanGdoN1, is presented as a proof-of-concept study. The residues varied for this library are shown in Figure 6-4. In SE3, position 9 is glutamate, whereas aspartate (in mSE3) has been found to work better here for MRI contrast (see Figure 6-1). In many native proteins with EF-hand motifs, such as Troponin C, this position contains an aspartate which coordinates Ca²⁺ (or Tb³⁺) *via* a water molecule.⁸⁻¹⁰ Serine at position 9 could also enable water coordination, or it could simply make the pocket too large. The side chain of alanine is even smaller than that of serine, and would almost certainly perturb the pocket too strongly, but alanine was included to examine the effect of a side chain lacking a hydrophilic group. For a negative control (to ensure that there would be beads with sequences not bound to Gd³⁺ and thus with no MRI contrast above background), the library will include arginine at this position. (Arginine is used instead of lysine because the latter is mass-degenerate with glutamate.) At position 3, asparagine is found in SE3 and mSE3. When an Asn3→Asp mutation is introduced into an LBT, however, the resulting sequence is surprisingly unable to bind Ln³⁺.¹¹ However, it is possible that if a mutation at Glu9 opens a

coordination space around the Gd^{3+} , the extra negative charge on the aspartate residue could be beneficial. Since Asn and Asp are of similar mass (and would probably be indistinguishable by MALDI-MS), the sequences with these variations have been capped using Boc-Asp(Bzl)-OH and Boc-Glu(Bzl)-OH, respectively. The amino acid identity at position 9 can thus be determined by the mass of the full-length peptide, and the identity at position 3 can be determined by the mass of the capped peptide.

Position	-1	0	1	2	3	4	5	6	7	8	9	10	11	12	13	14	15	K_D, Tb^{3+}	
Peptide																			
<u>SE3</u>		Y	I	D	T	N	N	D	G	W	I	E	G	D	E	L	L	A	38 nM
					D						A								
					N						D								
											E								
											R								
											S								

Figure 6-4. Library LanGdoN1: “Position 9 Optimization for MRI”. Residues at varied positions in the starting SE3 are shown in red. The results from this library have not yet been determined.

The results from this library have not yet been determined. There has been some initial difficulty with high background contrast seen with unmodified TentaGel resin, which is exacerbated by the presence of Gd^{3+} .⁶ Current work aims to reduce this, in order to distinguish different LBT-sequence-containing beads. Different buffers and metal-chelating agents to compete for low-affinity Gd^{3+} -binding sites are being tested to this end.

Conclusions

LBTs, such as mSE3, have been demonstrated to be viable MRI contrast agents *in vitro* when bound to Gd^{3+} . As a water molecule coordinated to the Gd^{3+} ion is necessary for maximum contrast, these LBT sequences will be distinct from the ones optimized for luminescence. The on-resin screen developed for selecting bright LBT sequences has therefore been modified to select for MRI contrast, but the split-and-pool peptide library design follows the same principles. The first library has been generated, but experimental details for the MRI-contrast selection require further optimization.

Experimental

6-0E. General Procedures

Peptide Synthesis and Purification.

LBT peptides were prepared by standard Fmoc-based SPPS procedures as described in Chapter 2 (2-0E), on an automated ABI 431A Peptide Synthesizer (Applied Biosystems). Peptides were purified by HPLC and verified by MALDI-TOF MS as described in Chapter 2 (2-0E). Concentrations of stock solutions of peptides and of ubiquitin fusion proteins were determined by UV absorption using the extinction coefficients of the tryptophan ($\epsilon_{280} = 5690 \text{ cm}^{-1} \text{ M}^{-1}$) and tyrosine ($\epsilon_{280} = 1280 \text{ cm}^{-1} \text{ M}^{-1}$) content in 6 M guanidine hydrochloride.¹²

Luminescence Titrations.

Titration were recorded on a Jobin Yvon Horiba Fluoromax-3 Spectrometer in a 1 cm path-length quartz cuvette, as described in Chapter 2 (2-0E). The buffer was 100 mM NaCl, 10 mM MOPS (pH 7.0). Aliquots of Tb^{3+} were added as described in section 2-0E. Luminescence titration spectra were again analyzed with the program SPECFIT/32,¹³ and calculated $\log \beta$ values were translated into the dissociation constants ($K_D = 10^{-\log \beta}$). Reported values are the average of three or four trials.

Determination of Tb^{3+} -bound water molecules.

Luminescence lifetimes were measured as described in Chapter 2 (2-0E), to determine τ_{H_2O} and τ_{D_2O} . The number of Tb^{3+} -bound water molecules, q , were then calculated as described in the literature.⁷

6-1. Assessment of Existing LBT Sequences for Gd^{3+} Binding.

Competitive Lanthanide Luminescence Titrations.

Competitive titrations were recorded on the same Jobin Yvon Horiba Fluoromax-3 Spectrometer in the 1 cm path-length quartz cuvette. Tryptophan-sensitized Tb^{3+} luminescence was collected by excitation at 280 nm and by recording emission at 544 nm; a 315 nm long-pass filter was used to avoid interference from harmonic doubling. Slit widths of 5 nm were used, with 1 second integration times. Spectra were recorded at 25°C, and were corrected for intensity using the manufacturer-supplied correction factors. Peptide or protein solutions were prepared in 3 mL buffer: 100 mM NaCl, 10 mM MOPS, pH 7.0.

Stock solutions of Gd^{3+} and Tb^{3+} were prepared from the LnCl_3 -hydrate salts (Sigma-Aldrich) as ~ 50 mM solutions in 1 mM HCl, and were diluted as needed. Exact concentrations were determined by colorimetric titrations using a standardized EDTA solution (Aldrich) and a Xylenol Orange indicator as described in the literature.¹⁴

For SE3: LBT Peptide was added to a concentration of 200 nM in a 3 mL solution of the NaCl/MOPS buffer described above, and a background data point was obtained. Next, Tb^{3+} was added to a concentration of 400 nM. Then, the competing Gd^{3+} was titrated: five 2.0 μL aliquots of 100 μM Gd^{3+} were added, followed by five 2.0 μL aliquots of 200 μM Gd^{3+} , followed by five 2.0 μL aliquots of 1 mM Gd^{3+} , and one 2.0 μL aliquot of 5 mM Gd^{3+} . After each addition, the solution was mixed by pipet-aspiration and a data point taken.

For SE3 ϵ and mSE3: LBT Peptide was added to a concentration of 1 μM in a 3 mL solution of the NaCl/MOPS buffer described above, and a background data point was obtained. Next, Tb^{3+} was added to a concentration of 2 μM . Then, the competing Gd^{3+} was titrated: five 2.0 μL aliquots of 200 μM Gd^{3+} were added, followed by five 2.0 μL aliquots of 1 mM Gd^{3+} , and five 2.0 μL aliquots of 5 mM Gd^{3+} . After each addition, the solution was mixed by pipet-aspiration and a data point taken.

Competitive luminescence titration spectra obtained in this fashion were analyzed with the program SPECFIT/32,¹³ which determines $\log \beta$ values (β = binding constant) using the equilibrium data. The known SE3- Tb^{3+} , mSE3- Tb^{3+} , or SE3 ϵ - Tb^{3+} $\log \beta$ was used as a constant in the algorithm. Calculated $\log \beta$ values were then translated into the dissociation constants ($K_D = 10^{-\log \beta}$). Reported values are based on three trials.

SE3: $\text{H}_2\text{N-YIDTNNDGWIEGDELLA-CONH}_2$

SE3 was prepared and characterized as described in Chapter 2 (2-2E).

$$\text{Log } \beta (\text{Tb}^{3+}, 1:1_{\text{NaCl/MOPS}}) \equiv 7.42 \text{ (see 2-2E)}$$

$$\text{Log } \beta (\text{Gd}^{3+}, 1:1_{\text{NaCl/MOPS}}) = 7.48 \pm 0.03$$

SE3 ϵ : $\text{H}_2\text{N-YIDTNNDAWIEGDELLA-CONH}_2$

SE3 ϵ was prepared and characterized as described in Chapter 5 (5-2E).

$$\text{Log } \beta (\text{Tb}^{3+}, 1:1_{\text{NaCl/MOPS}}) \equiv 5.79 \text{ (see 5-2E)}$$

$$\text{Log } \beta (\text{Gd}^{3+}, 1:1_{\text{NaCl/MOPS}}) = 5.86 \pm 0.06$$

mSE3: H₂N-**YIDTNNDGWIDGDELLA**-CONH₂

mSE3 was prepared and characterized as described in Chapter 2 (2-3E).

$\text{Log } \beta (\text{Tb}^{3+}, 1:1_{\text{NaCl/MOPS}}) \equiv 5.93$ (see 2-3E)

$\text{Log } \beta (\text{Gd}^{3+}, 1:1_{\text{NaCl/MOPS}}) = 6.07 \pm 0.03$

GPGdSE3-Ubiquitin:

GPGYIDTNNDGWIEGDELYIDTNNDGWIEGDELLAMQIFVKTLTGKTITLEVEPSDTIENVKAKIQDKEGIPPDQQRLIFAGKQLEDGRTLSDYNIQKESTLHLVLRRLRGG

GPGdSE3-ubiquitin was prepared and photophysically characterized as described in Chapter 4 (4-2E).

$\text{Log } \beta (\text{Tb}^{3+}:\text{protein}:\text{Gd}^{3+}, 1:1:0_{\text{NaCl/MOPS}}) \equiv 8.63$ (see 4-2E)

$\text{Log } \beta (\text{Tb}^{3+}:\text{protein}:\text{Gd}^{3+}, 2:1:0_{\text{NaCl/MOPS}}) \equiv 16.27$ (see 4-2E)

$\text{Log } \beta (\text{Tb}^{3+}:\text{protein}:\text{Gd}^{3+}, 1:1:1_{\text{NaCl/MOPS}}) = 16.65 \pm 0.01$

$\text{Log } \beta (\text{Tb}^{3+}:\text{protein}:\text{Gd}^{3+}, 0:1:1_{\text{NaCl/MOPS}}) = 9.02 \pm 0.15$

$\text{Log } \beta (\text{Tb}^{3+}:\text{protein}:\text{Gd}^{3+}, 0:1:2_{\text{NaCl/MOPS}}) = 16.32 \pm 0.01$

6-2. A Split-Pool Library to Optimize LBTs for MR-Imaging Studies.

Library “LanGdoN1: Position 9 Optimization for MRI”.

TentaGel Macrobeads (Rapp Polymere, Tübingen, Germany) were weighed into a fritted funnel (1 g, 0.21 mmol/g). Resin was swelled for 1 min. with DMF; for all swelling and reaction steps, N₂ gas was bubbled through to ensure complete mixing, and liquid was drained by vacuum filtration. All reactions were performed under atmosphere at room temperature.

An alanine residue was first coupled to the resin. Fmoc-Ala-OH (197 mg, 3 equiv.) and PyBOP (327 mg, 3 equiv.) were dissolved in ~6 mL of DMF, and added to the resin. DIPEA (290 μL , 8 equiv.) was then added to the mixture, and was allowed to react for 45 minutes. Resin was drained, and the step was repeated with fresh reagents for 45 minutes. The resin was then washed five times with DMF.

Deprotection of the Fmoc group was achieved by treatment with two 5 mL aliquots of 20% piperidine in DMF for about five minutes each. This solution was collected and diluted to 100 mL in methanol for UV analysis to determine yield ($\epsilon_{300(\text{Fulvene})} = 7800 \text{ M}^{-1}\text{cm}^{-1}$); obtained 143 μmol (68% yield).

Next, the HMBA linker was coupled. In 4 mL DMF were dissolved HMBA (165 mg, 5 equiv.), HOBt (166 mg, 5 equiv.), and DIC (165 μL , 5 equiv.), and the solution was added to the

resin and allowed to react for one hour. The resin was then filtered and washed five times with DMF.

To couple the β -alanine residue, the symmetric anhydride was made. In a 50 mL round-bottom flask equipped with a stir bar was added 665 mg Fmoc- β Ala-OH and 10 mL DCM (the former did not completely dissolve). Next, 165 μ L DIC was added and the solution turned clear, briefly, and then became cloudy again as product began to precipitate. The mixture was stirred under open atmosphere for 30 minutes at room temperature, and the solvent was then removed by rotary evaporation. The residue was dissolved in DMF and immediately added to the resin, along with 20 mg of DMAP; the mixture was allowed to react for three hours. Resin was then washed five times with DMF, and twice with DCM. The four residue spacer (–Gly-Pro-Pro-Arg–) was appended using standard Fmoc-based SPPS on the ABI 431A, as described in Chapter 2 (2-0E). For storage, the terminal Fmoc group was left attached, and the resin was washed with DCM; it was stored at 4°C until use.

For the split-and-pool library (as per Figure 1-10), the C-terminal residues –**GDELLA**– were synthesized on the ABI 431A, using standard Fmoc-based SPPS chemistry as described in Chapter 2 (2-0E), on 200 mg (~40 μ mol) of the TentaGel resin. The resin was then divided into five portions, each of which had one of the position 9 variable amino acids (Fmoc-Ala-OH, 10.0 mg; Fmoc-Asp(tBu)-OH, 13.2 mg; Fmoc-Glu(tBu)-OH, 13.6 mg; Fmoc-Arg(Pbf)-OH, 20.8 mg; or Fmoc-Ser(tBu)-OH, 12.4 mg; 32 μ mol of each) coupled by hand using PyBOP (16.6 mg, 32 μ mol) as an activating agent in DMF, with 11 μ L (64 μ mol) DIPEA. Resin was then pooled and the sequence –**NDGWI**– was coupled on the ABI. The resin was split again, this time into two portions. Using PyBOP (48.8 mg, 94 μ mol) as an activating agent, onto one portion Fmoc-Asn(Trt)-OH (48 mg, 85% of 94 μ mol) and Boc-Asp(Bzl)-OH (4.6 mg, 15% of 94 μ mol) were coupled in DMF; onto the other Fmoc-Asp(OtBu)-OH (33 mg, 85% of 94 μ mol) and Boc-Glu(Bzl)-OH (4.8 mg, 15% of 94 μ mol) were used. Finally, the resin was pooled to couple the final H₂N-**YIDT**– on the ABI, and cleave the N-terminal Fmoc protecting group. Side-chain-protecting groups were removed by treatment with the TFA cocktail (94% TFA, 2.5% EDT, 2.5% H₂O, and 1% TIS). The resin was then washed twice with DCM, twice with DMF, thrice with H₂O, and then with 40 mL of 100 mM HEPES pH 7.0 buffer. Resin was stored at 4°C until use by Kelly Daughtry in MRI contrast experiments.

A test cleavage was performed to verify the presence of the desired full-length and capped peptides. A few beads were treated overnight with fresh 28% NH₄OH at room temperature overnight, and then speedivac'ed to dryness. The white residue was dissolved in 50/50 water/acetonitrile; MALDI showed peaks corresponding to all of the expected masses.

Acknowledgements

I am grateful for our collaboration with Prof. Karen Allen's lab at Boston University; Kelly Daughtry did the MRI experiments, and provided me with the contrast image included in Figure 6-1. I am eternally grateful to Dr. Anne Reynolds for editing this chapter.

References

- (1) Pintacuda, G.; John, M.; Su, X.-C.; Otting, G. "NMR Structure Determination of Protein-Ligand Complexes by Lanthanide Labeling." *Acc. Chem. Res.* **2007**, *40*(3), 206-212.
- (2) Caravan, P.; Ellison, J. J.; McMurry, T. J.; Lauffer, R. B. "Gadolinium(III) Chelates as MRI Contrast Agents: Structure, Dynamics, and Applications." *Chem. Rev.* **1999**, *99*(9), 2293-2352.
- (3) Bottrill, M.; Kwok, L.; Long, N. J. "Lanthanides in magnetic resonance imaging." *Chem. Soc. Rev.* **2006**, *35*(6), 557-571.
- (4) Nitz, M.; Franz, K. J.; Maglathlin, R. L.; Imperiali, B. "A powerful combinatorial screen to identify high-affinity terbium(III)-binding peptides." *ChemBioChem* **2003**, *4*(4), 272-276.
- (5) Martin, L. J.; Sculimbrenne, B. R.; Nitz, M.; Imperiali, B. "Rapid Combinatorial Screening of Peptide Libraries for the Selection of Lanthanide-Binding Tags (LBTs)." *QSAR Comb. Sci.* **2005**, *24*(10), 1149-1157.
- (6) Daughtry, K.; Allen, K. N., Personal communication.
- (7) Beeby, A.; Clarkson, I. M.; Dickins, R. S.; Faulkner, S.; Parker, D.; Royle, L.; de Sousa, A. S.; Williams, J. A. G.; Woods, M. "Non-radiative deactivation of the excited states of europium, terbium and ytterbium complexes by proximate energy-matched OH, NH and CH oscillators: an improved luminescence method for establishing solution hydration states." *J. Chem. Soc., Perkin Trans. 2* **1999**, (3), 493-504.

- (8) Nitz, M.; Sherawat, M.; Franz, K. J.; Peisach, E.; Allen, K. N.; Imperiali, B. "Structural origin of the high affinity of a chemically evolved lanthanide-binding peptide." *Angew. Chem. Int. Ed.* **2004**, *43*(28), 3682-3685.
- (9) Rao, S. T.; Satyshur, K. A.; Greaser, M. L.; Sundaralingam, M. "X-ray structures of Mn, Cd, and Tb metal complexes of troponin C." *Acta Crystallogr. D* **1996**, *D52*(5), 997-1003.
- (10) Grabarek, Z. "Structural Basis for Diversity of the EF-hand Calcium-binding Proteins." *J. Mol. Biol.* **2006**, *359*, 509-525.
- (11) Martin, L. J.; Daughtry, K.; Allen, K. N.; Imperiali, B., Unpublished results.
- (12) Chazan, A. Peptide Property Calculator.
<http://www.basic.northwestern.edu/biotools/proteincalc.html>
- (13) Binstead, R.; Jung, B.; Zuberbühler, A. *SPECFIT/32 for Windows; Original Release 2000*, Version 3.0.39; Spectrum Software Associates, Marlborough, MA.: SPECFIT/32 provides global analysis of equilibrium and kinetic systems using singular value decomposition and nonlinear regression modeling by the Levenberg-Marquardt method., 2007.
- (14) Pribil, R. "Present state of complexometry. IV. Determination of rare earths." *Talanta* **1967**, *14*(6), 619-627.

Chapter 7

Using LBT Technology to Study the Protein Calcineurin

Introduction

The trivalent lanthanide ions (Ln^{3+}) have been widely exploited as protein probes. The similarity in ionic radii and oxophilic preferences to the divalent calcium ion (Ca^{2+}) (e.g. Table 1-1) has enabled the direct incorporation of these versatile ions into calcium-binding proteins.¹⁻⁵ A limitation to this approach is that native calcium-binding proteins with more than one calcium-binding motif cannot be site-specifically labeled with Ln^{3+} (Figure 7-1A). The development of LBT technology has enabled this limitation to be overcome: a single, specific Ca^{2+} -binding motif may be mutated with LBT residues, enabling a lanthanide ion to be incorporated only at that site (Figure 7-1B). A unique lanthanide-binding site is crucial for applications such as LRET.⁶

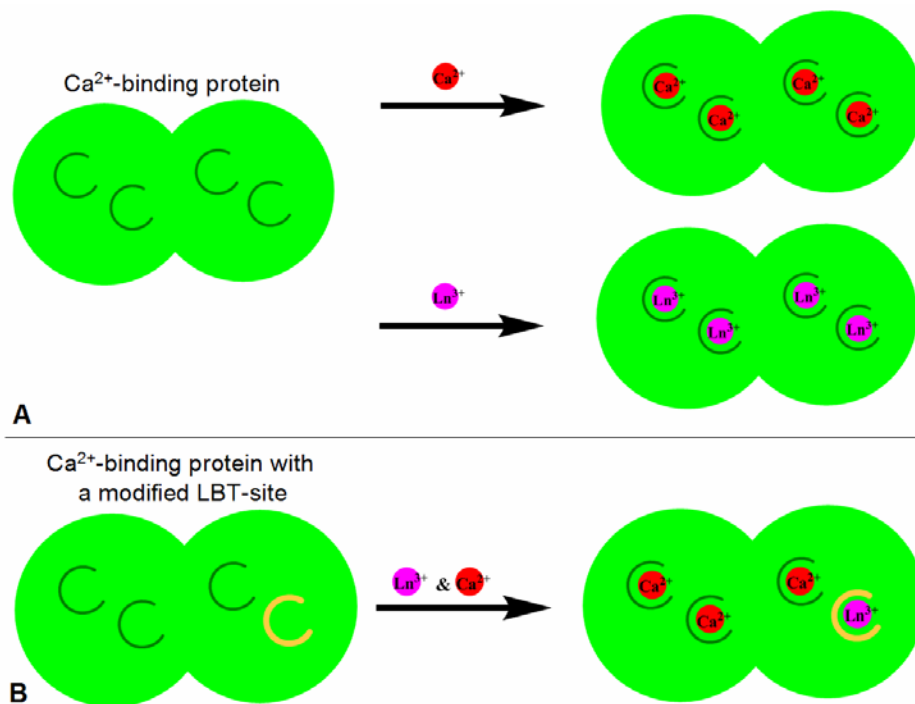


Figure 7-1. **A.** Native calcium-binding proteins with multiple calcium-binding motifs (dark green crescents) can be substituted with Ln^{3+} ions without bias for a particular site. **B.** When a specific site in a protein is modified to be LBT-like, it may be selectively labeled with Ln^{3+} , enabling the study of a more native-like protein with a unique spectroscopic handle for applications such as LRET. (Other sites, especially tight-binding sites, may also bind some Ln^{3+} , but can easily be made spectroscopically silent.)

A collaboration with Dr. Alina Iuga in the laboratory of Professor Patrick Hogan at Harvard Medical School aims to use lanthanide-binding motifs to study a specific calcium-

binding protein: Calcineurin (CN). The protein calcineurin is a unique Ser/Thr phosphatase that was originally found in neuronal cells, is involved in T-cell proliferation,⁷⁻⁹ and is the target of the immunosuppressive drug Cyclosporin A.¹⁰ CN is composed of two subunits: The larger A-subunit (CNA) contains the catalytic site, and the regulatory B-subunit (CNB) contains four Ca²⁺-binding motifs (Sites I – IV). The activation of the enzyme is controlled by calmodulin (CaM) and local calcium concentration [Ca²⁺].¹¹ CNA is composed of four domains: the N-terminal catalytic domain which has a zinc ion (Zn²⁺) and an iron ion (Fe²⁺ or Fe³⁺) in the active site, the CNB-binding domain, the CaM-binding domain, and the C-terminal autoinhibitory (AI) domain.¹² A crystal structure (Figure 7-2) shows the interaction of fully-occupied CNB with CNA, and highlights the site that has been reengineered for lanthanide-binding.⁸

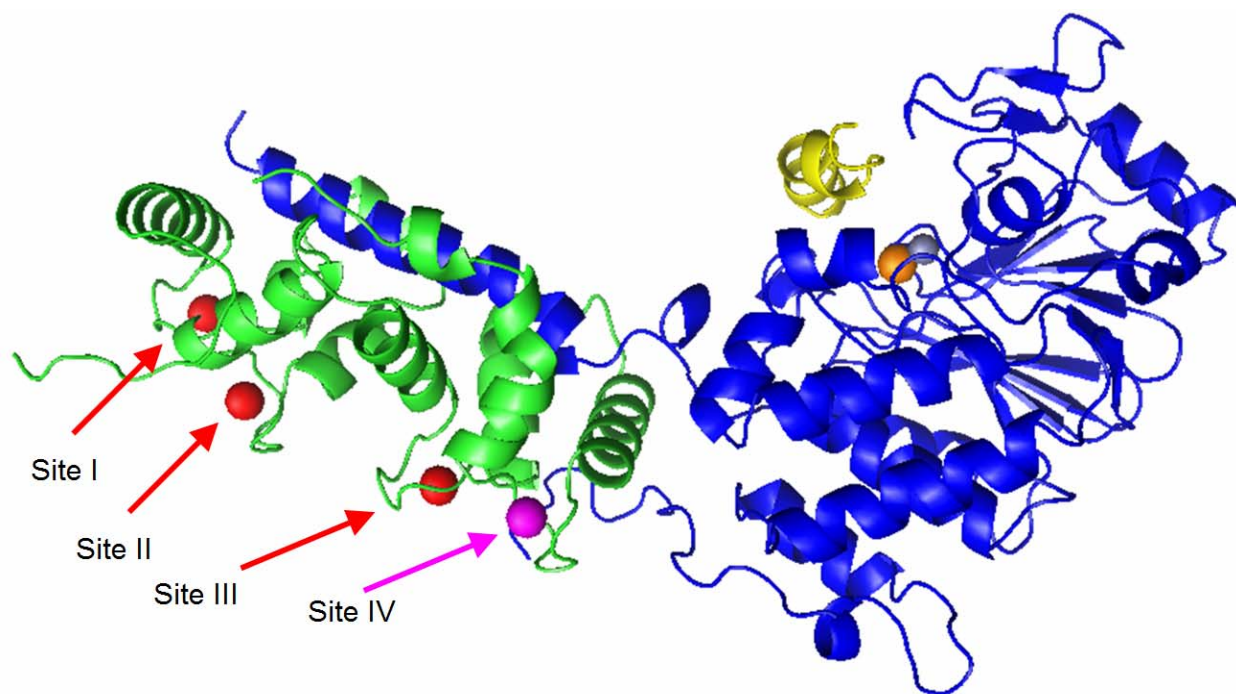


Figure 7-2. Crystal structure of calcineurin (from PDB ID# 1AUI),⁸ shown in cartoon form. Calcineurin A is shown in blue, and Calcineurin B is shown in green. The active site of CNA contains an Fe³⁺ ion (orange sphere) and a Zn²⁺ ion (grey sphere). The active site is blocked by the autoinhibitory domain, shown in yellow; the AI domain is also part of CNA but appears to be disconnected due to the unstructured Calmodulin-binding domain. In CNB, the four calcium ions are shown as spheres: Sites I – III (numbered left to right in the orientation shown) are colored red, and Site IV is colored magenta, and is indicated with a magenta arrow. Site IV has been modified to be LBT-like for the calcineurin mutants in these studies. (This figure was created using PyMOL.)

Interactions of CNA are outlined in Figure 7-3 (which is adapted from the literature¹³). Catalytic activity of CNA is up-regulated when Ca²⁺ binds to the regulatory sites on CNB, which alters the binding of the two subunits and lowers the K_m for a substrate peptide.¹⁴ Subsequent

binding of CaM, which increases V_{\max} , is necessary for CN to obtain maximal catalytic activity.¹⁴ Regulatory structural changes in CNA, which are modulated by the calcium-binding state of CNB¹³, are poorly understood and would benefit from further examination. For instance, the CaM binding domain is disordered in the crystal structure, but is believed to be ordered at low $[Ca^{2+}]$ when the regulatory sites of CNB are empty.¹³ Furthermore, the interaction of CaM with the CaM-binding domain¹⁵ has not been characterized in full-length CNA.¹⁶ Finally, although the autoinhibitory domain¹⁷ can be identified in the crystal structure (and is shown in yellow in Figure 7-2), it reportedly becomes disordered upon CaM binding.¹²

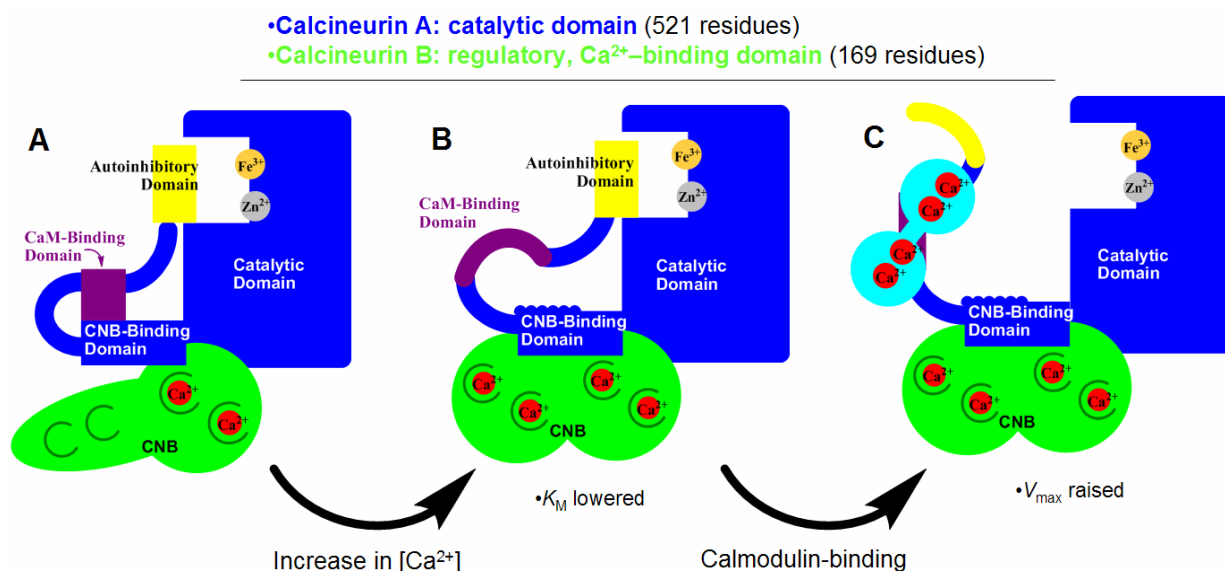


Figure 7-3. The effects of $[Ca^{2+}]$ and CaM on the enzymatic activity of calcineurin. **A.** At low $[Ca^{2+}]$, Sites I and II on CNB are unoccupied, and the CaM-binding domain (purple) of CNA is structured due to intrasubunit contacts. **B.** As local $[Ca^{2+}]$ increases, CNB Sites I and II become occupied. This enables the N-terminal portion of CNB to bind the CNB-binding domain of CNA, altering the structure of CNA such that the CaM-binding domain becomes disordered. (This is the state that appears in the crystal structure⁸ shown in Figure 7-2.) **C.** At high $[Ca^{2+}]$, fully occupied Calmodulin (turquoise, which also contains four calcium-binding motifs) binds to the CaM-binding domain, causing a further structural change in CNA that removes the AI domain from the active site. (This figure is adapted from figures in the literature.^{13,14})

A previous study by Horrocks *et al.* used Eu^{3+} and Tb^{3+} luminescence to probe the calcium-binding sites in CNB.³ However, Eu^{3+} had to be excited directly by a laser, and Tb^{3+} luminescence was suboptimal due to the presence of metal-coordinated water molecules and because only native tyrosine residues were used as sensitizers. Furthermore, interpretation of the results was complicated because all four metal-binding sites were occupied by Ln^{3+} . By applying our knowledge about the LBT, including ligand preferences and sequence optimization, we will be able to modify the calcium-binding site of our choosing (Site IV) to preferentially

chelate Tb^{3+} instead of Ca^{2+} . Furthermore, we will be able to introduce mutations to exclude water from the Tb^{3+} -binding site along with a tryptophan sensitizer in place of the weaker and more poorly placed tyrosine residues. In the future, we plan to use LRET to measure conformational changes of the CNA domains at high and low $[Ca^{2+}]$, and to study the interactions between the four calcium-binding sites.

Results and Discussion

7-1. Preliminary Studies and Mutations to Eliminate Background Luminescence

Based on the crystal structure of calcineurin⁸ (Figure 7-2), calcium-binding Site IV is situated closest to the catalytic domain of CNA, and to the conformationally mobile regions of interest such as the AI domain and the CaM-binding domain. There is general agreement in the literature that Site IV is a high-affinity site and is occupied regardless of $[Ca^{2+}]$ concentration.^{3,18,19} Therefore, this site was a logical choice for modification as an LBT for these experiments.

For initial studies, three CNB mutants were designed in collaboration with Dr. Alina Iuga and Prof. Patrick Hogan and cloned into a vector that expressed CNA and CNB in equal ratio; these mutants were designated CNm1, CNm2, and CNm3. The mutations involved the removal or addition of sensitizers, because wild-type CNB contains three tyrosine residues and no tryptophan residues. One (Tyr7) is near the N-terminus, far from any of the calcium-binding sites and is unlikely to be of consequence. The other two (Tyr99 and Tyr106) are at positions 0 and 7, respectively, in the Site III loop. (For reference, the complete sequence of CNB in the unmutated vector is included in Figure 7-4, and an alignment of the calcium-binding sites is included in Table 7-1.)

```

      2          11          21          31          41
      GNEASYPLE  MASHFDADEI  KRLGKRFFKKL  DLDNSGSLSV EEFMSLPELQ
      51          61          71          81          91
      QNPLVQRVID  IFDTDGNGEV  DEKEFIEGVS  QFSVKGDKQ  KLRFAFRIYD
      101         111         121         131         141
      MDKDGYISNG  ELFQVLKMMV  GNNLKDTQLQ  QIVDKTIINA  DKDGDGRISF
      151         161         170
      EEFAAVVGGL  DIHKKMVDD
  
```

Figure 7-4. Sequence of CNB used in this study. Two native cysteine residues (at positions 12 and 154) were mutated to alanine (underlined). The four calcium-binding EF-hand motifs are shown in bold-face; see also Table 7-1. Ala17 is indicated by an arrow.

Table 7-1. Alignment of the EF-Hand Motifs of Native Calcineurin-B with the LBT SE3^a

<i>Position</i>	-1	0	1	2	3	4	5	6	<u>7</u>	8	9	10	11	12	13	14	15
SE3	Y	I	D	T	N	N	D	G	<u>W</u>	I	E	G	D	E	L	L	A
Site I _(D31-E42)	-	-	D	L	D	N	S	G	<u>S</u>	L	S	V	E	E	-	-	-
Site II _(D63-E74)	-	-	D	T	D	G	N	G	<u>E</u>	V	D	F	K	E	-	-	-
Site III _(D100-E111)	-	-	D	M	D	K	D	G	<u>Y</u>	I	S	N	G	E	-	-	-
Site IV _(D141-E152)	-	-	D	K	D	G	D	G	<u>R</u>	I	S	F	E	E	-	-	-

^a Positions with metal-coordinating side chains (1, 3, 5, 9, and 12) are shown in bold-face. Position 7 (underlined) has a metal-coordinating backbone carbonyl.

The side chains of tyrosine residues 99 and 106 (especially Tyr106) are potentially capable of sensitizing a Tb³⁺ situated in Site III. Since only the signal from Site IV is desirable, mutant 1 (CNm1) contains a Tyr99→Phe mutation, mutant 2 (CNm2) contains that mutation as well as Tyr106→Phe, and mutant 3 (CNm3) contains both Tyr→Phe mutations as well as Lys142→Trp. The CNm3 Lys→Trp mutation was chosen because the side chain of Lys142 is at position 2 in the Site IV loop, analogous to qSE3 (Table 2-3). The intent was to create a mutant that would sensitize only a Site IV-bound Tb³⁺ (based on the crystal structure of CN, the side chain at this position points into solution, far from any other site).

The relative luminescence traces of these three mutants were approximately as expected (data not shown). Signals for CNm1 and CNm2 were barely above baseline. CNm3 has a noticeably stronger signal, but the intensity strength was almost exactly equal to wSE3 and approximately one tenth that of SE3 (Figure 7-5, below; see Table 2-3 for the sequence of wSE3), which is not sufficient for LRET. Nevertheless, the weak signal of CNm2 gave us confidence that luminescence from endogenous amino acids had been eliminated, and further mutation of Site IV to make it more similar to the optimized LBT sequence would afford a Tb³⁺ luminescence signal that could be used in LRET experiments.

7-2. Optimization of Site IV Luminescence Output in Calcineurin Mutants

Based on the experiments described above, a new mutant, CNm4, was designed. This mutant included the two Tyr→Phe mutations of CNm2 to eliminate unnecessary Tb³⁺ sensitization. In addition, two mutations were included to make Site IV much more LBT-like: Arg147→Trp will install the tryptophan sensitizer at the optimal^{20,21} EF-hand-position 7 (see Table 7-1), and Ser149→Glu will expel the metal-coordinated water molecule, increasing

luminescence,²² and making Site IV much more selective for Tb³⁺ over Ca²⁺.^{23,24} CNm4 was also made by Dr. Iuga in the Hogan laboratory. Table 7-2 includes the Site IV sequence of CNm4.

Table 7-2. Summary of the CNB-Site IV Sequences of LBT-Like Calcineurin Mutants ^{a,b}

<i>LBT position</i>	-1	0	1	2	3	4	5	6	<u>7</u>	8	9	10	11	12	13	14	15
<u>SE3</u>	Y	I	D	T	N	N	D	G	<u>W</u>	I	E	G	D	E	L	L	A
<i>CNB Site IV</i>	139	140	141	142	143	144	145	146	<u>147</u>	148	149	150	151	152	153	154	155
<u>CN</u> (wild type)	N	A	D	K	D	G	D	G	<u>R</u>	I	S	F	E	E	F	A	A
<u>CNm4</u>	N	A	D	K	D	G	D	G	<u>W</u>	I	E	F	E	E	F	A	A
<u>CNm5</u>	Y	A	D	K	D	G	D	G	<u>W</u>	I	E	F	E	E	F	A	A
<u>CNm6</u>	N	A	D	T	D	G	D	G	<u>W</u>	I	E	F	E	E	F	A	A
<u>CNm7</u>	N	A	D	K	N	G	D	G	<u>W</u>	I	E	F	E	E	F	A	A

^a Positions with metal-coordinating side chains (1, 3, 5, 9, and 12) are shown in bold-face. Position 7 (underlined) has a metal-coordinating backbone carbonyl.

^b Mutations to make Site IV more LBT-like are shown in red font.

Analysis of luminescence spectra of CNm4 verified that the new mutations led to a significant increase in intensity. CNm4 is roughly three times brighter than CNm3, and about half as bright as SE3 (Figure 7-5). Furthermore, results of luminescence decay experiments in deuterated solvent verified that water is excluded from Site IV-bound Tb³⁺ (Table 7-3; *vide infra*).

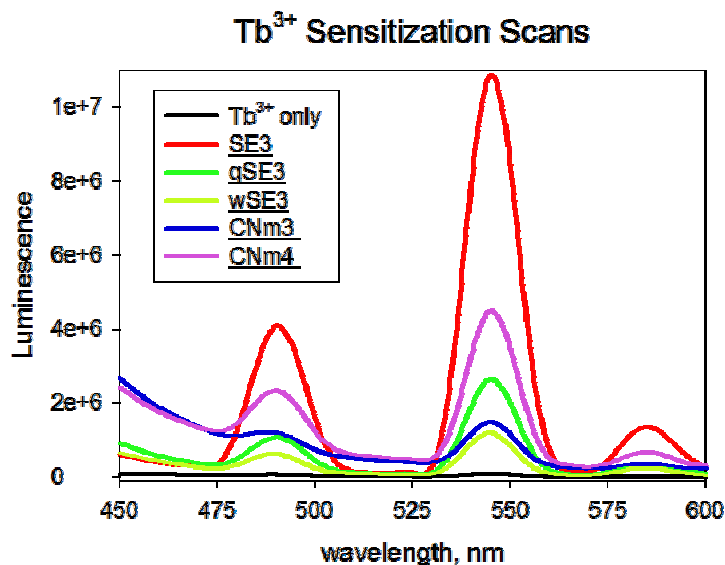


Figure 7-5. Luminescence scans comparing the ability of various LBTs and CN-mutants to sensitize Tb³⁺.

This success led us to design and express of three additional CN mutants, CNm5, CNm6, and CNm7. Each of these mutants, shown in Table 7-2 (*vide supra*), contains a single additional

mutation beyond CNm4. CNm5 contains a new tyrosine (Asn139→Tyr) that might further improve the luminescence output of this construct. CNm6 had a Lys142→Thr mutation that was hypothesized to improve metal affinity, based on the results of Library 4^{21,24,25} (Chapter 1). CNm7 mutated the metal-ligating residue Asp143→Asn, which has been shown to improve lanthanide-ion affinity by improving the electrostatic characteristics of the binding pocket.²⁶ (Also, LBT peptides with Asn3→Asp have been shown to be unable to sensitize Tb³⁺, for reasons that are unclear.²⁷)

A summary of the luminescence intensity and lifetimes of these mutants and CNm4 is included in Table 7-3. The mutation in CNm5 to add a tyrosine residue actually caused a significant decrease. In retrospect, this is perhaps not surprising if one compares the sequences and relative intensities of SE3 and SE4 (Table 4-1): the latter has no Tyr-1, but is brighter than the former. Based on Table 4-1, the more advantageous location to include a tyrosine residue is at position 8 (compare the sequences and relative intensities of SE2 and SE3). An additional CN mutant including this mutation (Ile148→Tyr) was therefore considered, but ultimately rejected due to published data about this position in the context of proteins.²⁸ Interestingly, while the Lys142→Thr mutation of CNm6 had no apparent effect, the Asp143→Asn mutation of CNm7 imparted a ~20% increase in luminescence.

Table 7-3. Luminescence Intensity and Bound Water Molecules for Calcineurin Mutants 4 – 7

	<i>LBT or Site IV Sequence</i> ^a	<i>Relative Intensity</i> ^b	<i>q</i> ^c
<u>SE3</u>	YIDTNNDGWIEGDELLA	1.00	0.08
<u>CNm4</u>	NADKDGDGWIEFEEF AA	0.49	0.08
<u>CNm5</u>	Y ADKDGDGWIEFEEF AA	0.35 ^d	N/D ^d
<u>CNm6</u>	NAD T DGDGWIEFEEF AA	0.50	-0.10 ^e
<u>CNm7</u>	NADK N GDGWIEFEEF AA	0.59	-0.01 ^e

^a Mutations differentiating CNm5, CNm6, and CNm7 from CNm4 are shown in bold-face.

^b Luminescence comparison of equal concentrations of peptide or protein construct saturated with Tb³⁺, normalized to that of SE3.

^c The number of bound water molecules, *q*, was determined by luminescence decay experiments as described in the literature.^{22,24}

^d Due to the decreased luminescence intensity of CNm5, the *q* value was not determined

^e Negative values of *q* such as these are within error indicating the presence of 0 water molecules coordinated to Tb³⁺.

All of the CN mutants listed in Table 7-3 were titrated with Tb³⁺ at a protein concentration of 50 nM in an attempt to determine a *K_D* value. However, all saturated at sub-stoichiometric concentrations of Tb³⁺, making the binding isotherm impossible to fit (data not shown). Titrations in acetate buffer, which should artificially reduce binding affinity, afforded

similar results; it is therefore not feasible to accurately compare the relative tightness of the mutants. Reasons for this result were unclear. Protein stock concentrations were verified by A_{280} UV absorbance in 6 M guanidinium chloride on multiple attempts with high consistency. Clearly, though, all are sufficiently tight for luminescence experiments including LRET. Given the superior luminescence properties of CNm7, it was chosen for use with most of the remaining experiments. Figure 7-6 shows the detail of Site IV in the crystal structure of native calcineurin with an overlay of the mutations made for CNm7.

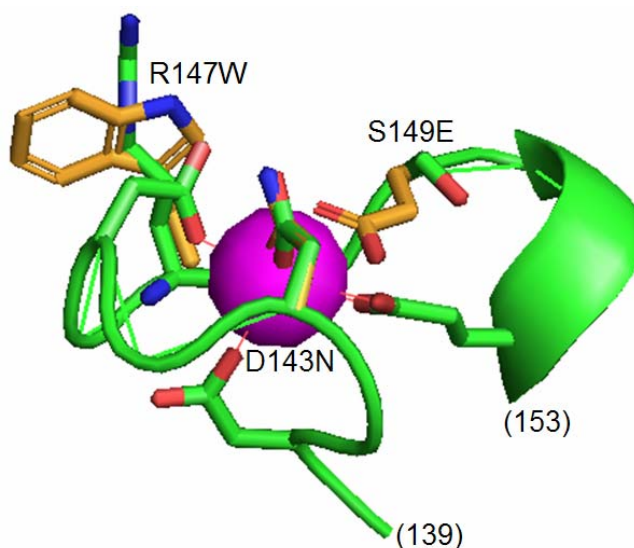


Figure 7-6. Detail of calcineurin-B, metal-binding Site IV, with an overlay of the mutations in CNm7. Coloration of calcineurin is as for Figure 7-2. Side chains of residues mutated for the CNm7 construct are shown with orange carbon atoms; mutated residues are indicated. (This figure was created using PyMOL.)

7-3. Use of Competitive Ligands to Study the Interactions of Site IV with Sites I – III

In addition to use as a potential LRET partner in distance measurements, LBT-containing calcineurin mutants can be used to study interactions of the CNB metal-binding sites. Previous studies have examined the four calcium-binding sites by using Eu^{3+} spectroscopy in wild-type CNB,³ or by using flow dialysis to study the calcium-binding properties of CNB mutants containing Glu→Lys mutations¹⁹ or Glu→Gln mutations¹⁸ at each of the four sites. These studies—and the general literature—confirm that Sites I and II are low-affinity, regulatory sites whereas Sites III and IV are structural sites with Site IV being the highest-affinity site. (See Table 7-1 or Figure 7-4 for the sequences of these sites.)

Due to evidence in the literature for “communication” amongst the four calcium-binding sites,¹⁸ CNm7 has been used to study these interactions in more detail. First, experiments were conducted in which CNm7, equilibrated with 2 equiv. Tb^{3+} , was subjected to high concentrations of a metal chelator such as EGTA or HEDTA (*N*-(hydroxyethyl)-ethylenediaminetriacetic acid). The speed with which the luminescence of the solution decreased was measured in the standard 100 mM NaCl 10 mM MOPS pH 7.0 buffer (excitation was at 280 nm, and emission was recorded at 544 nm). Observance of monoexponential decay curves verified the presence of a single terbium-binding site; curves in Figure 7-7 fit reasonably well to a mono-exponential, three-component decay curve $[I(t) = y_0 + a \cdot e^{-t/\tau}]$.

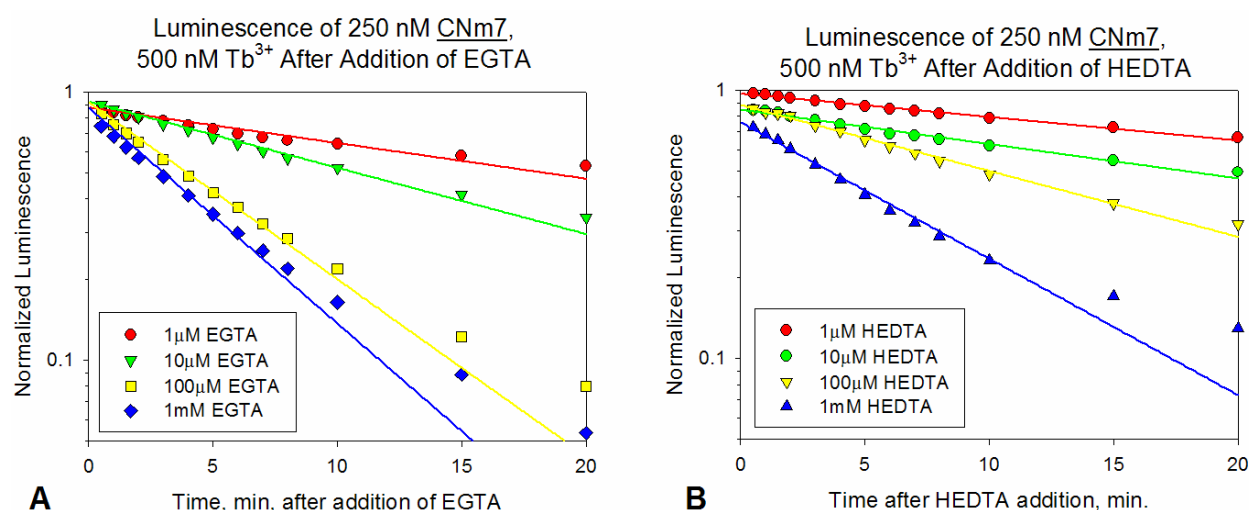


Figure 7-7. Addition of metal chelator (EGTA or HEDTA) to solutions of CNm7 and 2 equiv. Tb^{3+} causes monoexponential decay in luminescence.

The effect that occupancy of the other calcium-binding sites would have on the luminescence decrease was examined next. A slower rate would indicate that when one (or more) additional sites were bound to Ca^{2+} , Site IV metal affinity was improved. A constant amount of $[Ca^{2+}]_{free}$ must be available to bind Sites I – III, and can be obtained by using a metal/chelator buffering system.²⁹ (The desired $[Ca^{2+}]_{free}$ concentration must be within one log unit of the K_D between the chelator and Ca^{2+} .) Using the program WinmaxC32 (available on the web),²⁹ a series of buffered $[Ca^{2+}]_{free}$ was calculated, shown in Table 7-4. Note that in all cases, $[EGTA]_{free}$ is between 0.1 and 1 mM.

Table 7-4. Metal-Chelation Buffers to Make a Variety of Free $[\text{Ca}^{2+}]$ Concentrations ^{a,b}

$[\text{EGTA}]_{\text{total}}$	$[\text{Ca}^{2+}]_{\text{total}}$	$[\text{EGTA}]_{\text{free}}$	$[\text{Ca}^{2+}]_{\text{free}}$	Equiv. $[\text{Ca}^{2+}]_{\text{free}}$ ^c
1mM	740 μM	261 μM	1.00 μM	4.0 equiv.
1mM	587 μM	414 μM	500 nM	2.0 equiv.
1mM	415 μM	585 μM	250 nM	1.0 equiv.
1mM	254 μM	746 μM	120 nM	0.5 equiv.

^a In 100 mM NaCl, 10 mM MOPS, pH 7.0, 25°C

^b Calculated using WinmaxC32²⁹

^c At 250 nM CNm7

Experiments as in Figure 7-7 were conducted using the buffer conditions detailed in Table 7-4. CNm7 (250 nM) was equilibrated with 1 equiv. of Tb^{3+} and with the appropriate amount of $[\text{Ca}^{2+}]_{\text{total}}$. At $t = 0$, 1 mM EGTA was added and time points were taken. Results of these experiments are presented in Figure 7-8. Notably, when there is even enough $[\text{Ca}^{2+}]_{\text{free}}$ to occupy half of the CNm7 protein metal-binding sites (125 nM), the rate of luminescence decrease is notably slower than in the absence of Ca^{2+} with the same amount of $[\text{EGTA}]_{\text{free}}$. Presumably, the occupancy of Site III (the other tight-binding site) is responsible for this effect. This evidence corroborates with the published data, indicating cooperativity between Site IV and other calcium-binding sites. At $[\text{Ca}^{2+}]_{\text{free}}$ of 250 nM or above, the rate is further reduced because all available Site III motifs may be occupied.

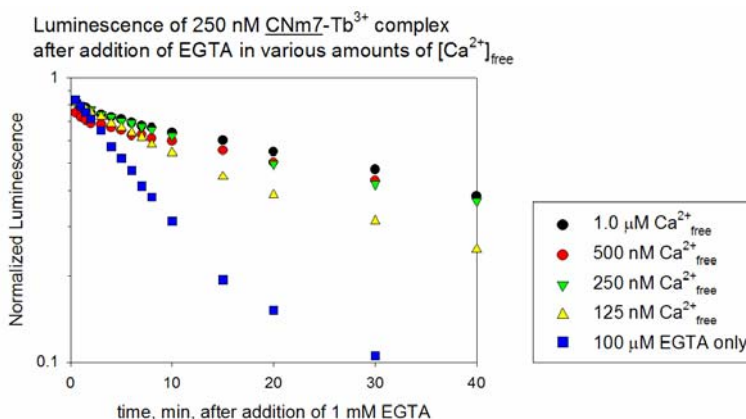


Figure 7-8. Luminescence decrease over time of CNm7 complexes with buffered²⁹ concentrations of $[\text{Ca}^{2+}]_{\text{free}}$. For the trials represented by black, red, green, and yellow data points, total concentration of EGTA was 1 mM, with at least 100 μM $[\text{EGTA}]_{\text{free}}$. For the trial represented by blue data points, no Ca^{2+} was present, and $[\text{EGTA}]_{\text{total}}$ was 100 μM .

7-4. Initial LRET Experiments using the construct CNm4-^BA17C-TMR

In LRET, as in all resonance energy transfer experiments, the choice of a suitable donor-acceptor pair is critical. Sufficient overlap between the emission spectrum of the donor (in this

case Tb^{3+}) and the excitation spectrum of the acceptor fluorophore is necessary to ensure measurable energy transfer (and therefore a value of R_0 that is commensurate with the target measurements). The distance, R , between Tb^{3+} and the acceptor fluorophore can be calculated as a function of R_0 (the Förster distance) and E (the percentage of energy transferred), shown in equation (3).³⁰ Values for E and R_0 can be determined as outlined in equations (4) and (5), respectively.³⁰ Values of the variables in these equations are as follows.^{6,30} The parameter τ_D is the lifetime of the donor alone; for this system it is the lifetime of unlabeled CNm7, which is 2.47 ms (*vide infra*). Similarly, τ_{DA} will be the lifetime of the donor (Tb^{3+}) in the presence of the acceptor fluorophore. The Förster distance R_0 is unique to each donor-acceptor pair, and is the distance between the donor and the acceptor such that $E = 0.5$. A randomized orientation for both the donor and the acceptor is assumed, and therefore κ^2 (the orientation factor) is set to be $2/3$. The refractive index, η , is 1.4 in water, and Q_D can be calculated by dividing the aforementioned τ_D by τ_{Tb} , the later of which is equal to 4.75 ms³¹. Finally, the spectral overlap term, J , can be calculated using the emission spectrum of the donor and the absorption spectrum of the acceptor (see the Experimental section).

$$R = R_0 \left[\frac{1}{E} - 1 \right]^{1/6} \quad (3)$$

$$E = 1 - \frac{\tau_{DA}}{\tau_D} \quad (4)$$

$$R_0 = 0.211 (\kappa^2 \eta^{-4} Q_D J)^{1/6} \quad (5)$$

For an initial attempt to study $[\text{Ca}^{2+}]$ -dependent conformational changes in calcineurin mutants, the mutant CNm4-B_{A17C}-TMR was made. This CNm4-based construct contains the mutation Ala17→Cys on the CNB subunit (see Figure 7-4). This cysteine residue was labeled with the tetramethylrhodamine (TMR) fluorophore (**3**), Figure 7-9. The value of J (equation (5)) was calculated to be $5.28 \times 10^{15} \text{ M}^{-1} \text{ cm}^{-1} \text{ nm}^4$, for LRET between Tb^{3+} and TMR, yielding a value of 59 Å for R_0 .

The residue Ala17 of CNB is located on an α -helix adjacent to calcium-binding Site I, leading us to posit that any conformational change upon occupancy of Site I would correspond to a distance change with respect to Site IV. Furthermore, the side chain of Ala17 was chosen for this mutation because it is at an ideal distance³² from the Site IV metal center (42.1 Å, Figure 7-10) for measurement. Unfortunately, UV analysis showed that this construct was labeled with

two equivalents of TMR, most likely due to the numerous native cysteine residues in the CNA subunit. The second TMR is believed to be attached to Cys153 on CNA, which is only 37.9 Å from the Site IV metal; Figure 7-10.³³

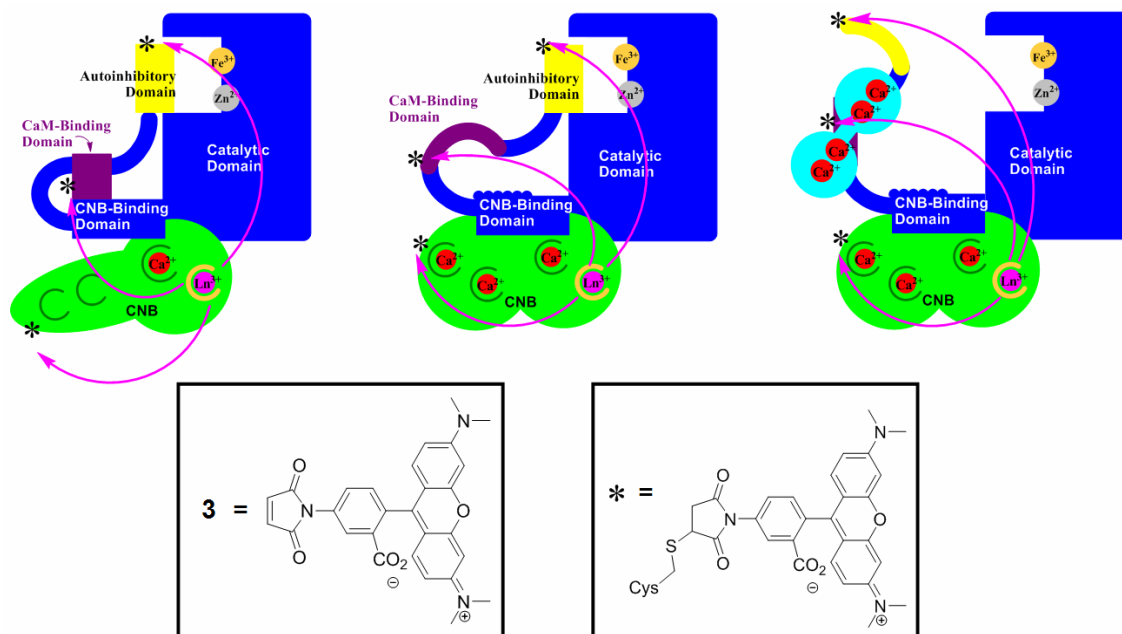


Figure 7-9. Plans for three possible calcineurin LRET experiments. (These experiments would not be conducted simultaneously, and are only shown as such here for illustrative purposes.) For CNm4-B_A17C-TMR the fluorophore is located on CNB near calcium-binding Site I. Ultimately, we would like to do LRET experiments with the acceptor on the CaM-binding domain and on the autoinhibitory domain.

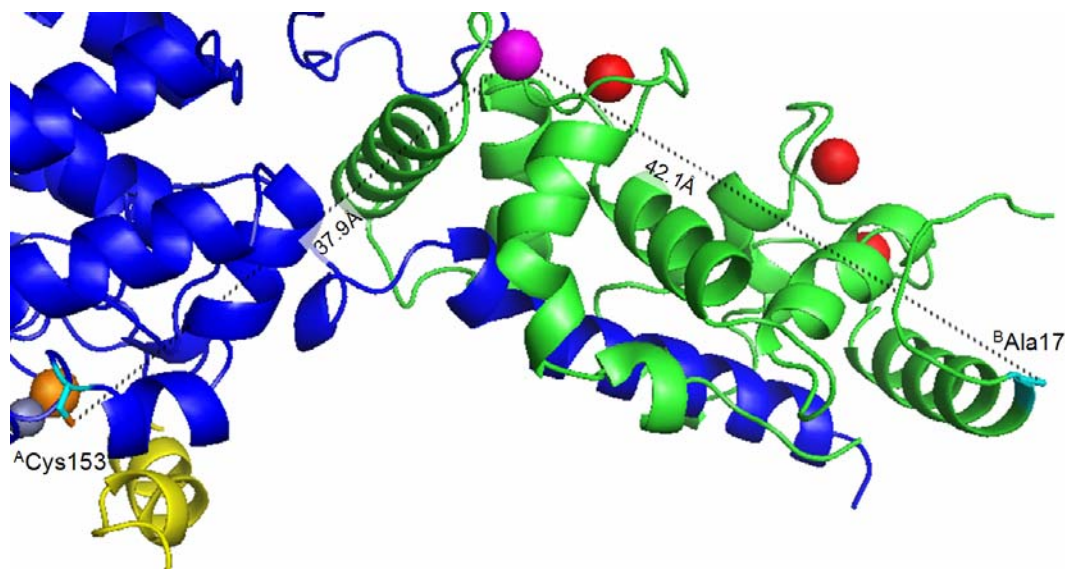


Figure 7-10. Detail of the calcineurin structure, showing the distances between the Site IV metal ion and ^BAla17 (42.1Å) and ^ACys153 (37.9Å). Coloration is as for Figure 7-2, with the residues of interest (^BAla17 and ^ACys153) shown in teal.

Results from an initial experiment, a gated luminescence scan with the CNm4-^BA17C-TMR construct, were promising. For this experiment, the solution was excited at 280 nm, and emission was recorded after a 50 μ s delay to allow for background fluorescence due to decay. Results are shown in Figure 7-11. Prior to addition of Tb^{3+} , no luminescence is seen. With CNm7 (which was used as the unlabeled control), the standard Tb^{3+} -luminescence peaks are observed, and with CNm4-^BA17C-TMR, an additional peak is seen, indicating that energy transfer from sensitized Tb^{3+} to the TMR moiety is occurring. However, from these data we cannot ascertain to which TMR the energy is transferred and/or whether it is $[Ca^{2+}]$ -dependent.

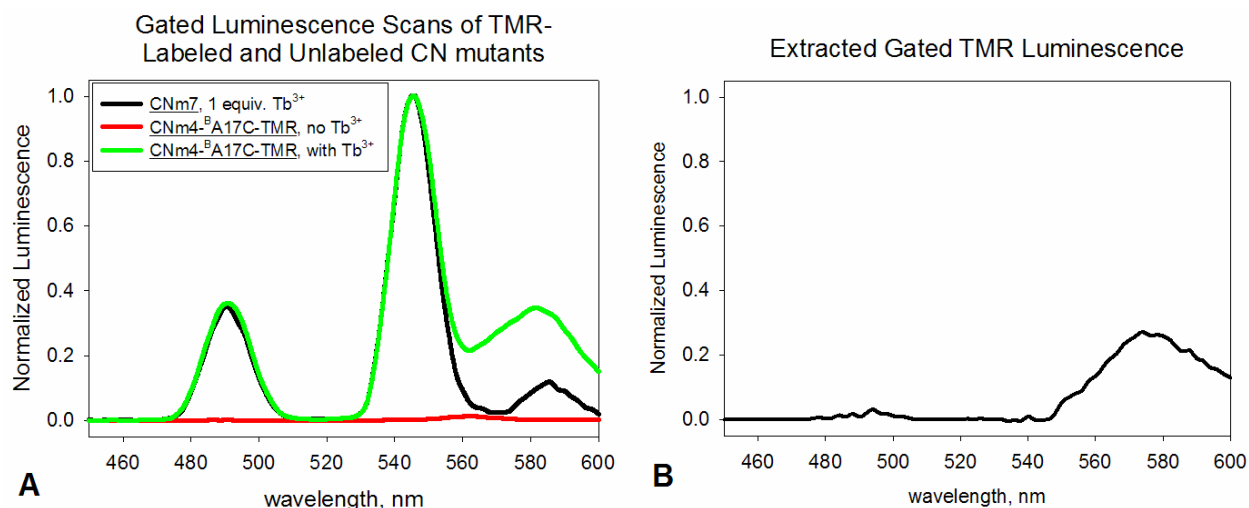


Figure 7-11. Gated luminescence scans of TMR-labeled and unlabeled LBT-containing calcineurin mutants. **A.** Luminescence scans of CNm7 or CNm4-^BA17C-TMR in the presence or absence of 1 equiv. Tb^{3+} . All scans were conducted at $[protein] = 2 \mu M$. **B.** Luminescence of the TMR fluorophore, obtained by subtracting the black curve in **A** from the green curve. (Expected maximum emission from TMR is 567 nm.)

Unfortunately, experiments to determine $[Ca^{2+}]$ -dependent distance changes have been unsuccessful. Luminescence decay curves were measured for CNm4-^BA17C-TMR with 1 equiv. Tb^{3+} while $[Ca^{2+}]$ was varied from 0 to 20 equivalents. Excitation was at 280 nm and emission was detected at 544 nm and 567 nm (the latter wavelength is the approximate emission maximum for TMR). Regardless of the amount of Ca^{2+} , the decay curves are superimposable (Figure 7-12). Based on the literature, a change in distance between donor and acceptor should be accompanied by a change in rate order,^{6,34} but this is not observed. This seems to indicate one of three things: 1) A17 does not move appreciably upon metal binding by Sites I and II; 2) the mutant CNm4-^BA17C-TMR has altered the calcium-affinity or binding-conformation of the CNB subunit; or 3) the additional TMR moiety is not conformationally mobile and is the

recipient of most—or all—of the energy transfer (perhaps due to a closer proximity to the Site IV Tb^{3+} ion). It is also possible that the protein was not fully decalcified upon purification, but an EGTA- Ca^{2+} is not an option for these experiments, as Tb^{3+} would be removed. A modified purification (perhaps involving Chelex[®] resin) is needed to ensure decalcified protein.

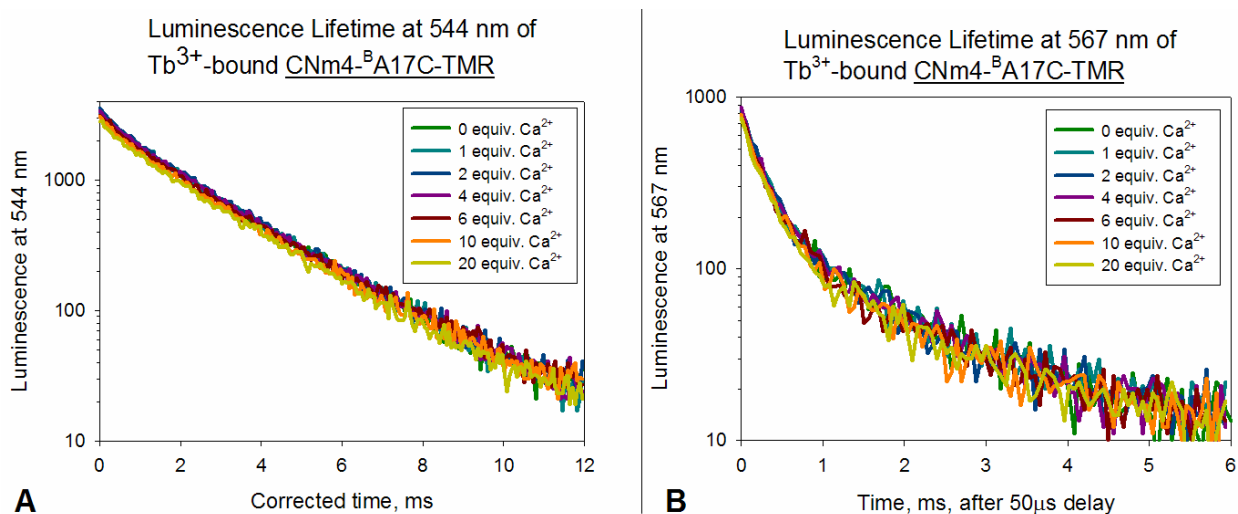


Figure 7-12. Luminescence decay curves of CNm4-B A17C-TMR (2 μM) with 1 equiv. Tb^{3+} are independent of $[\text{Ca}^{2+}]$. Excitation was at 280 nm; emission was recorded after a 50 μs delay. **A.** Emission at 544 nm. **B.** Emission at 567 nm.

7-5. A CNm4 Construct Labeled on the CaM-Binding Domain

The study of $[\text{Ca}^{2+}]$ -dependent changes in the structure and relative orientation of the CaM-binding domain by LRET is also of interest (see Figure 7-9). The CaM-binding-domain is believed to be structured at low $[\text{Ca}^{2+}]$ (when the N-terminal portion of CNB is partially unstructured) and unstructured when the metal-binding sites of CNB are fully occupied.^{12,13} Therefore, a residue on the CaM-binding domain of the CNA subunit, Ala378, was chosen to be mutated to cysteine and labeled with (3); this mutant is known as CNm4-A A387C-TMR. Although not visible in the crystal structure, A387 seems to be a reasonable distance³² from Site IV (~ 40 Å, based on nearby visible residues) and was therefore a good candidate for use in $[\text{Ca}^{2+}]$ -dependent LRET studies.

The construct CNm4-A A387C-TMR also had the mutation Cys153 \rightarrow Val in the CNA subunit, to preclude Cys153 from being labeled. Interestingly, UV studies still indicated this construct to be double-labeled, indicating that the A17C mutant may very well have one or more other cysteine residues inadvertently labeled by TMR. Unfortunately, CNm4-A A387C-TMR did not sensitize Tb^{3+} at all. The reason for this is unclear; perhaps one or both of the mutations

changed the CNA-CNB interaction such that the Site IV geometry was altered. Experiments with this construct are therefore no longer being pursued.

7-6. Generation of a Simpler System, with Only CNB, for Use in LRET Studies

A variety of reasons may have contributed to our inability to observe Ca^{2+} -dependent distance changes via LRET with the CNm4-^BA17C-TMR construct. It may have been due to non-specific labeling of cysteine residues with (3)—which could cause system instability, or give too many donor-acceptor pairs; it is also possible that the distance between Ala17 and Site IV is not affected by $[\text{Ca}^{2+}]$. A simpler system would provide a better platform to study the CNB system more efficiently.

There is precedence for using only the B-subunit of calcineurin (CNB) for studying the metal-binding sites.³ Therefore, it was decided to use a CNA-free system; that is, express CNBm7 (Figures 7-2, and 7-9, green) or CNBm7-A17C without CNA. Two plasmids (Figure 7-13) encoding these constructs were therefore generated. A peptide corresponding to the α -helical domain on CNA that binds CNB (e.g. Figure 7-2; the left-most blue-colored α -helix is this domain) would then be synthesized separately, and added to the solution as necessary. Thus, we would have a CNBm7 construct, with the lanthanide-binding Site IV and a single cysteine residue to label with the TMR fluorophore.

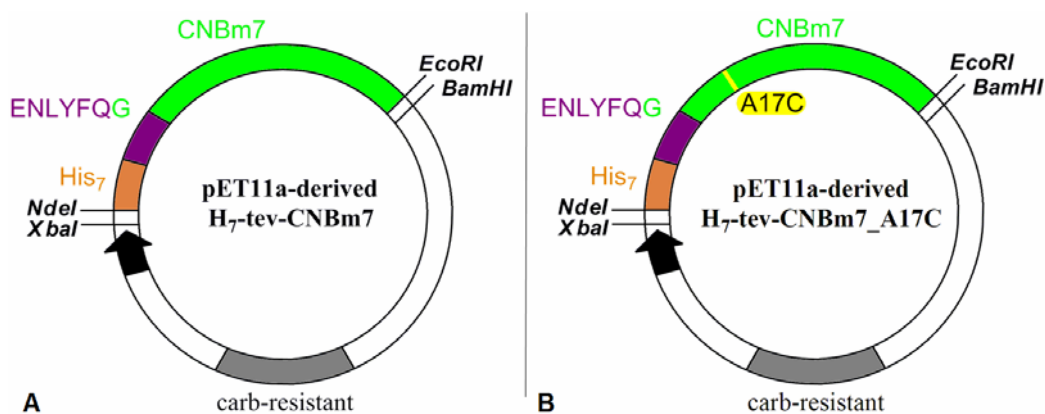


Figure 7-13. **A.** The plasmid for expressing (CNA-free) CNBm7. The N-terminal His₇-tag facilitates purification and the TEV-protease recognition site enables subsequent excision of the tag. **B.** The plasmid for expressing CNBm7-A17C.

The CNBm7 and CNBm7-A17C constructs (Figure 7-13) were expressed from BL21-(DE3)-gold cells and purified using IMAC (see the Experimental section). The His₇-tags were excised from both constructs by treatment with mTEV protease yielded the desired CNBm7 and

CNBm7-A17C products in good yields (about 70 mg/L). These proteins were then used in subsequent control experiments. To obtain pure, mono-labeled CNBm7-A17C-TMR construct, a modified procedure was used, diagrammed in Figure 7-14. Briefly, it was found that labeling of the cysteine with TMR during IMAC enabled the excess fluorophore (**3**) to be washed away. After elution and dialysis, treatment with mTEV protease allowed for excision of the His₇-tag and reverse-IMAC purification as before. A gel including this construct at different steps during the purification is shown in Figure 7-15; the fluorescence of the TMR tag was used as an alternative method of visualization. Based on UV-visible spectroscopic analysis, approximately 35% of the CNBm7-A17C construct is labeled with TMR.

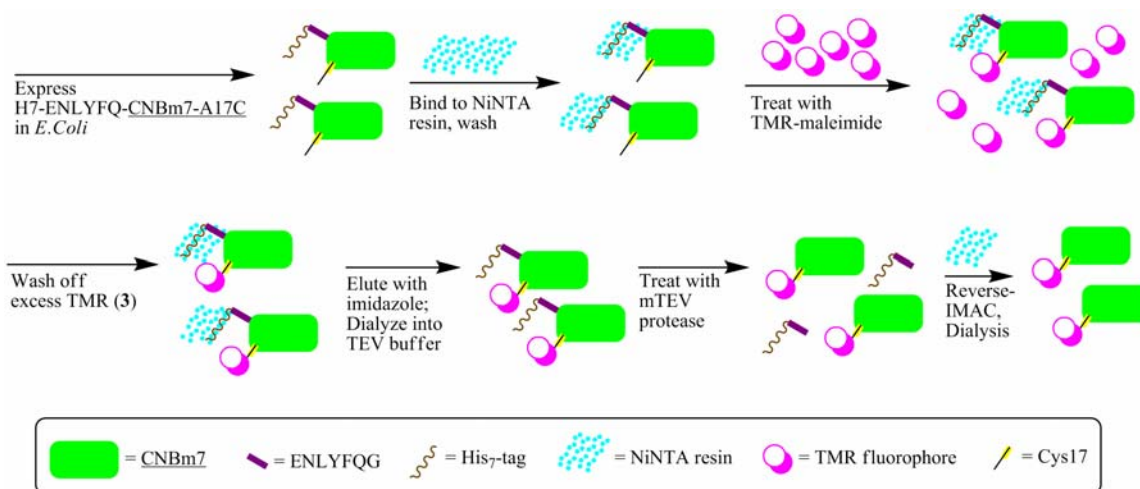


Figure 7-14. Method of generation and purification of CNBm7-A17C-TMR. (For a complete procedure, see the Experimental section.)

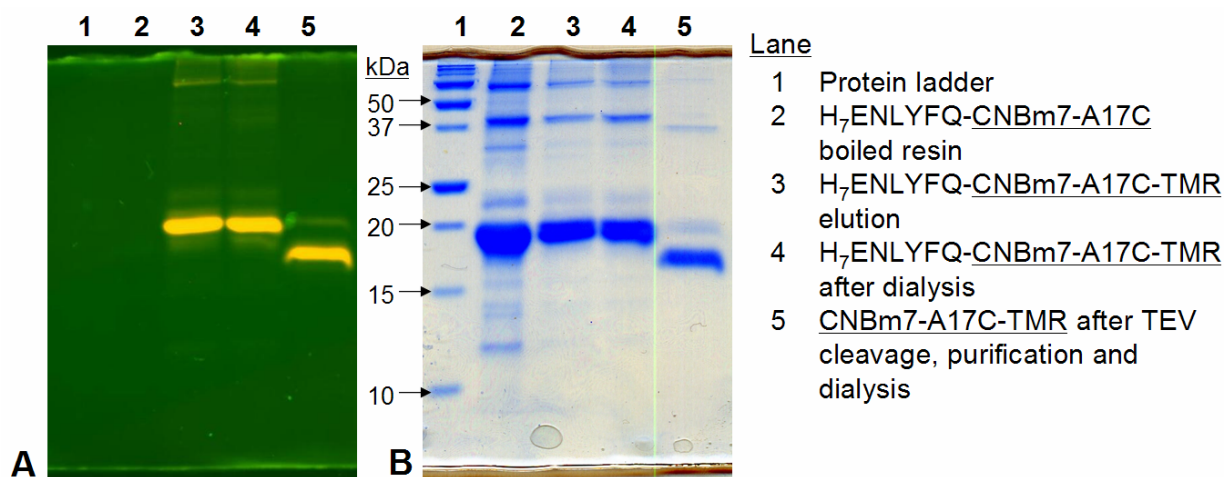


Figure 7-15. Gel of the purification of CNBm7-A17C-TMR. **A.** Illuminated with 280 nm light on a UV-transilluminator; the TMR fluorophore-labeled protein shows up as a yellow band (TMR emission maximum is about 567 nm). **B.** Stained with Gel-Code® Blue.

7-7. Generation of CNB-Binding Domain Peptides CaNAd α and P2465

Although the CNA-free system made expression and labeling of CNBm7 significantly easier, it was desirable to conduct experiments such as LRET in as native an environment as possible. Therefore, it would be necessary to have peptides corresponding to the α -helix of CNA to which CNB binds (see Figure 7-2, left). There is some discrepancy in the literature as to the peptide sequence that enables the most native-like mimic,^{19,35} and so two sequences—shown aligned in Table 7-5—were synthesized by SPPS.

Table 7-5. CNB-Binding Domain Peptides Synthesized

<i>Peptide</i>	<i>Sequence</i>
<u>CaNAdα</u> ^a	YWLPNFM V F T W S L P FVGEK V TEMLVNVLN I ASDDE
<u>P2465</u> ^b	DDEQFNSSPHPYWLPNFM V F T W S L P FVGEK V

^a “CaNAd α ” was named for “Calcineurin A peptide domain α -helix that binds CNB.” It includes CNA residues Tyr341 – Glu376, with the mutation Cys372→Ala. The final three residues (Asp-Asp-Glu) are not present in the crystal structure⁸, but were included to improve solubility.

^b “P2465” was named based on the literature.³⁵ It includes CNA residues Gln333 – Val361, as well as an additional N-terminal tripeptide (Asp-Asp-Glu) to improve solubility.

7-8. Photophysical Experiments with CNBm7

Initial photophysical experiments on CNBm7 showed that this construct sensitized Tb³⁺ and could be used in LRET experiments. The luminescence lifetime in H₂O was established to be 2.47 ms, and by determining lifetimes in varying percentages of deuteration, it was verified that water was excluded from the inner coordination sphere of Tb³⁺. Direct titrations were also performed, and similar to the CNA-containing mutants listed in Table 7-3, luminescence appeared to saturate at exactly 1 equiv. Tb³⁺. This was true in the presence of CaNAd α , P2465, or in the absence of both. This saturation is too sharp to obtain a K_D value, but it seems reasonable to estimate an upper limit of about ~10 nM.

LRET experiments on the labeled CNBm7-A17C-TMR construct have yielded results nearly identical to those with CNm4-^BA17C-TMR: LRET is observed, but shows no [Ca²⁺] dependence. Experiments were performed using 3 μ M protein (meaning, based on the UV, there was ~1 μ M CNBm7-A17C-TMR and 2 μ M unlabeled CNBm7-A17C). Parallel experiments were performed on solutions containing no peptide, or 6 μ M CaNAd α , or 6 μ M P2465. Results under all three conditions were essentially identical; the only difference noted was that the magnitude of the sensitized-Tb³⁺ luminescence in the presence of CaNAd α was about half that of the luminescence in the presence of P2465 or no CNA-domain peptide. (Results of separate

experiments indicated that the presence of CaNAd α slowed the rate at which CNBm7 Site IV became saturated with Tb^{3+} , but preincubation of metal ion and protein before LRET experiments compensated for this.)

Gated luminescence scans (compare to Figure 7-11) were performed at 0, 0.33, 0.67, 1.0 and 2.0 equivalents of Tb^{3+} , followed by 10 and then 50 equivalents of Ca^{2+} . Figure 7-16 includes only the results from the experiments in the presence of P2465 for brevity; these may be considered representative of the other two conditions (in the presence of CaNAd α and absence of CNA-domain peptide). The total luminescence output increased as $[Tb^{3+}]$ increased, and then decreased upon addition of $[Ca^{2+}]$ (Figure 7-16A). However, when these curves are normalized (Figure 7-16B), it is apparent that there is no significant change in the TMR signal (a change in LRET should be manifested as a change in the relative intensity of the signal around $\sim 567\text{ nm}^6$). Also, Figure 7-17 shows that the signal is consistent regardless of CNA-domain peptide used. Finally, luminescence decay experiments at 544 nm and 567 nm, as shown in Figure 7-12 for CNm4-B α 17C-TMR, were performed, and show no difference in τ_{DA} at the concentrations of $[Tb^{3+}]$ and $[Ca^{2+}]$ presented above (data not shown).

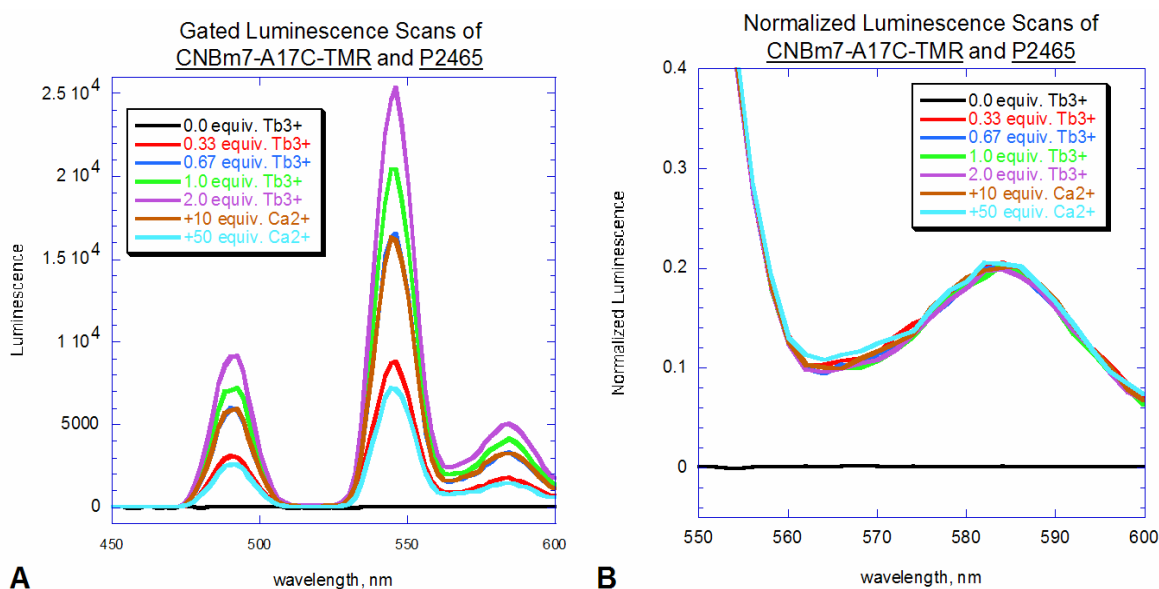


Figure 7-16. **A.** Different concentrations of $[Tb^{3+}]$ and $[Ca^{2+}]$ affect the absolute intensity of gated luminescence of the CNBm7-A17C-TMR construct in the presence of P2465 peptide. **B.** However, when the data is normalized, there is no change in the intensity of the TMR emission spectrum, as would be expected from a distance change between this acceptor and the Site IV Tb^{3+} ion.

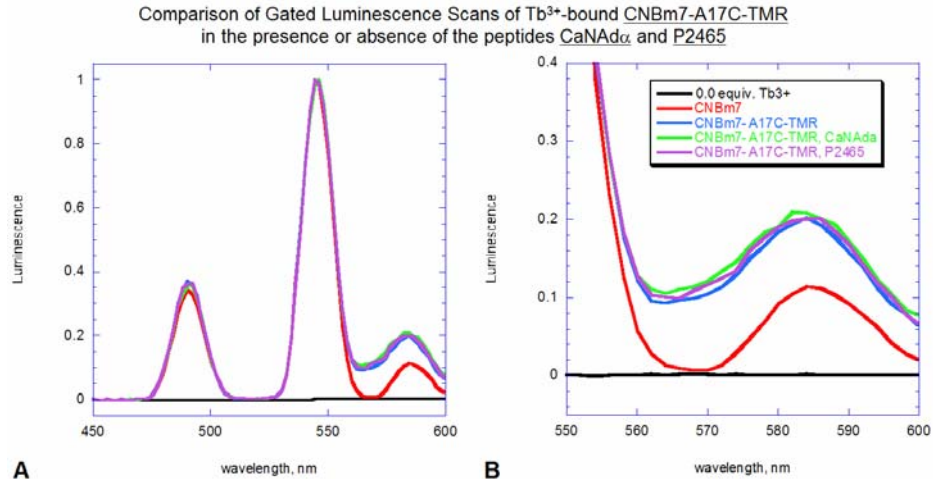


Figure 7-17. A. The presence or absence of a peptide (CaNAd α or P2465) based on the CNB-binding domain of CNA does not affect the Tb³⁺-to-TMR LRET of CNBm7-A17C-TMR in the presence of 50 equiv. [Ca²⁺]. **A.** Full trace including Tb³⁺-emission peaks. **B.** Detail of the TMR-emission region.

It is possible that trace Ca²⁺ in the buffer or the protein stock could pre-saturate Site I, but given that the experiment is run at a protein concentration that is at least an order of magnitude lower than K_D , this seems unlikely. Nevertheless, it would be prudent to conduct future experiments with Chelex[®]-treated buffer and protein stock to ensure complete decalcification. Given the results herein, it seems that Ala 17 was simply an unlucky target to pick. Future studies should focus on a different location on CNB, or label a different residue on CNA. For example, studies have been initiated with labeling a synthetic AI-domain peptide, which could then be incorporated into a CNm7 construct using Expressed Protein Ligation; this would have the additional advantage of precluding any doubly-labeled CNA.³⁶

Conclusions

The protein calcineurin has been modified such that the calcium-binding B-subunit contains an LBT-motif at calcium-binding Site IV. This enables the specific labeling of this site with Tb³⁺ for uses in experiments utilizing luminescence, while leaving the remaining three sites in the native form. Results of experiments on the brightest of these mutants, CNm7, corroborate published work indicating that calcium-binding by the CNB subunit is cooperative. Multiple constructs have been specifically labeled with a tetramethylrhodamine fluorophore at engineered cysteine residues for use in LRET experiments that probe [Ca²⁺]-dependent conformational changes. Unfortunately, [Ca²⁺]-dependent LRET has not yet been observed, even with the simplified CNBm7 system, most likely due to inopportune locations for the acceptor fluorophore.

Experimental

7-0E. General Procedures

Peptide Synthesis and Purification.

Preparation of peptides CaNAd α and P2465 was by standard Fmoc-based SPPS procedures as described in Chapter 2 (2-0E), on an automated ABI 431A Peptide Synthesizer (Applied Biosystems). NovaPEG Rink Amide LL resin (170 $\mu\text{mol/g}$) (EMD Biosciences, San Diego, CA) was used. These peptides were purified by HPLC and verified by MALDI-TOF MS as described in Chapter 2 (2-0E). Concentrations of stock solutions of peptides and of unlabeled fusion proteins were determined by the UV absorption using the extinction coefficients of the tryptophan ($\epsilon_{280} = 5690 \text{ cm}^{-1}\text{M}^{-1}$) and tyrosine ($\epsilon_{280} = 1280 \text{ cm}^{-1}\text{M}^{-1}$) content in 6 M guanidinium chloride.³⁷

Luminescence Titrations.

Titrations were recorded on a Jobin Yvon Horiba Fluoromax-3 Spectrometer in a 1 cm path-length quartz cuvette, as described in Chapter 2 (2-0E). As before, for direct titrations, the buffer was 100 mM NaCl, 10 mM MOPS; it was 100 mM NaOAc, 10 mM HEPES, pH 7.0 for qualitative comparisons. Aliquots of Tb^{3+} were added as described in section 2-0E; when saturation was reached (by 7 aliquots), the experiment was concluded. Because the calcineurin mutants saturated with substoichiometric [Tb^{3+}], the titration spectra could not be fit by SPECFIT/32¹⁵.

Relative Luminescence Intensity.

Comparative luminescence intensities of CN mutants were determined by comparing the luminescence of solutions containing 200 nM of a protein construct (or SE3) and 20 equiv. Tb^{3+} . (The luminescence of SE3 has been nominally defined as 1.00). Trials were done in triplicate and the luminescence (at 544 nm) was averaged.

Determination of Tb^{3+} -bound water molecules.

Luminescence lifetimes were measured as described in Chapter 2 (2-0E), to determine τ_{H2O} and τ_{D2O} . The number of Tb^{3+} -bound water molecules, q , could then be calculated as described in the literature.²²

SDS-PAGE Analysis.

The procedure for running SDS-PAGE gels is described in detail in Chapter 4 (4-2E). It should be noted, however, with all calcineurin proteins, it was helpful to add 1 mM EGTA to the loading buffer, to ensure that the CNB domain was completely free of Ca^{2+} when the gel was run; the presence of Ca^{2+} could affect protein migration and/or cause multiple bands to appear.

7-1E. Preliminary Studies and Mutations to Eliminate Background Luminescence

Luminescence Scans (non-gated)

Luminescence scans were conducted on the Jobin Yvon Horiba Fluoromax-3 Spectrometer in a 1 cm path-length quartz cuvette, with a 315 nm long-pass filter. As for direct titrations, the buffer was 100 mM NaCl, 10 mM MOPS. To the buffer was added 2 μM peptide or protein construct and 10 μM Tb^{3+} . For the calcineurin construct, the solution was allowed 10 minutes to equilibrate, as uptake of Tb^{3+} was not instantaneous as for the peptide constructs.

Scans were conducted with excitation at 280 nm at 25 °C. Emission was recorded at 5 nm increments from 450 – 600 nm (inclusive), with 1 second integration times. Slit widths were 5nm (excitation monochromator) and 10 nm (emission monochromator). When absolute comparison was needed, the emission at 545 nm was used.

CNA-His₆ tag: (The sequence of CNA used is the same in all calcineurin CN constructs, and is only included once here for brevity. The His₆-tag is used for purification.)

MSEPKAIDPK LSTTDRVKA VFPFPHRLT AKEVFDNDGK PRVDILKAHL MKEGRLEESV
ALRIITEGAS ILRQEKLLD IDAPVTVCGD IHGQFFDLMK LFEVGGSPAN TRYLFLGDYV
DRGYFSIECV LYLWALKILY PKTLFLLRGN HECRHLTEYF TFKQECKIKY SERVYDACMD
AFDCLPLAAL MNQQFLCVHG GLSPEINTLD DIRKLDRFKE PPAYGPMCDI LWSDPLEDFG
NEKTQEHFTH NTVRGCSYFY SYPAVCEFLQ HNNLLSILRA HEAQDAGYRM YRKSQTTGFP
SLITIFSAPN YLDVYNNKAA VLKYENNVMN IRQFNCSPPH YWLPNFMDFV TWSLPFVGEK
VTEMLVNVLN ICSDELGSE EDGFDGATAA ARKEVIRNKI RAIGKMARVF SVLREESSESV
LTLKGLTPTG MLPSGVLGG KQTLQSATVE AIEADEAIKG FSPQHKITSF EEAKGLDRIN
ERMPRRDAM PSDANLNSIN KALTSETNGT DSNGSNSSNI QHHHHHH

CNm1 (Sequence of CNBm1 shown; see above for that of the concurrently expressed CNA)

MGNEASYPLEMASHFDADEIKRLGKRFFKLLDLDNSGSLSVVEEFMSLPPELQQNPLVQRVIDIFDTD
GNGEVDFKEFIEGVSQFSVKGDKQKLRFAFRIFDMDKDYISNGELFQVLKMMVGNLKDQTQLQ
QIVDKTIINADKDGDRISFEEFAAVVGGGLDIHKKMVVDV

CNm1 was prepared by Dr. Alina Iuga, and was received as a stock in 100 mM NaCl, 50 mM HEPES pH 7.5, 2 mM β ME buffer. It was photophysically characterized by the non-gated luminescence scan as described above.

CNm2 (Sequence of CNBm2 shown; see above for that of the concurrently expressed CNA)

**MGNEASYPLEMASHFDADEIKRLGKRFFKLLDLDNSGSLSVVEEFMSLPQLQONPLVQRVIDIFDTD
GNGEVDFKEFIEGVSQFSVKGDKEQKLRFAFRIFDMDKDGFI SNGELFQVLKMMVGNLKDQTQLQ
QIVDKTI INADKGDGGRISFEEFAAVVGGGLDIHKKMVVDV**

CNm2 was prepared by Dr. Alina Iuga, and was received as a stock in 100 mM NaCl, 50 mM HEPES pH 7.5, 2 mM β ME buffer. It was photophysically characterized by the non-gated luminescence scan as described above.

CNm3 (Sequence of CNBm3 shown; see above for that of the concurrently expressed CNA)

**MGNEASYPLEMASHFDADEIKRLGKRFFKLLDLDNSGSLSVVEEFMSLPQLQONPLVQRVIDIFDTD
GNGEVDFKEFIEGVSQFSVKGDKEQKLRFAFRIFDMDKDGFI SNGELFQVLKMMVGNLKDQTQLQ
QIVDKTI INADWDGDGGRISFEEFAAVVGGGLDIHKKMVVDV**

CNm3 was prepared by Dr. Alina Iuga, and was received as a stock in 100 mM NaCl, 50 mM HEPES pH 7.5, 2 mM β ME buffer. It was photophysically characterized by the non-gated luminescence scan as described above.

Non-gated luminescence intensity at 545 nm: 1.48×10^6

7-2E. Optimization of Site IV Luminescence Output in Calcineurin Mutants

SE3: H₂N-YIDTNNDGWI**EGDELLA**-CONH₂

SE3 was prepared and photophysically characterized as described in Chapter 2 (2-2E).

It was photophysically characterized by the non-gated luminescence scan (see 7-1E), and as described in 7-0E.

Non-gated luminescence intensity at 545 nm: 1.09×10^7 ($\equiv 1.00$ for relative comparisons)
Relative luminescence intensity at 544 nm: 8.60×10^6 ($\equiv 1.00$ for relative comparisons)

qSE3: H₂N-YIDWNNDGLI**EGDELLA**-CONH₂

qSE3 was prepared and characterized as described in Chapter 2 (2-4E).

It was photophysically characterized by the non-gated luminescence scan (see 7-1E).

Non-gated luminescence intensity at 545 nm: 2.65×10^6

wSE3: H₂N-YIDTNNDGW**IDIDELLA**-CONH₂

wSE3 was prepared and characterized as described in Chapter 2 (2-4E).

It was photophysically characterized by the non-gated luminescence scan (see 7-1E).

Non-gated luminescence intensity at 545 nm: 1.19×10^6

CNm4 (Sequence of **CNBm4** shown; see 7-1E for that of the concurrently expressed **CNA**)

MGNEASYPLEMASHFDADEIKRLGKRFFKLLDLNSGSLSVVEEFMSLPQLQONPLVQRVIDIFD
TDGNGEVDFKEFIEGVSQFSVKGDKLRFQKLRFAFRIFDMDKDGFI SNGELFQVLKMMVGNLKD
TQLQ QIVDKTI INADKDGWIEFEEFAAVVGGLDIHKKMVVDV

CNm4 was prepared by Dr. Alina Iuga, and was received as a stock in 100 mM NaCl, 50 mM HEPES, 100 mM imidazole(\cdot HCl), 0.1 mM TCEP (*tris*-(carboxyethyl)phosphine) pH 7.5 buffer. It was photophysically characterized by the non-gated luminescence scan (see 7-1E), and as described in 7-0E.

Relative luminescence intensity at 544 nm: 4.25×10^6

Luminescence decay: $\tau_{H_2O} = 2.14$ ms; $\tau_{D_2O} = 2.47$ ms

Luminescence decay (+ 20 equiv. Ca^{2+}): $\tau_{H_2O} = 2.21$ ms; $\tau_{D_2O} = 2.52$ ms

CNm5 (Sequence of **CNBm5** shown; see 7-1E for that of the concurrently expressed **CNA**)

MGNEASYPLEMASHFDADEIKRLGKRFFKLLDLNSGSLSVVEEFMSLPQLQONPLVQRVIDIFD
TDGNGEVDFKEFIEGVSQFSVKGDKLRFQKLRFAFRIFDMDKDGFI SNGELFQVLKMMVGNLKD
TQLQ QIVDKTI IYADKDGWIEFEEFAAVVGGLDIHKKMVVDV

CNm5 was prepared by Dr. Alina Iuga, and was received as a stock in 100 mM NaCl, 50 mM HEPES, 100 mM imidazole(\cdot HCl), 0.1 mM TCEP pH 7.5 buffer. It was photophysically characterized as described in 7-0E.

Relative luminescence intensity at 544 nm: 3.01×10^6

CNm6 (Sequence of **CNBm6** shown; see 7-1E for that of the concurrently expressed **CNA**)

MGNEASYPLEMASHFDADEIKRLGKRFFKLLDLNSGSLSVVEEFMSLPQLQONPLVQRVIDIFD
TDGNGEVDFKEFIEGVSQFSVKGDKLRFQKLRFAFRIFDMDKDGFI SNGELFQVLKMMVGNLKD
TQLQ QIVDKTI INADTDGDWIEFEEFAAVVGGLDIHKKMVVDV

CNm6 was prepared by Dr. Alina Iuga, and was received as a stock in 100 mM NaCl, 50 mM HEPES, 100 mM imidazole(\cdot HCl), 0.1 mM TCEP pH 7.5 buffer. It was photophysically characterized as described in 7-0E.

Relative luminescence intensity at 544 nm: 4.27×10^6

Luminescence decay: $\tau_{H_2O} = 2.65$ ms; $\tau_{D_2O} = 2.93$ ms

CNm7 (Sequence of **CNBm7** shown; see 7-1E for that of the concurrently expressed **CNA**):

MGNEASYPLEMASHFDADEIKRLGKRFFKLLDLNSGSLSVVEEFMSLPQLQONPLVQRVIDIFD
TDGNGEVDFKEFIEGVSQFSVKGDKLRFQKLRFAFRIFDMDKDGFI SNGELFQVLKMMVGNLKD
TQLQ QIVDKTI INADKNGDGWIEFEEFAAVVGGLDIHKKMVVDV

CNm7 was prepared by Dr. Alina Iuga, and was received as a stock in 100 mM NaCl, 50 mM HEPES, 100 mM imidazole(\cdot HCl), 0.1 mM TCEP pH 7.5 buffer. It was photophysically characterized as described in 7-0E.

Relative luminescence intensity at 544 nm: 5.09×10^6

Luminescence decay: $\tau_{H_2O} = 2.21$ ms; $\tau_{D_2O} = 2.53$ ms

7-3E. Use of Competitive Ligands to Study the Interactions of Site IV with Sites I – III

Competition Kinetics with EGTA and HEDTA

“Competition Kinetics” experiments were conducted on the Jobin Yvon Horiba Fluoromax-3 Spectrometer in a 1 cm path-length quartz cuvette, with a 315 nm long-pass filter. The buffer was 100 mM NaCl, 10 mM MOPS. Experiments were conducted at volumes of 0.5 mL. After a baseline data point was taken, the protein construct CNm7 (250 nM) was incubated with 500 nM Tb^{3+} for at least 10 minutes, and a “maximum saturation” luminescence point was taken. Then, either EGTA or HEDTA stock was added to a concentration of 1 μ M, 10 μ M, 100 μ M or 1 mM (experiments were conducted at all concentrations with both, and done in triplicate; data points shown are averages of the three trials). A 5 μ L aliquot of EGTA or HEDTA was always used, so as to equally perturb the solution concentration each time; the stock concentration of chelator was simply adjusted as necessary. The cuvette was mixed by inversion, and a timer was started immediately after ejecting the pipet tip used to add EGTA or HEDTA. Time points were taken at 0.5, 1.0, 1.5, 2.0, 3.0, 4.0, 5.0, 6.0, 7.0, 8.0, 10, 15, 20, and 30 minutes.

Competition Kinetics with EGTA-buffered $[Ca^{2+}]$

Buffered- $[Ca^{2+}]$ competition kinetics experiments were also conducted on the Jobin Yvon Horiba Fluoromax-3 Spectrometer in the same quartz cuvette, with the 315 nm long-pass filter. The buffer was again 100 mM NaCl, 10 mM MOPS, and at volumes of 0.5 mL. After a baseline data point was taken, the protein construct CNm7 (250 nM) was incubated with 200 nM Tb^{3+} and Ca^{2+} (using one of the $[Ca^{2+}]_{total}$ detailed in Table 7-4) for at least 10 minutes, and a “maximum saturation” luminescence point was taken (which was an average of four points per construct). Then, EGTA stock was added to a concentration of 1 mM (experiments were conducted in triplicate; data points shown are averages of the three trials). The cuvette was mixed by inversion, and a timer was started immediately after ejecting the pipet tip used to add

EGTA. Time points were taken at 0.5, 1.0, 1.5, 2.0, 3.0, 4.0, 5.0, 6.0, 7.0, 8.0, 10, 15, 20, 30 and 40 minutes.

7-4E. Initial LRET Experiments using the construct CNm4-BA17C-TMR

Gated Luminescence Scans

Gated luminescence scans were conducted on the Jobin Yvon Horiba Fluoromax-3 Spectrometer equipped with a Spex 1934D3 phosphorimeter. A 0.5 mL, 1 cm path-length quartz cuvette was used. The buffer contained 100 mM NaCl and 10 mM MOPS. To the buffer was added 2 μ M protein construct; a background scan was always performed before adding Tb^{3+} .

Scans were conducted with excitation at 280 nm at 25 °C. Emission was recorded at 2 nm increments from 450 – 600 nm (inclusive). Slit widths were 5 nm (excitation monochromator) and 10 nm (emission monochromator). A 40 ms pulse of 280 nm excitation light was followed by a 50 μ s delay. Detection was then over a 10 ms window; 10 flashes were used per data point collected, and two runs were averaged. Metal (e.g. Tb^{3+}) was then added; see below for the specifics of different constructs. After all additions, the solution was allowed 10 minutes to equilibrate, as uptake of Tb^{3+} or Ca^{2+} was generally not instantaneous.

Determination of τ_D

Luminescence lifetimes were measured in a Jobin Yvon Horiba Fluoromax-3 Spectrometer, equipped with a Spex 1934D3 phosphorimeter. Samples were excited by a pulse of 280 nm light for 70 ms. Data were collected at 544 nm for 12 ms in 60 μ s increments following a 50 μ s delay. Slit widths were 5 nm for excitation and 10 nm for emission. Concentrations are detailed below with individual constructs. Data sets were fit to a single exponential decay (equation (1)), as described in Chapter 2.

$$I(t) = I(0)e^{-t/\tau} \quad (1)$$

Determination of τ_{DA}

Luminescence lifetimes were measured in the Jobin Yvon Horiba Fluoromax-3 Spectrometer, equipped with a Spex 1934D3 phosphorimeter. Samples were excited by a pulse of 280 nm light for 70 ms. Data were collected at 544 nm for 12 ms or 567 nm for 6 ms in 60 μ s increments following a 50 μ s delay. Slit widths were 5 nm for excitation and 10 nm for emission.

Concentrations are detailed below with individual constructs. Data sets were fit to a single exponential decay (equation (1)).

Determination of J

The value of J (for use in equation (5)) can be calculated as described in the literature, using equation (6).^{6,30} $F_D(\lambda)$ is the (normalized) luminescence output for the unlabeled Tb^{3+} -sensitizing construct at wavelength λ , as determined by the gated luminescence scan experiment described above. The value $\varepsilon(\lambda)$ is the extinction coefficient for the acceptor fluorophore (in this case TMR) at wavelength λ . This value was determined by taking an absorption spectrum from 450 nm – 600 nm (inclusive) of the construct at 2 nm increments, on a Shimadzu UV-2401PC UV-Visible spectrometer; the values were normalized and multiplied by ε_{\max} (95,000 $M^{-1}cm^{-1}$). $\Delta\lambda$ is the increment between measurements of $F_D(\lambda)$ and $\varepsilon(\lambda)$; in this case it is 2 nm. (Note that the sum from 450 to 600 is simply because those were the wavelengths used in this study; other donor-acceptor pairs would require summation over a different series of wavelengths.)

$$\frac{\sum_{\lambda=450}^{600} [F_D(\lambda) \cdot \varepsilon(\lambda) \cdot \lambda^4 \cdot \Delta\lambda]}{\sum_{\lambda=450}^{600} [F_D(\lambda) \cdot \Delta\lambda]} \quad (6)$$

CNm7 (see section 7-2E for the sequence and initial photophysical characterization of this construct)

CNm7 was characterized using the Gated Luminescence Scans and τ_D Determination described above. These were conducted at 2 μM protein with 2 μM Tb^{3+} , and were used in Figure 7-11 and as values for $F_D(\lambda)$ in equation (6).

τ_{00} equiv. Ca = 2.43 ms
 τ_{01} equiv. Ca = 2.45 ms
 τ_{02} equiv. Ca = 2.46 ms
 τ_{04} equiv. Ca = 2.46 ms
 τ_{06} equiv. Ca = 2.47 ms
 τ_{10} equiv. Ca = 2.51 ms
 τ_{20} equiv. Ca = 2.53 ms
 $\tau_D = 2.47 \pm 0.03$ ms

CNm4-^BA17C-TMR (Sequence of **CNBm4-A17C-TMR** shown; see 7-1E for that of the concurrently expressed **CNA**)

MGNEASYPLEMASHFDC(*TMR)DEIKRLGKRFKKLDLDNSGSLSVVEEFMSLPELQQNPLVQRVIDIFDTDGNGEVDKFKEFIEGVSQFSVKGDKKLRFAFRIFDMDKDGFI SNGELFQVLKMMVGNL KDTQLQQIVDKTIINADKDGWIEFEFEFAAVVGGLDIHKKMVVDV

CNm4-^BA17C-TMR was prepared by Dr. Alina Iuga, and was received as a stock in 100 mM NaCl, 50 mM HEPES, 100 mM imidazole·(HCl), 0.1 mM TCEP pH 7.5 buffer. It was photophysically characterized using the Gated Luminescence Scans and τ_{DA} Determination described above. These were conducted at 2 μ M protein with 2 μ M Tb³⁺, and were used in Figures 7-11 and 7-12. Table 7-6 includes these results.

Table 7-6. Gated Luminescence Scans and τ_{DA} Determination with 2 μ M **CNm4-^BA17C-TMR**

[Tb ³⁺]	[Ca ²⁺]	τ_{544} ^a	τ_{563} ^b	Remarks ^c
0.0 equiv.	0 equiv.	N/D ^d	N/D ^d	√
1.0 equiv.	0 equiv.	2.00 ms	0.49 ms	√ ^e
1.0 equiv.	1 equiv.	2.05 ms	0.47 ms	×
1.0 equiv.	2 equiv.	2.00 ms	0.46 ms	×
1.0 equiv.	4 equiv.	2.03 ms	0.46 ms	×
1.0 equiv.	6 equiv.	2.04 ms	0.47 ms	×
1.0 equiv.	10 equiv.	2.00 ms	0.46 ms	×
1.0 equiv.	20 equiv.	2.03 ms	0.45 ms	√

^a Included in Figure 7-12A

^b Included in Figure 7-12B

^c A check-mark (“√”) indicates that a Gated Luminescence Scan was taken at this concentration, but is not shown. An “×” indicates that a Gated Luminescence Scan was not taken.

^d Not determined (no signal)

^e Included in Figure 7-11

7-5E. A **CNm4** Construct Labeled on the CaM-Binding Domain

CNm4-^AA387C-TMR (Sequence of **CNA-^AA387C-TMR** shown; see 7-2E or 7-6E for that of the concurrently expressed **CNBm7**)

**MSEPKAIDPK LSTTDRVKA VPFPPSHRLT AKEVFDNDGK PRVDILKAHL MKEGRLEESV
ALRIITEGAS ILRQEKLLD IDAPVTVCGD IHGQFFDLMK LFEVGGSPAN TRYLFLGDYV
DRGYFSIECV LYLWALKILY PKTLFLLRGN HECRHLTEYF TFKQECKIKY SERVYDACMD
AFDCLPLAAL MNQQFLCVHG GLSPEINTLD DIRKLDRFKE PPAYGPMCDI LWSDPLEDFG
NEKTQEHFTH NTVRGC SYFY SYPVCEFLQ HNNLLSILRA HEAQDAGYRM YRKSQTTGFP
SLITIFSAPN YLDVYNNKAA VLKYENNVMN IRQFNCSPPH YWLPNFMDFV TWSLFPVGEK
VTEMLVNVLN ICSDELGSE EDGFDGC(*TMR)TAA ARKEVIRNKI RAIGKMARVF
SVLREESESV LTLKGLTPTG MLPSGVLSSG KQTLQSATVE AIEADEAIKG FSPQHKITSF
EEAKGLDRIN ERMPRRDAM PSDANLNSIN KALTSETNGT DSNGSNSNSNI QHHHHH**

CNm4-^AA387C-TMR was prepared by Dr. Alina Iuga, and was received as a stock in 100 mM NaCl, 50 mM HEPES, 100 mM imidazole(HCl), 0.1 mM TCEP pH 7.5 buffer. When it was photophysically characterized, it did not sensitize Tb³⁺.

7-6E. Generation of a Simpler System, with Only CNB, for Use in LRET Studies

Digestion of plasmids and inserts by restriction enzymes.

Digestion by restriction enzymes is described in detail in Chapter 4 (4-2E).

Ligation of new plasmids.

The ligation reaction strategy is described in detail in Chapter 4 (4-2E).

Transformation of competent cells

The transformation strategy is described in detail in Chapter 4 (4-2E).

“QuikChange[®]” Mutagenesis.

The procedure for QuikChange[®] Mutagenesis (Stratagene) is described in detail in Chapter 5 (5-6E).

Cleavage of constructs by mTEV protease.

The strategy for cleavage of constructs by mTEV protease is described in detail in Chapter 5 (5-6E). Briefly, protein was dialyzed into 100 mM NaCl and 50 mM PO₄³⁻, pH 8.0. Immediately prior to cleavage, 5 mM βME was added, and the solution was filtered through a 2 micron filter. The mTEV protease was then added (usually at around 1:500 dilution), and the reaction proceeded at room temperature overnight; it was analyzed by 15% SDS-PAGE.

Recipe for 1 liter of “eLB” expression medium (see also 5-5E)

10 g tryptone
5 g yeast extract
2 mL of 1 M MgSO₄
20 mL of 50× “M” buffer (1.25 M Na₂HPO₄, 1.25 M KH₂PO₄, 2.50 M NH₄Cl, 0.25 M Na₂SO₄)
Deionized H₂O to 1 L, and autoclave
200 μL trace metals, added after autoclaving (to ultimately provide 50 μM Fe³⁺, 20 μM Ca²⁺, 10 μM Mn²⁺, 10 μM Zn²⁺, 2 μM Co²⁺, 2 μM Cu²⁺, 2 μM Ni²⁺, 2 μM Mo⁶⁺, 2 μM Se⁴⁺, 2 μM BO₃³⁻)

Gene for CNBm7

The gene for CNBm7 was ordered from BioBasic, Inc. (Markham, Ontario), and was received in a high-copy, pUC57 plasmid. An N-terminal His₇-tag was included to enable purification by IMAC, and a TEV protease cleavage site was included to facilitate subsequent removal of the His-tag. The sequence of the gene that was ordered is shown.

NdeI-H₇-ENLYFQ-CNBm7-*EcoRI*:

CATATGCATCACCACCACCATCACGGTCACGAAAATCTGTACTTTTCAGGGTAACG
AGGCATCTTATCCGCTGGAATGGCGAGCCATTTTCGACGCTGATGAAATTAAC
GTCTGGGCAAACGTTTCAAGAACTGGACCTGGATAACAGCGGCTCCCTGTCTG
TGGAAGAATTTATGTCTCTGCCGGAGCTGCAACAGAATCCGCTGGTACAGCGCG
TAATCGACATCTTTGACACTGACGGCAACGGTGAAGTGGATTTCAAAGAGTTCAT
TGAAGGTGTTCCAGTTCCTCCGTGAAAGGTGATAAAGAACAGAACTGCGTTTC
GCTTCCGCATCTTCGACATGGACAAGGATGGCTTCATCTCTAACGGTGAAGTGT
TCCAGGTTCTGAAAATGATGGTTGGTAACAACCTGAAAGACACCCAAGTGCAGC
AGATTGTAGATAAAACCATCATCAACGCAGACAAAACGGCGATGGCTGGATCG
AATTTGAAGAGTTCGCCGCGGTGGTAGGTGGTCTGGACATTCACAAAAGATGG
TTGTTGATGTTTAAGAATTC

Cloning of the CNBm7 construct

The pET11a-based plasmid containing the gene encoding H₆-GPGdSE3-ubiquitin (see Chapters 4 and 5) was used as a template for the cloning. The plasmid was a gift from the labs of Prof. Karen Allen, and is carbenicillin-resistant. DH5 α cells (Stratagene) were transformed with this plasmid, plated on LB-carbenicillin-agar plates, and incubated overnight. A colony was picked and grown overnight; usable quantities of plasmid were extracted using a Miniprep (Qiagen) kit.

Other DH5 α cells were transformed with the pUC57 plasmid (*vide supra*) encoding the gene for CNBm7, plated on LB-carbenicillin-agar plates, and incubated overnight. A colony was picked and grown overnight; usable quantities of plasmid were extracted using a Miniprep kit.

The two plasmids were digested with restriction enzymes *NdeI* and *EcoRI* overnight at and purified as described (*vide supra*). The primers were then annealed as described (*vide supra*), and XL10-gold cells were transformed with the resulting plasmid; a colony was picked, grown, Miniprep, and sequenced to ensure that the correct gene was included. For expression, BL21 cells were transformed with the desired plasmid.

DNA sequence of the H₇-ENLYFOCNBm7 Plasmid:

ATGCATCACCACCACCATCACGGTCACGAAAATCTGTA CTTTCAGGGTAACGAGGC
ATCTTATCCGCTGGAAATGGCGAGCCATTTTCGACGCTGATGAAATTAACGTCTGG
GCAAACGTTTCAAGAACTGGACCTGGATAACAGCGGCTCCCTGTCTGTGGAAGA
ATTTATGTCTCTGCCGGAGCTGCAACAGAATCCGCTGGTACAGCGCGTAATCGAC
ATCTTTGACACTGACGGCAACGGTGAAGTGGATTTCAAAGAGTTCATTGAAGGTGT
TTCCCAGTTCTCCGTGAAAGGTGATAAAGAACAGAACTGCGTTTCGCTTTCCGCA
TCTTCGACATGGACAAGGATGGCTTCATCTCTAACGGTGAAGTGTCCAGGTTCTG
AAAATGATGGTTGGTAACAACCTGAAAGACACCCAACCTGCAGCAGATTGTAGATAA
AACCATCATCAACGCAGACAAAAACGGCGATGGCTGGATCGAATTTGAAGAGTTC
GCCGCGGTGGTAGGTGGTCTGGACATTCACAAAAAGATGGTTGTTGATGTTTAA

Expression and purification of the H₇-ENLYFOCNBm7 construct.

Starting from an overnight culture, BL21-(DE3)-Gold cells (Stratagene) expressing the desired fusion protein were grown in 1.0 L of eLB media containing carbenicillin antibiotic in a shaker at 37 °C. When the OD₆₀₀ reached 0.7, protein production was induced with 0.2 mM IPTG. After 5 hours, the cells were harvested by centrifugation and frozen at -80 °C until needed. Approximately 7.5 g of cell paste was obtained from a 1 L expression.

All purification was performed at 4 °C unless otherwise noted. Half of the cell pellet (0.5 L of eLB worth) was thawed and resuspended in a lysis buffer (50 mL of 300 mM NaCl, 50 mM PO₄³⁻, 10 mM imidazole, 2 mM βME, pH 8.0), to which was added 1 mg/mL lysozyme (chicken egg white, Aldrich), and 1:1000 Protease Inhibitor Cocktail Set III (Calbiochem), and incubated at 4 °C for 20 minutes. 12.5 mL of a 5% NP40 detergent solution (in lysis buffer) was then added, followed by 10 minutes of rocking. Cells were lysed by sonication (5 minutes at 3 intervals of 100 seconds with 100 second rests between intervals; 30% duty, 50% power), and cellular debris was pelleted by centrifugation (13K RPM for 55 min), and the soluble portion was filtered through a 2 micron filter. Supernatant was incubated for one hour with about 5 mL of NiNTA-agarose resin (Qiagen) at 4 °C, and poured into a 20 mL gravity-flow column, rerunning the flow-through to ensure complete binding. Resin was washed twice at room temperature with 30 mL wash buffer (identical to lysis buffer except for the concentration of imidazole, which was 20 mM). The CNBm7 construct was then eluted using ~40 mL of elution buffer (identical to the lysis buffer except for the concentration of imidazole, which was now 250 mM), and moved immediately to the cold (4 °C) room. The elution was analyzed by 15% SDS-PAGE and quantified using the Biorad BCA/BSA protein assay (obtained ~70 mg per L of eLB). Purified protein was immediately dialyzed to remove imidazole, and into a buffer suitable for

TEV cleavage (100 mM NaCl, 50 mM PO₄³⁻, pH 8.0), and stored at 4°C. The construct was then cleaved by mTEV protease as described (*vide supra*).

Cloning of the H₇-ENLYFQCNBm7-A17C construct.

The pET11a-based plasmid encoding H₇-ENLYFQCNBm7 was used as a template. Usable quantities of plasmid were extracted from transformed DH5α cells using a Miniprep (Qiagen) kit. Mutagenesis was conducted following the Quikchange (Stratagene) kit procedure (*vide supra*). The following primers were used (the altered nucleobases are shown in boldface.)

“QC_CNBm7_A17C_for”:
(GAAATGGCGAGCCATTT**C**ACT**G**TGATGAAATTAACGTCTGGG)

“QC_CNBm7_A17C_rev”:
(CCCAGACGTTTAATTT**C**AT**C**AGTCGAAATGGCTCGCCATTT**C**)

For expression, BL21 cells (Stratagene) were transformed with the desired plasmid.

DNA sequence of the H₇-ENLYFQCNBm7-A17C Plasmid:

```
ATGCATCACCACCACCATCACGGTCACGAAAATCTGTACTTTTCAGGGTAACGAGGC
ATCTTATCCGCTGGAAATGGCGAGCCATTTCACTGTGATGAAATTAACGTCTGG
GCAAACGTTTCAAGAACTGGACCTGGATAACAGCGGCTCCCTGTCTGTGGAAAGA
ATTTATGTCTCTGCCGGAGCTGCAACAGAATCCGCTGGTACAGCGCGTAATCGAC
ATCTTTGACACTGACGGCAACGGTGAAGTGGATTTCAAAGAGTTCATTGAAGGTGT
TTCCCAGTTCTCCGTGAAAGGTGATAAAGAACAGAACTGCGTTTCGCTTTCCGCA
TCTTCGACATGGACAAGGATGGCTTCATCTAACGGTGAACTGTTCCAGGTTCTG
AAAATGATGGTTGGTAACAACCTGAAAGACACCCAACTGCAGCAGATTGTAGATAA
AACCATCATCAACGCAGACAAAACGGCGATGGCTGGATCGAATTTGAAGAGTTC
GCCGCGGTGGTAGGTGGTCTGGACATCACAAAAGATGGTTGTTGATGTTTAA
```

Expression and purification of the H₇-ENLYFQCNBm7-A17C construct, and labeling by TMR

Starting from an overnight culture, BL21-(DE3)-Gold cells expressing the desired fusion protein were grown in 1.0 L of eLB media containing carbenicillin antibiotic in a shaker at 37 °C. When the OD₆₀₀ reached 0.7, protein production was induced with 0.2 mM IPTG. After 5 hours, the cells were harvested by centrifugation and frozen at -80 °C until needed. (Autoinduction was also found to be successful for both this and the CNBm7 construct; using autoinduction, 6.5 g of cell paste was obtained from 500 mL of expression medium.)

Purification was as for CNBm7 with the following exceptions. After loading the NiNTA resin with protein construct, half of the resin was then moved to a separate column for labeling. The buffer was changed to 100 mM NaCl, 50 mM HEPES pH 7.0 containing 0.1 mM TCEP.

Roughly 20 equivalents of TMR-maleimide (**3**) were added (0.5 mg, 1 μ mol, dissolved in 100 μ L DMSO), and the solution was rocked in the dark, overnight at 4°C. Excess fluorophore was then washed away, first with the (100 mM NaCl, 50 mM HEPES pH 7.0 containing 0.1 mM TCEP) buffer, although the resin remained a purple-pink color. The buffer was then changed back to (50 mL of 300 mM NaCl, 50 mM PO_4^{3-} , 20 mM imidazole, 2 mM β ME, pH 8.0), and the protein construct was eluted with 12 mL of elution buffer (50 mL of 300 mM NaCl, 50 mM PO_4^{3-} , 250 mM imidazole, 2 mM β ME, pH 8.0). The protein was immediately dialyzed into buffer for mTEV proteolytic cleavage (100 mM NaCl, 50 mM PO_4^{3-} , pH 8.0), and stored at 4°C. The construct was then cleaved by mTEV protease as described (*vide supra*).

7-7E. Generation of CNB-Binding Domain Peptides CaNAd α and P2465

CaNAd α : H₂N-YWLPNFM DVFTW SLPFVGEKVTEMLVNVLN IASDDE-CONH₂

CaNAd α was prepared using standard Fmoc-based SPPS as described in section 2-0E on NovaPEG Rink Amide LL resin, cleaved by TFA cocktail and purified by RP-HPLC. The peptide was dissolved in 20% DMF, 20% acetonitrile, and 60% water. Ammonium hydroxide was added to pH > 8.0 to help dissolution, and then the solution was acidified to pH < 6 by 2M acetic acid. The following HPLC gradient was used, with a 15 mL/min flow rate: 80:20 to 5:95 (water : acetonitrile, 0.1% TFA) over 25 minutes. Five minutes of 80:20 was run before the gradient, and six minutes of 5:95 was run after the gradient. (t_R = 28.4 min.). Exact mass calcd., 4220.9 [M+H⁺]; found 4221.7 [M+H⁺], 4244.3 [M+Na⁺] by MS (MALDI).

P2465: H₂N-DDEQFNSSPHPYWLPNFM DVFTW SLPFVGEKV-CONH₂

P2465 was prepared using standard Fmoc-based SPPS as described in section 2-0E on NovaPEG Rink Amide LL resin, cleaved by TFA cocktail and purified by RP-HPLC. The peptide was dissolved in 20% DMF, 20% acetonitrile, and 60% water. The subsequent purification, including acidification and HPLC gradient, was the same as for CaNAd α . (t_R = 23.6 min.). Exact mass calcd., 3830.3 [M+H⁺]; found 3828.9 [M+H⁺], 3850.8 [M+Na⁺] by MS(MALDI).

7-8E. Photophysical Experiments with CNBm7

CNBm7:

**GNEASYPLEMASHFDADEIKRLGKRFFKKLDLNSGSLSVVEEFMSLPQLQNPLVQRVIDIFD TDG
NGEVDFKEFIEGVSQFSVKGDKLRFQKLRFAFRI FDMKDGFISNGELFQVLKMMVGNNLKDTQLQQ
IVDKTIINADKNGDGWIEFEFFAAVVGGLDIHKKMVVDV**

The construct H₇-ENLYFQ-CNBm7 was prepared and cleaved by TEV protease as described above (section 7-6E). After mTEV cleavage, NaCl was added to the buffer to a concentration of 300 mM, and imidazole to a concentration of 20 mM. His-tag peptide, uncleaved protein, and mTEV protease were removed by reverse IMAC (running the solution by gravity through NiNTA resin). The solution containing CNBm7 was then dialyzed into 100 mM NaCl, 50 mM HEPES pH 7.5. Purity was assessed by SDS-PAGE (15% gel; section 4-2E), and concentration determined by UV A₂₈₀ (section 2-0E). It was photophysically characterized to verify that Tb³⁺ bound using Direct Titrations (2-0E), and using the Gated Luminescence Scans and τ_D Determination described above (section 7-4E). These were conducted at 2 μ M protein with 2 μ M Tb³⁺, and were used in Figures 7-11 and 7-12.

$$\text{Log } \beta (\text{Tb}^{3+}, 1:1_{\text{NaCl/MOPS}}) = 9.06 \pm 0.11$$

$$\text{Luminescence decay (no peptide): } \tau_{H_2O} = \tau_D = 2.61 \text{ ms; } \tau_{D_2O} = 3.05 \text{ ms}$$

$$+ \text{CaNA}\alpha: \tau_D = 2.63 \text{ ms}$$

$$+ \text{CaNA}\alpha + 20 \text{ equiv. Ca}^{2+}: \tau_D = 2.61 \text{ ms}$$

Gated Luminescence Scans were conducted at 2 μ M CNBm7. After a background scan was taken, scans were taken after the additions of 2 equiv. Tb³⁺, 20 equiv. Ca²⁺, and finally 2 equiv. CaNA α . No significant change was observed; the scan with 2 equiv. Tb³⁺ is included in Figure 7-17.

CNBm7-A17C:

**GNEASYPLEMASHFDCDEIKRLGKRFFKKLDLNSGSLSVVEEFMSLPQLQNPLVQRVIDIFD TDG
NGEVDFKEFIEGVSQFSVKGDKLRFQKLRFAFRI FDMKDGFISNGELFQVLKMMVGNNLKDTQLQQ
IVDKTIINADKNGDGWIEFEFFAAVVGGLDIHKKMVVDV**

The construct H₇-ENLYFQ-CNBm7-A17C was prepared and cleaved by TEV protease as described above for H₇-ENLYFQ-CNBm7 (section 7-6E). After mTEV cleavage, NaCl was added to the buffer to a concentration of 300 mM, and imidazole to a concentration of 20 mM. His-tag peptide, uncleaved protein, and mTEV protease were removed by reverse IMAC (running the solution by gravity through NiNTA resin). The solution containing CNBm7-A17C was then dialyzed into 100 mM NaCl, 50 mM HEPES pH 7.5. Purity was assessed by SDS-PAGE (15% gel; section 4-2E), and concentration determined by UV A₂₈₀ (section 2-0E). It was

photophysically characterized to verify that Tb³⁺ bound (7-0E), and using the τ_D Determination described above (section 7-4E). These were conducted at 2 μ M protein with 2 μ M Tb³⁺.

Luminescence decay (no peptide): $\tau_{H_2O} = \tau_D = 2.71$ ms; $\tau_{D_2O} = 3.14$ ms

CNBm7-A17C-TMR:

**GNEASYPLEMASHFDC(*TMR)DEIKRLGKRFKKLDLNSGSLSVVEEFMSLPQLQONPLVQRVID
IFDTDGNGEVDFKEFIEGVSQFSVKGDKEQKLRFAFRIFDMDKDGFI SNGELFQVLKMMVGNLK
DTQLQQIIVDKTI INADKNGDGIWIEFEEFAAVVGLLDIHKKMVVDV**

The construct H₇-ENLYFQ-CNBm7-A17C-TMR was prepared and cleaved by TEV protease as described above (section 7-6E). After mTEV cleavage, NaCl was added to the buffer to a concentration of 300 mM, and imidazole to a concentration of 20 mM. His-tag peptide, uncleaved protein, and mTEV protease were removed by reverse IMAC (running the solution by gravity through NiNTA resin). The solution containing CNBm7-A17C-TMR was then dialyzed into 100 mM NaCl, 50 mM HEPES pH 7.5. Purity was assessed by SDS-PAGE (15% gel; section 4-2E). Figure 7-15 shows this gel; Figure 7-15A takes advantage of the fluorescence of the TMR moiety. Concentration was determined by the comparison of a protein assay and the concentration of TMR based on UV absorbance (A₅₅₁): CNBm7-A17C was ~35% labeled; while not ideal, this was sufficient for the LRET experiments.

It was photophysically characterized to verify that Tb³⁺ bound using Direct Titrations (2-0E), and using the Gated Luminescence Scans and τ_{DA} Determination described above (section 7-4E). All of these experiments were conducted at 2.9 μ M protein, which corresponds to 1 μ M (labeled) CNBm7-A17C-TMR. (For calculating equivalents, 2.9 μ M—total CNBm7-A17C protein content—was used.) Tables 7-7, 7-8, and 7-9 include the results for this construct with no CNA-domain peptide, CaNAd α , and P2465, respectively.

Table 7-7. Gated Luminescence Scans and τ_{DA} Determination with 1 μ M CNBm7-A17C-TMR (2.9 μ M total CNBm7-A17C protein)

[Peptide]	[Tb ³⁺]	[Ca ²⁺]	τ_{544}	τ_{563}	Remarks ^a
None	0.00 equiv.	0 equiv.	N/D ^b	N/D ^b	√
None	0.33 equiv.	0 equiv.	2.47 ± 0.02 ms	1.64 ± 0.13 ms	√
None	0.67 equiv.	0 equiv.	2.47 ± 0.01 ms	1.59 ± 0.09 ms	√
None	1.00 equiv.	0 equiv.	2.43 ± 0.01 ms	1.51 ± 0.09 ms	√
None	2.00 equiv.	0 equiv.	2.46 ± 0.01 ms	1.35 ± 0.08 ms	√
None	2.00 equiv.	50 equiv.	2.50 ± 0.02 ms	1.59 ± 0.12 ms	√ ^c

^a A check-mark (“√”) indicates that a Gated Luminescence Scan was taken at this concentration, but is not shown.

^b Not determined (no signal)

^c Included in Figure 7-17.

Table 7-8. Gated Luminescence Scans and τ_{DA} Determination with 1 μM CNBm7-A17C-TMR (2.9 μM total CNBm7-A17C protein) in the Presence of 5.82 μM CaNAAd α Peptide

[CaNAAd α]	[Tb ³⁺]	[Ca ²⁺]	τ_{544}	τ_{563}	Remarks ^a
5.82 μM	0.00 equiv.	0 equiv.	N/D ^b	N/D ^b	√
5.82 μM	0.33 equiv.	0 equiv.	2.58 ± 0.02 ms	2.38 ± 0.33 ms	√
5.82 μM	0.67 equiv.	0 equiv.	2.50 ± 0.02 ms	2.00 ± 0.26 ms	√
5.82 μM	1.00 equiv.	0 equiv.	2.47 ± 0.02 ms	2.29 ± 0.33 ms	√
5.82 μM	2.00 equiv.	0 equiv.	2.50 ± 0.02 ms	1.02 ± 0.07 ms	√
5.82 μM	2.00 equiv.	20 equiv.	2.50 ± 0.02 ms	1.21 ± 0.09 ms	√
5.82 μM	2.00 equiv.	50 equiv.	2.56 ± 0.02 ms	1.60 ± 0.11 ms	√ ^c

^a A check-mark (“√”) indicates that a Gated Luminescence Scan was taken at this concentration, but is not shown.

^b Not determined (no signal)

^c Included in Figure 7-17.

Table 7-9. Gated Luminescence Scans and τ_{DA} Determination with 1 μM CNBm7-A17C-TMR (2.9 μM total CNBm7-A17C protein) in the Presence of 5.82 μM P2465 Peptide

[P2465]	[Tb ³⁺]	[Ca ²⁺]	τ_{544}	τ_{563}	Remarks ^a
5.8 μM	0.00 equiv.	0 equiv.	N/D ^b	N/D ^b	√ ^c
5.8 μM	0.33 equiv.	0 equiv.	2.48 ± 0.02 ms	1.47 ± 0.11 ms	√ ^c
5.8 μM	0.67 equiv.	0 equiv.	2.47 ± 0.01 ms	1.30 ± 0.09 ms	√ ^c
5.8 μM	1.00 equiv.	0 equiv.	2.47 ± 0.01 ms	1.17 ± 0.08 ms	√ ^c
5.8 μM	2.00 equiv.	0 equiv.	2.47 ± 0.01 ms	1.25 ± 0.08 ms	√ ^c
5.8 μM	2.00 equiv.	20 equiv.	2.48 ± 0.01 ms	1.24 ± 0.07 ms	√ ^c
5.8 μM	2.00 equiv.	50 equiv.	2.53 ± 0.02 ms	1.77 ± 0.13 ms	√ ^{c,d}

^a A check-mark (“√”) indicates that a Gated Luminescence Scan was taken at this concentration.

^b Not determined (no signal)

^c Included in Figure 7-16.

^d Included in Figure 7-17.

Acknowledgements

I am grateful for our collaboration with Professor Patrick G. Hogan and Dr. Alina Iuga at Harvard Medical School. Alina did all of the cloning, expression and purification of all of the CNA-containing mutants, including the labeling of the two CNm4 mutants. I thank Dr. Bianca Sculimbrene for helpful discussions about how to interpret LRET data. I am eternally grateful to Galen Loving and Elvedin Luković for editing this chapter.

References

- (1) Barbieri, R.; Bertini, I.; Cavallaro, G.; Lee, Y.-M.; Luchinat, C.; Rosato, A. "Paramagnetically induced residual dipolar couplings for solution structure determination of lanthanide binding proteins." *J. Am. Chem. Soc.* **2002**, *124*(19), 5581-5587.
- (2) Pidcock, E.; Moore, G. R. "Structural characteristics of protein binding sites for calcium and lanthanide ions." *J. Biol. Inorg. Chem.* **2001**, *6*(5-6), 479-489.
- (3) Burroughs, S. E.; Horrocks, W. D., Jr.; Ren, H.; Klee, C. B. "Characterization of the Lanthanide Ion-Binding Properties of Calcineurin-B Using Laser-Induced Luminescence Spectroscopy." *Biochemistry* **1994**, *33*(34), 10428-10436.
- (4) Lee, L.; Sykes, B. D. "Use of lanthanide-induced nuclear magnetic resonance shifts for determination of protein structure in solution: EF calcium binding site of carp parvalbumin." *Biochemistry* **1983**, *22*(19), 4366-4373.
- (5) Capozzi, F.; Casadei, F.; Luchinat, C. "EF-hand protein dynamics and evolution of calcium signal transduction: an NMR view." *J. Biol. Inorg. Chem.* **2006**, *11*, 949-962.
- (6) Sculimbrene, B. R.; Imperiali, B. "Lanthanide-Binding Tags as Luminescent Probes for Studying Protein Interactions." *J. Am. Chem. Soc.* **2006**, *128*(22), 7346-7352.
- (7) Klee, C. B.; Crouch, T. H.; Krinks, M. H. "Calcineurin: A calcium- and calmodulin-binding protein of the nervous system." *Proc. Natl. Acad. Sci. USA* **1979**, *76*(12), 6270-6273.
- (8) Kissinger, C. R.; Parge, H. E.; Knighton, D. R.; Lewis, C. T.; Pelletier, L. A.; Tempczyk, A.; Kalish, V. J.; Tucker, K. D.; Showalter, R. E.; Moomaw, E. W.; Gastinel, L. N.; Habuka, N.; Chen, X.; Maldonado, F.; Barker, J. E.; Bacquet, R.; Villafranca, J. E. "Crystal structures of human calcineurin and the human FKPB12-FK506-calcineurin complex." *Nature* **1995**, *378*, 641-644.
- (9) Feske, S.; Rao, A.; Hogan, P. G., "The Ca²⁺-calcineurin-NFAT signaling pathway." In *CALCIUM: A Matter of Life or Death*, Krebs, J.; Michalak, M., Eds. Elsevier: Amsterdam, **2007**; 41, pp 365-401.
- (10) Jin, L.; Harrison, S. C. "Crystal structure of human calcineurin complexed with cyclosporin A and human cyclophilin." *Proc. Natl. Acad. Sci. USA* **2002**, *99*(21), 13522-13526.
- (11) Klee, C. B.; Ren, H.; Wang, X. "Regulation of the Calmodulin-stimulated Protein Phosphatase, Calcineurin." *J. Biol. Chem.* **1998**, *273*(22), 13367-13370.
- (12) Hubbard, M. J.; Klee, C. B. "Functional Domain Structure of Calcineurin A: Mapping by Limited Proteolysis." *Biochemistry* **1989**, *28*, 1868-1874.

- (13) Yang, S.-A.; Klee, C. B. "Low Affinity Ca²⁺-Binding Sites of Calcineurin B Mediate Conformational Changes in Calcineurin A." *Biochemistry* **2000**, *39*, 16147-16154.
- (14) Stemmer, P. M.; Klee, C. B. "Dual Calcium Ion Regulation of Calcineurin by Calmodulin and Calcineurin B." *Biochemistry* **1994**, *33*, 6859-6866.
- (15) Binstead, R.; Jung, B.; Zuberbühler, A. *SPECFIT/32 for Windows; Original Release 2000*, Version 3.0.39; Spectrum Software Associates, Marlborough, MA.: SPECFIT/32 provides global analysis of equilibrium and kinetic systems using singular value decomposition and nonlinear regression modeling by the Levenberg-Marquardt method., 2007.
- (16) Ye, Q.; Li, X.; Wong, A.; Wei, Q.; Jia, Z. "Structure of Calmodulin Bound to a Calcineurin Peptide: A New Way of Making an Old Binding Mode." *Biochemistry* **2006**, *45*, 738-745.
- (17) Hashimoto, Y.; Perrino, B. A.; Soderling, T. R. "Identification of an Autoinhibitory Domain in Calcineurin." *J. Biol. Chem.* **1990**, *265*(4), 1924-1927.
- (18) Gallagher, S. C.; Gao, Z.-H.; Li, S.; Dyer, R. B.; Trewhella, J.; Klee, C. B. "There Is Communication between All Four Ca²⁺-Binding Sites of Calcineurin B." *Biochemistry* **2001**, *40*, 12094-12102.
- (19) Feng, B.; Stemmer, P. M. "Interactions of Calcineurin A, Calcineurin B, and Ca²⁺." *Biochemistry* **1999**, *38*(38), 12481-12489.
- (20) MacManus, J. P.; Hogue, C. W.; Marsden, B. J.; Sikorska, M.; Szabo, A. G. "Terbium luminescence in synthetic peptide loops from calcium-binding proteins with different energy donors." *J. Biol. Chem.* **1990**, *265*(18), 10358-10366.
- (21) Martin, L. J.; Sculimbrene, B. R.; Nitz, M.; Imperiali, B. "Rapid Combinatorial Screening of Peptide Libraries for the Selection of Lanthanide-Binding Tags (LBTs)." *QSAR Comb. Sci.* **2005**, *24*(10), 1149-1157.
- (22) Beeby, A.; Clarkson, I. M.; Dickins, R. S.; Faulkner, S.; Parker, D.; Royle, L.; de Sousa, A. S.; Williams, J. A. G.; Woods, M. "Non-radiative deactivation of the excited states of europium, terbium and ytterbium complexes by proximate energy-matched OH, NH and CH oscillators: an improved luminescence method for establishing solution hydration states." *J. Chem. Soc., Perkin Trans. 2* **1999**, (3), 493-504.
- (23) Drake, S. K.; Lee, K. L.; Falke, J. J. "Tuning the Equilibrium Ion Affinity and Selectivity of the EF-Hand Calcium Binding Motif: Substitutions at the Gateway Position." *Biochemistry* **1996**, *35*(21), 6697-6705.

- (24) Nitz, M.; Sherawat, M.; Franz, K. J.; Peisach, E.; Allen, K. N.; Imperiali, B. "Structural origin of the high affinity of a chemically evolved lanthanide-binding peptide." *Angew. Chem. Int. Ed.* **2004**, *43*(28), 3682-3685.
- (25) Nitz, M.; Franz, K. J.; Maglathlin, R. L.; Imperiali, B. "A powerful combinatorial screen to identify high-affinity terbium(III)-binding peptides." *ChemBioChem* **2003**, *4*(4), 272-276.
- (26) Marsden, B. J.; Hodges, R. S.; Sykes, B. D. "Proton NMR studies of synthetic peptide analogs of calcium-binding site III of rabbit skeletal troponin C: Effect on the lanthanum affinity of the interchange of aspartic acid and asparagine residues at the metal ion coordinating positions." *Biochemistry* **1988**, *27*(11), 4198-4206.
- (27) Martin, L. J.; Daughtry, K.; Allen, K. N.; Imperiali, B., Unpublished results.
- (28) Grabarek, Z. "Structural Basis for Diversity of the EF-hand Calcium-binding Proteins." *J. Mol. Biol.* **2006**, *359*, 509-525.
- (29) Patton, C.; Thompson, S.; Epel, D. "Some precautions in using chelators to buffer metals in biological solutions." *Cell Calcium* **2004**, *35*, 427-431.
- (30) Lakowicz, J. R., *Principles of Fluorescence Spectroscopy*. Kluwer Academic/Plenum Publishers: Boston, 1999;
- (31) Root, D. D.; Shanguan, X.; Xu, J.; McAllister, M. A. "Determination of Fluorescent Probe Orientations on Biomolecules by Conformational Searching: Algorithm Testing and Applications to the Atomic Model of Myosin." *J. Struct. Biol.* **1999**, *127*(1), 22-34.
- (32) Vogel, K. W.; Vedvik, K. L. "Improving Lanthanide-Based Resonance Energy Transfer Detection by Increasing Donor-Acceptor Distances." *J. Biomol. Screening* **2006**, *11*(4), 439-443.
- (33) Iuga, A.; Hogan, P. G., Personal communication.
- (34) Selvin, P. R.; Hearst, J. E. "Luminescence energy transfer using a terbium chelate: Improvements on fluorescence energy transfer." *Proc. Natl. Acad. Sci. USA* **1994**, *91*, 10024-10028.
- (35) Anglister, J.; Ren, H.; Klee, C. B.; Bax, A. "NMR identification of Calcineurin B residues affected by binding of a Calcineurin A peptide." *FEBS Letters* **1995**, *375*, 108-112.
- (36) Iuga, A.; Martin, L. J.; Imperiali, B.; Hogan, P. G., Unpublished results.
- (37) Chazan, A. Peptide Property Calculator.
<http://www.basic.northwestern.edu/biotools/proteincalc.html>

Appendix Select SPECFIT Data Files

A-1.) SE3, direct Tb³⁺ titration

X/Z Mode	Nm	Nw	Nc	Model	X-axis	Y-axis	Z-axis	Path	Temp, C				
1	13	1	2	1	0	2	0	1	25				
13	0	1.33E-08	2.66E-08	3.99E-08	5.32E-08	6.65E-08	9.97E-08	1.33E-07	1.66E-07	1.99E-07	2.65E-07	3.32E-07	3.98E-07
13	5E-08	4.99E-08	4.99E-08	4.99E-08	4.99E-08	4.99E-08	4.99E-08	4.98E-08	4.98E-08	4.98E-08	4.98E-08	4.98E-08	4.98E-08
[H+]	1.00E-07	1.00E-07	1.00E-07	1.00E-07	1.00E-07	1.00E-07	1.00E-07	1.00E-07	1.00E-07	1.00E-07	1.00E-07	1.00E-07	1.00E-07
544nm	0	41859.93	75255.5	106133.8	132244.1	147871.4	187826.4	212612.6	214625.9	221610.3	241726.5	248663.8	254491.2

A-2.) GdSE3, direct Tb³⁺ Titration

X/Z Mode	Nm	Nw	Nc	Model	X-axis	Y-axis	Z-axis	Path	Temp, C								
1	17	1	2	1	0	2	0	1	25								
17	0	1.33E-08	2.66E-08	3.99E-08	5.32E-08	6.65E-08	9.97E-08	1.33E-07	1.66E-07	1.99E-07	2.66E-07	3.32E-07	3.98E-07	4.64E-07	7.96E-07	1.13E-06	1.46E-06
17	4.99E-08	4.99E-08	4.99E-08	4.99E-08	4.98E-08	4.98E-08	4.98E-08	4.98E-08	4.98E-08	4.97E-08	4.97E-08	4.97E-08	4.97E-08	4.97E-08	4.97E-08	4.97E-08	4.96E-08
[H+]	1.00E-07	1.00E-07	1.00E-07	1.00E-07	1.00E-07	1.00E-07	1.00E-07	1.00E-07	1.00E-07	1.00E-07	1.00E-07	1.00E-07	1.00E-07	1.00E-07	1.00E-07	1.00E-07	1.00E-07
544nm	0	70604.55	119748.9	182111.3	244648.6	293614.3	397095.7	456972.9	495481.8	512843.6	559760.3	588067.6	587105.7	595785.6	606934.2	611530.1	603268.3

A-3.) SE3, Competitive titration between Tb³⁺ and Gd³⁺

X/Z Mode	Nm	Nw	Nc	Model	X-axis	Y-axis	Z-axis	Path	Temp, C								
1	17	1	3	1	0	2	0	1	25								
17	0	6.64E-08	1.33E-07	1.99E-07	2.65E-07	3.31E-07	4.63E-07	5.95E-07	7.27E-07	8.59E-07	9.90E-07	1.65E-06	2.31E-06	2.97E-06	3.62E-06	4.28E-06	7.56E-06
17	4.98E-07	4.98E-07	4.98E-07	4.98E-07	4.97E-07	4.97E-07	4.97E-07	4.96E-07	4.96E-07	4.96E-07	4.95E-07	4.95E-07	4.95E-07	4.94E-07	4.94E-07	4.94E-07	4.93E-07
17	2E-07	2.00E-07	1.99E-07	1.99E-07	1.99E-07	1.99E-07	1.99E-07	1.99E-07	1.99E-07	1.99E-07	1.98E-07	1.98E-07	1.98E-07	1.98E-07	1.98E-07	1.98E-07	1.98E-07
[H+]	1.00E-07	1.00E-07	1.00E-07	1.00E-07	1.00E-07	1.00E-07	1.00E-07	1.00E-07	1.00E-07	1.00E-07	1.00E-07	1.00E-07	1.00E-07	1.00E-07	1.00E-07	1.00E-07	1.00E-07
544nm	1223260	1076998	991304.4	878468.2	795024.7	742422.1	639632.3	563986.9	511617.7	462172.7	430247.2	293897.7	229977.7	196493.4	173920	155264.4	97292.34

Curriculum Vitae for LANGDON J. MARTIN

Education

- 2003–2008** **Graduate Student** in Chemistry
Massachusetts Institute of Technology, Cambridge, MA
Ph.D. in spring, 2008
Thesis: *Development of Lanthanide-Binding Tags (LBTs) as Powerful and Versatile Peptides for Use in Studies of Proteins and Protein-Interactions*
- 1999–2003** **B. A., Magna Cum Laude**, with Honors in Chemistry
Kalamazoo College, Kalamazoo, MI
Thesis: *Synthesis and Polymerization with a Cycloaliphatic Epoxide*
- 2001–2002** **Study Abroad** at Waseda University, Tokyo, Japan

Research Experience

- 2003–2008** **Doctoral Research** with Professor Barbara Imperiali
Massachusetts Institute of Technology, Cambridge, MA
Generation of LBT (Lanthanide-Binding Tag) peptides and peptide-libraries by solid-phase peptide synthesis; cloning, expression, and purification of LBT-protein fusion constructs; characterization of LBTs and LBT-protein constructs by luminescence spectroscopy including LRET
- 2002** **Undergraduate Research** with Professor Dean C. Webster
North Dakota State University, Fargo, ND
Small-molecule synthesis with a cycloaliphatic epoxide monomer; polymerization; characterization of the synthetic polymer

Teaching Experience

- 2003–2004, 2007** **Teaching Assistant** in Chemistry
Massachusetts Institute of Technology, Cambridge, MA
- 5.07: Biological Chemistry, Fall 2007
 - 5.12: Organic Chemistry I, Fall 2004: Head Teaching Assistant
 - 5.301: Chemistry Laboratory Techniques, January-term 2004
 - 5.12: Organic Chemistry I, Fall 2003
- 2004–2007** **Demonstration Leader**, M.I.T. Chemistry Outreach program
Gave 1–2 hour demonstrations and explanations of chemistry experiments at New England area high schools (at nine schools over four years)

Awards and Honors

- 2007** **Wyeth Scholar**
Awarded to M.I.T. graduate students in recognition of accomplishments in research and for delivering excellent lectures at the Graduate Research Symposium in Organic and Bioorganic Chemistry
- 2005** **Department of Chemistry Award for Teaching**
Recognizes outstanding Teaching Assistants; earned from work performed in Course 5.12 (Organic Chemistry I), Fall 2004
- 2003** **Phi Beta Kappa**, Kalamazoo College
- 2003** **Kalamazoo College American Chemical Society Award**
Awarded to a graduating senior for excellence in course-work and the Senior Individualized Project
- 2000–2003** **H. P. and Genevieve Connable Scholarship**, Kalamazoo College
- 1999–2003** **Kalamazoo College Honors Scholarship**
- 1998** **Eagle Scout**, Boy Scouts of America

Publications

- (3) N. R. Silvaggi, L. J. Martin, H. Schwalbe, B. Imperiali, K. N. Allen. “Double-Lanthanide-Binding Tags for Macromolecular Crystallographic Structural Determination.” *J. Am. Chem. Soc.* **2007**, *129*, 7114 – 7120
- Highlighted in *C&E News*, 16 May 2007, *85 (21)*, p.31
- (2) L. J. Martin, M. J. Hähnke, M. Nitz, J. Wöhnert, N. R. Silvaggi, K. N. Allen, H. Schwalbe, B. Imperiali. “Double-Lanthanide-Binding Tags: Design, Photophysical Properties, and NMR Applications.” *J. Am. Chem. Soc.* **2007**, *129*, 7106 – 7113
- Highlighted in *C&E News*, 16 May 2007, *85 (21)*, p.31
 - Featured in Faculty of 1000 Biology, F1000 Factor 6.4:
<http://www.f1000biology.com/article/id/1087761/evaluation>
- (1) L. J. Martin, B. R. Sculimbrene, M. Nitz, B. Imperiali. “Rapid Combinatorial Screening of Peptide Libraries for the Selection of Lanthanide-Binding Tags (LBTs).” *QSAR Comb. Sci.* **2005**, *24*, 1149 – 1157

Poster Presentations

- (1) L. J. Martin, N. R. Silvaggi, K. N. Allen, B. Imperiali. “Lanthanide-Binding Tags: Protean Tools for Protein Studies.” Gordon Research Conference *Chemistry and Biology of Peptides*: Ventura, CA; February **2008**
- (2) L. J. Martin, N. R. Silvaggi, K. N. Allen, B. Imperiali. “Double-Lanthanide-Binding Tags: Powerful and Versatile Protein Probes.” 234th National ACS Meeting: Boston, MA; August **2007**